# Proteomic and Metabolomic Profiling in the Stroke-Prone Spontaneously Hypertensive Rat and Chromosome 2 Congenic Strains

**Thesis submitted for the degree of Doctor of Philosophy (Ph.D.)**

**in the College of Medical, Veterinary and Life Sciences**

**November 2013**

**Sofia Tsiropoulou, M.Res.**

BHF Glasgow Cardiovascular Research Centre
Institute of Cardiovascular and Medical Sciences
College of Medical, Veterinary and Life Sciences
University of Glasgow

# Declaration

I declare that this thesis has been written entirely by myself and is a record of research performed by myself, unless otherwise acknowledged. Liquid chromatography / mass spectrometry was conducted by Mr William Mullen for the proteomics experiments and Dr. Karl Burgess for the metabolomics experiments. Processing of proteomics data on MaxQuant was conducted by Dr. David Sumpton. Collection of plasma and urine samples used for metabolomics screening was performed by researchers at the BHF/GCRC. Setting up of wire and pressure myographs, vessel mounting and normalisations for the myography experiments were done by Mrs Elisabeth Beattie. This work has not been submitted previously for a higher degree and was carried out under the supervision of Dr. Martin W. McBride, Professor Anna F. Dominiczak and Dr. Richard J. Burchmore.

---

Sofia Tsiropoulou

# Acknowledgements

Firstly, I wish to acknowledge my supervisors, Dr. Martin W. McBride, Professor Anna F. Dominiczak and Dr. Richard J. Burchmore for their support and advice. In particular, I would like to thank Dr. McBride for his supervision and guidance over the past four years and during the production of this thesis. Thanks also to Dr. Delyth Graham, Dr. John D. McClure and Miss Elisabeth Beattie for their advice and technical assistance.

I would like to express my appreciation to several people in the Glasgow Polyomics and the Beatson Institute for their help in the 'omics' studies. Prof. Reiner Breitling, for his vital input and constructive criticism. Dr. Andris Jankevics, not only for his constant assistance in the bioinformatic analyses, but also for our adventurous trips and bike-service sessions. Dr David Sumpton and Dr Sergio Lilla for their help in the proteomics analysis.

A very big thank you to my closest friends for being there when their support was most needed. Dimi, thank you for the inspirational conversations over our daily coffee breaks. Aurelie and Guto, thank you for all your help and encouragement. Louise, Dashti and Scott, thank you for the great fun in and out of the office. My dearest Finola, I am extremely grateful to you for all your kindness and invaluable support and for putting up with me till the end of this task.

Finally, I cannot express enough my gratitude towards my family, especially my parents, Aleka and Niko, for their un-wavering support and constant encouragement throughout my studies. I could not have achieved any of this without them. Μαμά, μπαμπά, σας ευχαριστώ που πιστέψατε σε μένα και πάντα στεκόσαστε πλάι μου σε κάθε μου προσπάθεια, έστω κι εξ αποστάσεως.

Thank you

Σας ευχαριστώ

Funding for this project was provided by the Scottish Universities Life Sciences Alliance (SULSA).

# Table of Contents

# List of Figures

# List of Tables

# List of Accompanying Material (CD)

The list-level of the contents represents the folders, subfolders and documents included in the supplemented hard copy (CD).

## Chapter 3 - Urine / Plasma metabolomics

- Plasma
  - Baseline
    - Plasma_base_IC3_19_IPA
    - IDEOM_v18_Plasma_POSNEG__baseline_comparions
  - Salt
    - Plasma_salt_IC4_44_IPA
    - IDEOM_v18_plasma_POSNEG_salt_comparisons
  - Salt v Baseline
    - Plasma_salt_v_base_SHRSP_IC_Trans_(13)+Trans unique_(28)_IPA
    - IDEOM_v18_plasma_POSNEG_salt_v_baseline_comparisons
- Urine
  - Baseline
    - Urine_base_IC3_41_IPA
    - IDEOM_v18_urine_POSNEG_baseline_comparisons
  - Salt
    - Urine_salt_IC4_21_IPA
    - IDEOM_v18_urine_POSNEG_salt_comparisons
  - Salt v Baseline
    - IDEOM_v18_urine_POSNEG_salt_v_baseline_comparisons

## Chapter 5 - SILAC proteomics

- MaxQuant Parameters Summary
- Common_HLA_HLB_1056
- Common_HLA_HLB_Fold change significant_203
- HLA_analysis ready_340
- HLB_analysis ready_289
- PerseusDataTable_Expanded_MajorityIDs_1998

# Chapter 6 - S1P stimulated VSMC metabolomics

- S1P_v_vehicle_comparisons
- S1P comparisons
- vehicle comparisons

# Abbreviations, Acronyms & Symbols

| | |
|---|---|
| ∩ | Intersection |
| ~ | Approximately |
| ˚C | Degrees Celcius |
| µ | Micro (prefix) |
| ACTA2 | Alpha Smooth Muscle Actin 2 |
| ADP | Adenosine Diphosphate |
| ANP | Atrial Natriuretic Peptide |
| ATP | Adenosine Triphosphate |
| AngII | Angiotensin II |
| ANOVA | Analysis of Variance |
| APS | Ammonium Persulphate |
| AQP2 | Aquaporin 2 |
| ATP | Adenosine Triphosphate |
| BCA | Bicinchoninic Acid |
| BP | Blood Pressure |
| BSA | Bovine Serum Albumin |
| CAD | Coronary Artery Disease |
| Chr | Chromosome |
| CO | Cardiac Output |
| cAMP | Cyclic AMP |
| CVD | Cardiovascular Disease |
| DAB | Diaminobenzidine Tetrahydrochloride |
| DAPI | 4'-6-Diamidino-2-Phenylindol |
| DMEM | Dulbecco's Modified Eagle's Medium |
| DMSO | Dimethyl Sulphoxide |
| DTT | Dithiothreitol |
| EC | Endothelial Cell |
| ECL | Enhanced Chemiluminescence |
| ECM | Extracellular Matrix |
| EDG | Endothelial Differentiation Gene |
| EDHF | Endothelium-Derived Hyperpolarisation Factor |
| EDRF | Endothelium-Derived Relaxation Factor |
| EDTA | Ethylene Diamine Tetra-Acetic Acid |
| EGTA | Ethylene Glycol Tetra-Acetic Acid |
| eNOS | Endothelial Nitric Oxide Synthase |
| ERK | Extracellular Signal-Regulated Kinase |
| ESI | Electrospray Ionisation |
| ET-1 | Endothelin I |
| FCS | Fetal Calf Serum |
| FITC | Fluorescein Isothiocyanate |
| g | Gram(s) |

| | |
|---|---|
| *g* | Gravitational force |
| GAPDH | Glyceraldehyde 3-Phosphate Dehydrogenase |
| GPCR | G-protein-Coupled Receptor |
| GRK | G-protein-Coupled Receptor Kinase |
| GSTM1 | Glutathione S-Transferase Mu 1 |
| GTP | Guanosine Triphosphate |
| GWAS | Genome Wide Assossiation Studies |
| $dH_2O$ | Distilled Water |
| h | Hours |
| $H_2O_2$ | Hydrogen Peroxide |
| HEPES | 4-(2-hydroxyethyl)-1-piperazineethanesulphonic acid |
| HILIC | Hydrophilic Interaction Liquid Chromatography |
| HRP | Horseradish Peroxidase |
| HTN | Hypertension |
| ICC | Immunocytochemistry |
| IF | Immunofluorescence |
| IgG | Immunoglobulin G |
| IHC | Immunohistochemistry |
| IP | Immunoprecipitation |
| IPA | Ingenuity Pathway Analysis |
| IPI | International Protein Index |
| kDa | Kilodalton(s) |
| KEGG | Kyoto Encyclopedia of Genes and Genomes |
| L | Litre(s) |
| LC | Liquid Chromatography |
| L-NAME | N-Nitro-L-Arginine Methyl Ester |
| m | Milli (prefix) |
| M | Molar(s) |
| mA | Milliamp(s) |
| MAPK | Mitogen-Activated Protein Kinase |
| min | Minute(s) |
| ml | Millilitre(s) |
| mmHg | Millimetres of Mercury |
| MLC | Myosin Light Chan |
| MLCK | Myosin Light Chain Kinase |
| MRA | Mesenteric Resistance Artery |
| MS | Mass Spectrometry |
| n | Nano (prefix) |
| NO | Nitric Oxide |
| OD | Optical Density |
| PBS | Phosphate-Buffered Saline |
| PCA | Principal Component Analysis |
| PDGF | Platelet Derived Growth Factor |

| | |
|---|---|
| $PGI_2$ | Prostacyclin |
| Pen/strep | Penicillin / Streptomycin |
| PFA | Paraformaldehyde |
| Pi | Inorganic Phosphate |
| PI3K | Phosphatidylinositol 3-Kinase |
| PKC | Protein Kinase C |
| PMSF | Phenylmethylsulphonyl Fluoride |
| PTM | Post Translational Modifications |
| QTL | Quantitative Trait Loci |
| QC | Quality Control |
| rcf | Relative Centrifugal Force |
| RhoA | Ras Homolog Gene Family, Member A |
| Rock | Rho Kinase |
| ROS | Reactive Oxygen Species |
| PRLC | Reverse Phase Liquid Chromatography |
| rpm | Revolutions per Minute |
| RT | Retention Time |
| r.t | room temperature |
| SAPK / JNK | Stress-Activated Protein Kinase / c-Jun N-Terminal Kinase |
| S1P | Sphingosine-1-Phosphate |
| S1PR1 / S1P1 | Sphingosine-1-Phosphate Receptor |
| SBP | Systolic Blood Pressure |
| SDS | Sodium Dodecyl Sulphate |
| SDS-PAGE | Sodium Dodecyl Sulphate Polyacrylamide Gel Electrophoresis |
| SEM | Standard Error of the Mean |
| SHR | Spontaneously Hypertensive Rat |
| SHRSP | Stroke-Prone Spontaneously Hypertensive Rat |
| SP | Short for SHRSP |
| SW2a | SP.$WKY_{Gla}$2a Congenic Strain |
| SW2k | SP.$WKY_{Gla}$2k Congenic Strain |
| TBS | Tris - Buffered Saline |
| TBST | 0.1% Tween-20 in TBS |
| TPR | Total Peripheral Resistance |
| v (vs) | Versus |
| v/v | Units volume per unit volume |
| VCAM-1 | Vascular Cell Adhesion Molecule-1 |
| VEGF | Vascular Endothelial Growth Factror |
| VSMC | Vascular Smooth Muscle Cell |
| w/v | Units weight per unit weight |
| WB | Western Blot |
| WHO | World Health Organisation |
| WKY | Wistar Kyoto |
| WS2a | WKY.$SP_{Gla}$2a Congenic Stain |

# Thesis Summary

Essential hypertension (EH) is considered one of the major contributors to the present pandemic of cardiovascular disease (CVD). EH has a largely obscure aetiology, which lies upon both environmental risk factors and underlying genetic traits. The stroke-prone spontaneously hypertensive rat (SHRSP) is an excellent model of human EH and exhibits salt sensitivity. Two quantitative trait loci (QTL) for blood pressure (BP) regulation have been identified on rat chromosome 2 (chr.2). On this basis, previous work in our laboratory focused on construction of chr.2 congenic strains, on both the SHRSP and Wistar-Kyoto (WKY) genetic backgrounds. In combination with microarray gene expression profiling in kidney from salt-loaded rats, two positional candidate genes for salt-sensitive hypertension were identified. Sphingosine-1-phosphate receptor 1 (*S1pr1*) and vascular adhesion molecule (*Vcam1*) lie on the chr.2 congenic interval implicated in salt-sensitivity. Additionally, studies on vascular smooth muscle cells (VSMC) demonstrated enhanced S1PR1-mediated sphingosine signalling in SHRSP compared to WKY. Finally, glutathione S-transferase mu 1 (*Gstm1*) was identified as another chr.2 candidate gene for BP regulation, lying outside the region implicated in salt-sensitivity.

This project attempts to comprehensively investigate the potential role of altered S1PR1 signalling in BP regulation and salt-sensitivity, through comparative proteomic and metabolomic profiling in WKY, SHRSP and chromosome 2 congenic and transgenic stains (WKY.SP$_{Gla}$2a, SP.WKY$_{Gla}$2a, SP.WKY$_{Gla}$2k and *Gstm1*-transgenic).

Characterisation of S1PR1 expression in renal and vascular tissue from 21 week-old salt-loaded rats, demonstrated below detection protein levels across parental and congenic strains. To further investigate the effect of the congenic interval and *Gstm1* on salt-sensitivity and BP regulation and identify putative biomarkers, high-throughput metabolomic screening of urine and plasma was conducted in parental, SP.WKY$_{Gla}$2k congenic and *Gstm1*-transgenic strains, on a normal-salt and high-salt diet. In both urine and plasma, salt-loading affected processes implicated in CVD, including inflammatory response, free radical scavenging and lipid metabolism. In urine, oleic acid, implicated in regulation of renin levels, was increased in the SHRSP and transgenic salt-sensitive strains compared to the WKY and 2k congenic salt-resistant strains, upon salt-loading. In plasma, known biomarkers of CVD were altered in SHRSP compared to the other three strains, at normal-salt, including L-proline and linoleic acid. Upon salt-loading, glutathione disulfide and sphingosine-1-

phosphate (S1P) were identified in high levels in the salt-sensitive strains. However, at normal-salt S1P was decreased in SHRSP compared to WKY and 2k congenic strains. Therefore, characterisation of the impact of S1P/S1PR1 signalling in the vasculature across the different strains was further investigated.

Initially, structure, mechanical properties and vascular reactivity of mesenteric resistance arteries (MRA) were studied in 16 week-old parental and reciprocal 2a congenic strains (WKY.$SP_{Gla}$2a and SP.$WKY_{Gla}$2a). There was no significant remodelling observed across the strains. However, SHRSP vessels were stiffer and this phenotype was under the control of the congenic segment. SHRSP exhibited hypercontractility, which was mediated by RhoA/Rock signalling pathway and was corrected by the transfer of the congenic interval in SP.$WKY_{Gla}$2a. SHRSP also displayed endothelial dysfunction, which was related to reduced nitric oxide (NO) bioavailability and was not improved by the congenic interval. The predominant regulatory mechanisms of contraction and relaxation in MRAs from WKY and WKY.$SP_{Gla}$2a were demonstrated to be different compared to SHRSP.

Subsequently, representation of these physiological differences in MRAs, at the molecular level, was investigated along with the effect of S1P-signalling in HTN. Comprehensive, high-throughput proteome profiling of S1P-stimulated primary mesenteric VSMCs from parental and 2a-reciprocal congenic strains, was achieved through triple stable isotope labelling (SILAC), LC-MS/MS analysis and MaxQuant quantification. Detection of few abundant phosphorylated proteins was attributed to lack of enrichment for phosphoproteome. Therefore, focus was placed on proteins whose differential expression between SHRSP and WKY was genetically regulated. These proteins mapped to pathways implicated in BP-regulation, including oxidative stress, vascular tone regulation and vascular remodelling. Glutathione S-transferase mu 1 (GSTM1) was upregulated in SHRSP, as opposed to down-regulated NAD(P)H oxidase quinone 1 (NQO1) and heme oxygenase 1 (HMOX1), suggesting different antioxidant mechanisms in health and disease. Natriuretic peptide receptor C (NPR3) which is implicated in vascular relaxation was increased in SHRSP, along with activators of RhoA contractile mechanism, such as caveolin1 (CAV1). Furthermore, RhoA/Rock signalling pathway was highly altered in SHRSP. Finally, differentially expressed proteins were related to sphingosine signalling, including superoxide dismutase 2 (SOD2) and collagen type III, alpha 1 (COL3A1).

To further investigate the metabolic effect of sphingosine signalling across the strains, and assess the contribution of the congenic interval, metabolomic profiling of primary

mesenteric VSMCs from parental and SP.WKY$_{Gla}$2a congenic strains, was performed at basal conditions and upon S1P-stimulation. A labelling-free, untargeted approach was employed, using HILIC-MS analysis and data processing through IDEOM. The effect of the congenic interval on the metabolic profile of SP.WKY$_{Gla}$2a was more profound under basal conditions. S1P-stimulation induced greater responses in SHRSP than WKY, indicating altered signalling. Furthermore the responses were different in each strain, suggesting a combined effect of the genetic background and the congenic interval on S1P signalling regulation. Inosine, which is implicated in purine metabolism, was significantly decreased in SHRSP compared to SP.WKY$_{Gla}$2a, at basal conditions, but was increased upon-S1P stimulation, implying that this S1P effect depends on the congenic interval. Moreover, tyramine, which has vasodilatory properties, was increased in stimulated SHRSP compared to basal conditions, indicating potential relation of sphingosine signalling with BP-regulation.

This study has combined high-throughput proteomic and metabolomic screenings with congenic and transgenic strains to capture a clearer picture of the pathophysiological processes that underlie HTN in SHRSP. Individual metabolites and proteins or pathways and processes identified to be altered in HTN, through this work, can be used for generation of new testable hypothesis towards the development of new therapeutic approaches against HTN.

# 1 Introduction

## 1.1 Cardiovascular Disease

Cardiovascular disease (CVD) refers to a class of disorders associated with the heart and vascular system, including coronary artery disease (CAD), cerebrovascular disease, hypertension, peripheral vascular disease, heart and renal failure. In the modern world, it represents a major cause of morbidity and mortality. In 2008, CVD was the leading cause of deaths attributed to non-communicable diseases (NCD), accounting for 17.3 million deaths or approximately 47% of the NCD deaths, according to the World Health Organisation (WHO, 2012). The rapid rise in the mortality of CVD over the last decades can be attributed primarily to modifiable environmental risk factors, such as poor diet, tobacco use and physical inactivity (Yusuf et al., 2001). However, CVD is also known to have a large heritable component, classifying it as a complex and multifactorial disease (Kathiresan and Srivastava, 2012).

Hypertension (HTN) is considered one of the major contributors to the present pandemic of CVD (Levenson et al., 2002a, Carretero and Oparil, 2000). The WHO 2012 statistics-report highlights the growing problem of raised blood pressure, which exhibits a high frequency affecting almost one in three adults (WHO, 2012). The actual prevalence and absolute burden of HTN was 26.4% (972 million) in 2000 and was predicted to increase by 60% (1.56 billion) by 2025. Although the relative numbers of hypertensive adults were greater in economically developed countries, the rate of increase in incidence of HTN was almost 7 times higher in the developing world. Moreover, prevalence was similar between men and women and increased with age, consistently in all regions (Kearney et al., 2005). Despite advances in the prognosis and primary prevention of HTN, treatment remains poor (Vidt and Borazanian, 2003, Kumar et al., 2013). Therefore, there is a pressing need for better understanding of the pathophysiological mechanisms and genetics of HTN towards the improvement of public health and socioeconomic conditions.

### 1.1.1 Hypertension: Causality and Classification

Hypertension is a disease of large phenotypic variance, characterised by elevated blood pressure (BP). Diagnosis of HTN is made when patient's average systolic/diastolic blood pressure (SBP/DBP) is consistently 140/90 mmHg or greater, although risk varies even at levels below 140/90 mmHg (pre-hypertensive; 120-139/80-89 mmHg) (Kshirsagar et al., 2006). BP is a complex trait because of interplay between heritable components and environmental factors. Modifiable risk factors for increased BP include elevated body mass

index (obesity), insulin resistance, high alcohol / salt intake, smoking, sedentary lifestyle, stress and low potassium / calcium intake. Conversely, age, family history of CVD, gender and ethnicity belong to non-modifiable risk factors (Poulter, 2003). The prevalence of HTN increases with age, and above the age of 50 years systolic HTN represents the most common form of HTN (Chobanian et al., 2003). The occurrence of the disease changes with race, age, geographic patterns, gender and socioeconomic status. Critically, there is a strong positive and continuous correlation between systolic BP (SBP) and the risk of cardiovascular disease (CVD) (stroke, myocardial infarction, and heart failure), renal failure and mortality (Chobanian et al., 2003, Carretero and Oparil, 2000).

According to the causality, HTN is classified in primary and secondary. Primary or essential hypertension (EH) is the dominant form, which accounts for 90-95% of cases of HTN (Carretero and Oparil, 2000). It is a disorder of largely obscure aetiology with lifestyle, environmental and genetic (Pickering, 1955, Marteau et al., 2005) components implicated in the occurrence. On the other hand, secondary hypertension is the least common form of HTN and is caused by another pre-existing medical condition, such as renovascular disease, renal failure, aldosteronism or tumours (Carretero and Oparil, 2000).

## 1.1.2 Essential Hypertension

### 1.1.2.1 Genetic Regulation of EH

EH is a heterogeneous disorder, with different patients having different causal factors that lead to high BP. However, in most of EH cases the causes are not clear. Since its description as a polygenic trait (Pickering, 1955), EH genetic predisposition has been extensively reviewed (Franceschini and Le, 2013, Padmanabhan et al., 2012). There are also preliminary studies on epigenetic regulation of EH by DNA methylation, histone modifications and microRNAs (Udali et al., 2013).

Early mechanistic insights into pathways altered in BP homeostasis came from studies on human Mendelian forms of HTN. These syndromes are caused by mutations in single genes which have large effects on BP and exhibit an early onset hypertension. Most of the mutated genes identified, correspond to rare variants which are associated with impaired sodium re-absorption (Table 1-1) (Munroe et al., 2013).

**Table 1-1. Mendelian / monogenic forms of hypertension.**[1]

| Condition | Mode of Inheritance | Pathway / Process | Chr | Gene and Biological Effect | References |
|---|---|---|---|---|---|
| Pseudohypoaldosteronism type 2; familial hyperkalemic hypertension; Gordons syndrome | Autosomal dominant and autosomal recessive | Renal electrolyte balance | 12p13, 17q21, 5q31, 2q36 | ***WNK1*** Gain-of-function mutations ***WNK4, KLHL3*** and ***CUL3*** Loss-of-function mutations | Wilson FH, 2001; Boyden LM, 2012; Louis-Dit-Picard H, 2012 |
| Hypertension associated with PPARγ mutations | Autosomal dominant | Adipocyte differentiation (HTN, IR,T2DM) | 3p25 | ***PPARγ*** Loss-of-function mutations | Barroso I, 1999 |
| Hypertension exacerbated by pregnancy | Autosomal dominant | Renal electrolyte balance | 4q31 | ***NR3C2*** Missense, loss-of-function mutation | Geller DS, 2000 |
| Familial hyperaldosteronism type 1; Glucocorticoid-remediable aldosteronism (GRA) | Autosomal dominant | Steroid / aldosterone synthesis | 8q24 | ***CYP11B1/CYP11B2*** chimeric gene | Lifton RP, 1999 |
| Congenital adrenal hyperplasia with CYP11B1 deficiency | Autosomal recessive | Steroid / aldosterone synthesis | 8q24 | ***CYP11B1*** Enzymatic defect mutation | White PC, 1991 |
| Corticosterone methyloxidase II deficiency | Autosomal recessive | Steroid / aldosterone synthesis | 8q24 | ***CYP11B2*** Enzymatic defect mutation | Pascoe L, 1992 |
| Congenital adrenal hyperplasia with CYP17A1 deficiency | Autosomal recessive | Steroid / aldosterone synthesis | 10q24 | ***CYP17A1*** Enzymatic defect mutation | Kagimoto M, 1988 |
| Hypertension and brachydactyly | Autosomal dominant | Sympathetic system | 12p12 | Unknown Inversion, deletion and reinsertion at 12p12.2 -p11.2 | Schuster H, 1996 |
| Apparent mineralocorticoid excess | Autosomal recessive | Steroid / aldosterone synthesis | 16p12 | ***HSD11B2*** Loss-of-function mutations | Stewart PM, 1996 |
| Liddle syndrome | Autosomal dominant | Renal electrolyte balance | 12p13, 16p12 | ***SCNN1B, SCNN1G*** Premature-stop-codon mutation | Shimkets RA, 1994 |

[1] Table 1-1 summarises main features of Mendelian forms of HTN, causative genes and processes affected. *WNK1/4*: lysine deficient protein kinase 1/4; *KLHL3*: Kelch-like protein 3; *CUL3*: cullin 3; *PPARγ*: peroxisome proliferator-activated receptor gamma; *NR3C2*: mineralocorticoid receptor; *CYP11B1*: 11β hydroxylase; *CYP11B2*: aldosterone synthase; *CYP17A1*: 17α hydroxylase; *HSD11B2*: 11β-hydroxysteroid dehydrogenase; *SCNN1B/G*: sodium channel nonvoltage-gated 1, β and γ subunits; IR: insulin resistance; *T2DM*: Type II diabetes mellitus; Chr: chromosome.

Recent advances in high-throughput genomic approaches have allowed more robust identification of genetic determinants of EH and BP. Human candidate genes studies have identified more than 110 genes to be potentially implicated in EH, such as angiotensin I converting enzyme (*ACE*), and nitric oxide synthase 3 (*NOS3*) genes (Benjafield and Morris, 2000, Bedir et al., 1999). However, the results were difficult to replicate, frequently due to poor study design or SNP (single nucleotide polymorphisms) coverage. Such studies analyse allelic frequencies of genetic markers (SNPs), tandem oligo-nucleotide repeats or gene copy number on a set of potential candidate genes, in patients and healthy individuals. Further, genetic linkage studies have identified susceptibility loci for EH and BP in every human chromosome so far (Cowley, 2006). This approach analyses the frequency by which adjacent SNPs/alleles are inherited with the trait of interest, while further fine mapping narrows down the genomic region of interest and identifies new genetic biomarkers. Several genetic linkage studies on human populations of different ethnicities have repeatedly associated the long arm of chromosome 2 (Chr.2q) with BP/EH regulation (Caulfield et al., 2003, Mocci et al., 2009, Rao et al., 2003). However, such approaches have been challenging due to the polygenic nature of BP regulation. This issue has been tackled by large-scale, genome-wide association studies (GWAS) (Table 1-2), which, over the past few years, have accelerated the current understanding of the genetic architecture of BP and EH. GWAS investigate dense sets of single nucleotide polymorphisms (SNP) with allele frequency greater than 5% in a population, located throughout the genome and their association with complex polygenic traits. In humans, common genetic biomarkers for EH/BP have been reported in 29 loci, by identifying SNPs within or between genes as in the case of *ATP2B1* (intron; (Levy et al., 2009)), *NPR3 - C5orf23* (intergenic; (Ehret, 2011)) and in regulatory regions as in the promoter region of *UMOD* (Padmanabhan et al., 2010) and *NOS3* (Salvi et al., 2012).

However, the reported genetic biomarkers represent, collectively, only a small fraction of BP heritability and have small size effects that do not explain BP phenotypic variance. Molecular and functional dissection of novel variants, using more detailed low-throughput analytical methods along with pathway analysis and in combination with advanced mapping (genome exon sequencing) and epigenetic studies may shed light into the aetiology of human EH (Padmanabhan et al., 2012). For example, in the case of *UMOD*, studies in transgenic mice homozygous for *UMOD* promoter risk variants demonstrated salt-sensitive hypertension and renal lesions, similar to those observed in homozygous individuals (Trudu et al., 2013).

**Table 1-2. Genetic loci associated with BP and/or hypertension identified in genome-wide association studies (GWAS). The loci are listed in chromosomal order.** [2]

| Locus | Chr | GWAS | Process / Pathway ; *Monogenic Syndrome* |
|---|---|---|---|
| ***M THFR (NPPA, NPPB)*** | 1p36.2 | CHARGE, GBPG, AGEN, ICBP, Gene-centric | Renal electrolyte balance |
| ***AGT*** | 1q42.2 | Gene-centric | Renal electrolyte balance, Vascular function |
| ***ULK4*** | | GBPG | |
| ***MECOM (MDS1)*** | 3q26.2 | GBPG, ICBP | |
| ***FGF5*** | 4q21.2 | GBPG, ICBP, AGEN | Angiogenesis |
| ***NPR3*** | 5p13.3 | ICBP, AGEN, Gene-centric | Renal electrolyte balance |
| ***HFE*** | 6p22.2 | ICBP, Gene-centric | *Hemochromatosis* |
| ***NOS3*** | 7q36.1 | HYPERGENES, Gene-centric | Endothelial function; *Pregnancy-induced HTN* |
| ***CACNB2*** | 10p12.3 | CHARGE, ICBP | ? Vascular / cardiac function |
| ***CYP17A1*** | 10q24.3 | CHARGE, GBPG, AGEN-BP, ICBP | Steroid/aldosterone synthesis; *17a-hydroxylase and/or 17,20-lyase deficiency* |
| ***PLEKHA7*** | 11p15.1 | CHARGE, ICBP | |
| ***SOX6*** | 11p15.2 | Gene-centric | Transcription |
| ***LSP1/TNNT3*** | 11p15.5 | Gene-centric | ? Endothelial function |
| ***ATP2B1*** | 12q21.3 | CHARGE, GBPG, AGEN, ICBP, Gene-centric | ? Vascular function |
| ***SH2B3*** | 12q24.1 | CHARGE, GBPG, ICBP | ? Endothelial function |
| ***TBX5-TBX3*** | 12q24.2 | CHARGE, ICBP | Development |
| ***CSK*** | 15q24.1 | CHARGE, GBPG, AGEN-BP, ICBP | Vascular function |
| ***UMOD*** | 16p12.3 | BP-extremes | ? Renal electrolyte balance, ? Renal function |
| ***ZNF652*** | 17q21.3 | GBPG, AGEN-BP, ICBP | |
| ***GNAS-EDN3*** | 20q13 | GBPG, ICBP | Vascular function |

[2] GWAS studies: CHARGE (Levy et al., 2009); GBPG (Newton-Cheh et al., 2009); AGEN-BP (Kato et al., 2011); ICBP (Ehret et al., 2011); Gene-centric (Johnson et al., 2011); BP-extremes (Padmanabhan et aal. 2010). *MTHFR*: methylene-tetrahydrofolate reductase; *NPPA*: atrial natriuretic peptide; *NPPB*: brain natriuretic peptide; *AGT*: angiotensinogen; *ULK4*: serine/threonine-protein kinase ULK4; *MECOM (MDS1)*: myelodysplasia syndrome protein 1; *FGF5*: fibroblast growth factor 5; *NPR3*: natriuretic peptide clearance receptor; *HFE*: human hemochromatosis protein; *NOS3*: nitric oxide synthase 3; *CACNB2*: voltage-dependent calcium channel B2 subunit; *CYP17A1*: cytochrome p450; *PLEKHA7*: plextrin-homology domain-containing family A member 7*; SOX6*: sex determining region y (SRY)-box 6; *LSP1/TNNT3*: leukocyte-specific protein 1 / troponin T type 3; *ATP2B1*: calcium/calmodulin-dependent ATPase isoform 1; *SH2B3*: lymphocyte-spesific adapter protein; *TBX5, TBX3*: T-box family genes; *CSK*: cytoplasmic tyrosine kinase; *UMOD*: uromodulin; *ZNF652*: zinc-finger protein 652; *GNAS*: guanine nucleotide binding protein, a-subunit stimulating; *EDN3*: endothelin 3.

#### 1.1.2.2 Salt Sensitivity

High salt intake is a major dietary risk factor contributing to EH with approximately one half of essential hypertensive patients demonstrating salt sensitivity. This chronic condition is characterised by exaggerated responses to changes in salt balance due to alteration of kidney function. Sodium retention, extracellular volume (ECV) expansion, increase of cardiac output and increased peripheral vascular resistance are some of the characteristic high salt-intake phenotypes that lead to elevation of SBP.

Salt sensitivity was arbitrarily classified by Weinberger et al. (Weinberger et al., 1986) as a difference of ≥10 mmHg in SBP between salt-loaded (2L of saline over 4h) and salt-depleted (10mmol sodium diet per day, plus oral furosemide) states and salt-resistance as a difference of ≤5 mmHg. Salt-sensitive patients exhibit a significantly reduced capacity to restore sodium balance, after increased salt intake, due to impaired pressure-natriuresis relationship (Luft et al., 1986, Rodriguez-Iturbe and Vaziri, 2007). The implication of genetic factors has been demonstrated in humans (Mei et al., 2012, Svetkey et al., 1996). A number of mutations have been found in genes implicated in BP regulation, by encoding for proteins that alter renal salt re-absorption in kidney. Specifically, the mutations affected circulation of mineralocorticoid hormones, renal ion channels and transporters and the mineralocorticoid receptor, causing Mendelian forms of hypertension and hypotension (Lifton et al., 2001). In addition, several genetic polymorphisms (SNPs) related to impaired sodium excretion, have been localised in quantitative trait loci (QTL) for salt sensitivity in genetic rat models (Johnson et al., 2009, Yagil et al., 2003). Other processes which have been associated with salt sensitivity include altered activity of neurohormonal systems, renal inflammation and oxidative stress (Laffer et al., 2006, Manning et al., 2005, Beeks et al., 2004). Salt sensitivity, apart from enhancing susceptibility to renal damage, is considered a major contributor to overall cardiovascular risk.

## 1.2 Blood Pressure Regulation

Circulation is a vital and highly regulated physiological function responsible for transportation of molecules (e.g. gases, nutrients and metabolism (by-)products) in the organism, across cells and organ tissues. The heart must pump against a variety of vascular beds (blood vessels) to transport blood to the organs, before it eventually returns to the heart via the veins, by flowing from areas of high to areas of low hydrostatic pressure. The force driving blood flow in the circulatory system is the mean arterial pressure (MAP), which is the result of the cardiac output (CO) multiplied by the total peripheral vascular resistance (TPR). CO represents the blood volume pumped by each heart ventricle per minute (~5.0 L/min) and depends on the heart rate and the amount of blood pumped from each ventricle per pulse (stroke volume). TPR is influenced by the individual resistance in each vessel, which is predominantly determined by the lumen diameter (Di). The Di is controlled by a number of physiological and neurohormonal mechanisms to maintain a normal MAP in the system (Vander, 2001a).

The kidney is a major organ involved in MAP regulation by controlling the blood volume and the myogenic tone (the vessel's physiological contractile tension relative to maximally dilated state) in the circulatory system. In response to decreases in sodium or BP, kidney produces renin, which acts through the renin-angiotensin-aldosterone system (RAAS) to cause sodium re-absorption, water retention and vasoconstriction, promoting an increase in BP (Vander, 2001b).

The autonomic nervous system can also regulate MAP through rapid activation of the sympathetic nervous system. Changes in BP are sensed by the baroreceptors in the vessels, which via signals to the vasomotor centre trigger secretion of hormones that affect the myogenic tone (a adrenoreceptors) and heart rate (β adrenoreceptors) to restore normal MAP (Julius, 1993).

Large vessels do not play significant role in TPR, and therefore MAP regulation, due to increased diameter and elasticity (compliance; $\delta V/\delta P$). On the contrary, TPR is primarily controlled by the microcirculation, the part of vasculature that is more sensitive to pressure-dependent diameter regulation, and consists of small arteries, pre-capillary arterioles, capillaries and venules, as well as elements of the lymphatic system (lymphatic capillaries and thoracic ducts). Increased resistance of these vessels, due to narrow Di and slow blood

flow as a result of the high total cross sectional area (CSA), lowers the MAP, under normal conditions (Figure 1-1) (Vander, 2001a).

In pathological conditions, including HTN, there is normally a disturbance in the CO or/and TPR.

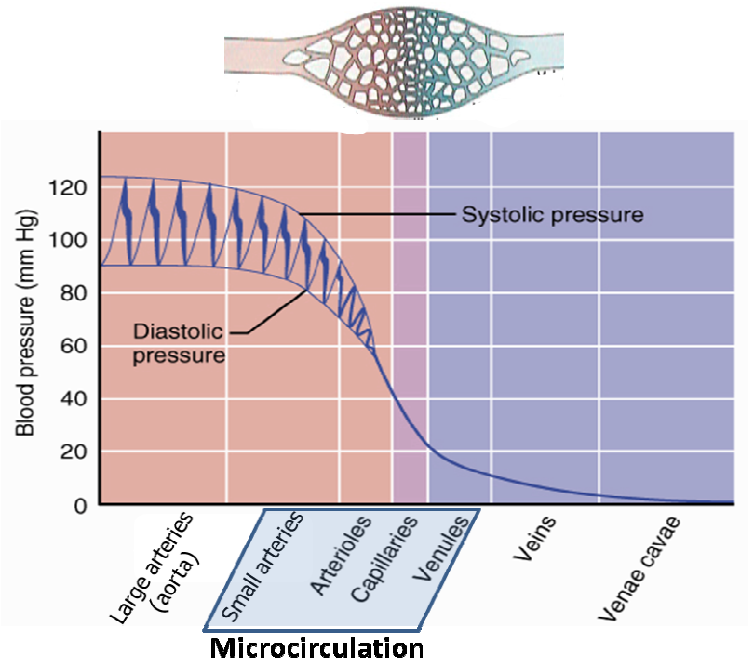


**Figure 1-1 - Systolic and diastolic blood pressures in the vascular system. The large drop in blood pressure is caused by the resistance vasculature (microcirculation), characterised by narrow lumen diameter and slow blood flow as a result of increased total cross sectional area (Adapted from Purves et al., Life: The Science of Biology, 4th Edition).**

## 1.2.1 Small Resistance Arteries in HTN

HTN is characterised by sustained increase in TPR, caused predominantly by pathological narrowing of small arteries (Di: 100-300μm) and precapillary arterioles (Di <100μm), which are considered a continuum rather distinct sites of resistance control (le Noble et al., 1998). This is evidenced by a large drop in BP across these vessels, which predicts a high resistance during HTN (Borders and Granger, 1986, Bohlen, 1986) (Figure 1-1). The lumen narrowing, observed in small arteries of both hypertensive animals (Briones et al., 2003, Arribas et al., 1997, Mulvany, 1988) and humans (Schiffrin, 1999, Rizzoni et al., 2003), is attributed to structural and functional alterations (Mulvany and Aalkjaer, 1990). Changes in structure of small resistance arteries, known as vascular remodelling, seem to be the result of abnormal organisation of extracellular material and have been significantly associated with the occurrence of cardiovascular events, including EH (Aalkjaer et al., 1987, Mathiassen et al., 2007, Muiesan et al., 2002). They have also been suggested to represent the most common and early form of target organ damage in human (Park and Schiffrin, 2001).

In addition, functional alterations refer, mainly, to impaired endothelial function and subsequent changes in the myogenic tone and Di, which are tonically modulated by endothelium-derived factors. Impaired endothelium-dependent responses in the resistance vasculature have been well documented in EH patients (Panza et al., 1990, Rossi et al., 1997, Taddei et al., 1992) and animal models (Ito and Carretero, 1992, Tuncer and Vanhoutte, 1993).

### 1.2.1.1 Vascular Smooth Muscle and Remodelling in HTN

In the arterial wall, the smooth muscle (SM) layer consists of vascular smooth muscle cells (VSMCs) in a matrix of collagen and elastin fibres and is known as *tunica media*. Depending on the vessel type, SM appears to be of variable thickness with the exception of capillary vessels, which consist only from endothelium. In response to physiological or chemical signals, SM can rapidly adapt its structural design to regulate the lumen diameter (Di) and meet vessel's functional demands.

It has been demonstrated that in EH patients and animal models the structure of small resistance arteries is abnormal, characterised by reduced Di and increased wall thickness to Di ratio (wall : lumen ratio), without change in wall mass (Aalkjaer et al., 1987, Rizzoni et al., 2003, Briones et al., 2003, Arribas et al., 1997). The mechanisms leading to such

abnormalities are not fully understood. Wall stress-induced changes in extracellular matrix proteins and neurohormonal environment as well as ROS have been suggested as potential mechanisms playing an important role (Lee et al., 1995, Touyz et al., 2003). The altered structure is considered to be the result of abnormal elastin and collagen re-arrangement in the vessel wall, rather than SM growth, known as inward eutrophic remodelling (Briones et al., 2003, Arribas et al., 1997, Mulvany, 1988).

Although structural changes in small arteries have been related to long-term elevated BP (Folkow, 1958), it is unclear whether remodelling is the cause or consequence of increased BP. Experiments in rats made hypertensive (Goldblatt technique) suggest that the remodelling is adaptive to increased BP (Deng and Schiffrin, 1991). On the contrary, increased media:lumen ratio has been observed in mesenteric resistance arteries (MRA) from rats (SHR) at a pre-hypertensive stage (Rizzoni et al., 1994). However, recent studies in humans show strong correlation between small artery remodelling and TPR, proposing that the structural changes are the result of myogenic tone rather than of pressure (Mathiassen et al., 2007). Such changes have, in turn, a positive feedback on TPR and BP.

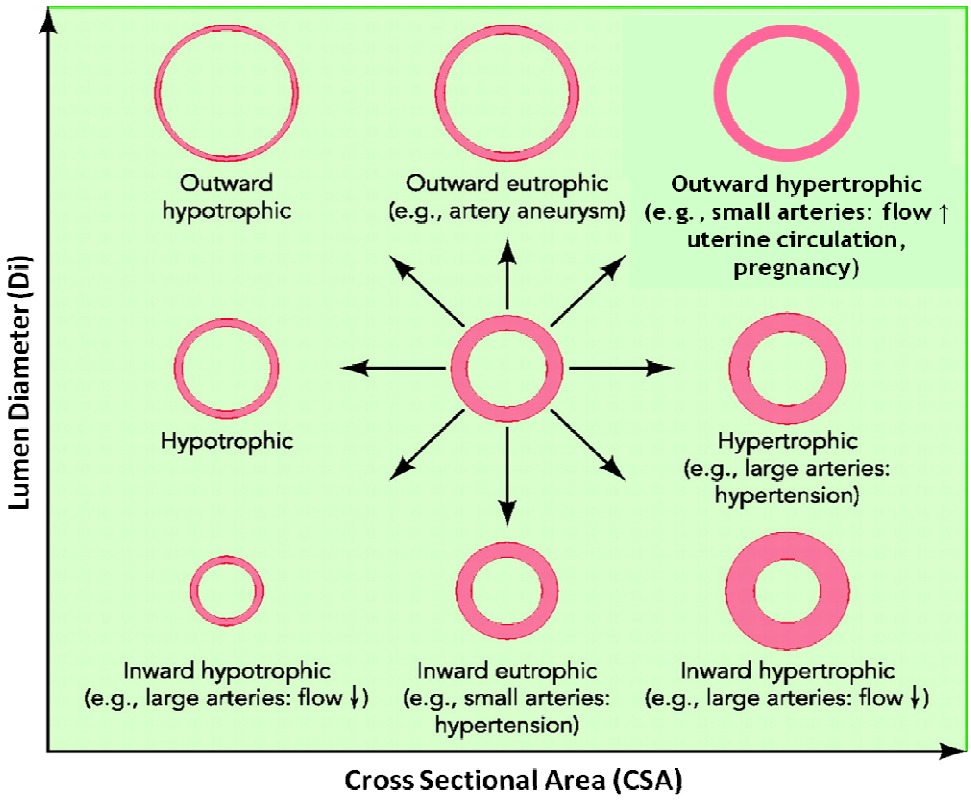


**Figure 1-2 - Vascular remodelling. Structural changes in the vascular smooth muscle are reflected as changes in the cross sectional area (CSA) and lumen diameter (Di) of the vessel. The relationship between CSA - Di determines the type of remodelling in small and large arteries. (Adapted from Mulvany et al., 1996)**

#### 1.2.1.2 Vascular Endothelium and Endothelial Dysfunction in HTN

The luminal surface of the entire cardiovascular system, from heart to capillary vessels, is lined by a monolayer of endothelial cells, the vascular endothelium or *tunica intima*. Apart from being a natural semi-selective barrier between circulating blood and tissue, the role of endothelium further expands into maintaining the balance between vasodilatation and vasoconstriction (myogenic tone), proliferation and migration of VSMCs (angiogenesis, SM growth, vascular remodelling) and thrombogenesis and fibrinolysis (inflammatory responses, coagulation) (Davignon and Ganz, 2004).

Upon exposure to mechanical or chemical stimuli, endothelial cells synthesise and secrete a variety of vasoactive factors (Félétou and Vanhoutte, 2006), which act primarily on the underlying SM to modulate myogenic tone and thereby vascular resistance. Vasodilators such as nitric oxide (NO), endothelium-derived hyper-polarisation factors (EDHF) and prostacyclin ($PGI_2$) increase vessel diameter and decrease resistance. The exact opposite effect is introduced by vasoconstrictors, including endothelin-1 (ET-1), angiotensin II (Ang II), prostanoids and reactive oxygen species (ROS) (Félétou and Vanhoutte, 2006, Vanhoutte et al., 2005). The relative contribution of each vasoactive mediator to endothelium-dependent responses varies according to the vessel size, the specific vascular bed, and the animal species. The mechanisms of action of these factors are discussed below and illustrated in Figure 1-3.

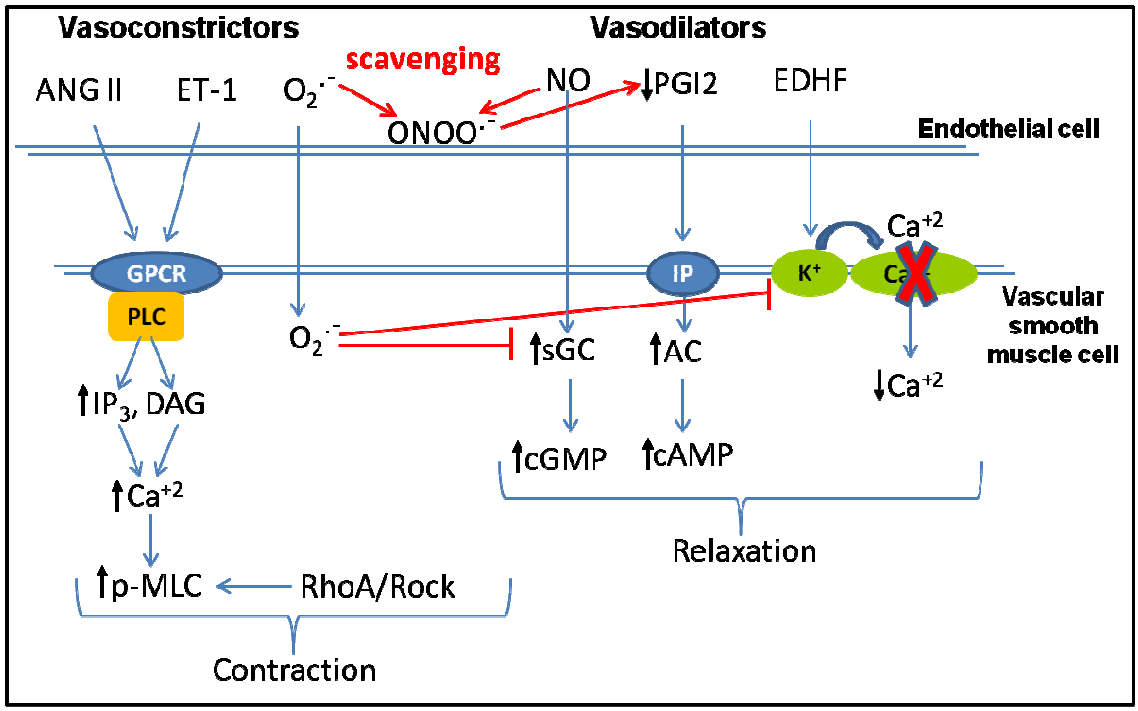


**Figure 1-3 - Endothelium-mediated contraction and relaxation in the smooth muscle. Vasoconstrictors and vasodilators released from endothelium upon stimulation, act on the smooth muscle through G-protein coupled receptors (GPCR), diffusion or membrane hyperpolarisation to cause contractile or vasodilatory responses, respectively. AngII, angiotensin II; ET-1, endothelin-1; $O_2^{\cdot -}$, superoxide; $ONOO^{\cdot -}$, peroxynitrate; NO, nitric oxide; PGI2, prostacyclin; EDHF, endothelium-derived hyperpolarisation factor; PLC, phospholipase C; IP3, inositol triphosphate; DAG, diacyloglycerol; $Ca^{+2}$, calcium; p-MLC, phosphorylated myosin light chain; Rock, Rho kinase; sGC, soluble guanyl cyclase; AC, adenyl cyclase; cGMP, cyclic guanosine monophosphate; cAMP, cyclic adenosin monophosphate; arrows indicate increased / decreased levels.**

The major regulator of cardiovascular homeostasis is considered to be NO, since apart from mediating vascular relaxation it also protects vascular wall from coagulation of blood and inflammatory responses leading to atherosclerosis (Harrison et al., 2010, Kubo-Inoue et al., 2002). Moreover, NO is known as the gate-keeper of endothelial function since it controls the production/action of other endothelium-derived mediators, including EDHF and ET-1 (Feletou et al., 2008). Its vasodilatory effects are predominantly exerted through stimulation of the soluble guanylyl cyclase (sGC) in the VSMCs and subsequent production of cyclic-GMP (Hobbs, 1997). In a similar manner, $PGI_2$ promotes SM relaxation by activating adenyl cyclase (AC) in the VSMCs, followed by generation of cyclic-AMP (Holzmann et al., 1980). On the contrary, the identity of EDHF is still not known. Several molecules have been proposed to complement the vasodilatory actions of NO and $PGI_2$, by causing membrane hyperpolarisation (opening of potassium channels) of VSMCs resulting in closure of voltage-

gated calcium channels (Feletou and Vanhoutte, 2009). C-type natriuretic peptide (CNP) has been identified as a potential EDHF, highly associated with regulation of relaxation in small resistance arteries (Barton et al., 1998, Chauhan et al., 2003, Steinmetz et al., 2004).

In the case of vasoconstrictors, peptides such as AngII and ET-1 exert their effects upon binding to a G-protein coupled receptor (GPCR) on the VSMC membrane. Regardless of the stimuli, the cellular mechanism leading to constriction involves initial elevation of cytosolic $Ca^{2+}$ levels, through efflux of extracellular $Ca^{2+}$ and release of intracellular $Ca^{2+}$ from sarcoplasmic reticulum. Subsequently, $Ca^{2+}$/calmodulin complex induces activation of myosin by the myosin light chain kinase (MLCK), to promote contraction. Contraction is further maintained by $Ca^{2+}$-sensitisation signalling, in which RhoA small G protein and its downstream effector, Rho kinase (RhoA/Rock) prevent activation of myosin light chain phosphatase (MLCP) (Webb, 2003, Wynne et al., 2009). On the other hand, ROS, superoxide anion ($O_2^-$) in particular, induce contraction mainly by increasing $Ca^{2+}$ mobilisation or sensitisation, direct depolarisation of the cell membrane or activation of endothelial enzymes which produce endothelium-derived contracting factors (EDCFs) (Jin et al., 1991, Tang et al., 2004, Vanhoutte et al., 2005).

#### *1.2.1.2.1 Endothelial Dysfunction*

Under physiological conditions release of endothelium-derived vasodilators predominate to maintain a normal vascular tone. Sustained shift of the equilibrium towards generation of endothelium-derived contracting factors (EDCF) results in endothelial dysfunction (Abdel-Sayed et al., 2003). In general, endothelial dysfunction is characterised by impaired endothelium-dependent relaxation of the SM to vasodilators such as acetylcholine, bradykinin and calcium ionophore. The reduced sensitivity of the vessel to such factors results from altered production and/or action of endothelium-derived vasodilators. Altered endothelial function is considered the hallmark in almost all forms of CVD (Félétou and Vanhoutte, 2006, Widlansky et al., 2003), including hypertension (Grunfeld et al., 1995, Potenza et al., 2005, Treasure et al., 1993), atherosclerosis (Ludmer et al., 1986, Kawashima and Yokoyama, 2004), CAD (Chan et al., 2003) and heart failure (Heitzer et al., 2005). Endothelial dysfunction has been shown to occur in small resistance arteries from both EH patients and animal models of HTN.

The mechanisms underlying endothelial dysfunction vary, depending on pathological, physiological and non-modifiable risk factors such as age and gender. In HTN, the impairment has been attributed to reduced synthesis and release of NO (Taddei et al., 1999,

Panza et al., 1993), and EDHF (Goto et al., 2004, Onaka et al., 1998) , or increased release of EDCFs (Luscher and Vanhoutte, 1986, Vanhoutte and Tang, 2008). It is still unclear whether endothelial dysfunction is a predictor, a risk factor or an end point of HTN, although it has been shown to precede establishment of high BP in young normotensive offspring of EH parents (Taddei et al., 1996). Moreover, inconsistent effects of antihypertensive drugs on endothelial function, despite correction of BP levels (Ghiadoni et al., 2012), further support the notion that endothelial dysfunction may be a primary event to BP increase.

An increasing body of evidence reveals oxidative stress as the common denominator of endothelial dysfunction in CVD, including EH (Griendling and FitzGerald, 2003a, Griendling and FitzGerald, 2003b). Oxidative stress occurs upon increased ROS production or reduced ability to scavenge ROS and/or impaired antioxidant activity (Touyz and Schiffrin, 2004). ROS have been involved in the inhibition of the three major endothelium-dependent vasodilatation pathways, i.e. NO, EDHF and $PGI_2$, by reducing NO bioavailability, inactivating NO and $PGI_2$ synthases or inhibiting sGC and decreasing the activity of channels implicated in the EDHF-mediated relaxation (Münzel et al., 2005, Zou et al., 2004, Liu et al., 2006, Kusama et al., 2005). Furthermore, ROS are known to induce VSMC contraction, as mentioned above (Félétou and Vanhoutte, 2006). It is still not clear whether vascular oxidative stress causes HTN in human, as only few antioxidant approaches have demonstrated improvement of endothelial function (Mistry et al., 2008, Duffy et al., 2001, Hamilton et al., 2002) as opposed to rat models of HTN (Hamilton et al., 2002, Graham et al., 2009, Savoia et al., 2006, Fennell et al., 2002). Furthermore, oxidative stress has been shown to precede the establishment of high BP in SHR rats (Nabha et al., 2005).

### 1.2.2 Treatments in HTN

Despite the extensive research in the battle against HTN, no treatment able to correct for all of the increased BP levels, oxidative stress and endothelial dysfunction has been found, to date. For improvement of HTN a selection of antihypertensive drugs is being used according to the individual's cardiovascular profile (BP readings, cardiovascular risk) and their response to the therapy (Mathiassen et al., 2007).

Traditionally, diuretics have been used as first line treatment to increase water and sodium excretion with subsequent reduction in CO and minor change of TPR (Shah, Littler 2004). Likewise, antagonists of β-adrenergic receptors (β-blockers) exert their therapeutic effects by lowering CO, but have no effect on endothelial function (Taddei et al., 2001). Calcium channel blockers improve endothelial function (Taddei et al., 2001), decrease contraction of the SM and consequently the TPR, however, they have been related to high risk of myocardial infarction. Blockers of AngII II receptors (ARB) or of its converting enzyme (ACE) increase dilatation of small arteries, leading to reduced TPR, without improving endothelial function (Schiffrin, 1998, Taddei et al., 1998). Antagonists of α-adrenergic receptors (α-blockers), which are less commonly used, decrease contraction of muscle fibres in the small arteries and hence the TPR. Finally, combination therapies, using more than one, are applied in the majority of cases, such as renin–angiotensin system inhibitors and calcium channel blockers, or renin–angiotensin system inhibitors and diuretics (Daskalopoulou et al., 2012, Frank, 2008). However, none of the modern therapies seem to have consistently long-term effects in lowering the pressure of EH patients. Unfortunately, their effects have not been assessed on TPR or small artery structure (Mulvany, 2012). It has been shown that therapies using substances with vasodilatory effects (Ca antagonists, ACE inhibitors, and receptor blockers (ARB)) can normalise small vessel structure, whereas beta-blocker treatments do not reduce TPR (Buus et al., 2004) and therefore do not correct the abnormal structure (Mathiassen et al., 2007, Agabiti-Rosei et al., 2009). Hence, treatment of HTN which focuses only on BP regulation could correct large artery and LV morphology, whereas for the normalisation of the crucial small resistance vessels structure vasodilator therapies are required (Mulvany, 2005, Mulvany, 2012, Schiffrin, 2010).

Apart from prescription of antihypertensive drugs, preventative lifestyles changes are essential in order to control BP levels and lower the risk of CVD and renal damage (Daskalopoulou et al., 2012).

## 1.3 HTN in Rats

The use of experimental animal models in studies of human diseases has been vital to the understanding of their pathophysiology. Using in-bred animal models ensures increased genetic homogeneity, reduced environmental effect through standardised housing criteria, and allows for controlled mating between diseased and healthy animals for linkage analysis (Graham et al., 2005).

Due to clear pathogenic (genetic, biochemical and physiological) similarity with humans, rodent models are extensively used in the investigation of the genetic, cellular and molecular basis of CVD in order to gain a better understanding of the long-term BP regulation. The rat, mouse and human genomes encode for a similar number of genes and almost all human genes have corresponding orthologues in the rat genome (Rat Genome Sequencing Project Consortium; 2004). Moreover, rodents are ideal experimental models in the drug research and testing due to their small size, short breeding time and simple husbandry.

Despite mice being the major model for mammalian genetic studies and manipulations, it is not the most appropriate model of human CVD, due to their small size and increased heart rate. On the contrary, rats have been widely bred to provide an animal model of human EH, due to their higher pathophysiological similarity to the human condition, as well as their bigger size which makes them more amenable to handling (Rapp, 2000).

### 1.3.1 Rat Models of HTN and Salt Disease

Most of the rat experimental models of HTN were developed from either Wistar-related or Sprague-Dawley stock, which share a common origin, using selective inbreeding, surgery, diet or drug treatment to induce HTN. A phylogenetic tree of 28 inbred laboratory rat strains used in the study of complex diseases, including HTN, has been generated recently, following their genome sequencing (Figure 1-4) (Atanur et al., 2013).

An example of a genetic model of HTN is the Dahl salt-sensitive (S) and salt-resistant (R) rats, which were bred on the basis of their BP after being fed a high salt diet (8% NaCl). On the other hand, genetically hypertensive rats (GH) and spontaneously hypertensive rats (SHR) are two models developed by rats selectively bred for high BP without any dietary or environmental stimuli. Rats with surgery-induced HTN include the Goldblatt model of renovascular HTN, in which one or both renal arteries have been constricted by use of a

small adjustable clamp (Goldblatt et al., 1934). Sabra HTN prone (SBH) and resistant (SBN) strains were selectively bred according to the response of BP to unilateral nephrectomy, treatment with deoxycorticosterone acetate and 1% NaCl to drink. Several rat hypertensive models have been generated using specific diet or drug treatments, such as high salt / fat / sugar diets, chronic inhibition of NO and chronic infusion of AngII. Despite the common genetic origin of the above strains, the genetic diversity amongst them is substantial and comparable to the divergence between unrelated humans (Doggrell and Brown, 1998, Dornas and Silva, 2011).

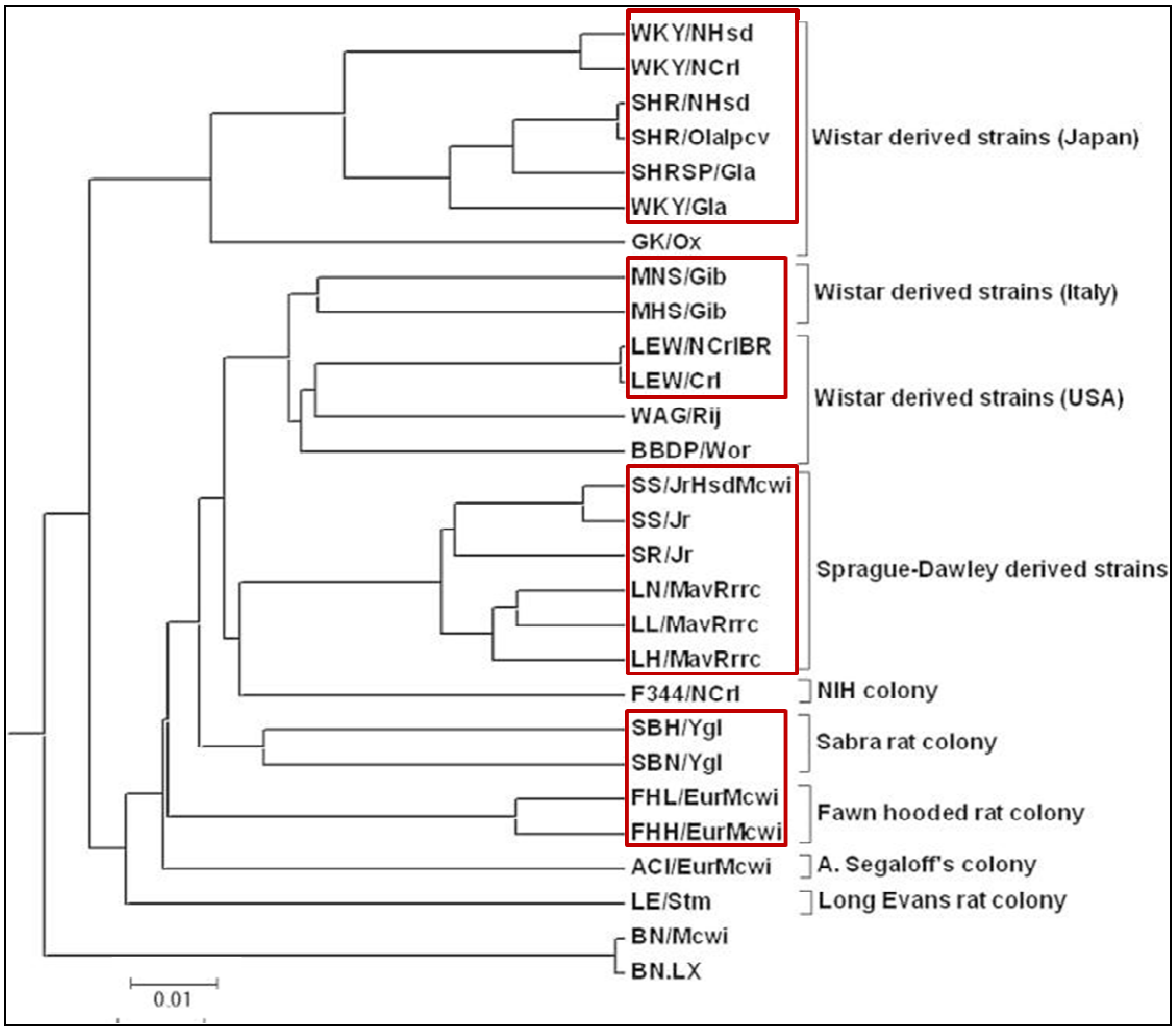


**Figure 1-4 - Phylogenetic tree of inbred experimental rat models used in studies of complex human diseases, including hypertension, diabetes and insulin resistance. The scale represents genetic distance based on whole genome comparisons, using Brown Norway (BN/Mcwi) as the reference strain (Atanur et al., 2013).**

### 1.3.2 The Stroke-Prone Spontaneously Hypertensive Rat (SHRSP)

The most commonly studied SHR is a breed established in the early '60s (1963), at the University of Kyoto, from Wistar-Kyoto (WKY) normotensive male with elevated BP mated to female with slightly elevated BP (Okamoto and Aoki, 1963). Further selective inbreeding of SHR more susceptible to stroke led to development of an SHR sub-strain, the stroke-prone SHR (SHRSP) (1974) (Yamori and Okamoto, 1974). The SHRSP spontaneously develops cerebral stroke as well as severe hypertension (>200 mmHg) early in life. The onset of spontaneous HTN is between 8 and 12 weeks of age and its magnitude is closely related to the incidence of stroke. SHRSP also exhibit sexual dimorphism, characterised by more pronounced HTN in male than in female animals. At 16 weeks of age, SBP reaches approximately 180 mmHg in male compared to 150 mmHg in females. Divergence in SBP between individual SHRSP colonies is observed, considering different husbandry regimes and criteria for selecting breeding pairs. Further hypertensive phenotypes and end organ damage exhibited by SHRSP include salt-sensitivity, proteinuria, left ventricular hypertrophy, and endothelial dysfunction (Yamori and Okamoto, 1974, Ohtaka, 1980, Tesfamariam and Halpern, 1988).

Because of the similarity in the pathophysiolology of stroke and EH between this strain and humans (Rapp, 2000), SHRSP is one of the most utilised experimental models for studying development, prognosis and treatment of EH, as well as interactions between genetics and environment. Its wide use in the genetic study of HTN involves genetic manipulations via generation of congenic (chromosomal segment replacement) and consomic (whole chromosome replacement) strains. Hilbert *et al.* (Hilbert et al., 1991) at the same time with Jacob *et al.* (Jacob et al., 1991) were the first to generate congenic strains of crosses between SHRSP and the normotensive control Wistar-Kyoto (WKY) in genetic linkage studies, aiming to locate candidate genes that regulate the quantitative trait of EH. However, SHRSP fail to display every phenotype of human EH. It is known that this strain do not exhibit spontaneous heart failure. Moreover, rats do not develop spontaneous atherosclerosis due to their plasma profile of high HDL levels (Fernandez et al., 1999) and absence of cholesteryl ester transfer protein (CETP) (Guyard-Dangremont et al., 1998), as well as their increased ability to convert cholesterol to bile acids (Horton et al., 1995).

SHRSP and WKY rats have been bred in Glasgow since September 1991. Integrity of colonies and hypertensive phenotype are ensured through selective mating of male SHRSP with SBP of 170-190 mmHg and female animals with SBP of 130-150 mmHg, measured by

tail cuff. Offspring start to develop HTN at 6-8 weeks of age and by 12-16 weeks they exhibit baseline SBP of 187 mmHg, compared to 134 mmHg for age-matched WKY (Figure 1-5A) (Graham et al., 2007, Koh-Tan et al., 2009). Consomic and congenic strains have been constructed and utilised in genome-wide linkage studies to identify candidate genes for BP regulation and salt-sensitivity, in SHRSP (Clark et al., 1996, McBride et al., 2003).

### 1.3.3 Congenic Strains in Genetic Screenings

Congenic strains are constructed by selective replacement of a chromosomal region closely linked to genes and other genetic elements, underlying a particular polygenic trait (e.g. EH) in the recipient strain, with the homologous region from the donor strain. Such regions of interest are known as quantitative trait loci (QTL). For identification of candidate genes underlying a trait, QTLs are the first to be determined via genome wide linkage scan by use of microsatellite markers. Subsequent generation of congenic and consomic strains verifies the existence of the QTL. Further breeding produces smaller congenic substrains, carrying a reduced size of the implicated chromosomal region for gene identification (Zhang et al., 1997). Finally genome-wide microarray expression profiling allows for identification of differentially expressed, candidate genes. In SHRSP, QTLs associated with BP regulation and salt-sensitivity have been identified on chromosomes 2, 3 and 14 (Clark et al., 1996, McBride et al., 2005, McBride et al., 2003). Moreover, construction of reciprocal congenic stains has previously been used in the genetic dissection of a BP QTL on rat chromosomes 1, 8, 9 and 13 (Clemitson et al., 2007, Zhang et al., 1997, Kumarasamy et al., 2011, Ariyarajah et al., 2004)

Previous work in our laboratory has led to construction of chr.2 congenic animals by mating of WKY (donor) and SHRSP (recipient) rats (Jeffs et al., 2000). A 'speed congenic' strategy was used, by combining a marker-directed breeding programme with genetic linkage maps, to achieve the congenic strains in 3-4 backcross generations (Jeffs et al., 2000). The strains were confirmed through genotyping. These animals exhibit significant reduction in SBP at baseline, when compared to SHRSP (Figure 1-5A). Total genome screening in the congenic strains (F2 generation) confirmed findings of Clark *et al*. (Clark et al., 1996) on the two QTLs for BP and salt-sensitivity identified on rat chr.2 (Jeffs et al., 2000, McBride et al., 2003). Further exclusion mapping studies on this chromosome, by use of the congenic animals, identified a potential 6-Mbp region harbouring candidate genes for salt sensitivity (Figure 1-5B). Subsequent microarray expression profiling carried out in whole kidneys from

salt-loaded parental and chr.2 congenic strains revealed differential expression of physiological candidate genes for BP and salt-sensitivity in HTN (Graham et al., 2007, McBride et al., 2003).

## 1.3.4 Candidate Genes for BP Regulation and Salt Sensitivity in SHRSP

### 1.3.4.1 Glutathione S-transferase Mu Type 1 (*Gstm1*)

One of the first positional and functional candidate genes for BP regulation identified in our laboratory on rat chr.2 was glutathione S-transferase mu type 1 (*Gstm1*) (Figure 1-5B) (McBride et al., 2003). *Gstm1* encodes for an enzyme belonging to the superfamily of glutathione S-transferases (GST), which catalyses ROS scavenging by conjugation to the reduced form of glutathione (GSH), and therefore participates in the endogenous defence against oxidative stress (Hayes and Pulford, 1995). Studies in the absence of salt loading demonstrated reduced renal mRNA and protein levels in young SHRSP (5 week old) and adult (16 week old) compared to SP.WKY$_{Gla}$2c* and WKY. Gene sequencing identified SNPs in coding and non-coding (promoter) regions (McBride et al., 2005). Moreover, combination antihypertensive treatment, using an ARB and a diuretic/vasodilator, did not restore *Gstm1* expression levels in young SHRSP, despite improvement of renal histopathological damages caused by sustained high BP (Koh-Tan et al., 2009). The above findings suggest involvement of *Gstm1* in the pathogenesis of HTN and occurrence of endothelial dysfunction, potentially via an oxidative stress pathway.

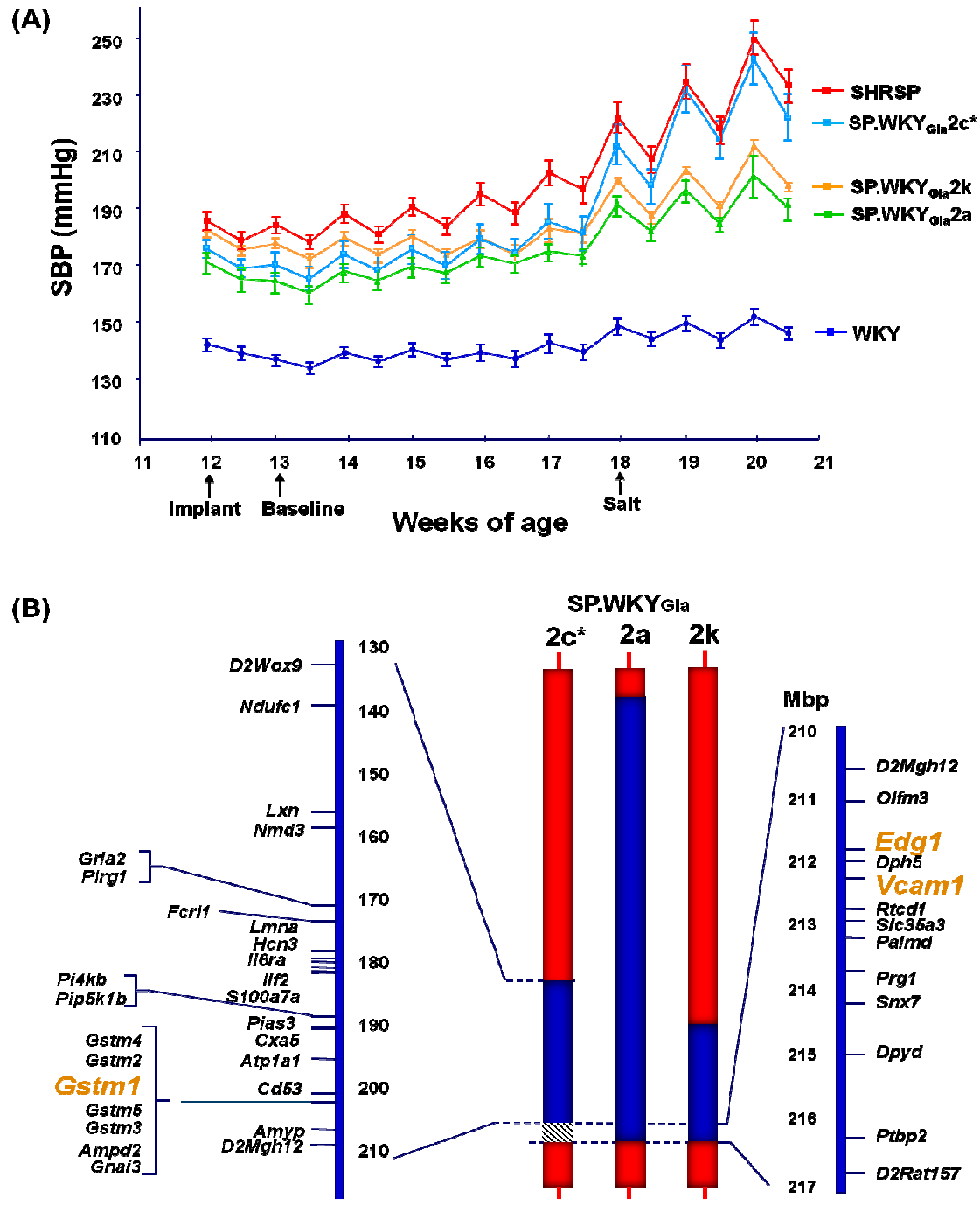


**Figure 1-5 - Identification of congenic interval and candidate genes for salt sensitivity and BP regulation. (A) Averaged weekly radiotelemetry recordings of night-time and day-time SBP in male WKY and SHRSP parental, SP.WKY$_{Gla}$2k, SP.WKY$_{Gla}$2a and SP.WKY$_{Gla}$2c* congenic strains. The animals were put on high-salt diet at 18 weeks of age. (B) Middle: Schematic map of chromosome 2 from congenic strains SP.WKY$_{Gla}$2a, 2k and 2c*. Blue bars: regions of WKY homozygosity, red bars: regions of SHRSP homozygosity, hatched bar: region of recombination and heterozygosity. Right: Physical map of a 6-Mbp congenic interval harbouring physiological candidate genes for salt sensitivity including *S1pr1 and Vcam1*. Left: Genetic map. The location of *Gstm1* is indicated outside of the region implicated in salt-sensitivity (McBride et al., 2003). A and B edited from Graham et al., 2007.**

### 1.3.4.2 Sphingosine-1-Phosphate Receptor 1 (*S1pr1*) and Vascular Cell Adhesion Molecule (*Vcam1*)

Sphingosine-1-phosphate receptor 1 (*S1pr1*) and vascular cell adhesion molecule (V*cam1*) were identified as two positional candidates for salt-sensitivity, lying on the 6-Mbp congenic interval of rat chr.2 (Graham et al., 2007). The proteins produced by the two genes are known to lie on a number of common and functionally important molecular pathways (Graham et al., 2007, Yogi et al., 2011, Bolick et al., 2005).

*S1pr1*, previously known as "endothelial differentiation gene 1" (*Edg1*), encodes for a G-protein coupled receptor (GPCR). It belongs to the family of receptors for sphingosine-1 phosphate (S1P), a lysophospholipid released mainly from platelets at sites of tissue injury or inflammation to promote angiogenesis (Sano et al., 2002, Lee et al., 1999). The S1P receptor family consists of five members: S1PR1/EDG1, S1PR2/EDG5, S1PR3/EDG3, S1PR4/EDG6, and S1PR5/EDG8 (Pyne and Pyne, 2000a). Upon activation by S1P, the receptors couple to heterotrimeric G-proteins (exchange of GDP for GTP: $G_i$, $G_q$, and $G_{12,13}$), which promote generation of second messengers to regulate a variety of cellular responses (Figure 1-6). Second messengers include phospholipase C (PLC), phospholipase D (PLD), adenylate cyclase (AC), intracellular $Ca^{2+}$ levels, ERK, and many others (Van Brocklyn et al., 1998, Pyne and Pyne, 2000b). Regulated responses include survival, proliferation, migration, angiogenesis, and actin cytoskeletal rearrangements (Spiegel and Milstien, 2003a). The expression profile of each member changes across the different tissues and cell types. S1PR1, S1PR2, and S1PR3 are the most widely expressed and therefore most studied, whereas S1PR4, and S1PR5 are expressed in limited tissues and their function is less clearly understood. S1PR1 is highly abundant in endothelial cells and has been shown to signal exclusively through coupling with $G_i$ (Windh et al., 1999). Its key role is the regulation of endothelial barrier functions, cell proliferation and migration, differentiation and vascular maturation (Kimura et al., 2000, Lee et al., 1998). Altered S1PR1 signalling has been implicated in the aetiology of cardiovascular disorders, including cardiac hypertrophy and inflammation (Yogi et al., 2011, Robert et al., 2001). Although the effects of S1P have been well documented, a major limitation in studying the role and signalling of discrete endogenous receptor subtypes has been the lack of subtype-selective agonists and antagonists, as well as poor receptor antibodies. Use of subtype-specific knockout mice has provided a powerful tool to overcome such challenges (Ishii et al., 2002, Liu et al., 2000). However, the *S1pr1* knock-out mouse shows embryonic lethality and the cardiac specific knock-out is not yet available. In recent

years, however, a number of such ligands (fingolimond - FTY720, SEW2871) have emerged and are undergoing clinical trials to determine their efficiency in treating acute kidney injury and autoimmune disorders such as multiple sclerosis by inducing lymphopenia (Kim et al., 2011, Lien et al., 2006).

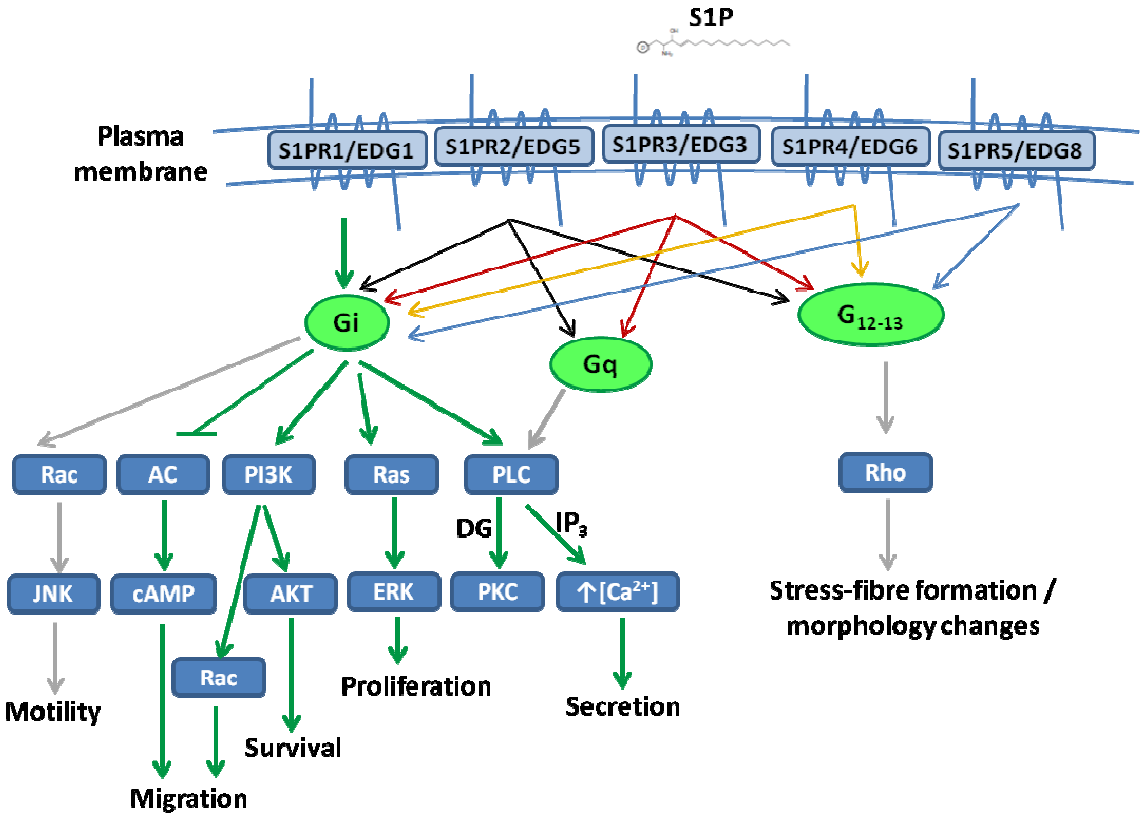


**Figure 1-6 - Overview of signalling pathways of S1P receptors (S1PR) and regulated cellular responses. Upon activation, all S1PR can couple to Gi proteins, all except S1PR1 couple to $G_{12-13}$ and finally the S1PR2 and S1PR3 receptors can also couple to Gq. Subsequently, the signal can be transduced through several second messengers to regulate different processes. S1PR1 couples exclusively to Gi, which then can activate either phospholipase C (PLC) to increase intracellular $Ca^{2+}$ levels, or Ras (small GTPases family) to promote proliferation, or phosphatidylinositol 3-kinase (PI3K) to induce survival and migration. It can also block adenylate cyclase (AC) to inhibit migration. Edg, endothelial differentiation gene; G, heterotrimeric G-proteins; Rac, subfamily of Rho GTPases ; Rho, small GTPases family; DG, diacylglycerol; $IP_3$, inositol triphosphate; JNK, C-Jun N-terminal kinase; cAMP, cyclic AMP; AKT, protein kinase B ; ERK, extracellular signal-regulated kinase; PKC, protein kinase C.**

V*cam1* is mainly expressed in endothelial cells after stimulation by cytokines, encoding for an adhesion molecule which functions as a pro-inflammatory marker. Alternative splicing results into two different transcripts encoding for two isoforms of VCAM1. The membrane-bound form allows adhesion of leukocytes (lymphocytes, monocytes, eosinophils, basophils) to vascular endothelium and subsequent trans-endothelial migration into arterial intima, and it also functions in signal transduction (Jager et al., 2000). The soluble isoform is used to monitor the membrane-bound VCAM1 expression and high levels are indicative of progressive formation of atherosclerotic lesions in human (Jager et al., 2000, Jang et al., 1994). Although hypertensive rat models, are not readily susceptible to atherosclerosis, due to a different lipoprotein profile from that of humans (i.e. low plasma levels of pro-atherogenic LDL and VLDL), increased expression of the soluble VCAM1 indicate potential kidney inflammation and low grade arterial stenosis.

Previous gene expression profiling in our laboratory, demonstrated differential expression of the two positional candidate genes, *S1pr1* and *Vcam1*, in kidneys from salt-loaded rats, and identified a number of SNPs in their promoter regions. mRNA expression of both genes was up-regulated in SHRSP compared to WKY and the SP.WKY$_{Gla}$2a and SP.WKY$_{Gla}$2k congenic strains. However, protein expression analysis in the salt-loaded kidneys showed reduced S1PR1 as opposed to increased VCAM1 in SHRSP relative to WKY and the congenic strains (Figure 1-7A and B). This lack of concordance in *S1pr1* mRNA and protein levels was suggestive of abnormal post-transcriptional regulation or protein turnover and subsequent altered S1PR1 signalling in HTN (Graham et al., 2007). Reduced protein levels could imply reduced renoprotection according to studies in rodents, which demonstrated a protective role of S1PR1 activation on renal function, characterised by suppression of pro-inflammatory molecules (Awad et al., 2006, Lien et al., 2006). Moreover, the renal levels of the pro-inflammatory marker VCAM1 were up-regulated in our SHRSP, indicating progressive kidney inflammation, a known key mechanism for inducing salt sensitivity (Rodriguez-Iturbe et al., 2002). However, recent studies on mesenteric primary VSMCs from WKY and SHRSP demonstrated that S1P-mediated S1PR1 activation up-regulated mitogenic and pro-inflammatory signalling, including induction of VCAM1 expression (Figure 1-7C and D). S1P/S1PR1 signalling was found to be altered in HTN, with related responses amplified in SHRSP, including activation of receptor tyrosine kinases (EGFR, PDGFR) and mitogenic kinases (MAPKs, SAPK/JNK) (Figure 1-7C), as well as expression of pro-inflammatory markers (ICAM1, VCAM1) and VSMC migration (Yogi et al., 2011).

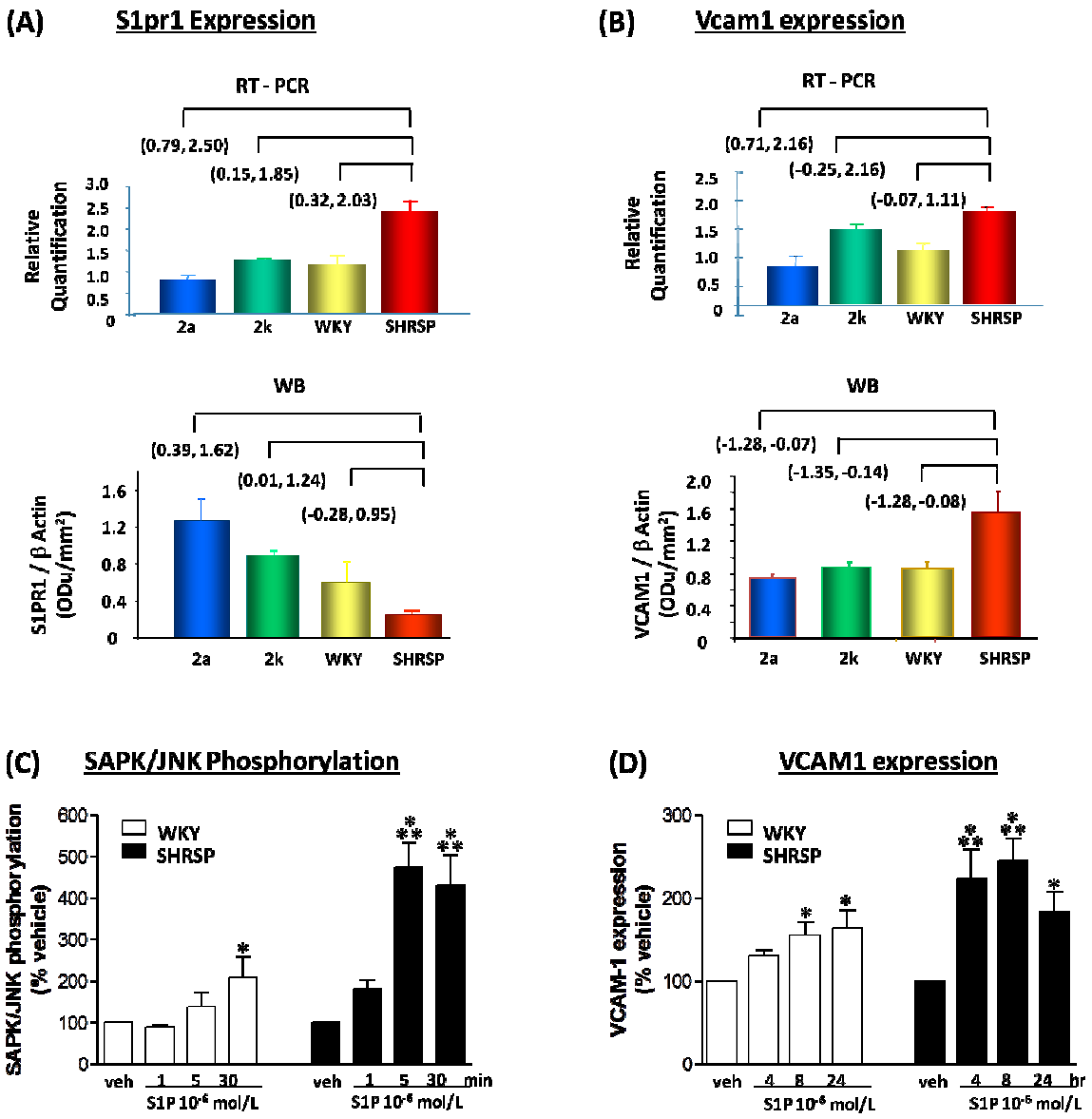


**Figure 1-7 - Differential renal expression of *S1pr1* and *Vcam1* candidate genes, and altered vascular S1P/S1PR1 signalling, in hypertension. (A) and (B): Differential mRNA (qRT-PCR; top graphs) and protein (WB; bottom graphs) expression levels of *S1pr1* and *Vcam1* in kidney from salt-loaded SHRSP compared to WKY and the SP.WKY$_{Gla}$2a, SP.WKY$_{Gla}$2k congenic strains. Statistical analysis was performed using 1-way ANOVA with Dunnett's posthoc test for multiple comparisons. Adapted from Graham et al., 2007. (C) and (D): Up-regulated mitogenic (SAPK/JNK phosphorylation) and pro-inflammatory (VCAM1 expression) responses upon S1P-stimulation in mesenteric primary VSMCs from WKY and SHRSP. Responses were mediated through S1PR1 and were augmented in SHRSP compared to WKY. *P< 0.05, ***P< 0.001 indicate statistical significance. Adapted from Yogi et al., 2011.**

To better comprehend / visualise the relationship between the two candidate genes and the pathways they are involved in, a hypothetical signalling network with S1PR1 (EDG1) at the apex, has been previously proposed using systems biology approaches (Graham et al., 2007). In this static model there is no concept of dynamic behaviour as it merely depicts protein-protein interactions, post-translational modifications (PTMs) and protein-DNA interactions (Figure 1-8). The rising argument is whether phenotypic differences between health and disease are driven exclusively by S1PR1 receptor via VCAM1 or by both candidate genes, which could be answered through enrichment of the pathway with dynamic data on the connectivities.

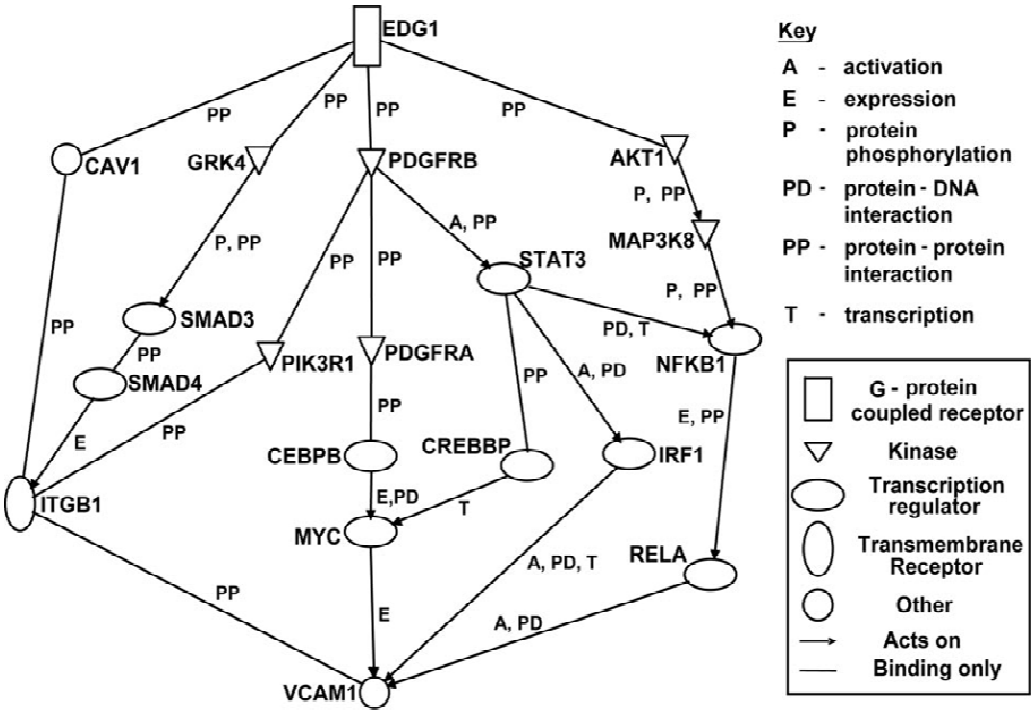


**Figure 1-8 - Transcriptional networks of *S1pr1* and *Vcam1* positional candidate genes. Static model of direct connections between S1PR1 and VCAM1 (generated by Ingenuity Pathway Analysis (IPA) software, Ingenuity Systems). The network is displayed graphically as nodes (gene products) and edges (the biological relationship between the nodes). Adapted from Graham et al., 2007.**

## 1.4 Systems Biology

Dynamic living systems sense their environment and respond to changes through complex cellular processes. Signal transduction and metabolic pathways are involved in every cellular response and are organized as highly interconnected networks, in which molecules participate in more than one reaction and there are several feedbacks. Therefore, any genetic alteration or exogenous perturbation results in a series of changes in the dynamic proteome and metabolome, which can be generally translated into phenotypic alterations. Thus, it becomes challenging to distinguish which metabolic processes / pathways are modified in each system, under different conditions.

Systems biology aims to interpret experimental evidence by reconstructing interconnected networks with increasing reliability, which would further allow rigorous predictions of cellular responses to specific perturbations. Crosstalk between networks provides holistic information on living systems for subsequent studies on diagnosis or prognosis of diseases. The emphasis is on the shift from working on individual molecules to work on networks which constitute the functional processes that link genetic and biochemical networks with biological phenotypes. To achieve this, mathematical modelling is combined with experimental validation, generating dynamic network maps with models describing their behaviour.

The use of mass spectrometry (MS)-based, high-throughput strategies permits precise and rapid proteome and metabolome screenings, which can capture changes in protein and metabolite profiles, as well as transient interactions between molecules. These approaches contribute to systematic mapping of cellular responses and the enrichment of static network maps obtained from genetic screens with dynamic data on their connectivity. Such combination of highly complementary network topology maps with inter-dependent dynamic data enables the study of cellular networks' function, from the physiological to the molecular level, and allows comparison of health and disease states.

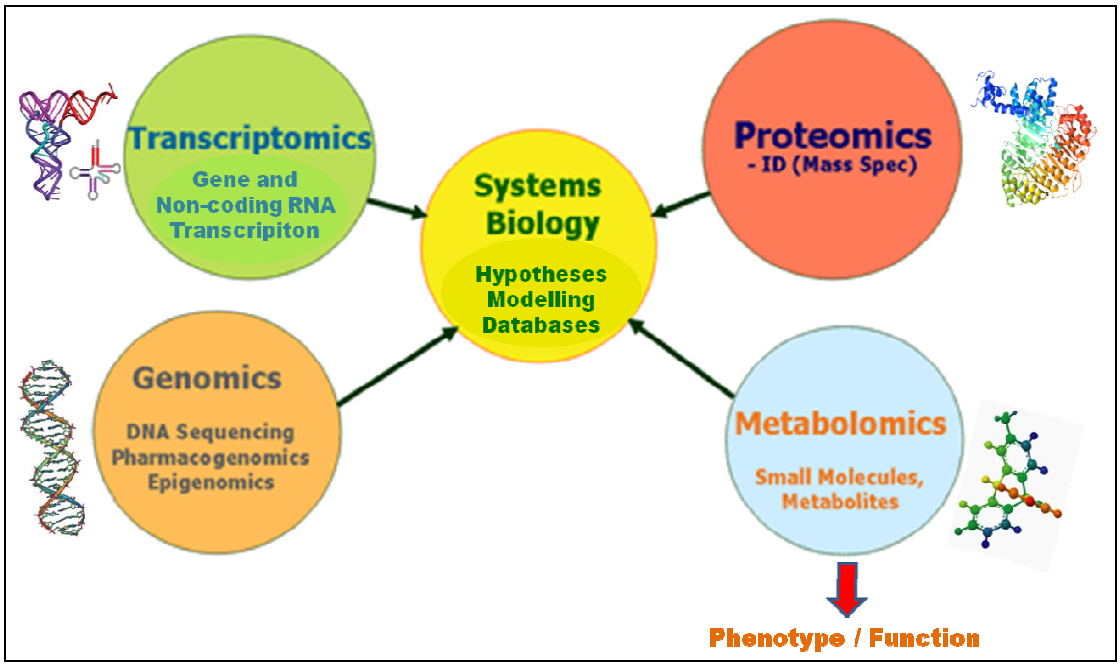


**Figure 1-9 - The 'omics' information universe. Systems biology aims to describe what can happen (genomics), what appears to be happening (transcriptomics), what makes it happen (proteomics) and what has happened and is happening (metabolomics) in a living system. Combination of this diverse yet complimentary information provides better understanding of the phenotype and function of the biological system.**

## 1.4.1 Proteomics

### 1.4.1.1 Mass Spectrometry-Based Quantitative Proteomics

Proteomics is the science often described as the next step after the sequencing of the human genome, as it is supported that there are many more proteins than there are corresponding genes in the genome. Proteomics focus on the study of protein structure and function and the ways they are produced and interact under different conditions within cells, in a system-wide manner. This highly sensitive and accurate 'omics' strategy provides a means towards a global view of cellular proteomes, which will improve our understanding of fundamental biological processes underlying a wide range of diseases and may facilitate discovery of new drugs. To date, the only global proteome (interactome) screening/quantification has been completed in *Saccharomyces cerevisiae* (Krogan et al., 2006, Gavin et al., 2006).

In highly complex dynamic systems, such as cells, proteins comprise the principal components of every cellular response to genomic changes or exogenous perturbations. Such responses involve the interplay of multiple protein modifications, interactions and signalling networks. Therefore, comprehensive protein characterisation is vital in revealing the mechanisms and underlying principles of biological processes, as well as in detecting unpredictable events. The complexity of proteomic changes has made their identification and characterisation quite challenging in modern cell biology.

Traditionally, techniques such as affinity purification of proteins and conventional column chromatography, combined with immunobloting, microscopy and mass spectrometry (MS), have been employed to measure abundance, modifications and interactions of proteins and have permitted extensive characterisation of many signalling pathways and cellular responses (Gingras et al., 2007, Kocher and Superti-Furga, 2007). However, limitations of such approaches include the need for specific antibodies or epitope-tagged proteins, the false-positive interactions difficult to distinguish from true specific signals, the need for extensive protein purification resulting in loss of weak binders and of course the restricted throughput (small-scale) which sheds light into a small part of the large interconnected protein networks in the cell. Therefore, such approaches were not suitable for large-scale interaction mapping.

Recent development of high-throughput, MS-based quantitative proteomics, highly sensitive and accurate, circumvents the above limitations, offering the potential to compare global proteomic outputs and gain molecular insights into cellular function and physiology, in

situations of health and disease. Large-scale, unbiased profiling of protein abundance (Andersen et al., 2005) and dynamics (Blagoev et al., 2003, de Hoog et al., 2004) provides data to improve characterisation of mechanisms of action and prediction of biomarkers. Monitoring of quantitative differences in proteomes and dynamic properties of proteins, including sub-cellular distribution, protein-protein interactions, turnover rates and PTMs (Mann, 2006, Ong et al., 2002), can be achieved by *in vitro* labelling of proteins. Labelling can be introduced either as chemical modifications (ICAT, iTRAQ) (Gygi et al., 1999, Ross et al., 2004), or as metabolic tags of peptides (Ong et al., 2004). Direct comparison of intensity signals between differentially labelled isotopes correspond to peptide and protein ratios. Metabolic labelling with stable heavy amino acid isotopes (SILAC) is proving to be a state-of-the-art, important tool for systems biology applicable from cell lines to primary cells, tissues (Ishihama et al., 2005) and animal models (Krüger et al., 2008, Sury et al., 2010). In combination with high-resolution MS-instruments and specialised data-processing bioinformatics tools, this powerful technique has led to a spectacular progress in rapid and accurate proteome screening of large proportions of mammalian proteomes (Graumann et al., 2008).

#### 1.4.1.2 Proteomics Instrumentation and Bioinformatic Analysis

Routine MS-screening of hundreds of proteins in complex sample mixtures, within few hours, has been mainly permitted due to continuous development of the instrumentation and bioinformatics tools for sample processing and data analysis (Makarov et al., 2006, Domon and Aebersold, 2006, Mueller et al., 2008).

Powerful mass spectrometers, such as the LTQ-Orbitraps, have become widespread in shotgun proteomics due to their high-mass precision and high-resolution in the rapid analysis of highly complex proteomes (Makarov et al., 2006, Olsen et al., 2005). Gigabytes of high-resolution MS data generated by proteomic analyses are processed through advanced computational software packages, essential for extraction, filtering, identification and quantification of such datasets. MaxQuant is a high-accuracy protein quantification platform developed by Cox *et al*. (Cox et al., 2009), which supports LTQ-Orbitrap instruments and enables high peptide identification rates. Combined with advanced modules for extensive bioinformatics and statistical analysis, these platforms represent powerful, unified computational analysis pipelines for quantitative proteomics. Perseus (http://www.perseus-framework.org), is such a module separately developed to complement MaxQuant workflow. Finally, pathway/network analysis performed on relevant databases, such as

Ingenuity Pathway Analysis (IPA; http://www.ingenuity.com), allows for biological interpretation and generation of new testable hypotheses.

However, such sensitive and automated technologies have the disadvantage of identifying a large number of contaminants. Additionally, during protein identification, partial overlap of the results from different quantification algorithms reflects imperfect overlap of different search engines (Searle et al., 2008, Yu et al., 2010). Because of this complexity, validating these events *in vitro* is difficult, despite the fact that they can provide a first step in establishing predictive models.

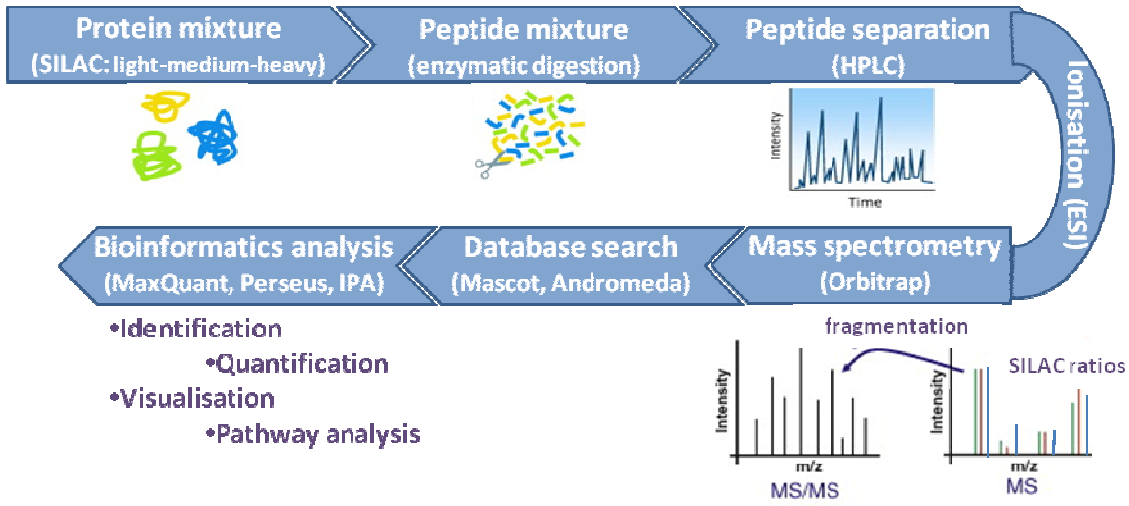


**Figure 1-10 – Quantitative shotgun proteomics. Differentially labelled protein samples (SILAC) are mixed in equal amounts and digested enzymatically into mixtures of chemically identical but isotopically distinct peptides. Peptides are then separated by high performance liquid chromatography (HPLC) and transferred into a mass spectrometer by electrospray ionisation (ESI). The mass spectra (MS) reveal intensity ratios of labelled peptide pairs/triplets, which assist relative quantification. Fragmentation spectra (MS/MS) of individual peptides contain information about peptide identity and are matched to protein sequence databases. Further bioinformatics analysis requires use of advanced algorithms, which enable protein identification and quantification, data visualisation and biological interpretation.**

## 1.4.2 Metabolomics

### 1.4.2.1 Metabolomics Analytical Platforms and Applications

Metabolomics is a rapidly growing field of post-genomic systems biology, complementary to the other 'omics' areas, focusing on comprehensive characterisation of living systems biochemistry (Arita, 2009). The metabolome of a biological system refers to its complete set of small molecules (metabolites). In contrast to genome and transcriptome which describe the potential of a cell, tissue or organism, metabolome represents the fingerprint of dynamic states that reflect the actual phenotypic status of the system (Breitling et al., 2008, Kell, 2006). Hence, metabolome screening offers an un-biased strategy towards characterisation of metabolic signatures/patterns driving phenotypic changes in disease and biomarker identification. Moreover, construction of dynamic metabolic maps would permit insights into physiological stress responses and pathological processes involved in disease development.

However, due to the highly diverse chemical nature of metabolites, a truly holistic metabolomics approach is not possible on a single analytical platform (Moco et al., 2007, Garcia et al., 2008). Therefore, current metabolomic studies are either targeted, focusing on specific metabolites or metabolic pathways of interest (Scalbert et al., 2009, Olszewski et al., 2010), or untargeted, aiming to identification of the most significant detectable changes in a system, but exhaustive coverage is not the goal (De Vos et al., 2007, Dunn et al., 2011). Normally, the latter approach is used in hypothesis-generating and biomarker identification studies (Sreekumar et al., 2009).

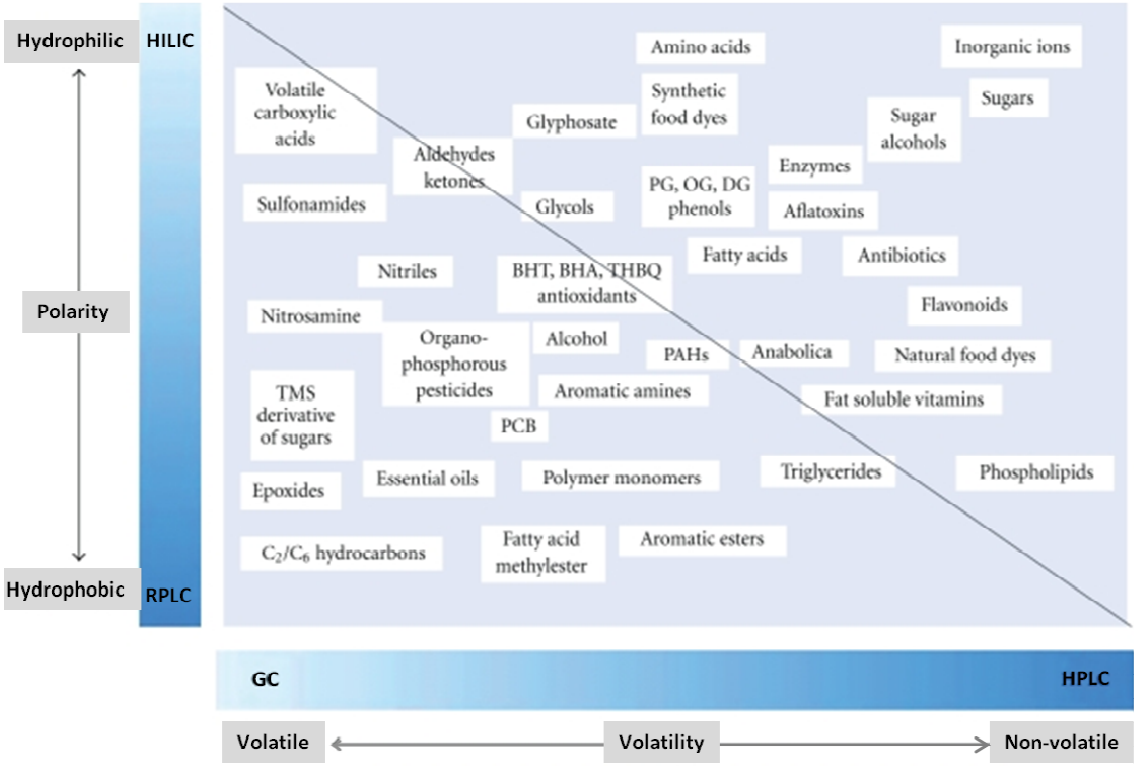


**Figure 1-11 – Metabolite diversity. The highly diverse chemical nature of metabolites requires use of multiple analytical platforms in order to achieve comprehensive characterisation of the metabolome. Gas chromatography (GC) and hydrophilic interaction liquid chromatography (HILIC) are the two most commonly used platforms in metabolomics analysis, coupled to MS. Adapted from Gratzfeld-Husgen and Schuster, 1996; Agilent Technologies.**

To sidestep limitations of individual analytical methods in global metabolic profiling, a multi-platform approach is required (Mandal et al., 2012, Naz et al., 2013, Suhre et al., 2010). However, recent advances in HPLC technologies and mass spectrometers, have made liquid chromatography coupled to mass spectrometry (LC-MS) increasingly popular in the field of metabolomics (Cubbon et al., 2010, Scalbert et al., 2009, Kamleh et al., 2008). Traditional reversed phase (RP) LC-MS, which is used for separation of hydrophobic small molecules on a non-polar stationary phase, is now complemented by the hydrophilic interaction LC (HILIC) approach which separates highly polar analytes on a hydrophilic stationary phase (Cubbon et al., 2010, Dunn et al., 2011, Scalbert et al., 2009). Therefore separation of a broader spectrum of metabolites is achieved. In combination with high-resolution mass analysers, such as the Orbitraps which offer accurate mass detection within 1ppm (Breitling et al., 2006, Moco et al., 2007) and much greater sensitivity over nuclear magnetic resonance (NMR) spectrometers, significantly improve metabolite identification. Moreover, quantitative changes are monitored simultaneously in hundreds of metabolites.

Nevertheless, presence of numerous structural isomers in biological systems makes confirmation of identifications extremely crucial. The two parameters most extensively used in identification are the LC retention time (RT) and MS/MS fragmentation spectra (Scalbert et al., 2009), which are normally compared to authentic standards or matched to public MS/MS databases. Despite all improvements in technologies and instrumentation, high technical and biological variability during robust characterisation of the extremely dynamic metabolome makes the use of large number of replicates (biological, technical, analytical) indispensable, to avoid inconsistent findings and increase confidence (Jankevics et al., 2011).

One of the major goals of metabolomics is the discovery of metabolic biomarkers, which are essential tools in clinical diagnostics as well as in monitoring progression of chronic diseases and responses to pharmacological treatments (Robertson, 2005, Rosner, 2009). Chronic diseases, such as CVD, are typically multifactorial, characterised by systemic pathological changes, which influence numerous metabolic processes. Therefore, identification of a single biomarker cannot, normally, display the disease complex status and is insufficiently powerful to provide a clinically useful diagnosis. High-throughput, quantitative metabolic profiling offers the advantage of detecting several biomarkers or characteristic metabolite patterns, either genetically controlled or being the result of drug interventions. This way, a more accurate representation of the condition is provided and understanding of metabolism disorders and their underlying mechanisms is improved.

The application of metabolomics in cardiovascular pathophysiology and genetics is a rapidly growing field, aiming to define a clearer metabolic picture for CVD prediction and progression. Accurate non-invasive techniques, carried out primarily on preparations of serum, plasma or urine (Giovane et al., 2008, Barderas et al., 2011, Waterman et al., 2010), have been combined with pattern-recognition algorithms to diagnose the presence and severity of the disease, as in the case of CAD (Brindle et al., 2002). A number of studies have focused and succeeded on establishing direct functional links between disease risk-genetic variants previously identified in GWAS, quantitative metabolic traits and an end-point of cardiovascular diseases. By integrating genomics with serum and urine metabolomics, such studies have allowed identification of new underlying biological processes and pathways in CVD (Illig et al., 2010, Suhre et al., 2011, Kettunen et al., 2012). Moreover, recent metabolomic studies are pointing at intestinal microbiota metabolism of nutrients as a potential risk factor for atherosclerosis pathogenesis (Koeth et al., 2013).

Therefore, data integration from high-throughput 'omics' studies will not only give insights into CVD pathophysiology, but will stress even more the importance of human metabolic individuality towards the development of new therapeutic strategies on a personalised medicine approach (Suhre et al., 2011).

#### 1.4.2.2 Metabolomics Bioinformatic Analysis

In order to extract valuable information from gigabyte-large LC-MS datasets, the use of automated and reliable bioinformatics algorithms is essential. A number of freely available applications has been developed to aid conversion, quantification and identification of LC-MS signals (Blekherman et al., 2011), complemented by advanced statistical software which extract significant features from such datasets (Madsen et al., 2010). IDEOM is a data processing pipeline developed for analysis of metabolomic LC/MS data from untargeted metabolomics studies (Creek et al., 2012). Its Excel graphical user interface (GUI) enables fast and easy conversion of raw LC-MS data into lists of putative metabolites, as well as advanced removal of noise and false identifications. This is achieved by implemented powerful processing tools, which perform automated filtering, peak annotation and metabolite identification with confidence levels and intensities (Smith et al., 2006b, Scheltema et al., 2011). Improved metabolite identification is based on mass and retention time matching to integrated databases. In addition, development of the PeakML.Viewer provides an environment for rapid inspection of peak quality (Scheltema et al., 2011). Subsequent interpretation of significant data through association with metabolic processes/networks and biomarker search, on web-servers such as IPA (http://www.ingenuity.com), allows for generation of new testable hypotheses and drug development.

However, sensitivity of automated technologies on metabolite identification is particularly challenged by the highly unstable nature of metabolome, artefact peaks (Moco et al., 2007, Neumann and Bocker, 2010, Scheltema et al., 2009) and the large number of structural isomers in biological samples. Confidence of the results is greater when observed metabolic changes can be related to each other or to processes/pathways known to be deregulated or lastly to gene and protein networks of other 'omic' studies (Loscalzo et al., 2007). Nonetheless, verification/validation of findings is vital before proceeding to generation of testable hypothesis and it minimally involves confirmation of the metabolite identity by further fractionation. In biomarker studies the result is usually validated in a different cohort of samples.

# Aims

Previously, microarray gene expression profiling in kidneys of salt-loaded WKY, SHRSP and chr.2 congenic strains, identified *S1pr1* and *Vcam1* as candidate genes predisposing to salt-sensitive HTN. In addition, studies in primary VSMCs from MRAs demonstrated association of S1P/S1PR1 signalling to specific pro-inflammatory pathways (VCAM1) through receptor tyrosine kinases, a process which was more pronounced in SHRSP compared to WKY. Moreover *Gstm1* was identified as a chr.2 positional and functional candidate for BP regulation, mapping outside the region implicated in salt-sensitivity.

The overall aim of this study is to dissect the functional role of these genes and of the chr.2 congenic interval in EH and salt-sensitivity in the SHRSP. A combination of chr.2 congenic and transgenic strains with high-throughput proteome and metabolome screenings is used in order to achieve robust identification and characterisation of altered signalling pathways and metabolic processes associated with predisposing risk factors and consequences of HTN.

The specific aims of this work are:

- to compare, *in vitro*, S1PR1 expression profile in renal and vascular tissue from 21 week-old, salt-loaded WKY, SHRSP and SP.WKY$_{Gla}$2a, SP.WKY$_{Gla}$2k congenic strains.

- to characterise salt-sensitivity and identify putative biomarkers through metabolic profiling of matched urine and plasma from 21 week-old, control and salt-loaded, WKY, SHRSP, SP.WKY$_{Gla}$2k congenic and *Gstm1*-transgenic strains.

- to examine, *ex-vivo*, MRA structure, mechanics and reactivity in vessel segments from 16 week-old WKY, SHRSP and SP.WKY$_{Gla}$2a, WKY.SP$_{Gla}$2a reciprocal congenic strains.

- to study, *in vitro*, S1P/S1PR1-mediated mitogenic signalling in mesenteric primary VSMCs from 16 week-old WKY, SHRSP and SP.WKY$_{Gla}$2a, WKY.SP$_{Gla}$2a reciprocal congenic strains.

- to extend the above study using MS-based quantitative SILAC-proteomic and metabolomic screenings for robust identification of S1P-mediated and genetically-driven changes in the global proteome and metabolome of VSMCs.

# 2 Materials and Methods

# 2.1 Materials

## 2.1.1 Biological Material

Inbred colonies of the parental WKY and SHRSP, the congenic SP.WKY$_{Gla}$2a, WKY.SP$_{Gla}$2a and SP.WKY$_{Gla}$2k and the *Gstm1*-transgenic rat strains have been maintained at the University of Glasgow, by brother-sister mating and microsatellite/single nucleotide polymorphism genotyping, to ensure homozygosity of screened loci (Luft et al., 1988). The rats were housed under controlled conditions of 21°C and 12-hour light/dark cycles. The pups were weaned at 4 weeks and housed according to sibling group and gender thereafter. All rats were maintained on normal rat chow (rat and mouse No.1 maintenance diet, Special Diet Services, UK) and water *ad libitum*. The salt-loaded groups were given a salt challenge (1% NaCl in drinking water) at 18 weeks of age, for 3 weeks. The research was conducted in conformity with Public Health Service policy on the humane care and use of laboratory animals.

Primary VSMCs previously isolated from thoracic aorta of the WKY and SHRSP rats, were grown in complete growth medium (section 2.1.4). Cell cultures were maintained for 10-12 passages.

## 2.1.2 Reagents

General chemicals, enzymes and any reagents used in this study were of the highest available grades. Handling of all hazardous reagents was in accordance with Control of Substances Hazardous to Health regulations. The reagents were obtained from the following suppliers:

- Avanti Polar Lipids Inc, Alabama, USA
  - *VPC23019 sphingolipids*
- AMS Biotechnology Ltd, Europe
  - *Detachin cell detachment solution*
- BD Biosciences, Oxford, UK
  - *Cell nylon filter 100µm*
- BioRad Laboratories Ltd, Hertfordshire, UK
  - *Ready gel tris-HCl 12%, Ready gel tris-HCl 10%*
- Dundee Cell Products Ltd, Dundee, UK

  - *DMEM-14 media (R0K0), DMEM-11 SILAC media (R6K6), DMEM-15 SILAC media (R10K8), dialysed FBS (MWCO 10,000 Da)*

- Enzo Life Sciences Inc (Biomol), UK
  - *D-erythro sphingosine-1-phosphate*
- Fisher Scientific Ltd, Loughborough, Leicestershire, UK
  - *Hepes, DMSO, Histoclear*
- GE Healthcare Bio-Sciences Ltd, Buckinghamshire, UK
  - *Full-range markers RNP800E, Amersham Hybond-P polyvinylidene fluoride (PVDF) membrane*
- Invitrogen Ltd, Paisley, UK
  - *Gibco high-glucose Dulbecco's modified Eagle medium (DMEM), Gibco Ham's F-12 nutrient mix, penicillin/streptomycin solution, gentamicin, L-glutamine, sodium pyruvate solution, trypsin-EDTA (0.5%-0.2%) solution, Prolong Gold*
- Lonza, Cambridge, UK
  - *Calcium and magnesium free Dulbecco's phosphate buffered saline (DPBS)*
- National Diagnostics, GA, USA
  - *Histomount*
- PAA Laboratories Ltd, Somerset, UK
  - *Foetal calf serum (FCS)*
- Promega Ltd, Southampton, UK
  - *Sequencing grade modified trypsin*
- Roche Diagnostics Ltd, Burgess Hill, UK
  - *Complete protease inhibitor cocktail*
- Sigma-Aldrich Company Ltd, Dorset, UK
  - *30% acrylamide/bis-acrylamide solution 37.5:1, bovine serum albumin (BSA), ponceau S, elastase (≥4 ui/mg), soybean trypsin inhibitor, N(G)-nitro-L-arginine methyl ester hydrochloride (L-Name), carbamoylcholine chloride (carbachol), L-(-)-noradrenalin bitatrate (+)salt monohydrate, sodium nitroprusside (SNP), fasudil dihydrochloride, IgG mouse / goat / rabbit*
- Vector Laboratories Inc, Burlingame, USA
  - *Vectashield, rabbit serum, goat serum*
- Worthington Biochemical Corp, Lakewood, UK
  - *Collagenase type I (>200 IU/mg)*

### 2.1.3 Kits

The kits used in this study were obtained from the following suppliers:

- Thermo Scientific, Waltham, MA, US
  - *Pierce BCA Protein Assay kit*
- GE Healthcare Bio-Sciences Ltd, Buckinghamshire, UK
  - *RPN2106 ECL Western Blotting Detection Reagents*
- AMS Biotechnology Ltd, Europe
  - *CNM Compartmental Protein Extraction kit*
- Vector Laboratories Ltd, Peterborough, UK
  - *Vectastain Universal Elite ABC kit*
  - *DAB Peroxidase Substrate Kit, 3,3'-diaminobenzidine*

### 2.1.4 Solutions & Media

In all the solutions used in this study high purity sterile water was used as dissolving agent, unless otherwise stated. Laboratory glassware was autoclave-sterilised and sterile, disposable plastic-ware was used.

- 6x SDS-PAGE sample buffer: 260mM Tris-HCl pH 6.8, 10% (w/v) SDS, 30% (v/v) glycerol, 0.012% (w/v) bromophenol blue, 6% (v/v) β-mercaptoethanol
- SDS-PAGE resolving buffer: 10-12% (v/v) acrylamide/bis-acrylamide, 375mM Tris pH 8.8, 0.1 % (w/v) SDS
- SDS-PAGE stacking buffer: 4% (v/v) acrylamide/bis-acrylamide, 125mM Tris pH 6.8, 0.1 % (w/v) SDS
- SDS-PAGE running buffer: 0.1 % (w/v) SDS, 25mM Tris, 192mM glycine
- SDS-PAGE transfer buffer: 25mM Tris, 192mM glycine, 20% (v/v) methanol
- Coomassie stain solution: 0.025% (w/v) Coomassie brilliant blue R-250, 40% (v/v) methanol, 10% (v/v) acetic acid
- Coomassie de-stain solution: 40% (v/v) methanol, 10% (v/v) acetic acid
- Ponceau S: 0.5% (w/v) Ponceau S in 1% (v/v) acetic acid
- Tris-buffered saline / Tween (TBST): 140mM NaCl, 20mM Tris pH 7.6, 0.1% (v/v) Tween-20

- Blocking buffer: 5% (w/v) BSA in TBST
- 10x Phosphate-buffered saline: 1.37M NaCl, 27mM KCl, 0.1M $Na_2PO_4$, 18mM $KH_2PO_4$, pH 7.4
- Citrate buffer: 8mM trisodium citrate, 2mM citric acid, pH 6.0
- Stripping Solution: 0.2M glycine in 1% (w/v) SDS, pH 2.2
- Krebs / Physiological salt solution (PSS): 119mM NaCl, 4.7mM KCl, 0.6mM $MgSO_4.7H_20$, 25mM $NaHCO_3$, 1.18mM $KH_2PO_4$, 11mM D-glucose, 2.5mM $CaCl_2.2H_20$, pH 7.4
- Calcium-free PSS: 23μM EDTA in PSS free of $CaCl_2$
- Potassium PSS (KPSS): 123mM KCl in PSS free of NaCl
- Paraformaldehyde (PFA) 4%: 12.5mM NaOH 1N, 4% (w/v) PFA in DPBS
- Metabolite extraction buffer: Chloroform : Methanol (100% v/v) : $ddH_2O$ (1:3:1)

All cell culture media were supplemented with 10% FCS and 5% 100 IU/ml Penicillin - 100μg/ml Streptomycin and were sterilized through a 0.2μm pore size filter, unless otherwise stated.

- Wash media: Ham's F-12 nutrient mix, 10mg/ml Gentamicin, 2mM L-glutamine, 4.8g/ml Hepes, serum free
- Complete growth media: DMEM with 4mmol/L L-glutamine, 4.5g/L D-glucose, 110 mg/L sodium pyruvate
- SILAC complete media: SILAC DMEM media containing unlabelled arginine and lysine amino acids (R0K0) / SILAC DMEM media containing $^{13}C$ labelled arginine and lysine amino acids (R6K6) / SILAC DMEM media containing $^{13}C$ and $^{15}N$ labelled arginine, and $^{13}C$ and $^{15}N$ labelled lysine amino acids (R10K8). Media were supplemented with 10% (v/v) dialysed FBS.
- Cryo-preservation media: 10% (v/v) DMSO in complete growth media
- Pre-digestion media: 3mg/ml Collagenase II in wash media

- Digestion media: 2mg/ml BSA, 2mg/ml Collagenase II, 0.12mg/ml Elastase, 0.36mg/ml soybean trypsin inhibitor in wash media
- Cell lysis buffer: *Buffer A*: 50mM $Na_4P_2O_7$, 50mM NaF, 50mM NaCl, 5mM $Na_2EDTA$, 10mM Hepes, 0.5% (v/v) triton X-100, pH 7.4; *Buffer B*: 1mM $Na_3VO_4$, 1mM PMSF, 2 tablets of complete EDTA-free protease inhibitor cocktail per 50ml

## 2.1.5 Primary Antibodies

Primary antibodies were purchased from the following suppliers and are listed in Table 2-1:

- Abcam, Plc., Cambridge, UK
- Cell Signaling Technologies, Inc., MA, USA - New England Biolabs, Ltd, UK
- Santa Cruz Biotechnology, Inc., CA, USA

**Table 2-1. List of primary antibodies used in the experiments**

| Primary antibodies | Description | Company | Reference | Dilution | Method |
|---|---|---|---|---|---|
| **HMOX1** | IgG1 monoclonal antibody raised in mouse immunised with synthetic peptide corresponding to aa 1-30 of human HMOX1 | Abcam | ab13248 | 1/250 | WB |
| **NPR3** | IgG polyclonal antibody raised in rabbit immunised with synthetic peptide corresponding to aa 400-500 of human NPR3 | Abcam | ab79164 | 1/500 | WB |
| **CAV1** | IgG polyclonal antibody raised in rabbit immunised with synthetic peptide corresponding to aa 1-17 of human CAV1 | Abcam | ab2910 | 1/500 | WB |
| **ACTA1** | IgG polyclonal antibody raised in rabbit immunised with synthetic peptide from N-terminus of human ACTA1 | Abcam | ab11317 | 1/500 | WB |
| **NQO1** | IgG polyclonal antibody raised in rabbit immunised with synthetic peptide from within residues 200 to C-terminus of human NQO1 | Abcam | ab34173 | 1/500 | WB |
| **GSTM1** | IgG polyclonal antibody raised in rabbit immunised with synthetic peptide from C-terminus of mouse GSTM1 | Provided by professor John D. Hayes | | 1/5000 | WB |
| **GAPDH** | IgG1 monoclonal antibody raised in mouse immunised with rabbit muscle GAPDH | Abcam | ab8245 | 1/5000 | WB |
| **EDG1** | IgG polyclonal antibody raised in rabbit immunised with synthetic peptide corresponding to aa 241-253 of human EDG1 | Abcam | ab23695 | 1/200 - 1/500 | WB |
| | | | | 1/100 - 1/1000 | IHC |
| | IgG polyclonal antibody raised in rabbit immunised with synthetic peptide from C-terminus of mouse EDG1 | Provided by Dr. Tim Palmer (PA1-1040) | | 1µg/ml | WB |

| Primary antibodies | Description | Company | Reference | Dilution | Method |
|---|---|---|---|---|---|
| **S1PR2** | IgG polyclonal antibody raised in goat immunised with synthetic peptide corresponding to C-terminus of human EDG5 | Santa Cruz | sc-16085 | 1/100 | WB |
| **S1PR3** | IgG monoclonal antibody raised in mouse immunised with synthetic peptide corresponding to C-terminal of human EDG3 | Abcam | ab12254 | 1/5000 | WB |
| **VCAM1** | IgG monoclonal antibody raised in rat immunised with glycoprotein fraction from cerebellum of 8-10 days old mice | Abcam | ab78712 | 1/100 | WB |
| **Na-K ATPase** | IgG1 monoclonal antibody raised in mouse immunised with full length native protein from rabbit renal outer-medulla | Abcam | ab7671 | 1/5000 | WB |
| **histone H1.0** | IgG1 monoclonal antibody raised in mouse immunised with ox liver histone H1.0 | Abcam | ab11079 | 1/500 | WB |
| **Vimentin** | IgG1 monoclonal antibody raised in mouse immunised with cytoskeletal vimentin extract of calf lens | Abcam | ab8978 | 1/500 | WB |
| **phospho-SAPK/JNK** | IgG polyclonal antibody raised in rabbit immunised with synthetic phospho-peptide corresponding to residues surrounding Thr183/Tyr185 of human SAPK/JNK | Cell Signaling | #4668 | 1/1000 | WB |
| **SAPK/JNK** | IgG polyclonal antibody raised in rabbit immunised with GST/human JNK2 fusion protein | Cell Signaling | #9252 | 1/1000 | WB |
| **phospho-ERK1/2** | IgG polyclonal antibody raised in rabbit immunised with synthetic phospho-peptide corresponding to residues surrounding Thr202/Tyr204 of human ERK1 | Cell Signaling | #9101 | 1/400 | WB |
| **ERK1/2** | IgG polyclonal antibody raised in rabbit immunised with synthetic peptide derived from a sequence in the C-terminus of rat ERK1 | Cell Signaling | #9102 | 1/400 | WB |
| **phospho-p38 MAPK** | IgG polyclonal antibody raised in rabbit immunised with synthetic phospho-peptide corresponding to residues surrounding Thr180/ Tyr182 of human p38 MAPK | Cell Signaling | #9211 | 1/1000 | WB |
| **p38 MAPK** | IgG polyclonal antibody raised in rabbit immunised with synthetic peptide derived from the sequence of human p38 MAPK | Cell Signaling | #9212 | 1/1000 | WB |
| **beta-Actin** | IgG1 monoclonal antibody raised in mouse immunised with synthetic peptide corresponding to N-terminus of the beta isoform of actin | Abcam | ab6276 | 1/10000 | WB |
| **ACTA2** | IgG2a monoclonal antibody raised in mouse immunised with synthetic peptide corresponding to N terminal amino acids 1-10 of alpha smooth muscle actin | Abcam | ab18147 | 1/100 - 1/1000 | IHC |
| | IgG polyclonal antibody raised in rabbit immunised with synthetic peptide corresponding to N-terminus of human SMCα-actin | Abcam | ab5694 | 1/100 | ICC |
| **AQP2** | IgG polyclonal antibody raised in goat immunised with synthetic peptide corresponding to C-terminus of human aquaporin 2 | Santa Cruz | sc-9882 | 1/100 - 1/2000 | IHC |

## 2.1.6 Secondary Antibodies

Secondary antibodies were purchased from the following suppliers and are listed in Table 2-2:

- Dako-Cytomation, Denmark
- Abcam, Plc., Cambridge, UK
- Vector Laboratories Ltd, Peterborough, UK

**Table 2-2. List of secondary antibodies used in the experiments**

| Secondary antibodies | Description | Company | Reference | Dilution | Method |
|---|---|---|---|---|---|
| **Anti-mouse IgG** | Horseradish peroxidase-conjugated, polyclonal antibody, raised in rabbit | Dako | #P0260 | 1/1000 - 1/2000 | WB |
| **Anti-rabbit IgG** | Horseradish peroxidase-conjugated, polyclonal antibody, raised in swine | Dako | #P0399 | 1/1000 - 1/2000 | WB |
| **Anti-goat IgG** | Horseradish peroxidise-conjugated, polyclonal antibody, raised in rabbit | Abcam | ab6741 | 1/200 | IHC |
| **Anti-mouse/rabbit IgG** | Biotinylated polyclonal antibody, raised in horse | Vector | #BA-1400 (Universal ABC kit) | 1/200 | IHC |

## 2.1.7 Software

- Image J V1.42, National Institutes of Health, Bethesda MD, USA
- LabChart 6.1.1, ADInstruments Ltd, Oxford, UK
- MyoView 1.1, DMT, Denmark
- Xcalibur 2.2.0 Thermo Fisher Scientific, Inc., MA, USA
- MaxQuant 1.1.1.25, 1.2.0.18, 1.2.2.6, Max Planck Institute, Martinsried, Germany
- Perseus 1.2.0.17, 1.2.7.4 Max Planck Institute, Martinsried, Germany
- Scaffold 3.2.0, Proteome Software, Inc., Portland, USA
- Mascot Server 2.3, Matrix Science Ltd, London, UK
- IDEOM V11 – V19, Glasgow Polyomics Facility, Glasgow, UK
- PeakML Viewer, Glasgow Polyomics Facility, Glasgow, UK
- Wallac Work-Out, Turku, Finland
- GraphPad Prism 4 for Windows, GraphPad Software, San Diego California USA

## 2.2 General Primary Cell Culture Methods

All cell culture was performed under sterile conditions in vertical laminar flow cabinets. Cells were cultured in 100mm x 20mm culture dishes or T25, T75 and T150 culture flasks with vented cups (Corning, UK) and were maintained in the appropriate media as sub-confluent cultures (70-80% confluence) at 37°C in a 5% $CO_2$ humidified incubator. Media was replaced every other day.

### 2.2.1 Isolation of Mesenteric Primary Rat VSMCs

Rat primary vascular smooth muscle cells derived from mesenteric arteries of 16 week-old male WKY, SHRSP, SP.WKY$_{Gla}$2a and WKY.SP$_{Gla}$2a rats were isolated by standard collagenase / elastase enzymatic digestion based on a modified version of the protocol described by Yogi and colleagues (Yogi et al., 2011). In summary, 1-3 animals were sacrificed by cervical dislocation and their mesenteric beds were excised and pooled in ice-cold wash media. Maximum storage time was 1h, on ice. Arteries were gently washed off of remaining blood with wash media and then incubated in pre-digestion media (10ml/mesenterium) for 15min, at 37˚C under agitation. Excess fat, connective tissue and adventitia were stripped off in petri dishes containing cold wash media. Clean mesenteric beds were incubated in digestion media (7ml/mesenterium) for 60-90min, at 37˚C under agitation. The digested vessel fragments were subsequently passed through a 21-gauge needle, to obtain a homogeneous suspension, and filtered through a 100µm nylon filter to remove debris. Cell suspension was centrifuged for 2-3min at 800g, re-suspended in 5ml complete growth media, distributed in a T25 flask and kept in a 5% $CO_2$ humidified incubator, at 37°C (passage 0). Media was replaced after 24h. Cells were cultured up to passage 8.

### 2.2.2 Culture and Passage of Primary Rat VSMCs

Cultures of primary cells were passaged at approximately 70-80% confluence, ensuring they were not subject to stress by over or under-confluence. Media was removed and cells were washed in DPBS. Trypsin-EDTA (700µl / 25cm$^2$) or Detachin (1ml / 25cm$^2$), a mild enzymatic solution, were added to the cells and incubated at 37°C for 5min or until the majority of cells were detached. In the case of trypsin-EDTA the enzymatic action was subsequently suspended by the addition of a triple-volume of complete media. Cells were

pelleted by centrifugation at 800g for 3min and re-suspended in either fresh growth media for plating or ice-cold lysis buffer for protein extraction.

### 2.2.3 Cryo-preservation of Primary Rat VSMCs

Cells were harvested as described in section 2.2.2, and re-suspended in cryo-preservation media at a density of approximately 2 x $10^6$ cells/ml. Cell suspension was aliquoted into sterile 1ml cryogenic vials and cooled at a constant -1°C / min down to -80°C, using isopropanol containers. After 24h vials were stored in liquid nitrogen.

For resuscitation, vials were quickly thawed at 37°C until culture was liquefied. Cells were carefully added into pre-warmed complete media and plated in a T25 flask. DMSO-containing medium was replaced the following day.

### 2.2.4 Characterisation of Mesenteric Primary Rat VSMCs

The purity of primary VSMC cultures (% VSMC) was assessed by positive immunofluorescent staining (ICC) for the SMC type-specific marker SMC-α-actin (ACTA2, polyclonal rabbit-anti human; ab5694).

At passage 2, cells were harvested and seeded onto sterile coverslips in 6-well plates and allowed to attach overnight. Media was then removed and cells were rinsed twice with DPBS, fixed in 4% PFA for 15min at rt and washed another three 5min times in DPBS. Cell permeabilisation with TritonX-100 (0.1% in DPBS) for 15min at rt was followed by three 5min DPBS washes. Cells were then incubated with 20% (v/v) serum/DPBS from the appropriate species that the secondary antibody was raised in, which was goat in this case, for 30min at rt, with one further DPBS wash. This was followed by incubation with the primary antibody (1:50 ACTA2 in 20% goat serum/DPBS) or an equivalent dilution of rabbit IgG used as a negative control, for 1h at rt. Excess primary antibody was removed by three 5min DPBS washes. Next, cells were incubated with secondary FITC-conjugated antibody (1:200 goat anti-rabbit IgG in 20% goat serum/DPBS), for 45min at rt. From this point on, coverslips were kept in the dark at all times to prevent photo bleaching of samples. Following a further three 5min DPBS washes to remove excess secondary antibody, coverslips were mounted onto a glass slide using Vectashield supplemented with propidium iodide (PI) for nuclei counter-staining. Coverslips were sealed with nail-varnish and left to dry overnight at rt, then stored at 4˚C. Cells were imaged under a Zeiss LSM 510 Meta confocal microscope (Carl Zeiss Ltd, Hertfordshire,UK) with compatible objectives, at x40 and x100 magnifications.

### 2.2.5 S1P-stimulation of Mesenteric Primary Rat VSMCs

At sub-confluence (~80%), complete growth media was washed off three times with DPBS. Cells were starved overnight (~16h) in serum-free regular DMEM media to induce growth arrest and synchronise cell cycles to the $G_0$ phase. Next day, starvation media was refreshed 30min prior to stimulation. Subsequently, cells were stimulated for 30min, at 37°C, with S1P ($10^{-6}$mol/L) or an equivalent amount of 4mg/ml BSA in $ddH_2O$ (S1P solvent: vehicle), used as a negative control. Stimulation was terminated by washing off the media three times with cold DPBS. After removing DPBS completely, dishes were left upturned to dry and kept temporarily in dry ice or stored at -80˚C until used for whole cell lysate preparation.

In one set of experiments, prior to S1P stimulation, cells were exposed for 30min to VPC23019 (S1PR1/S1PR3 antagonist, $10^{-5}$mol/L) or equal amount of the VPC solvent [vehicle: DMSO/1N HCl (95:5 v/v) diluted (1:20) in 3% BSA (in $ddH_2O$)], used as a negative control.

### 2.2.6 SILAC Labelling of Mesenteric Primary Rat VSMCs

Comparison of the whole proteome of the mesenteric primary VSMCs from WKY, WKY.$SP_{Gla}$2a, SP.$WKY_{Gla}$2a and SHRSP, was performed using stable isotope labelling with amino acids in cell culture (SILAC).

At passage 3, the complete growth media was washed off twice with DPBS and replaced by regular DMEM medium supplemented with 10% dialysed serum. After cells being adapted for 24h, media was washed off and replaced by differentially labelled SILAC media. WKY cells were grown in the control “light”- R0K0 condition, with $^{12}C_6{}^{14}N_4$ L-arginine (Arg0) and $^{12}C_6{}^{14}N_2$ L-lysine (Lys0). SHRSP were “heavy”- R10K8 labelled with $^{13}C_6{}^{15}N_4$ L-arginine (Arg 10; 10Da heavier) and $^{13}C_6{}^{15}N_2$ L-lysine (Lys8; 8Da heavier). The 2a congenic strains were “medium heavy”- R6K6 labelled with $^{13}C_6$ L-arginine (Arg6; 6Da heavier) and $^{13}C_6$ L-lysine (Lys6; 6Da heavier). Cells were grown in the labelled media for 6 divisions, to ensure uniform incorporation of isotopic amino acids into proteins. At passage 7, cells were stimulated with S1P ($10^{-6}$mol/L) as outlined in section 2.2.5 and harvested (section 2.2.2) to be used for proteome profiling.

### 2.2.7 Preparation of Whole Cell Lysates

For protein extraction, cells were harvested as described in section 2.2.2, washed in DPBS and centrifuged for 5min at 800g, 4°C. The pellet was then re-suspended in ice-cold lysis buffer (500µl / T150).

In stimulation experiments (section 2.2.5), after washing off media, petri dishes were left inverted to dry. Two 10cm dishes were used per condition (e.g. vehicle, S1P-stimulated). Dishes were placed on an ice-tray and cells were scrapped off in ice-cold lysis buffer (120µl / dish) and collected into an Eppendorf tube.

The suspension was incubated under rotation at 4°C for 30min and subsequently homogenised by 50 passes through a 25-gauge needle. Cell homogenates were centrifuged at 13,000 x g and 4°C for 15min and supernatant was stored at -80°C until required. Total protein concentration was measured using a BCA-based method as outlined in section 2.3.1.

### 2.2.8 Compartmental Protein Extraction from Cells

Enrichment of cellular compartments in protein was achieved using an Amsbio CNM Compartmental Protein Extraction Kit according to the manufacturer's instructions. Briefly, cells were harvested, counted using a haemocytometer and lysed in an ice-cold hypotonic buffer (C-provided) by passing the suspension through a needle base for approximately 70 times, while on ice. Lysate was compartmentalised in cytoplasmic, nuclear and membranic fractions by serial incubations (20min, 4°C) and centrifugations (20min, 15,000g, 4°C) in respective compartment extraction buffers. Hypotonic buffers C and N were used to break the cytoplasmic and nuclear membranes, respectively, whereas for extraction of membrane proteins the M buffer contained NP-40 detergent. Protein concentration of fractions was measured by BCA assay (section 2.3.1) and samples were stored at –80°C until required.

# 2.3 General Protein Methods

## 2.3.1 Determination of Protein Concentration

Protein concentrations were determined using a Pierce bicichoninic acid (BCA) Protein Assay kit according to the manufacturer's instructions. Serial dilutions of albumin protein standard (provided), ranging from 25µg/ml to 2000µg/ml, was prepared (in lysis buffer) to generate a concentration standard curve for each assay. BCA reagent was prepared by mixing reagents A and B (provided) at a ratio of 50:1. 5µl of the albumin standards / protein samples / lysis buffer (blank) were added to a 96-well plate, in duplicate. Volume in each well was adjusted to 25µl with lysis buffer. BCA reagent (copper sulphate and bicinchonic acid) was then added at a ratio of 8:1 (BCA : sample/standard). Plates were subsequently incubated in dark at 37°C for 15min. At this temperature, protein peptide bonds reduce copper ions in the BCA reagent ($Cu^{2+} \rightarrow Cu^{1+}$). Each $Cu^{1+}$ reacts with 2 molecules of BCA to produce a purple-coloured product detectable at 562nm. The optical density (OD) of the colour is directly proportional to the amount of protein in a sample. Absorbance at 562nm was determined using a Wallac Victor2 plate reader (Wallac, Turku, Finland). An average value of the two replicates was calculated. Concentration of protein in each sample was estimated from the linear equation of the standard curve by Work-Out software (Wallac) and the degree of dilution.

## 2.3.2 SDS-PAGE

In each experiment, equal amounts of protein samples (30-100µg) were diluted to an equal final volume, using $ddH_2O$. Proteins were then denatured by exposure to 1% v/v β-mercaptoethanol (1x sample buffer) and incubation at 70˚C, for 10mins. Samples were resolved by SDS-PAGE on gels of 4 % (w/v) acrylamide stacking buffer and 10-12 % (w/v) acrylamide resolving buffer, depending on the molecular weight of the proteins of interest. A 30% acrylamide / bis-acrylamide mixture was used to form the gels, which were polymerised by addition of APS and TEMED. Full range (10 - 250 kDa) Amersham Rainbow or See Blue Plus2 molecular weight markers were resolved alongside samples to allow size estimation of immunoreactive proteins. Electrophoresis was performed in 0.1 % (w/v) SDS running buffer, at a constant electric potential of 150 volts.

### 2.3.3 Coomassie Staining / De-staining

Following SDS-PAGE, gels containing the resolved proteins (section 2.3.2) were carefully stained in Coomassie solution for at least 30min, under gentle shaking. Gels were then de-stained in Coomassie de-staining solution, until protein bands become clearly visible.

### 2.3.4 In-gel Trypsin Digestion of Coomassie-stained proteins

All steps were performed in a laminar flow hood. Surfaces were cleaned with 70% (v/v) ethanol before use. Gloves were worn at all times to avoid keratin contamination. HPLC grade solvents were used to avoid polymers contamination.

Coomassie-stained gels were rinsed in $dH_2O$ for 10min and placed on a light-surface inside a fume hood. Each lane was divided in 6 subsequent pieces from higher to lower molecular weights. Excised gel pieces were placed in Eppendorf tubes and washed first in 100mM ammonium bicarbonate ($NH_4HCO_3$ - Sigma) and then in 50% (v/v) ACN/100mM $NH_4HCO_3$, pH 8, for another 30min at each stage, on shaker. To reduce peptides, treatment with 100mM $NH_4HCO_3$ / 45mM DTT (fresh) was performed at 60˚C for 30min. Samples were cooled down to rt and alkylated with 100mM iodoacetamide (IAA) (fresh) for 30min in the dark. In-gel reduction of disulphide bonds on cysteine by the mild agent DTT and alkylation of sulphydryl (SH) groups by IAA to prevent re-formation of disulphide bridges, before trypsin digestion, allows for wider protein coverage (Shevchenko et al., 1996). An extra 30min wash was performed in 50% (v/v) ACN/100mM $NH_4HCO_3$, on shaker. Gel pieces were subsequently de-hydrated in 100% (v/v) ACN for 10min and completely dried off in a vacuum centrifuge. Sufficient amount of sequencing grade trypsin (in 25mM $NH_4HCO_3$) was added to re-hydrate each gel piece at a protease/protein ratio of 1:100 to 1:20 (w/w). Protein was digested overnight at 37˚C. Next day, supernatant was transferred to a 96 well-plate. Gel pieces were washed initially with 5% (v/v) formic acid and then with 100% (v/v) ACN for 20min at each stage, at rt. Solvent was transferred to the respective well from the first extraction in the 96 well-plate. Combined extracts were completely dried off in a Speedvac and plate was stored at -20 ˚C until used for LC/MS.

### 2.3.5 Semi-dry Protein Transfer

Proteins separated by SDS-PAGE (section 2.3.2) were subsequently electro-transferred from the gel onto a Hybond-P PVDF membrane by semi-dry transfer. Briefly, gels, filter paper and the PVDF membrane were equilibrated in transfer buffer for 10mins. Then, they were placed on a semi-dry transfer apparatus in the following order: 3 layers of filter paper, then the PVDF membrane, followed by the gel and a further 3 layers of filter paper. Air bubbles from in-between the layers were removed, apparatus lid was placed on and constant current of 180mA was applied for 30-45min. Time of transfer was determined by the number, percentage and thickness of the gels, as well as by the size of the protein(s) of interest. To check the efficiency of the electro-transfer, membranes were finally stained with Ponceau-S for 5min and de-stained with $dH_2O$ and TBST.

### 2.3.6 Western Immunoblotting

Following transfer, PVDF membranes were washed in TBST for 5min prior to incubation with blocking buffer for at least 1h, at rt. Membranes were then probed with primary antibody overnight, at 4°C, under gentle shaking. Primary antibodies were diluted to appropriate concentrations (section 2.1.5) in blocking buffer. After six 5min washes in TBST, membranes were incubated with the appropriate HRP-conjugated secondary antibody diluted in blocking buffer (section 2.1.4), for 2h, at rt. A further six 5min washes in TBST were performed. Immunoreactive proteins were detected using Amersham ECL Western Blotting Detection reagents, as per the manufacturer's instructions. X-ray films were exposed to membranes for 1sec-30min, and developed using a Kodak X-OMAT 2000 developer. Band densitometric quantification (arbitrary units) was performed using ImageJ V1.42 and protein expression levels were normalised to expression levels of housekeeping/control proteins (GAPDH, β-actin).

### 2.3.7 Membrane Re-probing

After film exposure, membranes were washed off ECL buffer twice, for 5min in TBST. Bound antibodies were stripped off by incubation in stripping buffer for 30min, at rt, under mild shaking. Three 5min washes in TBST were followed by a 30min incubation in blocking buffer, at rt. Membranes were re-probed with new primary antibodies and the subsequent steps of immunodetection were performed as described in section 2.3.6.

## 2.4 Immunohistochemistry

Expression levels of S1PR1 in thoracic aortas and kidneys from 21 week-old, salt-loaded, WKY and SHRSP rats were detected by immunohistochemistry (IHC). Tissue collection and fixing (10% v/v formalin) was performed by Dr Caline Coh-Tan. Preparation of paraffinised sections was performed by Mr Andy Carswell.

Prior to histological staining, paraffin was removed from the cut sections by two 7min washes in Histoclear and rehydrated through an ethanol gradient of 100%, 95% and 70% for 7min at each stage and a final 7min rinse in $dH_2O$. Endogenous peroxidase was quenched by incubating slides for 15min in 0.3% (v/v) $H_2O_2$ in methanol, at rt. After two 10min washes in $dH_2O$, antigen was retrieved by heating at 95°C in citrate buffer for 15min, followed by two further 10min washes. Sections were incubated in 2% normal blocking serum (derived from the appropriate species that the secondary ab was raised in) in PBS, for 1h. Subsequently, primary antibodies against S1PR1 (ab23695; IgG rabbit polyclonal) and the positive controls AQP2 (sc-9882; IgG goat polyclonal) and ACTA2 (ab18147; IgGa2 mouse monoclonal), as well as equivalent IgGs (derived from same species primary ab was raised in - used as negative controls) were probed overnight. Antibodies and IgGs were diluted in the appropriate blocking serum at a range of 1/100 to 1/2000. Three 5min washes with PBS were followed by incubation with either biotinylated anti-mouse/rabbit (ABC universal kit) or HRP-conjugated anti-goat secondary antibody, diluted in blocking serum (1/200), at rt, for 30min or 1h, respectively. When ABC universal secondary antibody was used, sections were subsequently incubated with ABC complex for 30min, at rt. Sections were then washed three times in PBS and incubated with the chromogen diaminobenzidine hydrochloride with hydrogen peroxide (DAB substrate kit) for 5min, at rt. Sections were then counterstained with heamatoxylin for 2min, washed in cold running tap water for 5min and dehydrated through a reverse ethanol gradient of 70%, 95% and 100% for 7min at each stage with two final 7min washes in Histoclear. Histomount was used to mount the sections before observation under Olympus BX40 transmitted light microscope, at several magnifications. Positive immunostaining was seen as a dark brown and nuclei appeared blue/purple.

## 2.5 General Ex-Vivo Drug Interventions

Mesenteric resistance arteries (MRA) were isolated from WKY, SHRSP, WKY.$SP_{Gla}$2a and SP.$WKY_{Gla}$2a rats to investigate vascular reactivity by wire myography and vascular remodelling by pressure myography. Animals were sacrificed at 16 weeks of age under terminal anaesthesia with isoflurane. Mesenteries were excised and placed in ice-cold physiological salt solution (PSS). Third order MRAs (2–3 mm in length) were dissected of adherent connective tissue, and stored in PSS at 4˚C, overnight. Tissue collection as well as myograph set up, vessel mounting and normalisations were performed by Mrs Elisabeth Beattie.

### 2.5.1 Wire Myography

Vessel segments were suspended on two stainless steel wires on a four-channel small vessel myograph (DanishMyoTech (DMT), Atlanta, GA). Changes in isometric tension of vessels were detected by a force transducer and recorded by the LabChart (v6.1.1) data acquisition package. Segments were maintained in organ bath chambers filled with PSS pH 7.4, at 37˚C and gassed with 95% $O_2$ - 5% $CO_2$. To achieve maximal contraction, vessels were first allowed to stabilize for 30min at resting tension and then exposed for a further 30min to a predetermined optimal active tension for rat MRAs (lumen diameter normalised to 90% of the diameter expected at transmural pressure of 100 mmHg) (Falloon et al., 1995). Viability of vessels was assessed by a contractile response to treatment with high potassium PSS (KPSS) and maximal active tension between vessels was calculated. Following three PSS washes, vessels were left to rest for 30min. Contractile responses to cumulative doses of the α-adrenergic receptor agonist, noradrenalin (NA, $10^{-9}$ to $3x10^{-5}$ M), were measured first in the absence and again after two PSS washes, in the presence of the Rho-kinase (ROCK) inhibitor Fasudil (3μM) (Asano et al., 1987). Changes in tension in the presence of Fasudil provided a measure of the contribution of Rho kinase pathway on the basal tone. The degree of contraction was calculated and expressed as percentage of the maximal response at $3x10^{-5}$ NA without Fasudil. Similarly, relaxation in response to cumulative doses of the cholinergic agonist carbachol ($10^{-8}$ to $10^{-5}$ M) was assessed in the absence and presence of the endothelial nitric oxide synthase (eNOS) inhibitor, L-NAME (100μM). Changes in tension in the presence of L-NAME indicated effect of endothelial NO on the regulation of basal tone. Relaxation was calculated and expressed as a percentage of sub-maximal (~80%)

contraction to NA at $3x10^{-6}$M. Finally, MRAs were washed 3 times with PSS and allowed to stabilize for 10min. Endothelium-independent vasorelaxation was assessed using cumulative doses of an external donor of NO, the sodium nitroprusside (SNP, $10^{-8}$ to $10^{-5}$M) in a similar manner. Dose response curves were plotted on GraphPad Prism 4. Relaxation and contraction responses were expressed as percentages of the maximal response and statistical analysis was performed using two-way analysis of variance (ANOVA) followed by Bonferroni's multiple comparison test, on GraphPad Prism 4. Differences were considered statistically significant at $P<0.05$.

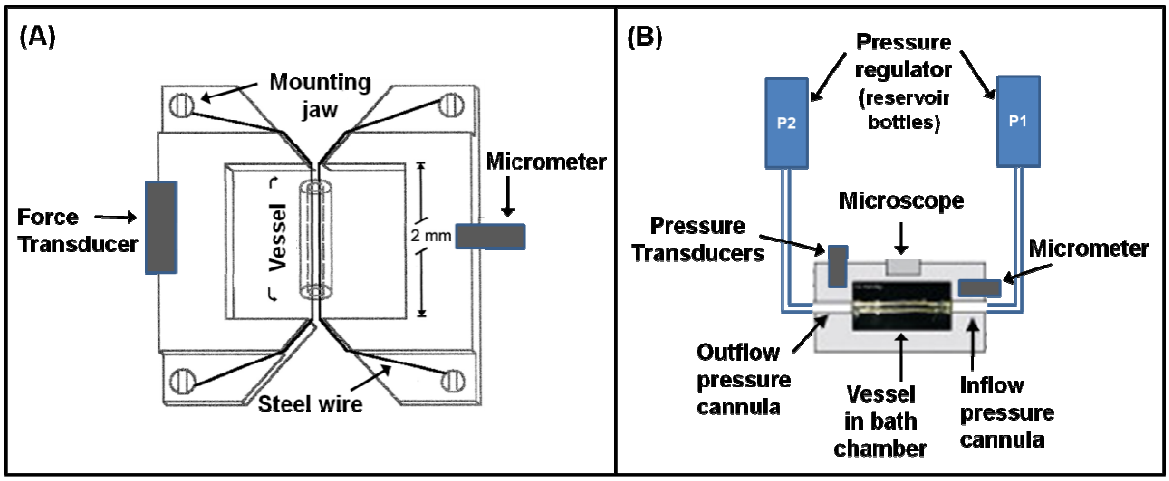


**Figure 2-1. Myography systems. (A) Wire myograph. The vessel segment is mounted on two steal wires. The adjustable jaw is connected to a micrometer screw and the fixed jaw to the force transducer. (B) Pressure myograph. The vessel is mounted onto two glass cannulas. Inflow and outflow pressures are controlled by adjusting the height of Ca-free PSS reservoirs on a tower and are continually recorded by two in-line pressure transducers.**

## 2.5.2 Pressure Myography

Pressure myography is the method of choice for studying structure and mechanics of small vessels, which under exposure to intraluminal pressures assume a physiological shape (Halpern and Osol, 1986; Mulvany and Aalkjaer, 1990).

Vessel segments were tied on the two glass cannulas of a pressure myograph (DMT p100 pressure system, Denmark) using nylon ties. Two in-line pressure transducers continually recorded inflow and outflow pressures, which were controlled by adjusting the height of Ca-free PSS reservoirs on a tower. A Zeiss Axiovert 25 inverted microscope equipped with a CCD Sony XC-75CE monochrome video camera was used to capture a real time video image of the vessel, displayed on a PC monitor by MyoView 1.1 software (DMT,

Denmark). Lumen (internal) and vessel wall (external) diameters were measured at a x200 magnification. Within the bath chamber, MRAs were maintained in Ca-free PSS, pH 7.4, at 37˚C and gassed with 95% $O_2$ - 5% $CO_2$. Vessel lumen was flushed to remove any remaining debris or blood and the segment was straightened without any stretching, by adjusting the micrometer. Vessels were subjected to gradually increasing intraluminal pressure from 10-110 mmHg at 10 and 20 mmHg intervals, lasting 10min each. Internal ($D_i$; lumen width) and external ($D_e$) diameters of vessels were measured and used to calculate structural and mechanical parameters. Structural parameters included cross sectional area (CSA = ($\pi$ / 4) x ($D_e^2$ - $D_i^2$)) and wall to lumen ratio (Wall / lumen = ($D_e$ - $D_i$) / $2D_i$). Mechanical parameters were calculated as previously described by Baumbach and Heistad (Baumbach and Heistad, 1989) and included: Circumferential wall strain = ($D_i$ – $D_0$) / $D_0$, where $D_0$ is the diameter at the lowest intraluminal pressure of 10 mmHg and $D_i$ is the observed internal diameter for a given pressure. Circumferential wall stress = (P x $D_i$) / $D_e$ - $D_i$ where P is the intraluminal pressure. Response curves were plotted on GraphPad Prism 4. Statistical analysis of structural and mechanical parameters was performed using two-way analysis of variance (ANOVA) followed by Bonferroni's multiple comparison test. The strain-stress relation was fitted to an exponential curve for each vessel and the slope of the curve was determined. The slopes were compared between groups using unpaired Student's t-test. Differences were considered statistically significant at $P<0.05$.

# 2.6 Proteomic Profiling

## 2.6.1 Sample Preparation

Comparisons of whole proteome from 16 week-old WKY, SHRSP, WKY.$SP_{Gla}$2a and SP.$WKY_{Gla}$2a were performed on 30min S1P-stimulated primary VSMCs (section 2.2.6). To optimise the experimental design (comparison of 3 experimental groups at a time) triple SILAC labelling (section 2.2.5) was performed, allowing comparison of the proteome from all four groups in just two experiments: (A) WKY - WKY.$SP_{Gla}$2a - SHRSP and (B) WKY - SP.$WKY_{Gla}$2a - SHRSP. After differential labelling cells from each strain were harvested and mixed at 1:1:1 ratio, based on cell number counted with a haemocytometer (Hausser Scientific, US). Following cell lysis (section 2.2.7), the mixed-lysates were processed using SDS-PAGE (section 2.3.2), gel was stained with Coomassie (section 2.3.3) and each lane was divided into 6 gel slices to reduce the complexity of samples for LC separation. Subsequently,

each slice underwent in-gel trypsin digestion (section 2.3.4) and the eluates were stored as individual samples at -80˚C, until used for proteome profiling. The sample preparation procedure is illustrated in Figure 2-2A.

### 2.6.2 Liquid Chromatography – Tandem Mass Spectrometry Analysis

For proteomic profiling, the chemically identical and isotopically distinct SILAC tryptic peptides were distinguished by polarity and mass using reversed-phase rapid separation liquid chromatography (RSLC) operated on a nano-HPLC flow system (Ultimate 3000, Dionex, Camberley, UK), which provides ultrafast, ultrahigh-resolution LC separations using high flow rates. Initially, samples were loaded onto a Dionex 100µm x 2cm, 5µm/100Å pore size, C18 nano trap column, in ACN (98:2) and 0.1% formic acid solution. Samples were then washed off into an Acclaim PepMap C18 nano column 75µm x 15cm, 2µm/100Å pore size at a flow rate of 0.3µm/min. The nano-system was maintained at 35 °C in a column oven. Elution of samples was carried out for 100min, using a gradient of solvent A: 0.1% formic acid versus solvent B: acetonitrile, starting at 5% B and rising to 50% B. Eluted peptides were electrosprayed into an Orbitrap Velos Fourier Transformation mass spectrometer via a Proxeon nanoelectrospray ion source (2.5kV ionisation voltage, 200 °C capillary temperature, Thermo Fisher Hemel, UK). These mass spectrometers enable faster and more reliable detection and identification of proteins in complex mixtures and were operated in positive ion and MS-MS mode, scanning from 380 to 2000 amu. Top 20 most intense ions from each full scan, depending on signal intensity, were isolated for MS/MS fragmentation by collision-induced dissociation (CID) at 35% collision energy. The resulting fragments were detected at ion resolutions of 60,000 for MS scans and 7,500 for MS/MS scans. This work was done by Prof H. Mischak's laboratory.

### 2.6.3 Proteomic Data Processing

Raw MS/MS Orbitrap Velos spectra were extracted using Xcalibur (version 2.2) and processed on MaxQuant software (versions 1.1.1.25, 1.2.0.18 or 1.2.2.6) specific for MS-based quantitative proteomics (Cox et al., 2009). MaxQuant 'Quant' interface initially detected three-dimensional peak and isotope patterns and assembled them into SILAC triplets for quantification. Peptide fragment spectra were filtered through Andromeda, a peptide search engine integrated into the MaxQuant environment (Cox et al., 2011), being unique in accurately distinguishing and identifying co-fragmented peptides from mixture

spectra. Derived peak lists were searched using the Mascot search engine against the mouse and/or rat International Protein Index (IPI version 3.68; minimally redundant but maximally complete combined database) or SwissProt Rodentia peptide sequences database (2011; best annotated database). Cysteine carbamidomethylation was selected as the fixed modification; methionine oxidation, N-terminal protein acetylation, phosphorylation of serine, threonine and tyrosine sites and heavy isotopes of lysine and arginine (Lys6, Lys8, Arg6, Arg10) were selected as variable modifications. MS/MS ion data were searched with a relative peptide mass tolerance of 20ppm. Minimum required peptide length was 6 amino acids. A maximum of two missed cleavages was allowed per tryptic peptide. MaxQuant 'Identify' interface allowed statistical filtering and quantification of identified peptides/proteins (Cox and Mann, 2008). Data extraction and processing through MaxQuant were performed by Dr D. Sumpton, Dr S. Lilla and Dr S. Zanivan (The Beatson Institute). The output of the MaxQuant/Mascot workflow was subsequently submitted to the Perseus platform (version 1.2.0.17 or 1.2.7.4) for bioinformatics analysis and visualisation (http://www.perseus-framework.org). Proteins were filtered for differential expression, using a fold change cut-off of 1.3 (FC=±1.3). To explore relevant biological pathways, networks and processes, all differentially regulated proteins with SwissProt/IPI identifiers, corresponding expression values and FC were imported into Ingenuity Pathway Analysis (Ingenuity®Systems, www.ingenuity.com). Each identifier was mapped to the corresponding protein in the Ingenuity® Knowledge Database. A cut-off of FC=±1.3 was set again to filter for significance. These so called Network Eligible molecules were then overlaid to biological canonical pathways, functions and diseases based on the existing information in the database. Also, networks of Network Eligible molecules were algorithmically generated based on their connectivity. The score for each network represents the degree of relevance of a network to the given list of Network Eligible molecules. The data analysis process is illustrated in Figure 2-2B. Selected differentially expressed proteins were validated by immunoblotting.

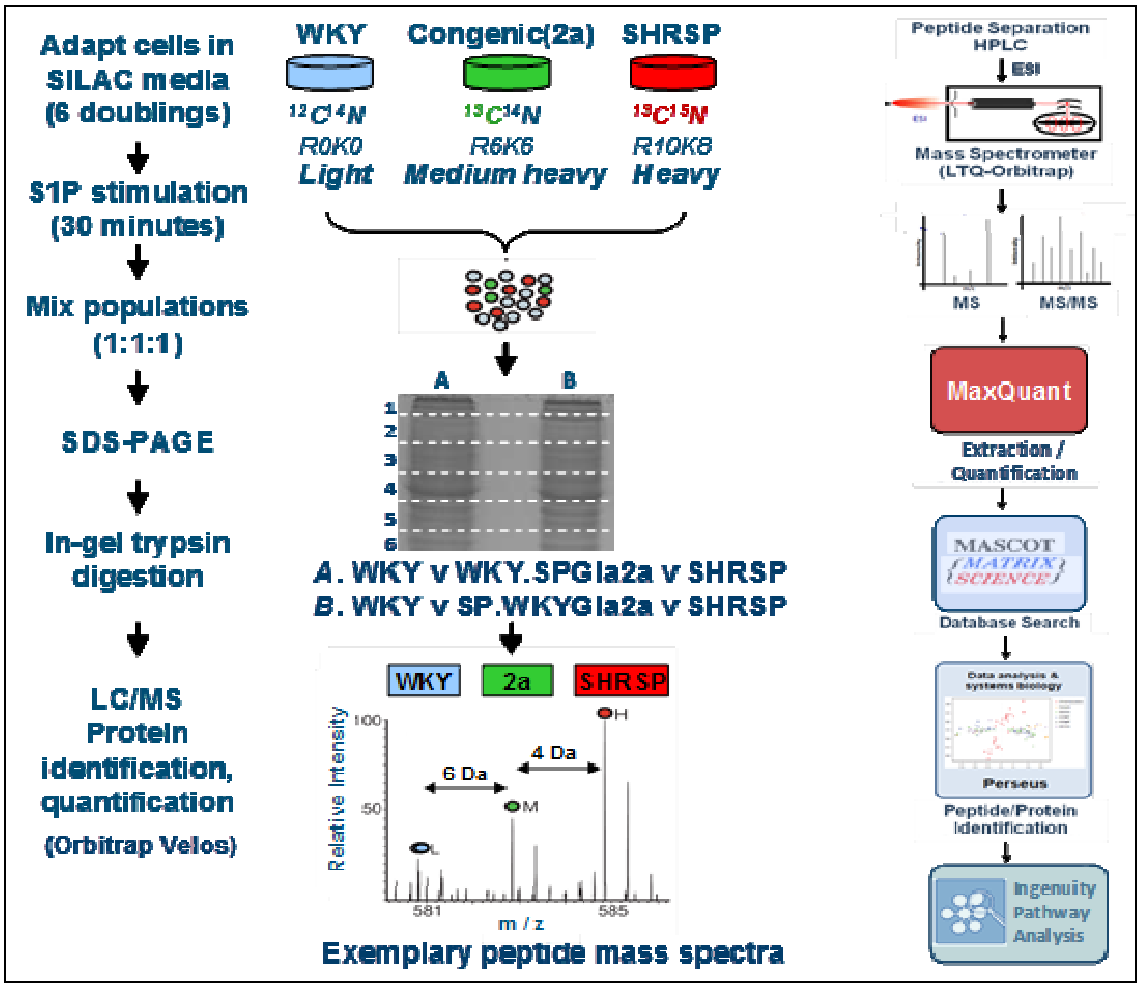


**Figure 2-2 - SILAC proteome profiling of parental and congenic primary S1P-stimulated VSMC. (A) Experimental workflow. Primary mesenteric VSMCs from 16 week-old animals are adapted in DMEM supplemented with 10% dialysed serum, for 24h. Subsequently, cells are transferred into differentially isotope-labeled SILAC media for metabolic labeling. WKY are grown in control "light" condition with $^{12}C_6{}^{14}N_4$ L-arginine (Arg0) and $^{12}C_6{}^{14}N_2$ L-lysine (Lys0), SHRSP are "heavy" labelled with $^{13}C_6{}^{15}N_4$ L-arginine (Arg10) and $^{13}C_6{}^{15}N_2$ L-lysine (Lys8), 2a congenics are "medium" labelled with $^{13}C_6$ L-arginine (Arg6) and $^{13}C_8$ L-lysine (Lys6). After 6 divisions, to ensure isotopic amino acid incorporation, cells are serum-starved overnight, stimulated with S1P ($10^{-6}$M) for 30 min, harvested and mixed in equal numbers (1:1:1, $10^6$): experiment *A*. $WKY_L$ - $WKY.SP_{Gla}2a_M$ - $SHRSP_H$, experiment *B*. $WKY_L$ - $SP.WKY_{Gla}2a_M$ - $SHRSP_H$. Following cell lysis the mixed-lysate (50 µg) is resolved by SDS-PAGE and visualized by Coomassie staining. Each lane (*A, B*) is divided into 6 slices and digested in-gel by trypsin before analysed by LC coupled to MS/MS. Differences in intensity of peptide peak-ratios reflect differences in protein abundance. (B) MS/MS data analysis workflow. Tryptic peptides separated by rapid LC are directed to the Orbitrap Velos mass analyser, through ESI. Raw MS/MS spectra are extracted using Excalibur, filtered and quantified through MaxQuant and associated with amino acid sequences on Mascot search engine. Data is uploaded to Perseus platform for further bioinformatics analysis, and to IPA database for association with relevant biological pathways.**

# 2.7 Metabolomic Profiling

## 2.7.1 Sample Preparation

Mesenteric primary VSMCs from 16 week-old WKY, SHRSP and the two 2a congenic strains were treated for 30mins with S1P or vehicle (section 2.2.5), harvested (section 2.2.2) and lysed in metabolite extraction buffer, as described below. Four biological replicates of each strain were analysed.

Matched urine and plasma samples were collected from 21 week-old male WKY, SHRSP, SP.WKY$_{Gla}$2k congenic and *Gstm1*-transgenic rats fed normal or high-salt (1% NaCl in drinking water) diet as described in section 2.1.1. At 21 weeks of age, rats were housed individually in metabolic cages for 24 hours prior to sacrifice. Urine samples were collected over a 24h period, while stored at 4˚C. Aliquots were snap frozen into liquid nitrogen ($N_{2(l)}$) and stored at -80˚C until use. Blood samples were collected in EDTA at sacrifice, immediately placed on ice and centrifuged within 1h at 1000g, for 10min. Plasma was extracted, aliquoted, snap frozen into $N_{2(l)}$ and stored at -80˚C. Metabolites were extracted from a maximum of 4 biological replicates of matched urine and plasma from each strain, as described below. Salt intervention and sample collection was done by researchers at the Glasgow Cardiovascular Research Centre (BHF/GCRC).

Metabolites were extracted using a slightly modified version of Folch method (Folch et al., 1957). Chloroform was used as the non-polar and methanol as the polar extracting solvents along with water, at a ratio of 1:3:1 (v/v), allowing the extraction of both non-polar and polar, water-soluble and organic-soluble metabolites. Samples were vortex-mixed in metabolite extraction buffer for 1h, at 4°C and then centrifuged at 13.000 g for 3min, at 4°C. Supernatant was stored at -80˚C until metabolomic profiling was performed.

## 2.7.2 Hydrophilic Interaction Liquid Chromatography – Mass Spectrometry

Metabolites were separated by polarity and hydrophilicity using a ZIC-HILIC 4.6mm x 15cm column (Merck SeQuant, Sweden) running at 300µl/min, on a UltiMate 3000 Rapid Separation LC system (Thermo Fisher, UK). Separation is based on weak electrostatic interactions (hydrogen bonds and polar-polar interactions) occurring between hydrophilic metabolites and the zwitterionic stationary phase. Mobile phase gradient ran from 20% $H_2O$-80% ACN to 80% $H_2O$-20% ACN in 30min, followed by a wash at 5% ACN-95% $H_2O$ for 6min

and equilibration at 20% $H_2O$-80% ACN for 8min. HILIC column is much more efficient (peaks up ~38% of molecules) compared to other columns, especially in highly complex samples such as urine. Eluted metabolites were directed via heated electrospray ionisation (ESI) to an Orbitrap Exactive mass analyser (Thermo Fisher), which exhibits ultrahigh mass accuracy and resolution and was operated in both positive and negative detection ion modes. The work was done by researchers at the Glasgow Polyomics Facility.

### 2.7.3 Metabolomic Data Processing

Raw MS data, from positive and negative modes, generated in Orbitrap Exactive was processed using version11/version19 IDEOM Excel interface tools, a standard pipeline suitable for metabolomic LC/MS data analysis (Creek et al., 2012). In specific, raw data was converted into a functional format by msconvert, XCMS library (R-package) was then used for peak picking (Smith et al., 2006a) and mzMatch for related peak annotation, filtering and grouping of samples (Scheltema et al., 2011). IDEOM further allowed for metabolite identification by mass and retention time (RT), using several comprehensive metabolomic and metabolic pathway databases (e.g. HMDB, KEGG, Metacyc) and RT lists of standards (authentic metabolites), as well as for relative quantification using internal standards. IDEOM also enabled advanced visualisation and multivariate statistics by exporting data to R. PeakML Viewer was used for rapid inspection of data quality (peak shape, intensity, confidence levels) and dataset comparisons (Scheltema et al., 2011). Metabolite intensities were corrected for total MS intensity (TIC: total ion current). Student's unpaired t-test was employed to filter for significance, using a p-value (p-val) threshold of 0.05. Datasets containing KEGG identifiers, corresponding expression values and p-val were then uploaded onto Ingenuity Pathway Analysis (IPA) software (Ingenuity®Systems, www.ingenuity.com). Each identifier was mapped to the corresponding metabolite in the Ingenuity® Knowledge Database. A cut-off p-value<0.05 was set to identify significantly changing molecules, called Network Eligible molecules. When overlaid to a global molecular network generated by Ingenuity® Knowledge Database, networks of Network Eligible molecules were algorithmically generated based on their connectivity. Individual metabolites and networks were associated with metabolic processes/pathways and biomarker search. The data analysis pipeline is illustrated in Figure 2-3.

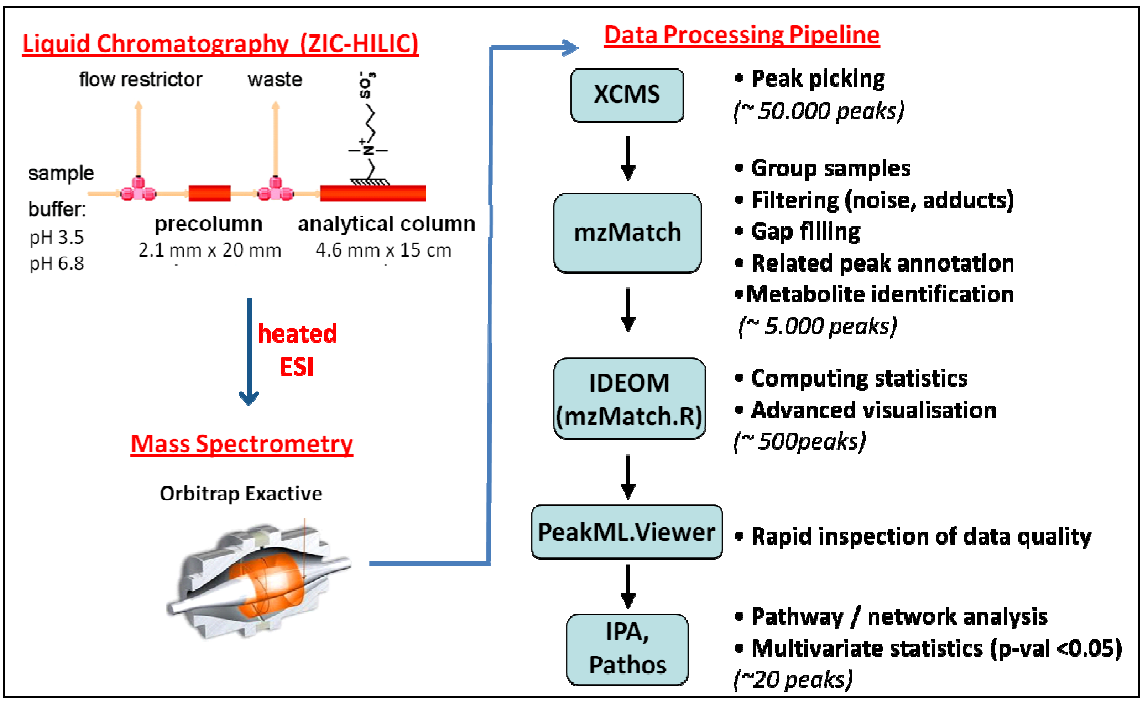


**Figure 2-3 - Metabolomic analysis: sample processing and MS data analysis pipeline. Analytes extracted from cell lysates or biofluids, by methanol/chloroform for 1h at 4°C, are separated by zwitterionic - hydrophilic interaction liquid chromatography (ZIC-HILIC) according to their hydrophilicity, eluted and directed to the Orbitrap Exactive mass analyser through heated electrospray ionisation (H-ESI). Peaks are extracted from raw MS spectra using the XCMS library and processed through the mzMatch/IDEOM pipeline for metabolite identification and further bioinformatics analysis. The number of detected peaks is remarkably reduced along the extensive filtering process. Metabolites reaching statistical significance are finally uploaded to Ingenuity Pathway Analysis (IPA) database for association with metabolic processes and biological interpretation.**

## 2.8 Statistical Analysis

*In vitro* experiments were performed in triplicate on 3 independent occasions, unless otherwise stated. *Ex vivo* myography experiments were carried out with 4 to 12 rats per group. Statistical analysis was performed using Microsoft Excel and Prism Graphpad 4 commercially available software. Results are expressed as Mean ± standard error of the mean (SEM). For specific two-group comparisons, unpaired Student's t-test was used. Comparisons across multiple groups and conditions were made by two-way analysis of variance (ANOVA) followed by Bonferroni's multiple correction test. Statistical significance was considered for p-values <0.05 (two-tailed).

Proteomic data were filtered for fold change, FC ≥ ±1.3. Metabolomic data were filtered for significance using unpaired Student's t-test for p-value <0.05. Canonical pathway analysis identified the pathways from the IPA library that were most significantly associated with the datasets. Proteins/metabolites from the dataset that met the FC/p-value cut-off and were mapped to a pathway in the Ingenuity Pathway Knowledge Base (IPKB) were considered for the analysis.

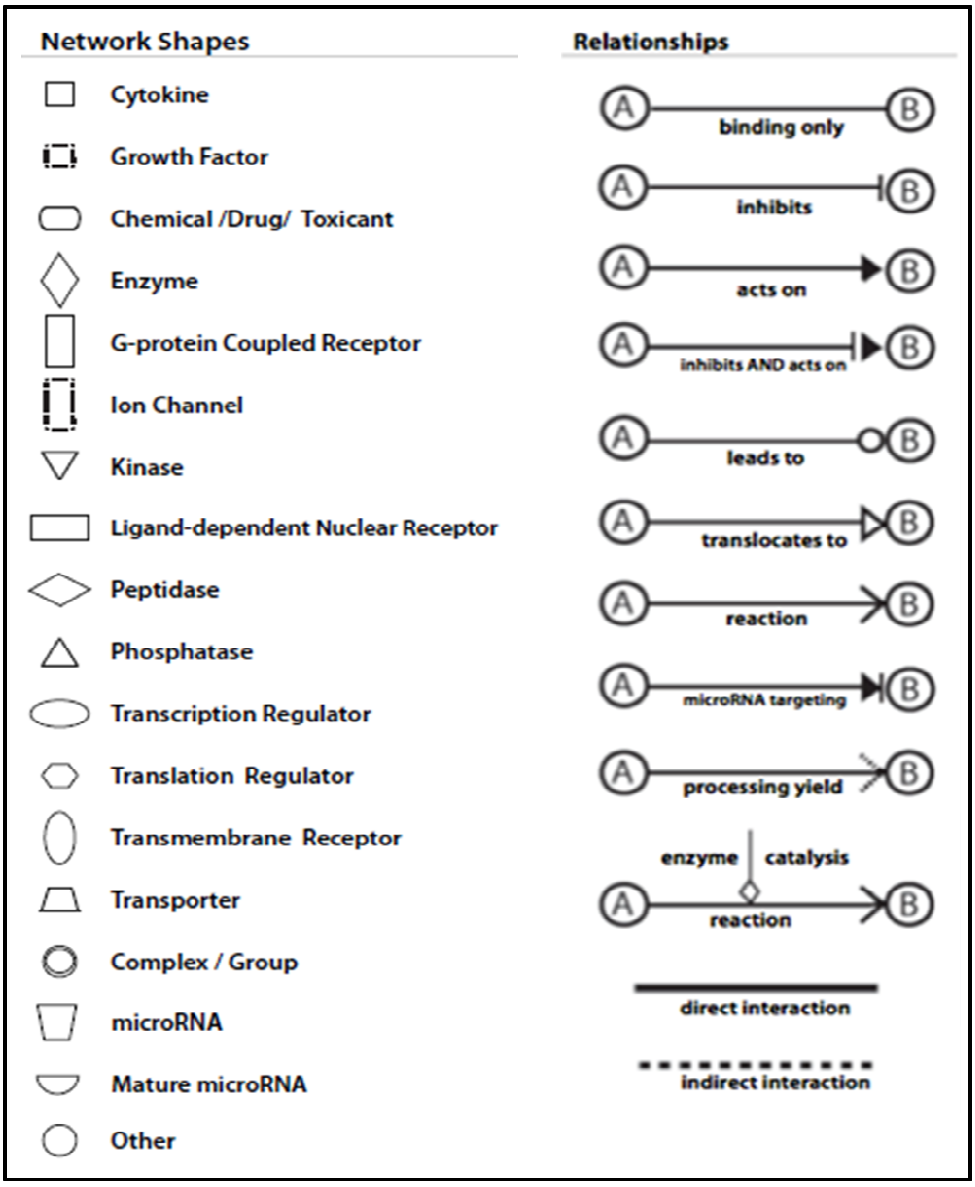


**Figure 2-4 - IPA annotations. This table provides a key of the main features of IPA Network Explorer and Canonical Pathways, including molecule shapes and relationship labels and types. (Ingenuity® Systems, http://www.ingenuity.com).**

# 3 Effects of Salt Loading on S1PR1 Expression and Signalling and on BP Regulation in Salt-Sensitive Rats

# 3.1 Introduction

Essential hypertension (EH) is regularly characterised by exaggerated responses to increased dietary sodium, mainly due to impaired kidney function (Luft et al., 1986). SHRSP, a well-characterised model of human EH, also exhibits salt sensitivity (Ohtaka, 1980, Tesfamariam and Halpern, 1988, Yamori and Okamoto, 1974)**.** Genome-wide linkage studies have identified two QTLs on rat chromosome 2 associated with BP regulation and salt sensitivity (Clark et al., 1996). To confirm and further dissect the genetic components of these QTLs, congenic strains have been generated, using WKY as the donor of chr.2 segments and SHRSP as the recipient strain (Figure 3-1A). Two congenic strains generated by introgression of a 64-cM congenic interval, SP.WKY$_{Gla}$2a (SW2a), and of a smaller 10-cM segment part of the 64-cM region, SP.WKY$_{Gla}$2k (SW2k), exhibit significantly lower SBP to SHRSP, at baseline and under salt-loading. Moreover, they display similarly reduced sensitivity to salt, compared to responses in SHRSP (Figure 3-1B) (Graham et al., 2007). Microarray expression profiling in renal tissue from baseline and salt-loaded parental and chr.2 congenic strains has detected differentially expressed candidate genes for BP and salt-sensitivity. At baseline, *Gstm1* was identified as a positional and functional candidate for BP regulation (McBride et al., 2003). A *Gstm1*-transgenic strain has been constructed in our laboratory, by insertion of the WKY gene into the SHRSP background, demonstrating significantly reduced SBP, similar to that of SW2a and SW2k at baseline, yet upon salt loading an exaggerated increase in SBP is observed (Figure 3-1). Under salt-loading, V*cam1* and *S1pr1* have been identified as two candidate genes for salt-sensitive BP regulation. These genes demonstrated elevated mRNA levels in SHRSP compared to WKY and the SW2a and 2k congenic strains. However, S1PR1 protein levels were decreased in SHRSP, suggestive of abnormal post-transcriptional regulation or protein turnover and subsequent altered signalling in hypertension (Graham et al., 2007).

Therefore, genetic alterations, as well as exogenous perturbations can lead to substantial alterations in the phenotype, through large and diverse impact on numerous metabolic processes. Comprehensive and accurate characterisation of changes in the highly dynamic metabolome, which represents best the actual phenotypic state of a biological system (Breitling et al., 2008, Kell, 2006), can be achieved by use of high-throughput approaches. In metabolomic studies, body fluids are of significant value because of their metabolite-rich content, which reflects at least in part, the actual state of each cell, tissue

and organ in an organism. Plasma and urine are the most commonly used biofluids, due to their availability and ease of collection. In comparison to plasma, urine offers the extra advantages of non-invasive collection, multiple sampling over a period of time and greater stability and resistance to oxidation or precipitation, thus generating more reproducible profiles (von Zur Muhlen et al., 2009). Alterations in the metabolic fingerprint of urine and plasma are representative of the complex pathophysiology during progression of chronic diseases, such as EH. The application of metabolomics in cardiovascular research is an emerging field aiming to define a clearer metabolic picture of CVD for improved prognosis, diagnosis and therapy evaluation (Giovane et al., 2008, Barderas et al., 2011). In clinical diagnostics, the main focus is on identification of disease biomarkers and biofluid samples are typically collected from control and drug treated or diseased subjects. Large-scale metabolomic screenings, using advanced instrumentation and bioinformatics tools, permit discovery of distinct and defined metabolite patterns instead of single biomarkers, which are more informative of the disease complex status.

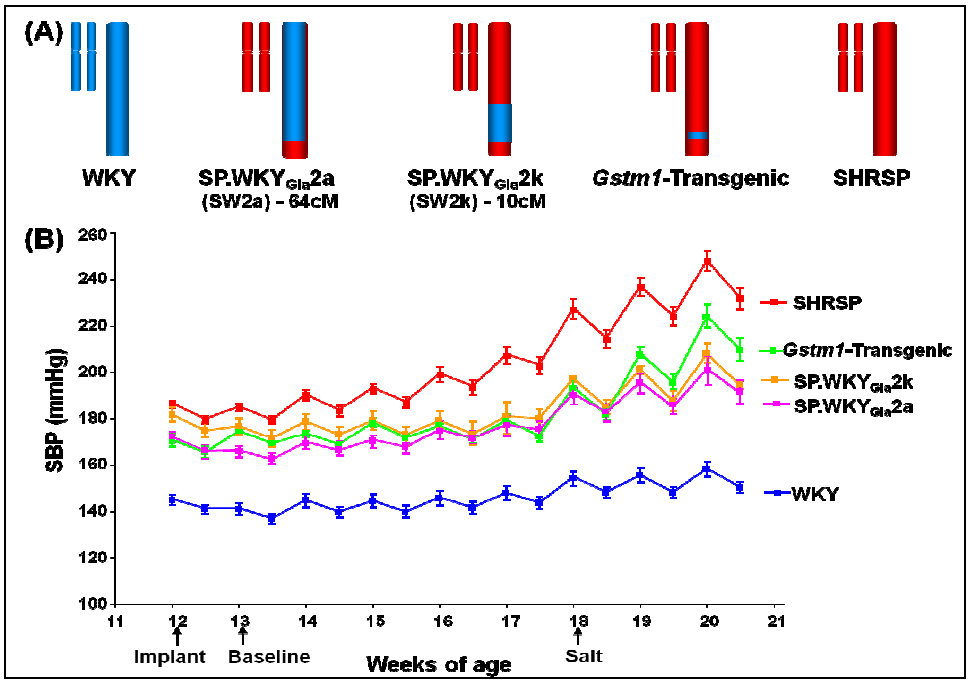


**Figure 3-1 - Chromosome 2 congenic and transgenic strains generated by WKY (donor) and SHRSP (recipient) mating. (A) Schematic of chr.2 from parental, SW2a and SW2k congenic and *Gstm1*-transgenic strains, showing location and size of congenic regions, as well as approximate integration site of the *Gstm1* gene. Blue bars: regions of WKY homozygosity, red bars: regions of SHRSP homozygosity. (B) Averaged weekly radiotelemetry recordings of night-time and day-time SBP in male parental, SW2a and SW2k congenic and *Gstm1*-transgenic strains, under baseline and salt-loaded conditions. Animals were put on high-salt diet at 18 weeks of age. Edited from Graham et al., 2007.**

## Aims

This work is a follow up of previous studies on rat renal tissue identifying *Gstm1* as a candidate gene for BP regulation and *S1pr1* as a candidate for salt sensitivity. We used 21 week-old, WKY and SHRSP parental in combination with SW2a and SW2k congenic and *Gstm1*-transgenic strains aiming to:

- characterise S1PR1 protein expression upon salt-loading, in renal and vascular tissue and compare the expression profiles across salt-resistant (WKY, SW2a, SW2k) and salt-sensitive (SHRSP) strains, by the means of immunohistochemistry (IHC) and western blot (WB) analysis.

- characterise the metabolic profile (signatures/patterns) of salt-sensitivity and identify urine and plasma biomarkers, by comparisons across salt-resistant (WKY, SW2k) and salt-sensitive (SHRSP, *Gstm1*-transgenic) strains, under normal-salt (baseline) and salt-loaded conditions. Untargeted metabolomic screening of urine and plasma was performed (Figure 3-2).

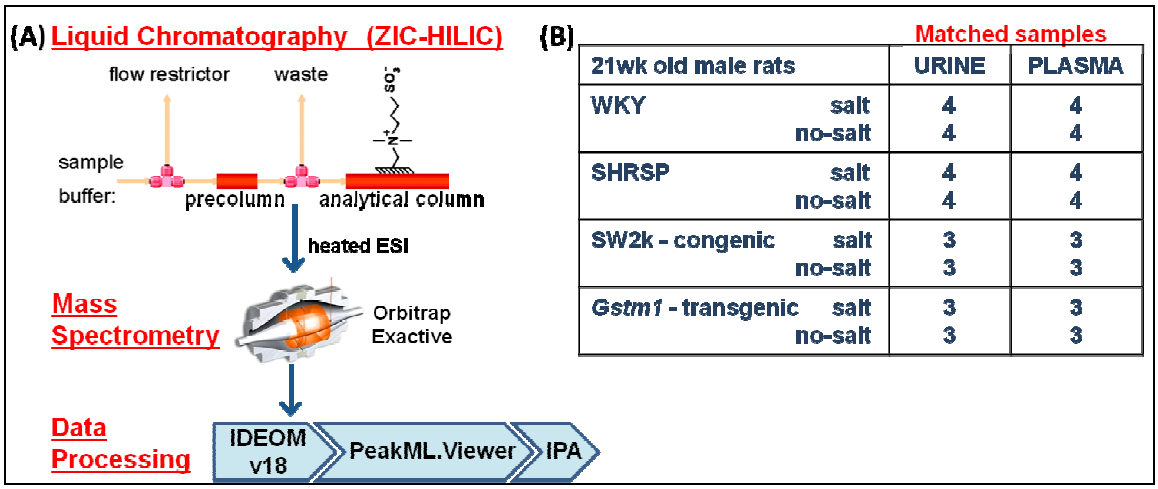


| 21wk old male rats | | URINE | PLASMA |
|---|---|---|---|
| WKY | salt | 4 | 4 |
| | no-salt | 4 | 4 |
| SHRSP | salt | 4 | 4 |
| | no-salt | 4 | 4 |
| SW2k - congenic | salt | 3 | 3 |
| | no-salt | 3 | 3 |
| *Gstm1* - transgenic | salt | 3 | 3 |
| | no-salt | 3 | 3 |

**Figure 3-2 - Metabolomics analysis of urine and plasma from parental, SW2k-congenic and *Gstm1*-transgenic rats. Matched samples were collected from 21 week-old rats, at baseline and under salt-loading. (A) Experimental process. Metabolites were separated by ZIC-HILIC and analysed on an Orbitrap Exactive mass spectrometer. Raw peaks were filtered, identified, quantified and statistically analysed through the IDEOM v18 stringent pipeline and uploaded to databases for biological interpretation. (B) Experimental design. Four biological replicates for WKY and SHRSP and three for SW2k congenic and *Gstm1*-transgenic strains were analysed.**

# 3.2 Results

## 3.2.1 S1PR1 expression in tissues from salt-loaded rats

### 3.2.1.1 S1PR1 renal expression in salt-loaded WKY, SHRSP and congenic strains

S1PR1 expression in kidney from 21 week-old, salt-loaded WKY and SHRSP was assessed by IHC, as described in section 2.4. S1PR1 levels were below detection in the kidney medulla and cortex from both strains (Figure 3-3B and C, bottom panels). Negative IgG controls showed no detectable staining as expected (Figure 3-3; A: left panel, B and C: bottom panels) and positive immunostaining for aquaporin2 (AQP2) gave intense signal on the periphery of medullary collecting ducts and cortical collecting tubules, in kidney from WKY (Figure 3-3A; right panel).

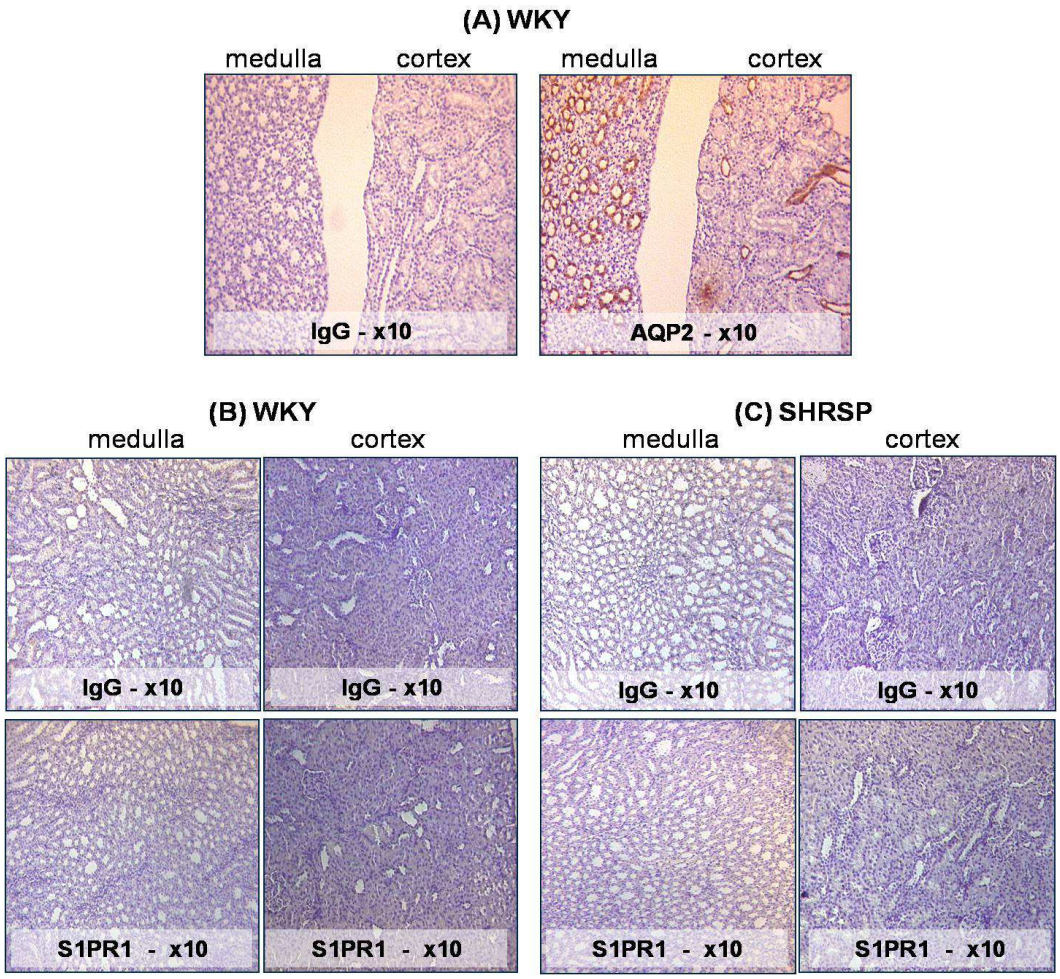


**Figure 3-3 - Characterisation of S1PR1 expression in kidney (medulla and cortex) from 21 week-old, salt-loaded WKY and SHRSP rats, by IHC. (A) Tissue from WKY. Left panel: Isotype (goat IgG) negative control; right panel: positive immunostaining for AQP2, 1/1000. Tissues from WKY (B) and SHRSP (C). Top panels: Isotype (rabbit IgG) negative control; bottom panels: immunostaining for S1PR1, 1/100. Magnification x10.**

To increase concentrations of low abundance proteins, enrichment for cellular compartments was performed on whole kidney homogenates from 21 week-old salt-loaded parental and SW2a and SW2k congenic strains. Western blot for S1PR1 (47 kDa) detected a single strong band in the membrane fraction and a single fainter band in the cytoplasmic fraction, at the expected MW (Figure 3-4; top panels). Expression levels in the membrane fraction were similar across all four strains. Cytoplasmic levels appeared increased in SW2k. Cross-contamination of cellular compartments was tested by stripping and re-probing the membranes for compartment specific markers. GAPDH cytoplasm specific and $Na^+/K^+$ATPase membrane specific markers showed considerable cross-contamination, however enrichment of fractions appeared to be sufficient for detection of S1PR1 (Figure 3-4; middle and bottom panels).

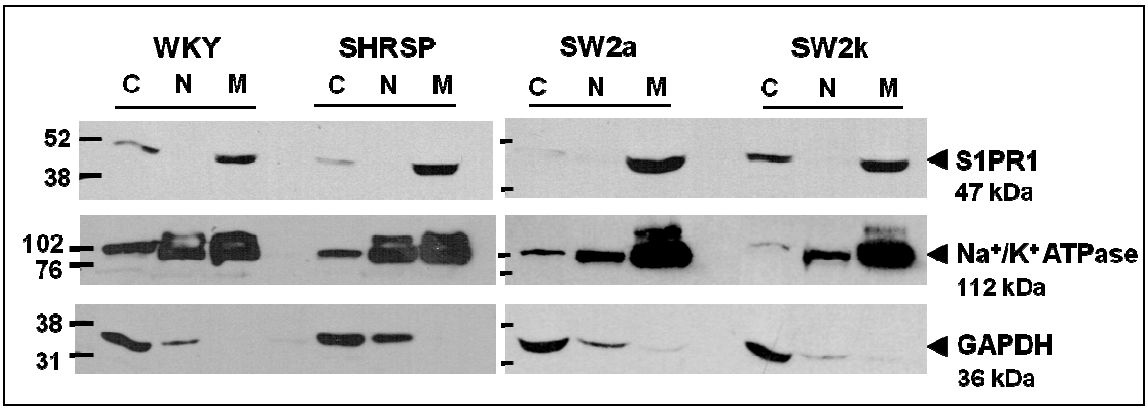


**Figure 3-4 - S1PR1 expression in protein enriched, cellular compartments of whole kidney homogenate, from 21 week-old, salt-loaded parental and SW2a and SW2k congenic strains. Representative immunoblots for S1PR1 (top panel). Membranes were stripped and re-probed with compartment specific markers: $Na^+/K^+$ ATPase membrane marker (middle panel); GAPDH cytosolic marker (bottom panel). Protein loaded: 80 μg (C: cytosolic, N: nuclear, M: membranic fractions). Results are representative of 2 experiments.**

### 3.2.1.2 S1PR1 vascular expression in salt-loaded WKY and SHRSP

S1PR1 expression in thoracic aortas from 21 week-old, salt-loaded WKY and SHRSP was assessed by IHC, as described in section 2.4. S1PR1 levels were below detection in the SM of thoracic aortas from both strains (Figure 3-5B and C, bottom panels). Negative IgG controls showed no detectable staining as expected (Figure 3-5; top panels) and positive immunostaining for α-SMactin2 (ACTA2) (Figure 3-5A; bottom panel) gave widespread signal in the SM of carotid artery from WKY.

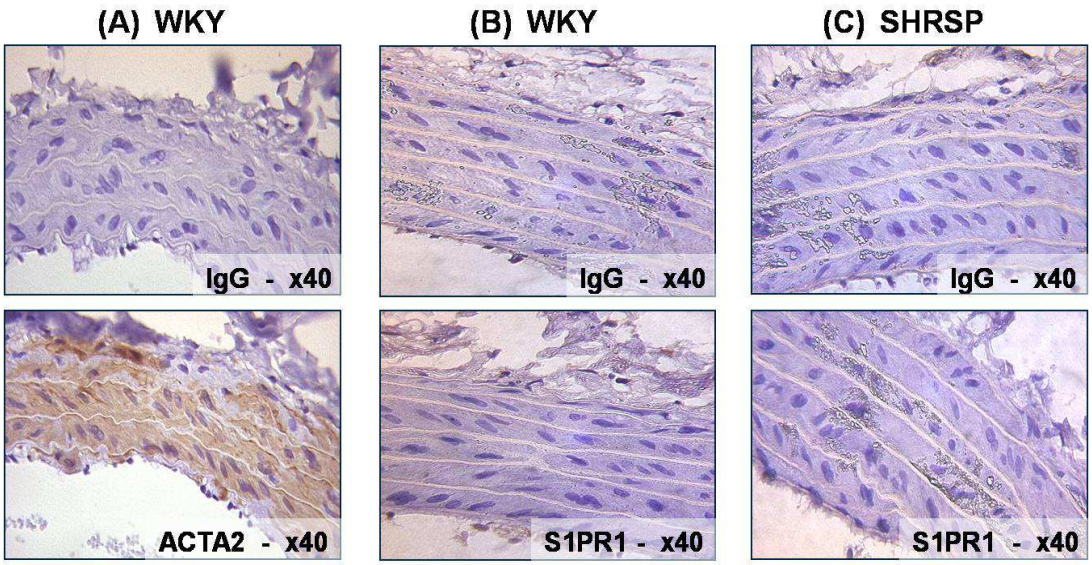


**Figure 3-5 - Characterisation of S1PR1 expression in thoracic aorta from 21 week-old, salt-loaded WKY and SHRSP rats, by IHC. (A) Carotid artery from WKY. Top panel: Isotype (mouse IgG) negative control; bottom panel: positive immunostaining for ACTA2, 1/1000. Thoracic aorta from WKY (B) and SHRSP (C). Top panels: Isotype (rabbit IgG) negative control; bottom panels: immunostaining for S1PR1, 1/100. Magnification x40.**

### 3.2.2 Urine and Plasma Metabolomics and Bioinformatics Analysis

To further investigate the role of candidate genes in salt-sensitive HTN, and assess the effects of salt-loading on BP regulation and sphingosine metabolism, untargeted metabolic profiling was carried out in urine and plasma matched samples from 21 week-old WKY, SHRSP, SW2k congenic and *Gstm1*-transgenic strains, under baseline and salt-loaded conditions. Extracted metabolites from urine and plasma were processed on a ZIC-HILIC - MS platform, as detailed in section 2.7. Stringent filtering of extracted MS data containing thousands of peaks (~50.000) using IDEOM v18, led to identification of a reduced number of positively and negatively ionised putative metabolites (Figure 3-6A): 4849_Plasma_Pos / 3254_Plasma_Neg; 6395_Urine_Pos / 4116_Urine_Neg. The number of metabolites identified in plasma samples were almost two thirds of those identified in urine. Next, metabolites' intensities were corrected to the summed MS intensity (TIC: total ion current) to minimise the uncontrollable effect of exogenous factors (quantification errors). Identification lists of positive and negative modes were then combined (PosNeg) to give the list of putative metabolites to be further analysed: 820_Plasma_PosNeg and 1336_Urine_PosNeg (Figure 3-6A).

The quality of urine and plasma filtered data was assessed by generation of principal component analysis (PCA) plots, which represent the profile of a linear combination of the metabolites identified for each sample. Two representative PCA score plots, where all plasma or urine samples (baseline and salt-loaded) have been plotted together for increased reliability, are illustrated in Figure 3-6B and C, respectively. In both plots, the normotensive and salt-resistant WKY clustered separately from the other three strains under baseline and salt-loading. *Gstm1*-transgenic strain seemed to always cluster together with SHRSP, unlike SW2k which generally displayed more separated clusters, especially at baseline. Moreover, the metabolic profiles between baseline and salt-loaded conditions appeared to be discrete across all strains, although in some plots WKY and WKY-salt clusters exhibited partial overlapping, such as in plasma_positive (Figure 3-6B). Finally, cluster separation in plasma was clearer compared to urine profile.

(A)

| (IDEOM v18) | Plasma Positive | Plasma Negative | Plasma PosNeg (TIC) | Urine Positive | Urine Negative | Urine PosNeg (TIC) |
|---|---|---|---|---|---|---|
| Peaks Detected (mzMatch filter) | 4849 | 3254 | | 6395 | 4116 | |
| Metabolites Identified (central database) | 552 | 387 | 820 | 964 | 610 | 1336 |

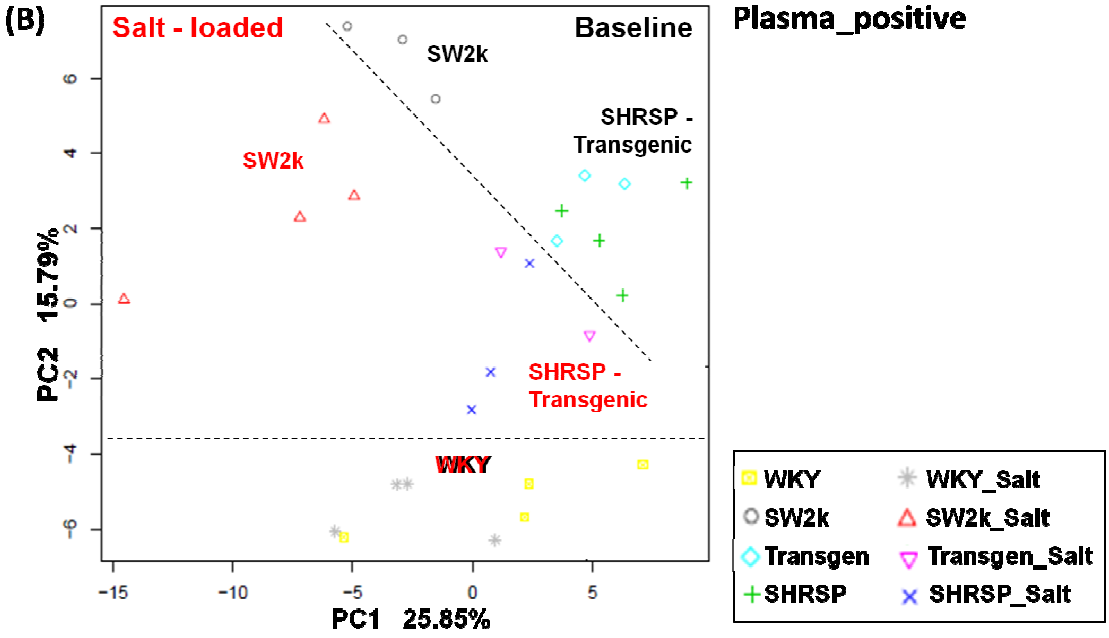


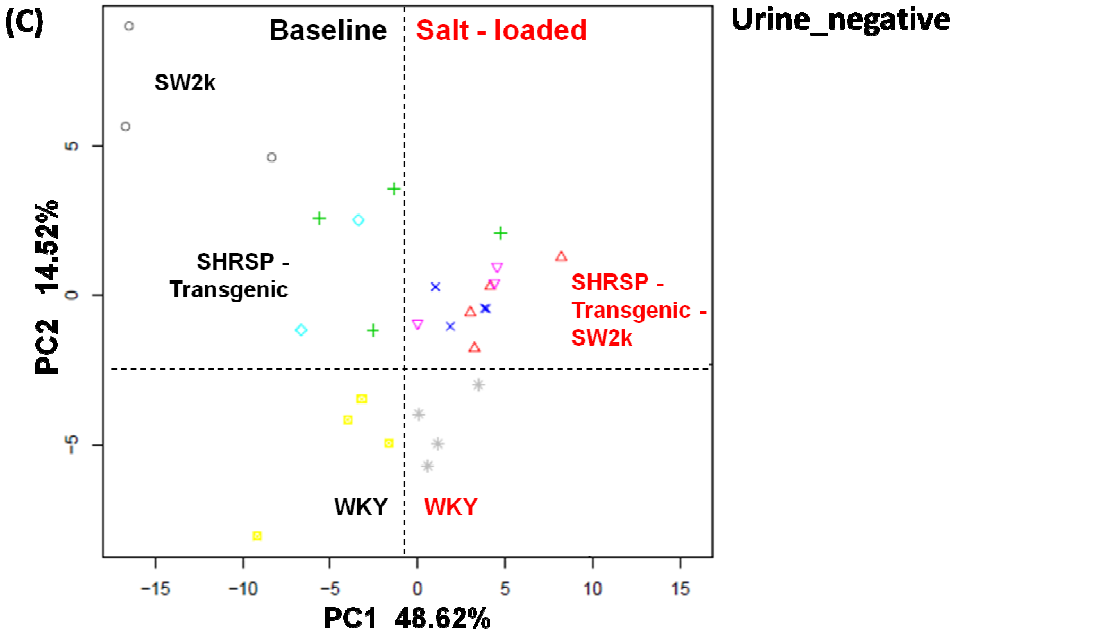


**Figure 3-6 - Orbitrap Exactive MS-data filtering and visualisation on IDEOM v18. (A) Peaks were picked using XCMS, filtered using mzMatch and matched to a set of databases for metabolite identification. The table summarises numbers of putative metabolites identified in the positive and negative modes and collectively (posneg), after correcting for total intensity (TIC), across plasma or**

**urine samples, in all four stains. (B)-(C) PCA score plots for plasma_positive and urine_negative samples, respectively, were generated in R using data from all strains and both baseline and salt-loaded conditions. PC1 and PC2 represent the percentages of metabolites that drive the separation of samples along the axes. Dashed lines indicate separation between WKY and the other strains or between baseline and salt-loaded groups.**

Subsequently, pair-wise comparisons were performed both across strains, under baseline or salt-loading (Figure 3-7), and across salt-challenged conditions (salt_v_baseline) (Figure 3-8), in urine and plasma. Unpaired t-test was utilised to determine significance (p-val <0.05). Approximately one third of the identified metabolites, in each of the comparisons at baseline and at salt-loaded conditions, were found to be significantly changed, both in urine and plasma. The only exception was the plasma comparison under salt-loading between *Gstm1*-tansgenic and SW2k, which exhibited a smaller ratio of significant differences (610_total / 105_significant) (Figure 3-7A). In the comparisons across baseline and salt-loading, WKY displayed lower ratio of significant changes in plasma compared to the other three strains (555_total / 71_significant). However, in urine, WKY had similar ratio to SW2k, which was smaller than these of SHRSP and the transgenic (Figure 3-8).

When data was uploaded onto IPA, approximately one half of the significant metabolites were identified by their KEGG IDs (Figure 3-7A and Figure 3-8A). These significant 'analysis ready' molecules were used for biological interpretation and biomarker analysis. Tables of original data (IDEOM v18) and of significantly changing metabolites, for all comparisons and intersections of interest, are included in the 'Urine' and 'Plasma' subfolders of the 'Chapter 3 - Urine, Plasma metabolomics' folder, in the hard copy (CD) accompanying this thesis.

(A)

| 21 weeks old rats, ± salt (IDEOM v18) | Plasma PosNeg | | | Urine PosNeg | | |
|---|---|---|---|---|---|---|
| | All | p-val <0.05 | IPA (analysis ready) | All | p-val < 0.05 | IPA (analysis ready) |
| SHRSP v WKY (baseline) | 579 | 167 | 86 | 914 | 258 | 125 |
| SHRSP v SW2k (baseline) | 598 | 132 | 62 | 977 | 237 | 111 |
| SHRSP v Trans (baseline) | 585 | 125 | 52 | 880 | 254 | 121 |
| SHRSP v WKY (salt) | 593 | 185 | 86 | 933 | 368 | 161 |
| SHRSP v SW2k (salt) | 614 | 158 | 68 | 892 | 364 | 174 |
| Trans v SW2k (salt) | 610 | 105 | 56 | 844 | 269 | 129 |
| Trans v WKY (salt) | 582 | 133 | 61 | 905 | 281 | 127 |

(B)

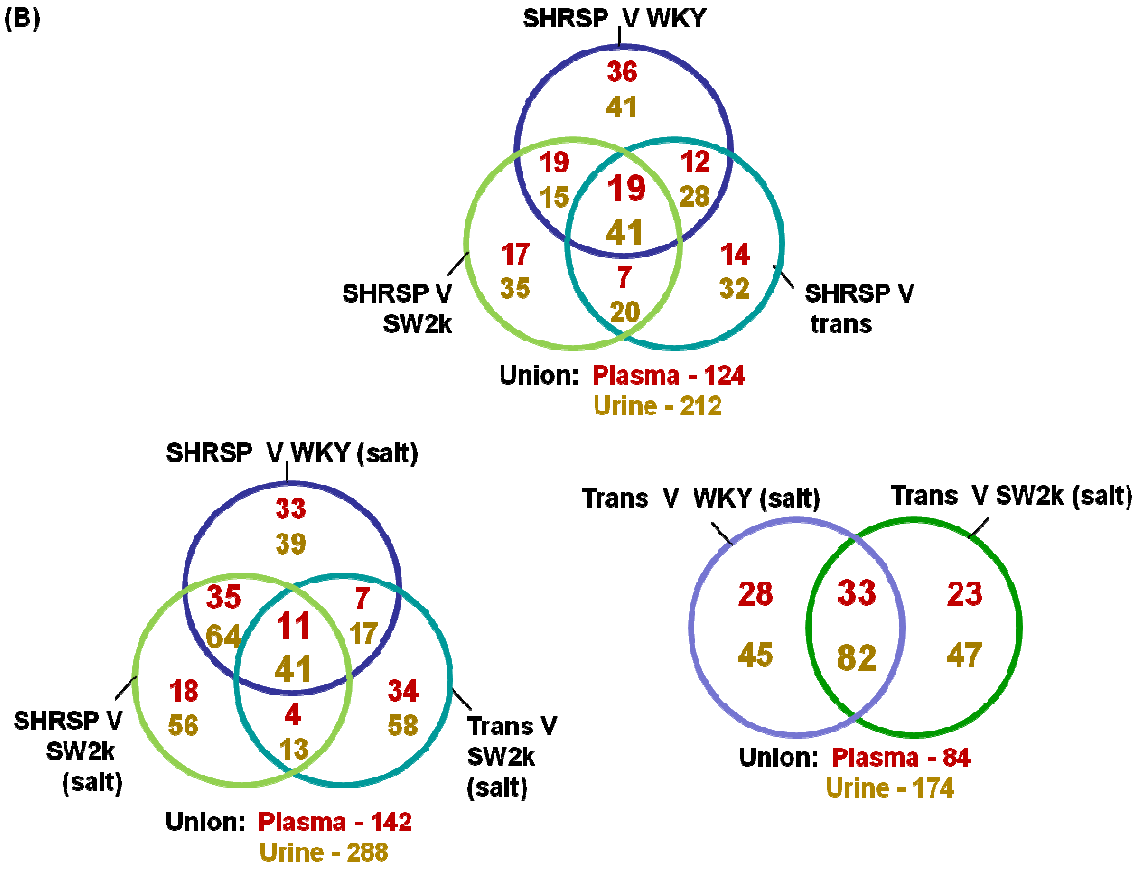


**Figure 3-7 - Comparisons of interest between WKY, SHRSP, SW2k congenic and *Gstm1*-transgenic strains, at baseline and salt-loading, in plasma and urine. (A) Summary table of numbers of putative metabolites identified collectively in positive and negative modes (posneg), of significantly changing metabolites (p-val <0.05) and of significant metabolites identified on IPA as 'analysis ready', across the comparisons. (B) Venn-diagrams of 'analysis ready' metabolites for comparisons of interest.**

(A)

| Salt Comparisons (IDEOM v18 ) | Plasma PosNeg | | | Urine PosNeg | | |
|---|---|---|---|---|---|---|
| | All | p-val <0.05 | IPA (analysis ready) | All | p-val <0.05 | IPA (analysis ready) |
| WKY_salt v WKY | 555 | 71 | 31 | 908 | 355 | 154 |
| SHRSP_salt v SHRSP | 600 | 160 | 64 | 926 | 235 | 102 |
| SW2k_salt v SW2k | 608 | 136 | 61 | 963 | 414 | 199 |
| Trans_salt v Trans | 609 | 115 | 45 | 840 | 220 | 103 |

(B)

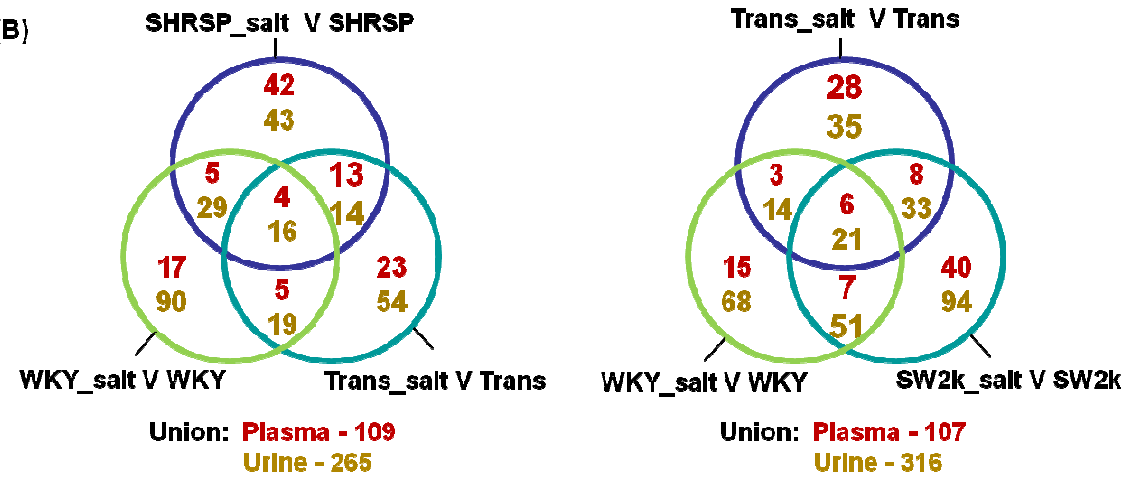


**Figure 3-8 - Comparisons of interest across baseline and salt-loaded conditions in plasma and urine from WKY, SHRSP, SW2k congenic and *Gstm1*-transgenic strains. (A) Summary table of numbers of putative metabolites identified collectively in positive and negative modes (posneg), of significantly changing metabolites (p-val <0.05) upon salt-challenge, and of significant metabolites identified on IPA as 'analysis ready', across different comparisons. (B) Venn-diagrams of 'analysis ready' metabolites for comparisons of interest.**

#### 3.2.2.1 Urine metabolomic profiling at baseline and upon salt-loading

At baseline, comparison of SHRSP urine metabolic profile to the other three strains identified 41 common, significantly changing metabolites across the three comparisons: SHRSP_v_WKY, SHRSP_v_Trans and SHRSP_v_SW2k (Figure 3-7B; top venn-diagram). The above metabolites mapped to a variety of functions and diseases on IPA, rather than highlighting a few specific ones. Of the 41, 25 displayed consistent direction of change, with 24 being constantly increased and 1 decreased in SHRSP. Table 3-1 summarises data for some of the metabolites. 19 out of the 24 increased metabolites were detected only in SHRSP and exhibited fold changes (FC) between 2.610 and 9535.108. Complete data for all 41 metabolites can be found in the 'Urine/Baseline/Urine_base_IC3_41_IPA' supplementary table.

Further network analysis on IPA explored potential relation of the 41 significant metabolites to GSTM1 and GSTM5 (rat and human homologues), in an attempt to more restrictively identify molecules implicated in the improved BP phenotype of *Gstm1*-transgenic compared to SHRSP (Figure 3-9). N-acetyl-L-cysteine (NAC) was an interesting metabolite connected to GSTM5 through molecules implicated in oxidative stress, lipid metabolism and CVD. NAC was reduced in SHRSP compared to WKY (FC=-2.006) and SW2k (FC=-2.101), but its levels were highly increased in comparison to *Gstm1*-transgenic (FC=202.72).

**Table 3-1. Subset of the 41 'in common' urine metabolites exhibiting consistent, significant change across the comparisons of SHRSP versus WKY, SW2k and *Gstm1*-transgenic, at baseline. Data were generated on IDEOM v18. Green: decreased and red: increased metabolite levels.**

| KEGG id | Putative metabolite | Fold Change | P-value | Fold Change | P-value | Fold Change | P-value |
|---|---|---|---|---|---|---|---|
| | | SHRSP v WKY | | SHRSP v SW2k | | SHRSP v Trans | |
| C03089 | 5-methylthio-D-ribose | 802.718 | 0.001 | 802.718 | 0.001 | 802.718 | 0.001 |
| C02376 | 5-methylcytosine | 561.482 | 0.003 | 561.482 | 0.003 | 561.482 | 0.003 |
| C03793 | N6,N6,N6-trimethyl-L-lysine | 72.784 | 0.009 | 72.784 | 0.009 | 72.784 | 0.009 |
| C06325 | 2-quinolinecarboxylic acid | 72.749 | 0.009 | 72.749 | 0.009 | 29.701 | 0.008 |
| C03404 | tyrosine methyl ester | 45.489 | 0.005 | 45.489 | 0.005 | 45.489 | 0.005 |
| C10454 | methyleugenol | 23.719 | 0.001 | 23.719 | 0.001 | 23.719 | 0.001 |
| C00275 | mannose-6-phosphate | 22.214 | 0.004 | 22.214 | 0.004 | 22.214 | 0.004 |
| C08276 | 3-(methylthio)propionic acid | 17.090 | 0.005 | 17.090 | 0.005 | 17.090 | 0.005 |
| C01047 | N5-ethyl-L-glutamine | 13.427 | 0.002 | 13.427 | 0.002 | 13.427 | 0.002 |
| C00438 | N-carbamoyl-L-aspartic acid | 11.043 | 0.010 | 11.043 | 0.010 | 11.043 | 0.010 |
| C12453 | acetylpseudotropine | 6.075 | 0.005 | 6.075 | 0.005 | 6.075 | 0.005 |
| C03002 | N-caffeoylputrescine | 5.382 | 0.016 | 5.382 | 0.016 | 5.382 | 0.016 |
| C00670 | sn-glycero-3-phosphocholine | 5.320 | 0.013 | 5.320 | 0.013 | 5.320 | 0.013 |
| C06156 | D-glucosamine 1-phosphate | 3.843 | 0.018 | 3.843 | 0.018 | 3.843 | 0.018 |
| C01026 | dimethylglycine | 952.889 | 0.001 | 1.614 | 0.016 | 952.889 | 0.001 |
| C02220 | 2-aminomuconate | -2.156 | 0.028 | -1.737 | 0.013 | -3.069 | 0.001 |

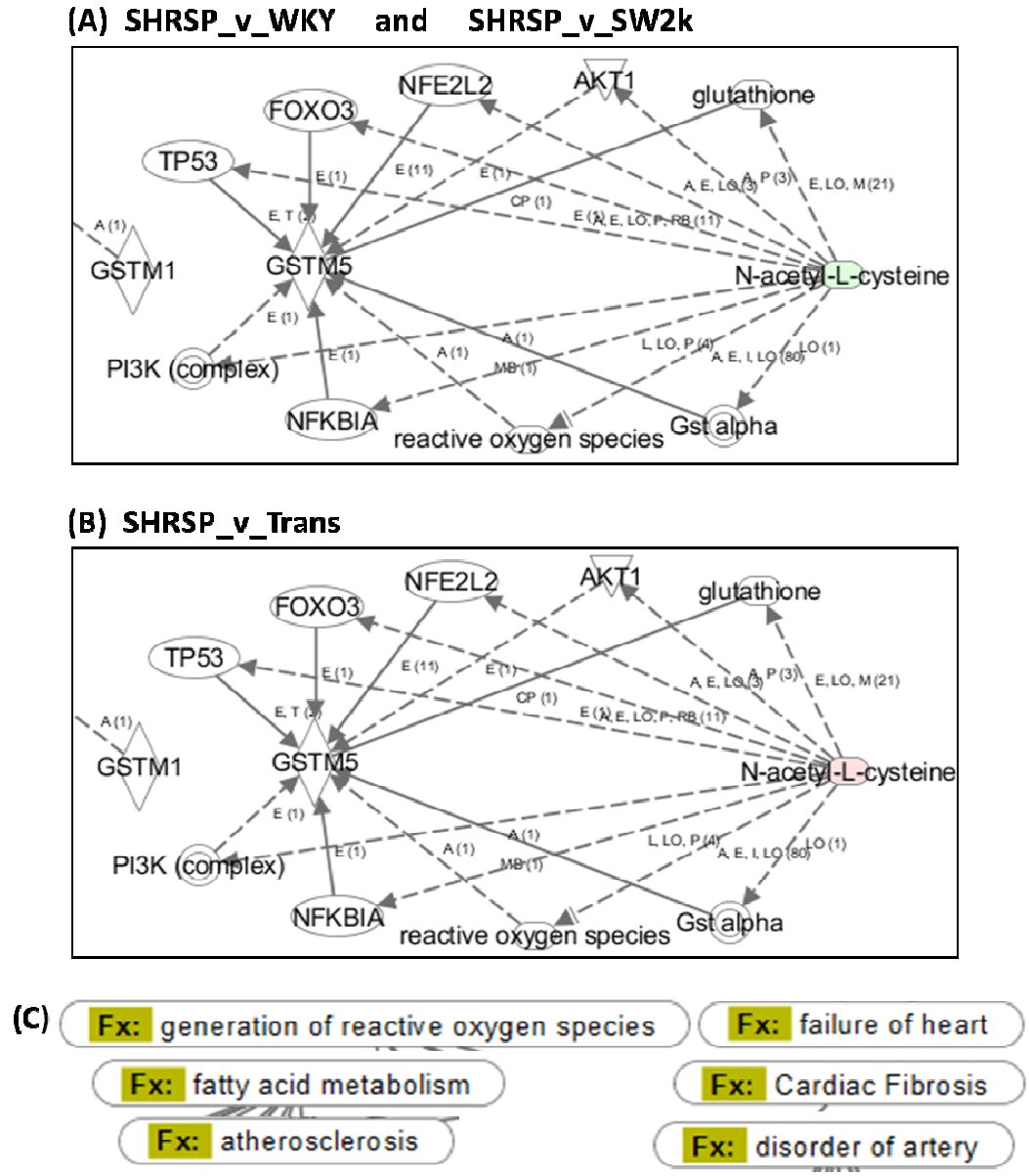


**Figure 3-9 - Ingenuity Pathway Analysis (IPA) network associating urine N-acetyl-L-cysteine with GSTM1 and GSTM5 (glutathione S-transferase mu 1/5). N-acetyl-L-cysteine (NAC) baseline levels were significantly deceased in the SHRSP_v_WKY and SHRSP_v_SW2k comparisons (A) and significantly increased in the SHRSP_v_ *Gstm1*-transgenic comparison baseline (B). (C) NAC was associated to GSTM5 through molecules implicated in ROS generation, fatty acid metabolism, arterial and cardiac disorders. TP53: tumour protein p53; FOXO3: forkhead box O3; NFE2L2: nuclear factor (erythroid-derived 2)-like 2; AKT1: serine-threonine protein kinase AKT1; PI3K: 1-phosphatidylinositol 3-kinase; NFKBIA: nuclear factor of kappa light polypeptide gene enhancer in B-cells inhibitor, alpha; Gst alpha: glutathione S-transferase alpha. Colour indications: green - decrease, red - increase, white - not detected.**

Subsequently, urine metabolic profiles of salt-loaded animals were compared. Comparison of the SHRSP and *Gstm1*-transgenic salt-sensitive versus the WKY and 2k salt-resistant strains identified 21 metabolites that were changing across all four comparisons: SHRSP_v_WKY, SHRSP_v_SW2k, Trans_v_WKY and Trans_v_SW2k. 14 of these metabolites were consistently increased in the salt-sensitive strains and all but one were detected only in the SHRSP and *Gstm1*-transgenic, having FC that ranged from 3.313 to 5555.425. Table 3-2 summarises data for some of the metabolites. Complete data for all 21 metabolites can be found in the 'Urine/Salt/Urine_salt_IC4_21_IPA' supplementary table.

**Table 3-2. Subset of the 21 'in common' urine metabolites exhibiting significant change across the comparisons of SHRSP and *Gstm1*-transgenic versus WKY and SW2k, under salt loading. Data were generated on IDEOM v18. Green: decreased and red: increased metabolite levels.**

| KEGG id | Putative metabolite | Fold Change | P-value | Fold Change | P-value | Fold Change | P-value | Fold Change | P-value |
|---|---|---|---|---|---|---|---|---|---|
| | | SHRSP v WKY | | SHRSP v SW2k | | Trans v WKY | | Trans v SW2k | |
| C00715 | 2-amino-4-hydroxyaminopteridine | 3.313 | 0.001 | 3.313 | 0.001 | 5.056 | 0.017 | 5.056 | 0.017 |
| C01801 | 2-deoxy-D-ribose | -1.321 | 0.015 | -1.411 | 0.029 | 1.622 | 0.009 | 1.330 | 0.043 |
| C00632 | 3-hydroxyanthranilic acid | 304.287 | 0.001 | 304.287 | 0.001 | 546.148 | 0.004 | 546.148 | 0.004 |
| C02230 | 3-methylguanine | -1.241 | 0.001 | -1.344 | 0.008 | 1.281 | 0.001 | 1.183 | 0.019 |
| C03672 | 4-hydroxyphenyllactic acid, (DL)-isomer | -2.199 | 0.000 | 67.177 | 0.001 | -1.418 | 0.006 | -1.292 | 0.039 |
| C00221 | beta-D-glucose | 6.801 | 0.031 | 9.604 | 0.033 | 9.974 | 0.013 | 14.085 | 0.023 |
| C16526 | gondoic acid | 2.103 | 0.001 | 2.103 | 0.001 | 3.989 | 0.001 | 3.989 | 0.001 |
| C05842 | N'-methyl-2-pyridone-5-carboxamide | 3167.422 | 0.002 | 3167.422 | 0.002 | 5555.425 | 0.006 | 5555.425 | 0.006 |
| C00712 | oleic acid | 6.043 | 0.005 | 6.043 | 0.005 | 13.526 | 0.022 | 13.526 | 0.022 |
| C00408 | S-pipecolic acid | -1.613 | 0.018 | 2283.527 | 0.007 | -1.319 | 0.037 | 2792.030 | 0.006 |
| C10172 | stachydrine | 591.528 | 0.007 | 591.528 | 0.007 | 1348.975 | 0.004 | 1348.975 | 0.004 |
| C00178 | thymine | 37.785 | 0.004 | 37.785 | 0.004 | 63.453 | 0.021 | 63.453 | 0.021 |

Further network analysis on IPA associated 3-hydroxyanthranilic acid (consistently increased), oleic acid (consistently increased), pipecolic acid (decreased in comparisons with WKY) and 2-deoxy-D-ribose (decreased in SHRSP) with molecules implicated in lipid metabolism, inflammatory response, CVD and oxidative stress (Figure 3-10).

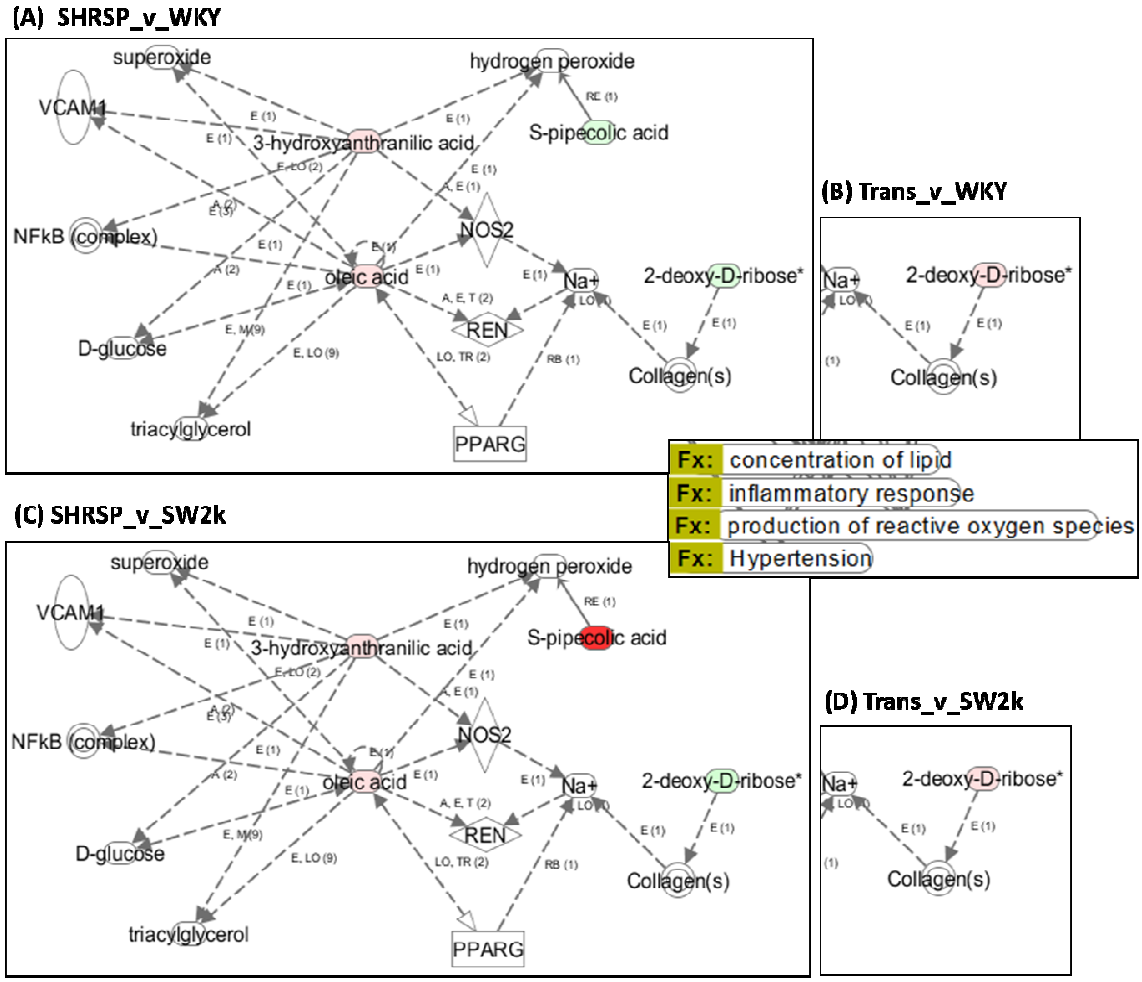


**Figure 3-10 - IPA network of urine metabolites significantly changing in the salt-sensitive versus the salt-resistant strains, upon salt-loading. (A) Changes in the SHRSP_v_WKY. (B) Changes in the *Gstm1*-transgenic _v_WKY followed same direction as in SHRSP_v_WKY apart from 2-deoxy-D-ribose. (C) Changes in the SHRSP_v_SW2k. (D) Changes in the *Gstm1*-transgenic _v_ SW2k comparison. The altered metabolites were associated to molecules implicated in lipid metabolism, inflammatory response, ROS production, CVD. VCAM1: vascular cell adhesion molecule 1; NFkB: nuclear factor kappa-light-chain-enhancer of activated B cells; NOS2: nitric oxide synthase 2; REN:renin; PPARG: peroxisome proliferator-activated receptor gamma; $Na^+$: sodium. Colour indications: green - decrease, red - increase, white - not detected. Asterisk indicates more than one potential isomers.**

Finally, assessment of peak quality for the metabolites of interest that were identified in the urine comparisons, was performed on peakML.Viewer. Figure 3-11 illustrates the peak chromatograms of selected metabolites which demonstrated relatively good peak shape and reproducibility.

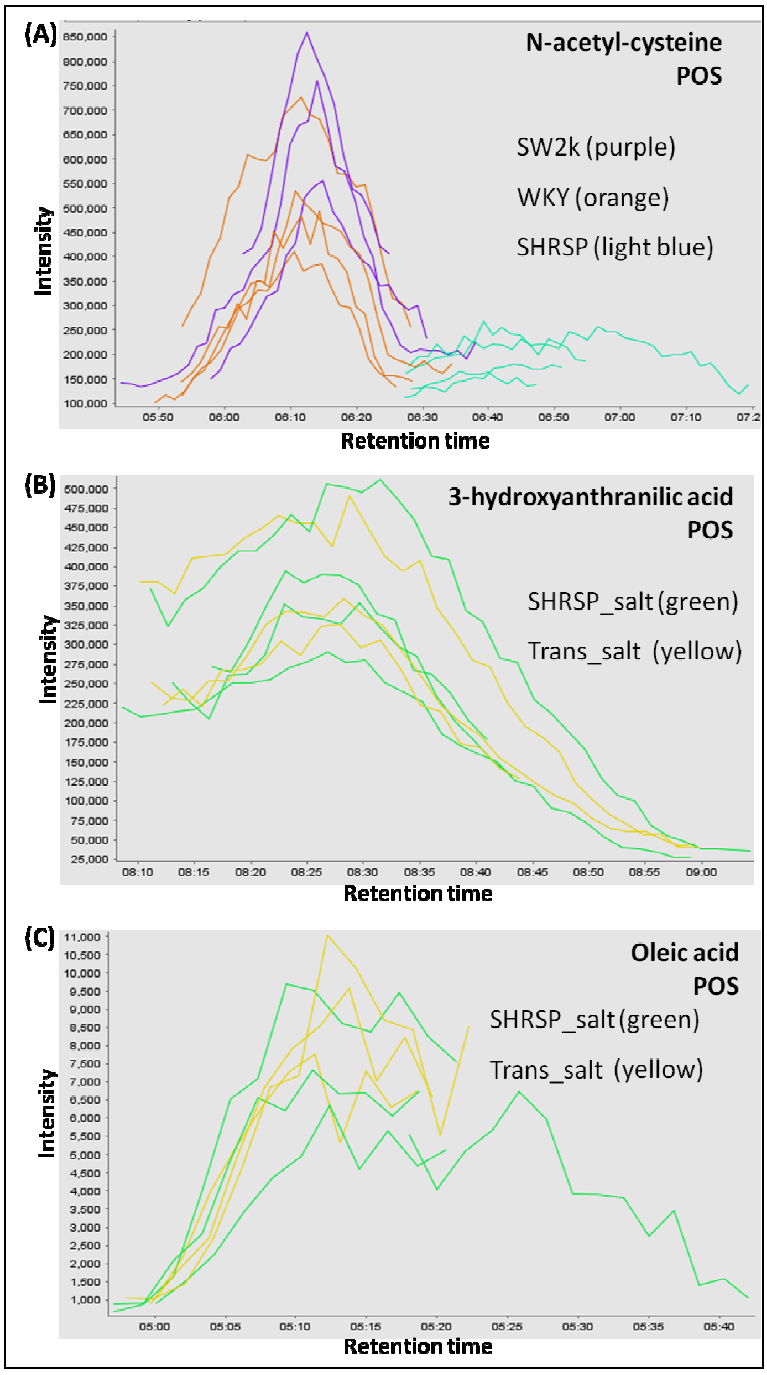


**Figure 3-11 - PeakML chromatograms of metabolites of interest identified in urine comparisons across WKY, SHRSP, SW2k and *Gstm-1* transgenic strains, at baseline or salt-loaded conditions. (A) N-acteyl-cysteine exhibited significant decrease at baseline in SHRSP compared to WKY and SW2k and was not detected in the transgenic. At salt-loading, (B) 3-hydroxyanthraniclic acid and (C) oleic acid were increased in SHRSP and transgenic animals compared to WKY and SW2k. The x-axis indicates the retention time and the y-axis the intensity.**

#### 3.2.2.2 Plasma metabolomic profiling at baseline and upon salt-loading

At baseline, comparison of SHRSP plasma metabolic profile to the other three strains identified 19 common, significantly changing metabolites across the three comparisons: SHRSP_v_WKY, SHRSP_v_Trans and SHRSP_v_SW2k (Figure 3-7B; top venn-diagram). Association to functions and diseases on IPA did not highlight a particular process, rather, each metabolite was implicated in different functions. 18 out of the 19 metabolites exhibited consistent direction of change, with 17 showing constantly elevated and 1 diminished levels in SHRSP (Table 3-3). Of the 17 increased metabolites 5 were detected only in SHRSP and exhibited FC raging from 3.701 to 4005.273.

Similarly to the urine analysis, further network analysis on IPA investigated potential relation of the 19 significant metabolites to GSTM1 and GSTM5, attempting to more restrictively identify plasma metabolic components implicated in the improved BP phenotype of *Gstm1*-transgenic compared to SHRSP. 5 metabolites were connected to GSTM5 and related to ROS and lipid metabolism (Figure 3-12). L-proline, 1-acylglycerophosphocholine and phosphatidylethanolamine belonged to the consistently increased in SHRSP metabolites. Moreover, L-proline was unique to SHRSP, with FC=4005.273 over the other three strains. Another metabolite of interest was the linoleic acid, the only consistently reduced metabolite in SHRSP, having a FC of -7.176 in SHRSP_v_WKY, -8.207 in SHRSP_v_Trans and -7.301 in SHRSP_v_SW2k comparison (Table 3-3). Moreover, an interesting hit exhibiting inconsistent change was the sphingosine-1-phosphate (S1P). S1P was significantly decreased in SHRSP compared to WKY (FC= -72.654) and SW2k (FC=-58.345), but did not change in comparison to transgenic animals (FC=1.504, p-val=0.0954).

**Table 3-3. Subset of the 19 'in common' plasma metabolites exhibiting significant change in SHRSP compared to WKY, SW2k and *Gstm1*-transgenic, at baseline. Data were generated on IDEOM v18. Green: decreased and red: increased metabolite levels.**

| KEGG id | Putative metabolite | Fold Change | P-value | Fold Change | P-value | Fold Change | P-value |
|---|---|---|---|---|---|---|---|
| | | SHRSP v WKY | | SHRSP v SW2k | | SHRSP v Trans | |
| C05131 | (1-ribosylimidazole)-4-acetate | 2.465 | 0.046 | 19.400 | 0.012 | 19.400 | 0.012 |
| C04715 | (20S,22S,25S)-22,25-epoxyfurost-5-ene-3beta,26-diol | 14.038 | 0.001 | 1.362 | 0.020 | 16.096 | 0.001 |
| C04230 | 1-acylglycerophosphocholine | 3927.009 | 0.000 | 5268.337 | 0.000 | 267.237 | 0.001 |
| C01301 | 3,7,12-trihydroxycholestan-26-al | 27.344 | 0.001 | 1.513 | 0.017 | 23.220 | 0.000 |
| C00632 | 3-hydroxyanthranilic acid | 6.974 | 0.000 | 6.974 | 0.000 | 6.974 | 0.000 |
| C05828 | 3-methylimidazoleacetic acid | 5.103 | 0.010 | 3.881 | 0.017 | 6.929 | 0.012 |
| C04780 | 8-((1R,2R)-3-oxo-2-((Z)-pent-2-enyl) cyclopentyl) octanoic acid | 3.666 | 0.020 | 2.263 | 0.034 | 3.024 | 0.024 |
| C05519 | allo-L-threonine | 1.570 | 0.000 | 1.450 | 0.029 | 1.153 | 0.034 |
| C01888 | aminoacetone | 1.492 | 0.000 | 1.456 | 0.009 | 1.157 | 0.043 |
| C02862 | butyrylcarnitine | 195.648 | 0.001 | 195.648 | 0.001 | 1.903 | 0.003 |
| C00256 | D-lactic acid | 3.701 | 0.004 | 3.701 | 0.004 | 3.701 | 0.004 |
| C01190 | glucosylceramide | 12.411 | 0.000 | 12.411 | 0.000 | 12.411 | 0.000 |
| C00581 | glycocyamine | 166.404 | 0.009 | 110.143 | 0.009 | 107.098 | 0.009 |
| C00148 | L-proline | 4005.273 | 0.000 | 4005.273 | 0.000 | 4005.273 | 0.000 |
| C01595 | linoleic acid | -7.176 | 0.002 | -8.207 | 0.009 | -7.301 | 0.008 |
| C00157 | phosphatidylcholine | -1.568 | 0.022 | 308.914 | 0.007 | 8234.086 | 0.001 |
| C00350 | phosphatidylethanolamine | 119.584 | 0.009 | 119.584 | 0.009 | 214.250 | 0.001 |
| C00315 | spermidine | 15.060 | 0.007 | 15.060 | 0.007 | 15.060 | 0.007 |
| C01004 | trigonelline | 1.500 | 0.006 | 1.425 | 0.022 | 272.302 | 0.001 |

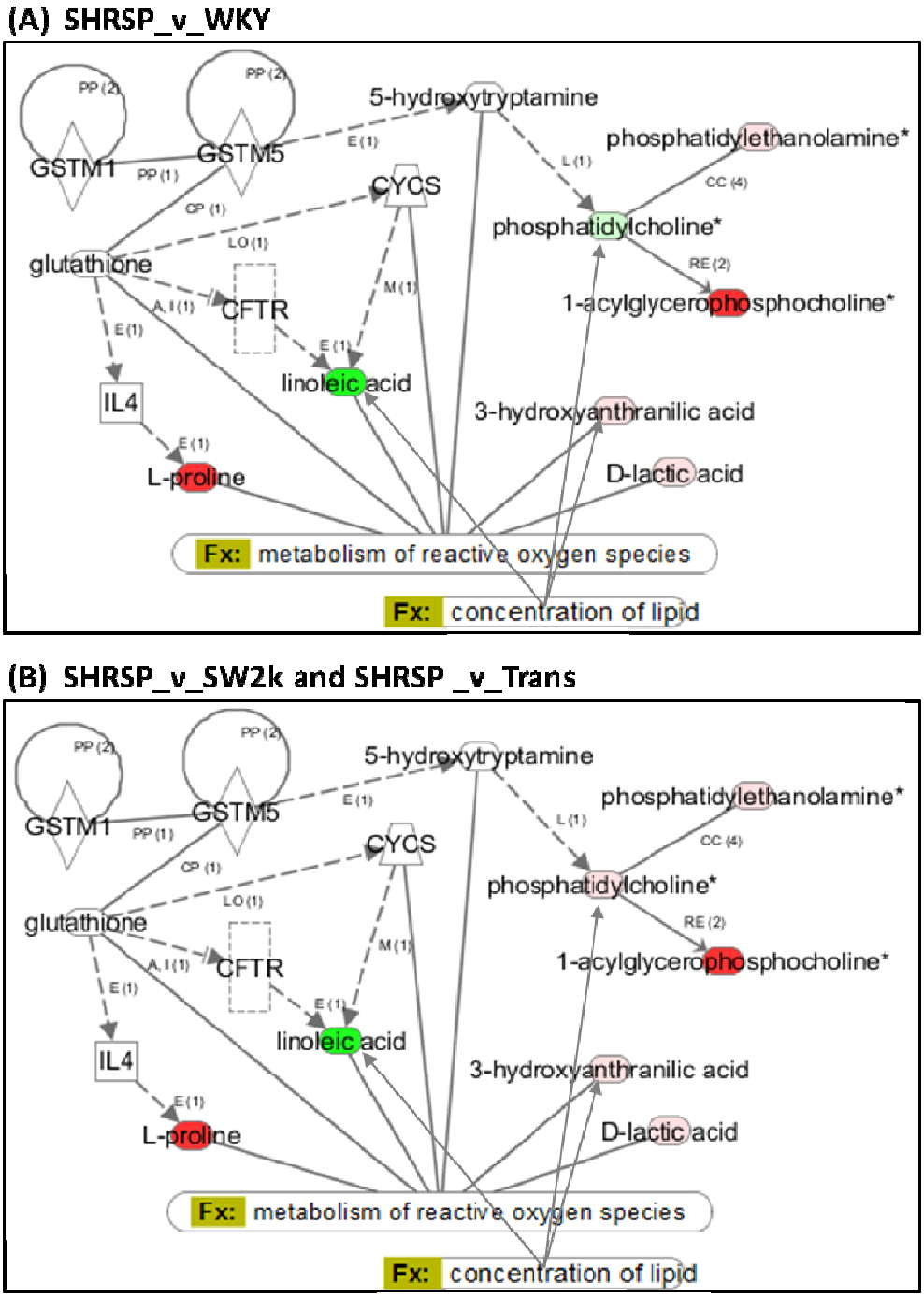


**Figure 3-12 - IPA network associating plasma metabolites, which significantly change at baseline in SHRSP versus WKY, SW2k and *Gstm1*-transgenic, with GSTM1 and GSTM5. (A) Changes in the SHRSP_v_WKY comparison. (B) Changes in the SHRSP_v_SW2k and SHRSP_v_ *Gstm1*-transgenic comparisons followed a common pattern. Five metabolites were associated to GSTM5 and the majority of molecules in the network mapped to ROS and lipid metabolism. IL4: interleukin 4; CFTR: cystic fibrosis transmembrane conductance regulator; CYCS: cyctochrome C, somatic. Colour indications: green - decrease, red - increase, white - not detected. Asterisk indicates more than one potential isomers.**

Subsequently, plasma metabolic profiles in salt-loaded animals were compared. As in the urine analysis, comparison of the salt-sensitive versus the salt-resistant strains identified 44 metabolites that were changing across all four comparisons: SHRSP_v_WKY, SHRSP_v_SW2k, Trans_v_WKY and Trans_v_SW2k. Of the above metabolites 3 were consistently decreased and 19 increased in the salt-sensitive strains. Of those increased 11 were detected only in SHRSP and *Gstm1*-transgenic, having FC that ranged from 1.580 to 382.770. Table 3-2 summarises data for some of the metabolites. Complete data for all 44 metabolites can be found in the 'Plasma/Salt/Plasma_salt_IC4_44_IPA' supplementary table.

Further investigation identified glutathione disulfide (GSSH) as a potentially interesting metabolite, which was detected only in salt-sensitive strains. GSSH displayed increased concentrations in SHRSP (FC=10.718) and *Gstm1*-transgenic (FC=26.31) compared to WKY and SW2k (Table 3-4). However, in the comparison between SHRSP and transgenic the change was not significant (FC=-2.455; p-val=0.0562).

**Table 3-4. Subset of the 44 'in common' plasma metabolites exhibiting significant change across the comparisons of SHRSP and *Gstm1*-transgenic versus WKY and SW2k, under salt loading. Data were generated on IDEOM v18. Green: decreased and red: increased metabolite levels.**

| KEGG id | Putative metabolite | Fold Change | P-value | Fold Change | P-value | Fold Change | P-value | Fold Change | P-value |
|---|---|---|---|---|---|---|---|---|---|
| | | SHRSP v WKY | | SHRSP v SW2k | | Trans v WKY | | Trans vSW2k | |
| C04230 | 1-acylglycero phosphocholine | 551.272 | 0.004 | 1005.104 | 0.008 | 450.080 | 0.042 | -5.263 | 0.006 |
| C01801 | 2-deoxy-D-ribose | 1.462 | 0.034 | 1.436 | 0.022 | 1.652 | 0.242 | 1.620 | 0.259 |
| C05332 | 2-phenethylamine | 4.373 | 0.036 | 4.373 | 0.036 | 5.557 | 0.046 | 5.560 | 0.046 |
| C05582 | 4-hydroxy-3-methoxyphenylacetic acid | -1.292 | 0.381 | 1.015 | 0.951 | 2.036 | 0.020 | 2.670 | 0.023 |
| C00300 | creatine | 1654.942 | 0.001 | -1.127 | 0.290 | 1209.068 | 0.027 | -1.538 | 0.023 |
| C00256 | D-lactic acid | 2.338 | 0.017 | 2.338 | 0.017 | 1.841 | 0.126 | 1.840 | 0.126 |
| C00864 | D-pantothenic acid | 18.582 | 0.005 | -1.604 | 0.009 | 38.272 | 0.081 | 1.280 | 0.302 |
| C00127 | glutathione disulfide | 10.718 | 0.003 | 10.718 | 0.003 | 26.313 | 0.046 | 26.310 | 0.046 |
| C00530 | hydroquinone | -1.560 | 0.145 | -1.134 | 0.369 | 2.448 | 0.007 | 3.370 | 0.026 |
| C15809 | iminoglycine | 2.109 | 0.005 | -1.712 | 0.003 | 4.322 | 0.036 | 1.200 | 0.130 |
| C02043 | indole-3-lactic acid | 2.059 | 0.187 | -1.321 | 0.426 | 5.104 | 0.030 | 1.880 | 0.017 |
| C00337 | L-4,5-dihydroorotic acid | -2.353 | 0.008 | -2.984 | 0.026 | -3.690 | 0.007 | -4.762 | 0.015 |
| C02700 | L-formylkynurenine | 2.480 | 0.046 | 2.480 | 0.046 | 3.136 | 0.032 | 3.140 | 0.032 |
| C00155 | L-homocysteine | -1.406 | 0.082 | -1.446 | 0.063 | -1.919 | 0.006 | -1.961 | 0.004 |
| C00148 | L-proline | 2719.667 | 0.016 | 1.126 | 0.475 | 3993.938 | 0.006 | 1.650 | 0.000 |
| C00157 | phosphatidylcholine | -1.487 | 0.011 | 243.483 | 0.023 | 28.719 | 0.017 | 265.690 | 0.038 |
| C00350 | phosphatidylethanolamine | 23.247 | 0.023 | 31.966 | 0.018 | 7.319 | 0.008 | 24.660 | 0.029 |
| C01004 | trigonelline | 1.086 | 0.600 | -1.061 | 0.689 | 1.942 | 0.009 | 1.690 | 0.014 |
| C00366 | uric acid | 1.509 | 0.282 | 1.418 | 0.338 | 1.716 | 0.026 | 1.610 | 0.039 |

Finally, the metabolic effect of salt-loading on plasma was assessed in each strain individually, by comparing profiles between baseline and salt-loaded conditions. Comparisons across *Gstm1*-transgenic and the salt-resistant strains identified 28 significant changes unique to the transgenic. Of these, 9 were in common with SHRSP and 6 exhibited consistent increase across the two salt-sensitive strains, with FC ranging from 1.439 to 961.421 (Table 3-5). Complete data for all unique and common metabolites can be found in the 'Plasma/Salt_v_Baseline/Plasma_salt_v_base_SHRSP_IC_Trans_(13)+ Trans_unique_(28) _IPA' supplementary table.

**Table 3-5. Subset of the plasma metabolites exhibiting significant change in SHRSP and *Gstm1*-transgenic or in the transgenic alone (unique), upon salt-loading. Data were generated on IDEOM v18. Green: significantly decreased and red: significantly increased metabolite levels.**

| KEGG id | Putative metabolite | Fold Change | P-value | Fold Change | P-value | Fold Change | P-value | Fold Change | P-value |
|---|---|---|---|---|---|---|---|---|---|
| | | WKY_salt v WKY | | SW2k_salt v SW2k | | SHRSP_salt v SHRSP | | Trans_salt v Trans | |
| C05453 | 7alpha,12alpha-dihydroxy-5beta-cholestan-3-one | 1.274 | 0.229 | 1.021 | 0.881 | 739.619 | 0.000 | -1.491 | 0.043 |
| C00121 | ribose | 1.082 | 0.681 | 1.613 | 0.100 | 1.520 | 0.023 | 1.584 | 0.007 |
| C06124 | sphingosine-1-phosphate | | | 1.283 | 0.278 | 82.300 | 0.035 | 88.898 | 0.006 |
| C06772 | diethanolamine | | | 1.279 | 0.283 | 1.477 | 0.014 | 1.548 | 0.002 |
| C11512 | methyl jasmonate | -1.103 | 0.159 | 1.201 | 0.284 | 4.056 | 0.000 | -2.755 | 0.049 |
| C06184 | N-methylpelletierine | | | | | 1.978 | 0.001 | 3.255 | 0.003 |
| C01028 | N6-hydroxy-L-lysine | 1.291 | 0.095 | 1.264 | 0.222 | 1.439 | 0.000 | 1.914 | 0.028 |
| C02477 | alpha-tocopherol | | | -568.542 | 0.960 | 961.421 | 0.038 | -2.026 | 0.033 |
| C01740 | octylamine | | | 1.128 | 0.576 | 34.195 | 0.021 | 45.689 | 0.020 |
| C00141 | alpha-ketoisovaleric acid | 1.108 | 0.635 | 1.140 | 0.596 | 1.214 | 0.218 | -1.168 | 0.030 |
| C00219 | arachidonic acid | 1.076 | 0.721 | 1.020 | 0.940 | 1.008 | 0.976 | 1.582 | 0.041 |
| C00221 | beta-D-glucose | 1.082 | 0.318 | 1.036 | 0.825 | 1.062 | 0.516 | -1.447 | 0.035 |
| C00158 | citric acid | 1.180 | 0.593 | 1.080 | 0.764 | 1.477 | 0.100 | 1.365 | 0.009 |
| C00530 | hydroquinone | -1.339 | 0.192 | -2.497 | 0.102 | -1.199 | 0.489 | 3.218 | 0.034 |
| C02989 | L-methionine sulfoxide | | | | | | | 22.257 | 0.022 |

Further investigation identified sphingosine-1-phosphate to be consistently and highly increased in both SHRSP (FC=82.300) and the transgenic (FC=88.898), under salt-loading (Table 3-5). Arachdonic acid was another molecule of interest, which displayed significantly increased concentrations only in salt-loaded transgenic animals (FC=1.582). 'Diseases and Function' analysis on IPA implicated the two metabolites in several pathological processes known to be related to salt, including CVD and BP regulation, inflammatory response, ROS producion and lipid metabolism.

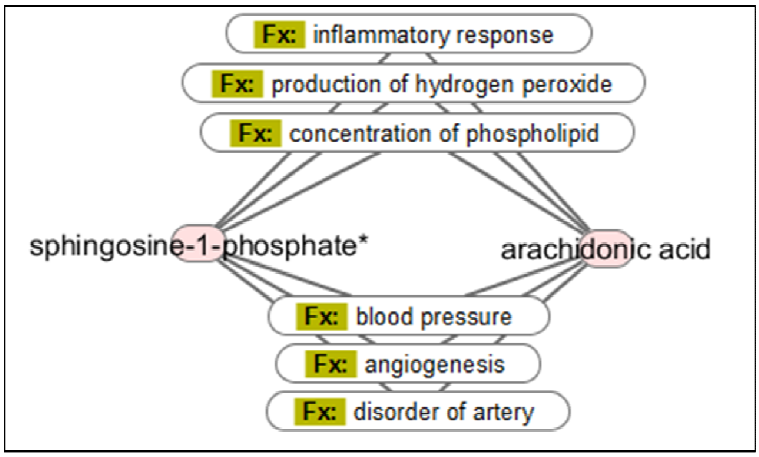


**Figure 3-13 - 'Disease and function' analysis on IPA for significantly changing metabolites upon salt-loading, in salt-sensitive strains. Sphingosine-1-phosphate was consistently increased across SHRSP (FC=82.300) and *Gstm1*-transgenic (FC=88.898). Arachidonic acid exhibited elevated concentrations only in salt-loaded transgenic (FC=1.582). The two metabolites were associated on IPA with a number of processes and pathological conditions including, inflammatory response, ROS production, lipid metabolism, BP, angiogenesis and artery disorders. Red indicates increase. Asterisk indicates more than one potential isomers.**

Finally, assessment of peak quality for the metabolites of interest, that were identified in the plasma comparisons, was performed on peakML.Viewer. Figure 3-14 illustrates the peak chromatograms of selected metabolites which demonstrated good peak shape and reproducibility.

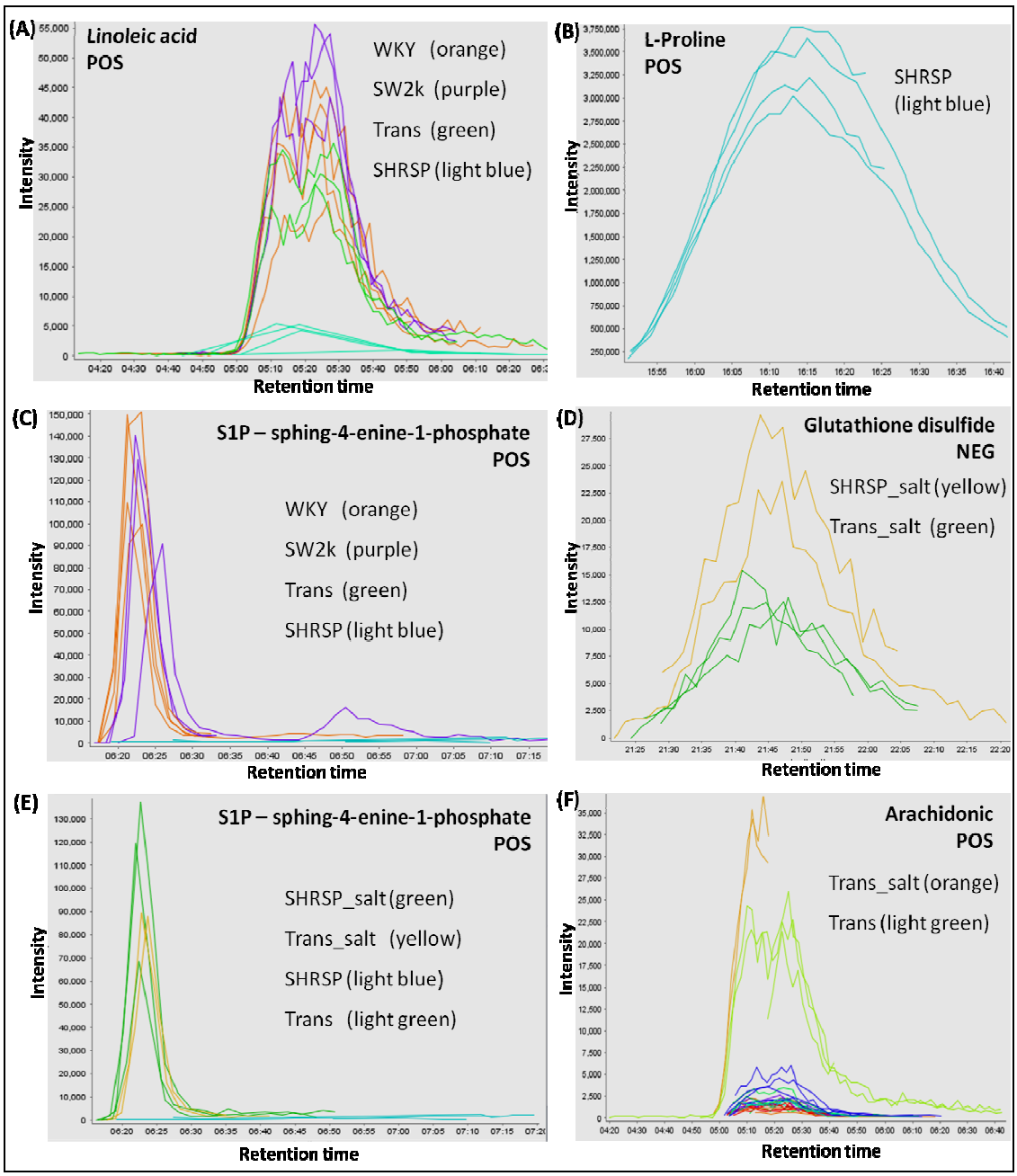


**Figure 3-14 - PeakML chromatograms of metabolites of interest identified in plasma comparisons across WKY, SHRSP, SW2k and *Gstm-1* transgenic strains, at baseline or salt-loaded conditions. (A) Linoleic acid baseline levels were significantly decreased in SHRSP compared to the other three strains. (B) L-proline was a 'unique' SHRSP metabolite, not detected in the other strains, at baseline. (C) S1P exhibited decreased baseline concentrations in SHRSP and the transgenic strain compared to WKY and SW2k. (D) Glutathione disulfide was detected only in SHRSP and transgenic , upon salt-loading and displayed increased levels in SHRSP. (E) Upon salt-loading S1P increased in both SHRSP and the transgenic compared to baseline levels. (F) Arachidonic acid displayed high levels in the transgenic, which were even more elevated under salt-loading. The x-axis indicates the retention time and the y-axis the intensity.**

## 3.3 Discussion

Previous microarray profiling in whole kidney from salt-loaded rats demonstrated differential expression of *S1pr1*, a candidate gene for salt-sensitivity, across WKY, SHRSP and chr.2 congenic strains (Graham et al., 2007). Following up from these studies, this work aimed to further investigate whether the effects of altered gene expression were represented at the protein level, in kidneys from salt-loaded parental and SW2a and SW2k congenic rats. The investigation was also extended to vascular tissue, since S1PR1 is known to play significant role in the vasculature (Spiegel and Milstien, 2003b, Fujii et al., 2012).

The protein levels of S1PR1 in both salt-loaded kidney and thoracic aorta were below detection when tested with IHC. To circumvent this issue, WB analysis was performed in kidney enrichments for membrane fraction and demonstrated similar expression levels across parental and congenic animals. This inconsistency between mRNA and protein levels implies abnormal post-transcriptional regulation or protein turnover. In thoracic aorta enrichments, previous work in our lab demonstrated consistently low detection of S1PR1 levels across the strains.

To further investigate the role of candidate genes in salt-sensitive HTN, and assess the effects of salt-loading on BP regulation and sphingosine signalling, a more comprehensive, untargeted, metabolic profiling was carried out in urine and plasma from rats, on normal-salt and salt-loaded diets. In this study, apart from the parental and the SW2k congenic strains, the *Gstm1*-transgenic strain was included. The aim was to also assess the role of *Gstm1*, a chr.2 positional and functional candidate for BP-regulation (McBride et al., 2003), on the metabolic level and to investigate its implication in salt-sensitivity.

Identified metabolites in plasma were almost two thirds of those identified in urine. This could be the result of the fact that urine samples were collected over a 24h period. During this space of time, while urine is exposed to the environment, further chemical reactions and oxidation changes of the dynamic urinary metabolome are possibly allowed to take place, leading to greater inter-sample variability. PCA plots for urine and plasma were generated to assess the variability within and across groups. In both urine and plasma, clustering indicated different profiles between normal-salt and salt-loaded groups, in each strain, with the exception of WKY in plasma. This may illustrate the fact that WKY are resistant to salt-loading, maintaining low BP levels. In addition, WKY and SW2k displayed more different profiles to the SHRSP and *Gstm1*-transgenic strains, which were clustering

together, and this differential clustering was consistent across urine and plasma and across baseline and salt-loading. It is therefore suggested that the two salt-resistant strains, WKY and SW2k, handle salt-loading in a different way, as opposed to the salt-sensitive strains which exhibit consistently similar profiles across normal-salt and salt-loaded conditions. However, variability within groups was large, which can be attributed to the small number of replicates, in combination with the highly dynamic nature of the metabolome.

Considering time limitations, from a large number of comparisons across urine and plasma, across strains and across conditions, focus was placed on particular intersects according to the most interesting questions to be tested in each case. At baseline, SHRSP was compared to each of the other three strains, in order to investigate the metabolic components associated with increased BP in SHRSP and improved BP in SW2k and *Gstm1*-tansgenic. Under salt-loading, the SHRSP and *Gstm1*-transgenic salt-sensitive strains were compared to the WKY and SW2k salt-resistant strains, in order to examine metabolic changes implicated in a protective or a pathogenic manner in salt-sensitivity. Lastly, comparisons within each strain before and after salt-loading were performed to characterise how each strain responds to salt-loading.

Comparison of urine profiles under normal-salt, demonstrated that SHRSP was equally different to the other three strains, and therefore 'in common' changing metabolites, were further investigated as components associated with BP regulation. The most interesting finding was N-acetyl-cysteine (NAC), which exhibited decreased levels in SHRSP compared to WKY and SW2k, but was not detected in the transgenic animals. Moreover, IPA network analysis identified several connections between NAC and the human homologue of GSTM1, GSTM5. However, N-acetyl-cysteine is a synthetic derivative of cysteine, exhibiting antioxidant properties (Mansano et al., 2012) and being implicated in artery vasodilation and protection against acute renal failure in rats (de Araujo et al., 2005, Alencar et al., 2003). It has been and is extensively being used in clinical trials as a treatment for a wide range of human diseases, including HTN and renal failure (NCT00569465, NCT00736866 - clinical trial identifiers). Therefore, further investigation is needed into the origin of this metabolite (microbiota?) in our animals, which was the single isomer identified with high confidence.

Subsequent investigation of the effect of salt-loading in urine profiles of salt-resistant and salt-sensitive strains, demonstrated responses of similar magnitude for the resistant WKY and SW2k. However, the sensitive SHRSP and transgenic seemed to respond in a different way to salt-loading, as indicated through the venn diagrams. Therefore, the few

metabolites changing 'in common' and in the same direction between SHRSP and the transgenic may include molecules implicated in salt-sensitivity. 3-hydroxyanthranilic acid and oleic acid were two metabolites consistently elevated in SHRSP and the transgenic, compared to WKY and SW2k. 3-hydroxyanthranilic acid, an intermediate of tryptophan degradation, has protective effects against inflammation through scavenging of free radicals, induction of the antioxidant HMOX1 (heme-oxygenase 1) protein expression and reduction of VCAM1 protein expression (Opitz et al., 2007). Therefore, increased levels in the salt-sensitive strains imply increased tryptophan degradation, which may act in a protective manner against stress induced by salt-loading. Moreover, oleic acid, a monounsaturated fatty acid, has been implicated in increased production of ROS (reactive oxygen species) (Lu et al., 1998), and the up-regulation of renin transcription through the transcription factor PPARg (peroxisome proliferator-activated receptor-gamma) (Todorov et al., 2007). Increased renin transcription suggests potentially increased levels of angiotensin II, which regulates vasoconstriction. Furthermore, a paradigm of how angiotensin II may be implicated in the pathogenesis of salt-dependent HTN has been recently described (Blaustein et al., 2012). Hence, raised BP in salt-sensitivity may be regulated by increased levels of oleic acid. The above responses may be mediated by the congenic interval due to the different profiles between salt-sensitive and salt-resistant strains.

Finally, comparisons across normal-salt and salt-loaded conditions within each strain indicated different responses across strains, as observed through venn diagramms. However, due to time limitations, further analysis of these urine comparisons was not performed.

Subsequent comparisons of plasma profiles under normal-salt, exhibited a similar pattern to this of urine, with SHRSP having a consistently different profile to this of the other three strains. Focus on 'in common' metabolites changing consistently across the three comparisons, identified L-proline and linoleic acid as potentially interesting and they were also associated to human GSTM5 and metabolism of ROS, on IPA. L-proline is an amino acid that has been reported to support generation of ROS through its oxidised form (Donald et al., 2001) and also to reduce the antioxidant activity of SOD (superoxide dismutase) in rat erythrocytes (Roecker et al., 2012). Therefore, increased levels of L-proline only in SHRSP suggest implication in the elevated BP phenotype, as well as a protective effect of the congenic interval, and potentially the *Gstm1,* through down-regulation of L-proline levels. In addition, levels of linoleic acid were consistently decreased in SHRSP. Linoleic acid, an unsaturated fatty acid is known to down-regulate protein expression of eNOS (endothelial

nitric oxide synthase) in endothelial cells (Artwohl et al., 2004) and increase NAD(P)H oxidase activity (Lassegue and Clempus, 2003) in VSMC. Moreover, linoleic acid plasma levels were shown to be inherited in families with CVD (Shah et al., 2009). Thus, decreased levels of linoleic acid in SHRSP may imply a protective adaptation against increased oxidative stress in these animals, which is most likely mediated by the congenic interval, but further investigation is needed. Another interesting finding was the significantly reduced S1P levels in SHRSP compared to WKY and SW2k, but not to the transgenic strain, which suggests that *Gstm1* does not regulate S1P levels.

Next, the plasma metabolic profiles upon salt-loading were compared across the salt-sensitive and salt-resistant strains. Responses between SHRSP and *Gstm1*-transgenic shared less 'in common' metabolites, indicating different handling of salt-loading and supporting similar findings in urine. An interesting metabolite that was consistently elevated in the salt-sensitive strains was the glutathione disulfide (GSSH). GSSH is the oxidised form of glutathione, a known antioxidant (Pompella et al., 2003). Increased GSSH levels are potentially a marker of increased oxidative stress upon salt-loading in salt sensitivity. Furthermore, it could be suggested that although *Gstm1* expression in the transgenic strain is beneficial at baseline causing decrease in BP, salt-loading hampers this beneficial effect.

Finally, the plasma profiles at normal-salt and salt-loaded conditions were compared within each strain to assess differential responses to salt-loading. Again, the majority of identified metabolites were unique to each strain, suggesting different handling of salt. The major finding of this analysis was the consistent increase of S1P upon salt-loading, in both the SHRSP and *Gstm1*-transgenic salt-sensitive strains, which suggests regulation of S1P levels by salt. This increase reaches S1P levels of WKY and SW2k at baseline and can be interpreted as protective in the regulation of BP and oxidative stress under salt loading.

In conclusion, urine analysis proved to be more challenging than plasma, as urinary metabolic profiles are known to be more susceptible to environmental factors and therefore more variable. However, oleic acid was identified in urine as a candidate biomarker for salt sensitivity. In plasma, glutathione disulfide could represent a marker of increased oxidative stress in salt-sensitivity. Moreover, L-proline and linoleic acid were suggested to be implicated in BP regulation in HTN. For the analysis to be complete, further validation of the findings to authentic standards by MS/MS fractionation and verification by WB and enzymatic activity assays, would be essential before any generation of new testable hypothesis.

# 4 Functional and Molecular Characterisation of Mesenteric Resistance Arteries from WKY, SHRSP and Chromosome 2 Congenic Strains

# 4.1 Introduction

Elevated BP in HTN is mediated by increased peripheral vascular resistance, which is principally determined through the myogenic tone of microcirculation, including resistance arteries (Borders and Granger, 1986, Bohlen, 1986). Alterations in the structure and function of resistance arteries regulate blood flow and pressure, through vascular remodelling and modulation of myogenic tone (Mulvany and Aalkjaer, 1990).

Adaptive changes in structure and elasticity of mesenteric resistance arteries (MRA) in hypertensive rat models (SHR/SHRSP) are characterised by narrowing of the lumen and increased wall:lumen ratio, which may increase vascular resistance, even at full dilatation, and vascular stiffening caused by abnormal elastin and collagen organisation (Arribas et al., 1997, Briones et al., 2003, Briones et al., 2009, Mulvany, 1988). However, the mechanisms involved in vascular remodelling, are not clear. Antioxidant therapies in SHR/SHRSP have been shown to improve the wall:lumen ratio in MRAs (Chen et al., 2001, Park et al., 2002, Rizzoni et al., 1998). Therefore, oxidative stress, along with wall stress, changes in the extracellular matrix proteins deposition and the neurohormonal environment, have been suggested as potential mechanisms contributing to the vascular remodelling (Lee et al., 1995, Touyz et al., 2003).

In addition, alterations of function in resistance arteries occur as a result of imbalance between vasodilatation and vasoconstriction. The principal vasodilators are nitric oxide (NO), prostacyclin ($PGI_2$) and endothelium-derived hyperpolarising factors (EDHF). EDHF is the main vasodilatory pathway in small resistance arteries, whereas $PGI_2$ and NO are more prominent in large vessels (Shimokawa et al., 1996). Yet, NO is considered the major regulator of cardiovascular homeostasis (Feletou et al., 2012). The principal vasoconstrictors include endothelin-1, prostanoids, angiotensin II and superoxide anions (Félétou and Vanhoutte, 2006). Normal function of endothelium, which is the source of the vasoactive factors, maintains the physiological vascular tone. Imbalance in availability of vasoactive factors results in endothelial dysfunction, the common denominator of cardiovascular diseases, including hypertension (Grunfeld et al., 1995, Potenza et al., 2005, Treasure et al., 1993). In SHRSP, EDHF-mediated responses have been reported to be impaired in resistance arteries (Goto et al., 2004, Sunano et al., 1999). Moreover, endothelium-dependent relaxation responses are diminished due to low NO bioavailability, despite the generally increased eNOS activity and unaffected endothelial NO production (McIntyre et al., 1997,

Kerr et al., 1999, Ma et al., 2001). In SHRSP, NO bioavailability is reduced due to enhanced levels of the NO scavenger, superoxide anion, indicating implication of ROS in endothelial dysfunction (Hamilton et al., 2004). Increased production of the superoxide anion has been mainly attributed to endothelial xanthine oxidase, NADPH oxidase (NOX) and uncoupled eNOS (Grunfeld et al., 1995, Kerr et al., 1999, Suzuki et al., 1998, Zalba et al., 2000, Hamilton et al., 2001). Inhibition of eNOS by administration of L-NAME, decreased vascular superoxide levels in SHRSP (Grunfeld et al., 1995, Hamilton et al., 2001, Kerr et al., 1999). In general, therapeutic approaches using antioxidants demonstrate an improvement in the endothelial function (Fennell et al., 2002, Savoia et al., 2006).

Apart from the endothelium-dependent modulation, the contractile state of SM is also regulated by neurotransmitters, hormones and other chemical signals, as well as changes in the load or length, which affect directly the VSMCs (Webb, 2003). The contractile activity in SM is controlled by the balance between $Ca^{2+}$/calmodulin-dependent MLC kinase (MLCK) and MLC phosphatase (MLCP) activity, whereby de-phosphorylation of MLC promotes relaxation. MLCP activity is controlled by the RhoA small G protein and its downstream effector Rho kinase (RhoK), which de-activates the phosphatase, maintaining the contracted state of MLC in VSMCs (Seko et al., 2003, Webb, 2003). Inhibition of RhoK using pharmacological antagonists, such as Fasudil, has been shown to induce relaxation hence reduction in BP (Tsounapi et al., 2012, Uehata et al., 1997, Yang et al., 2011) and correct SMC hypercontractions (Mukai et al., 2001, Tsounapi et al., 2012) in *in vivo* and *ex vivo* studies on animal models of HTN, suggesting that inhibition of RhoK improves endothelial dysfunction in HTN in the SHR model. Recent publications also support a potential antioxidant role of fasudil, which is partly exerted through elevation of NO production (Guan et al., 2012, Ma et al., 2011), potentially leading to further inhibition of RhoA, in VSMC (Sauzeau et al., 2000, Wu et al., 1996).

In addition, vasoactive compounds can also be produced and secreted by platelets, as in the case of sphingolipids, which are known to impact on vascular remodelling and endothelial dysfunction in HTN (Bolz et al., 2003, Ohanian et al., 2012, Spijkers et al., 2011). Sphingosine-1-phosphate (S1P) is an important bioactive lipid that influences vascular tone and VSMC function through selective binding of S1PR1, S1PR2 and S1PR3 receptors (Coussin et al., 2002, Lee et al., 1998, Murakami et al., 2010) (subtypes present in the vasculature)(Peters and Alewijnse, 2007). S1P signalling has been related to inflammation in HTN; specifically, it has been suggested to regulate pro-inflammatory vascular signalling

through receptor tyrosine kinases (RTK) (Tanimoto et al., 2004). Moreover, RTK transactivation has been shown to further trigger activation of MAP kinases, including p38MAPK and SAPK/JNK, known mitogenic signal transducers implicated in pro-inflammatory pathways and VSMC inflammation (Eguchi et al., 2001, Linseman et al., 1995, Yogi et al., 2011). These S1P/S1PR1-mediated pro-inflammatory effects were upregulated in mesenteric VSMCs from hypertensive SHRSP (Yogi et al., 2011). Furthermore, it has been demonstrated that the S*1pr1* (*Edg1*) receptor is a candidate gene implicated in salt-sensitive HTN in the SHRSP model, exhibiting elevated mRNA expression in kidney from these animals (Graham et al., 2007). Taken together the above data signify the potential importance of altered S1P/S1PR1 signalling in vascular remodelling and endothelial dysfunction in HTN.

### 4.1.1 Aims

Previous construction of chr.2 congenic strains, both on the WKY and SHRSP genetic backgrounds, resulted in improved BP phenotypes (Graham et al., 2007) (Figure 4-1). This series of experiments used 3rd order-mesenteric resistance arteries (MRA) from 16-week-old normotensive WKY, hypertensive SHRSP and the WKY.$SP_{Gla}$2a (WS2a) and SP.$WKY_{Gla}$2a (SW2a) reciprocal congenic strains aiming to:

- to compare the structure, mechanics and vascular function of MRAs across the strains, as well as to assess the effect of the chr.2 congenic interval on these phenotypes.
- to investigate the underlying regulatory mechanisms of MRA vascular reactivity across the strains and their association with the congenic interval.
- to establish mesenteric primary VSMC cultures, in order to examine S1P/S1PR1 signalling across the strains.

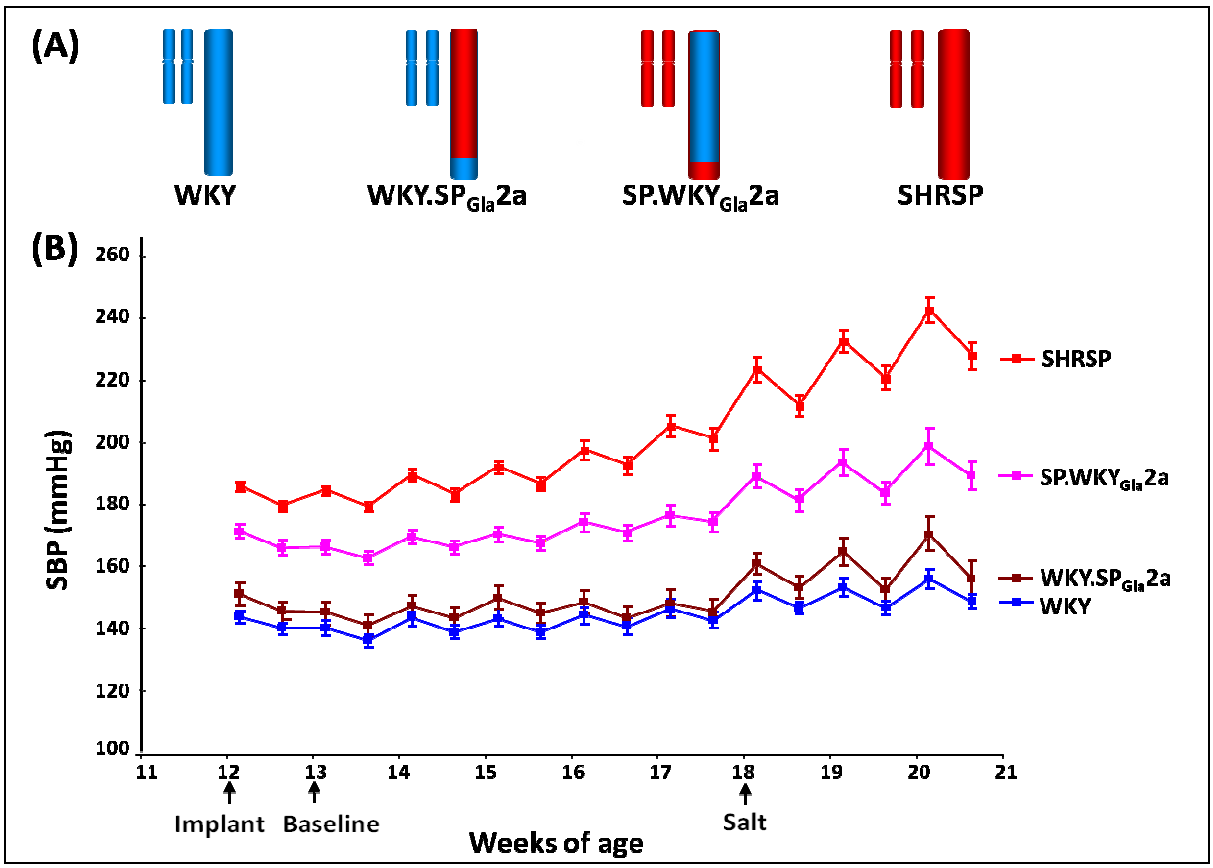


**Figure 4-1 - Chromosome 2 reciprocal congenic strains generated by WKY and SHRSP mating. (A) Schematic of chr.2 from parental, WKY.SP$_{Gla}$2a and SP.WKY$_{Gla}$2a congenic strains, showing location of the congenic interval. Blue bars: regions of WKY homozygosity, red bars: regions of SHRSP homozygosity. (B) Averaged weekly radiotelemetry recordings of night-time and day-time SBP in male parental and WKY.SP$_{Gla}$2a and SP.WKY$_{Gla}$2a congenic strains, under baseline and salt-loaded conditions. Animals were put on high-salt diet at 18 weeks of age. Edited from Graham et al., 2007.**

# 4.2 Results

## 4.2.1 Structural and mechanical properties of MRAs from WKY, SHRSP and 2a congenic strains

Vascular structure and mechanics of MRAs from 16 week old WKY, SHRSP and the SP.WKY$_{Gla}$2a and WKY.SP$_{Gla}$2a congenic strains were assessed by subjecting vessel segments to a stepwise increase of intraluminal pressure (from 10 to 110 mmHg) on a pressure myograph, as described in section 2.5.2.

MRAs from SHRSP exhibited smaller, yet not significantly, external diameter at pressures greater than 60mmHg (De; Figure 4-2A), compared with the other three strains. SHRSP internal diameter (Di; Figure 4-2B) also appeared slightly diminished relative to WKY and SP.WKY$_{Gla}$2a, and significantly smaller to WKY.SP$_{Gla}$2a, at high pressures (80-120mmHg, $P<0.05$). Wall : lumen ratio, wall thickness and cross-sectional area (CSA) (Figure 4-2C,D and E) tended to decrease in SHRSP and both the 2a congenic strains compared with WKY, but only reached significance in WKY.SP$_{Gla}$2a versus WKY arteries ($P<0.05$; 10-20mmHg for wall : lumen ratio, 10-20 and 80-110mmHg for wall thickness, 100-110mmHg for CSA). SHRSP and SP.WKY$_{Gla}$2a demonstrated intermediate phenotypes for these three parameters. The above data are summarised in Table 4-1.

**Table 4-1. Morphometric parameters of pressurised MRAs.**

| Group | External diameter (μm) (110mmHg) | Lumen diameter (μm) (110mmHg) | Wall/lumen ratio (%) (20mmHg) | Wall thickness (μm) (110mmHg) | Cross-section area (μm$^2$) (110mmHg) |
|---|---|---|---|---|---|
| **WKY** | 436 ± 15.0 | 314 ± 10.8 | 0.196 ± 0.02* | 61 ± 5.2* | 72486 ± 7518* |
| **WS2a** | 438 ± 12.3 | 348 ± 12.7 | 0.132 ± 0.011 | 45 ± 2.5 | 55450 ± 3266 |
| **SW2a** | 443 ± 10.1 | 328 ± 13.0 | 0.181 ± 0.019 | 58 ± 4.1 (40-60mmHg)* | 69333 ± 4730 |
| **SHRSP** | 402 ± 13.9 | 294 ± 18.6* | 0.197 ± 0.025 | 55 ± 3.5 | 58907 ± 2847 |

**Values are means ± SEM** ***p<0.05 vs WS2a**

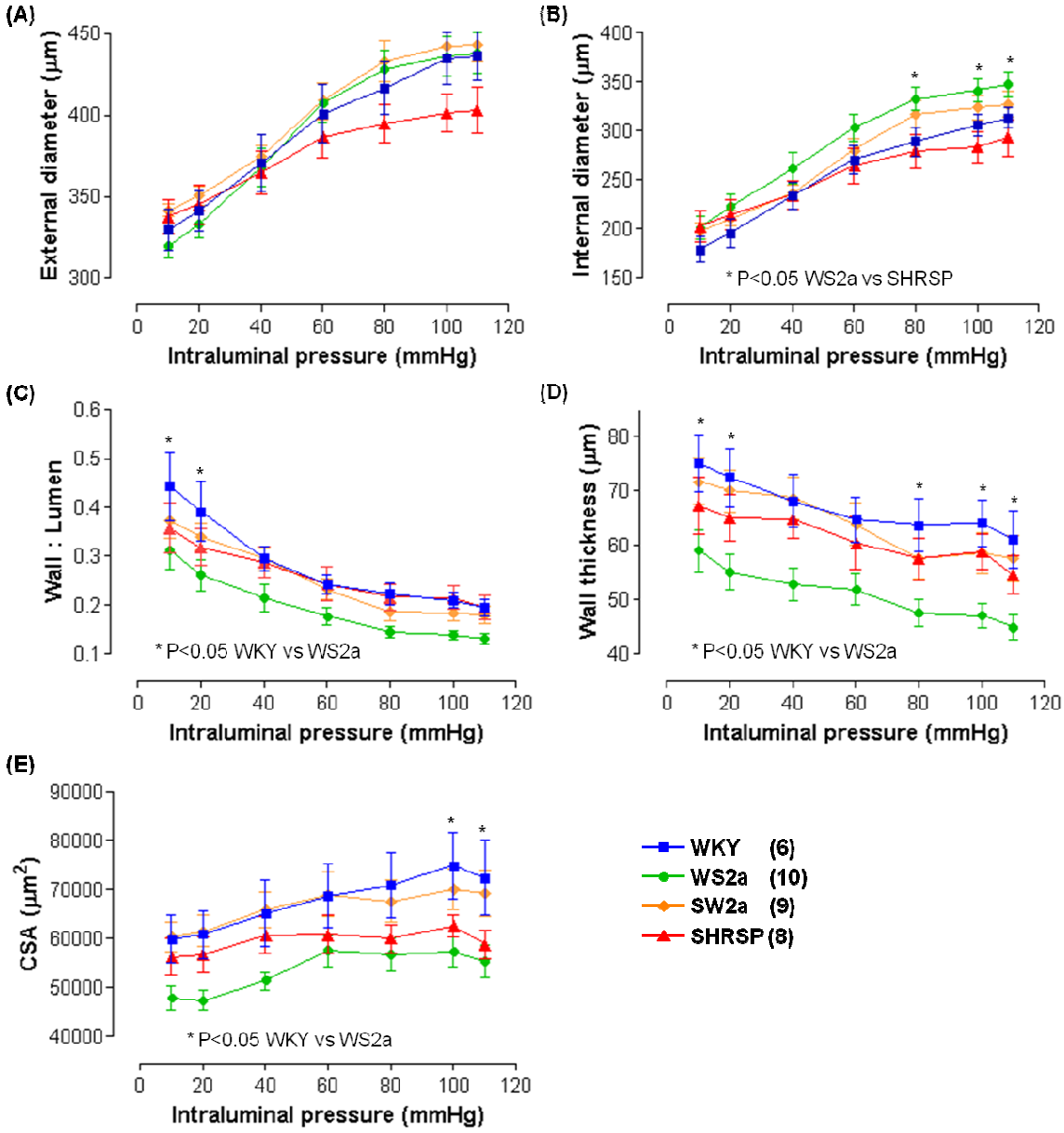


**Figure 4-2 - Comparison of structural properties of MRAs from 16 week old parental WKY and SHRSP and congenic WKY.SP$_{Gla}$2a and SP.WKY$_{Gla}$2a strains. (A) External diameter, (B) internal diameter, (C) wall : lumen ratio, (D) wall thickness and (E) cross-sectional area (CSA) in dependency to applied intraluminal pressure, on fully relaxed MRA, as measured by pressure myography. Data are expressed as mean ±SEM; n=number of animals is indicated in parenthesis; *P*-values indicate statistical difference between strains calculated by two-way ANOVA (rat strain – pressure), followed by Bonferroni test.**

Subsequently, vascular stiffness of MRAs was assessed by measuring stress and strain of the arterial wall. Wall stress was significantly enhanced only in WKY.$SP_{Gla}$2a, at high pressures (80-110mmHg), in comparison to all other strains (Figure 4-3A). Wall strain was significantly lower in SHRSP relative to WKY as well as WKY.$SP_{Gla}$2a, at pressures between 60 and 110mmHg ($P<0.001$ and $P<0.01$, respectively) (Figure 4-3B). Incremental distensibility, at low pressures (10-40mmHg), followed a similar pattern between strains sharing genetic background, with SHRSP-background strains (SHRSP and SP.$WKY_{Gla}$2a) exhibiting smaller values than WKY-background strains (WKY and WKY.$SP_{Gla}$2a) (Figure 4-3C). Finally, wall stiffness, described by the stress - wall strain relationship, was increased in SHRSP compared with WKY and the congenic strains, however it did not reach significance ($p=0.055$) (Figure 4-3D). Increased stiffness is indicated by the leftward shift of the curve and the higher β value, which represents the curve slope. Data are summarised in Table 4-2.

**Table 4-2. Mechanical parameters of pressurised MRAs.**

| Group | Stress (x $10^6$ dynes/$cm^2$) (20mmHg) | Wall strain (110mmHg) | Incremental distensibility (% $mmHg^{-1}$) (20mmHg) | β-slope |
|---|---|---|---|---|
| **WKY** | 0.041 ± 0.004 *** | 0.870 ± 0.106 ### | 0.901 ± 0.162 | 4.053 ± 0.376 |
| **WS2a** | 0.058 ± 0.004 | 0.755 ± 0.076 ## | 0.942 ± 0.189 | 4.497 ± 0.278 |
| **SW2a** | 0.044 ± 0.004 *** | 0.669 ± 0.071 | 0.599 ± 0.128 | 5.310 ± 0.828 |
| **SHRSP** | 0.042 ± 0.005 *** | 0.468 ± 0.066 | 0.602 ± 0.123 | 7.221 ± 0.928 |

**Values are means ± SEM**

***** P<0.001 vs WS2a ###, ## P<0.001, 0.01 vs SHRSP**

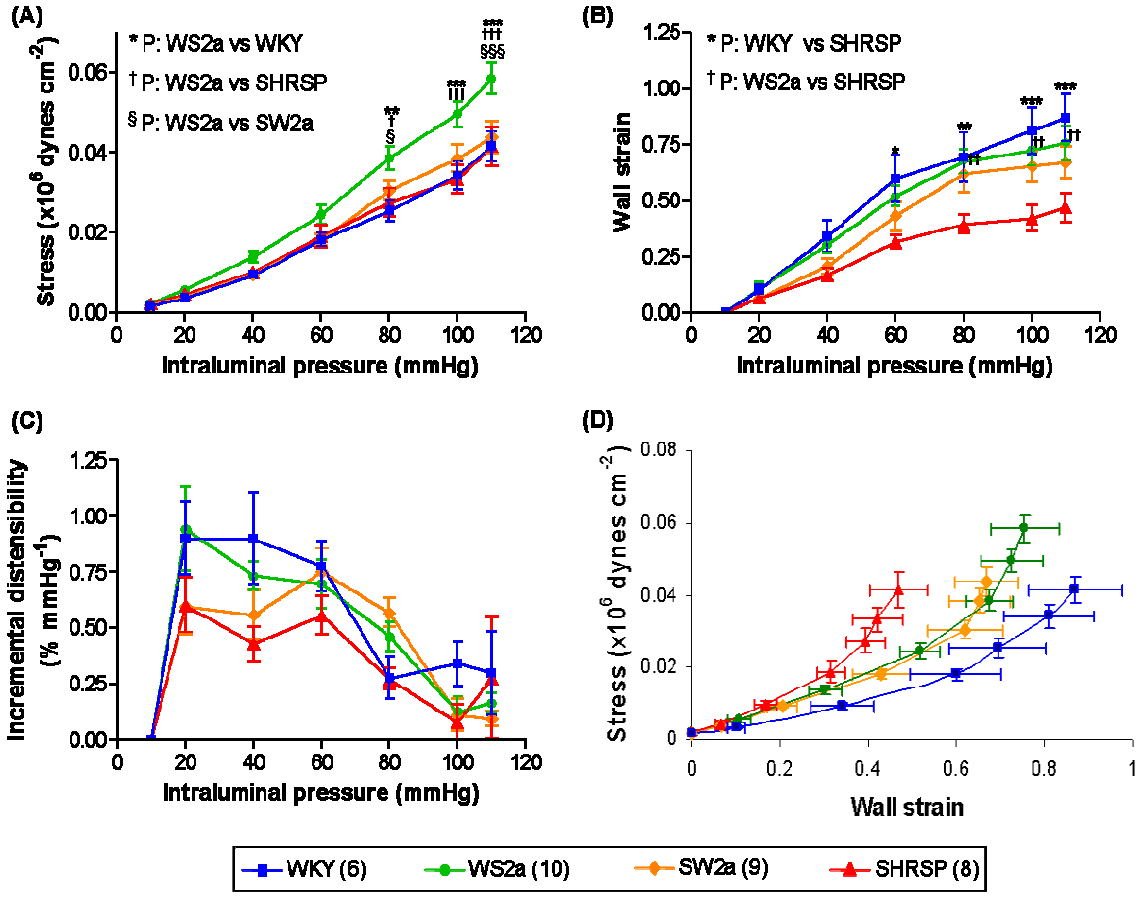


**Figure 4-3 - Comparison of mechanical parameters of MRAs from 16 week old parental WKY and SHRSP and congenic WKY.SPGla2a and SP.WKYGla2a strains. (A) Stress, (B) wall strain and (C) incremental distensibility in dependency to applied intraluminal pressure, on fully relaxed MRA. (D) Stress-strain relationship. Data are expressed as mean ±SEM; n=number of animals is indicated in parenthesis; *,**,*** P< 0.05, 0.01, 0.001 indicate statistical difference between strains calculated by two-way ANOVA (rat strain – pressure), followed by Bonferroni test.**

### 4.2.2 Vascular reactivity and endothelial function of MRAs from WKY, SHRSP and 2a congenic strains

Vascular reactivity and endothelial function of MRAs from 16 week old WKY, SHRSP and SP.WKY$_{Gla}$2a and WKY.SP$_{Gla}$2a congenic strains were assessed by exposing vessels to cumulative doses of a vasodilator / vasoconstrictor, and measuring the responses on a wire myograph, before and after pharmacological inhibition of certain relaxation / constriction pathways, as described in section 2.5.1.

To evaluate alpha-adrenergic-induced contractile responses of MRAs, isolated arteries were treated with increasing doses of noradrenalin (NA) ($10^{-9}$ to $3x10^{-5}$M). Responses were measured before and after RhoK inhibition with fasudil (3μM, 30min before NA stimulation) to assess the involvement of RhoA/Rho kinase pathway on the basal tone. Inhibition of RhoK decreased similarly NA-induced contraction in WKY, WKY.SP$_{Gla}$2a and SP.WKY$_{Gla}$2a, without reaching significance (Figure 4-4A, B and D). On the contrary, in SHRSP, the fasudil-induced decrease in contraction to high NA doses was significantly greater compared to untreated MRAs ($3x10^{-6}$M, $P<0.01$). Moreover, the contraction curve was slightly shifted to the right, indicating a lower sensitivity to NA in fasudil-treated versus untreated arteries from SHRSP (Figure 4-4C). Further, comparison of responses across strains, in untreated MRAs, demonstrated significantly enhanced contractility in SHRSP versus WKY and the two congenic strains ($3x10^{-6}$ to $10^{-5}$M). SP.WKY$_{Gla}$2a NA-induced contraction was also increased relative to WKY, whereas WKY.SP$_{Gla}$2a exhibited similar responses to WKY. Finally, a small leftward shift of the SHRSP curve indicated higher sensitivity to NA (Figure 4-4E). After RhoK inhibition, SHRSP high contractile responses to NA remained significantly different to the other three stains ($3x10^{-6}$ to $10^{-5}$ M), despite the corrected levels as described above (Figure 4-4F). The above data are summarised in Table 4-3.

**Table 4-3. Contractile responses to noradrenalin in untreated and fasudil-treated MRAs.**

| Group | Noradrenaline<br>Active effective pressure (kPa)<br>($3 \times 10^{-6}$ M) | Noradrenaline + Fasudil<br>Active effective pressure (kPa)<br>($3 \times 10^{-6}$ M) |
|---|---|---|
| **WKY** | 23.18 ± 2.54 *** , # | 17.38 ± 2.17 *** , ##, § |
| **WS2a** | 25.92 ± 3.89 *** | 20.90 ± 5.87 |
| **SW2a** | 32.85 ± 2.22 ** | 27.10 ± 2.02 |
| **SHRSP** | 41.45 ± 1.85 ## | 31.26 ± 3.42 §§ |

**Values are means ± SEM**

***,** P < 0.001, 0.01 vs SHRSP ##, # P < 0.01, 0.05 vs SW2a

§§,§ P < 0.01, 0.05 vs untreated

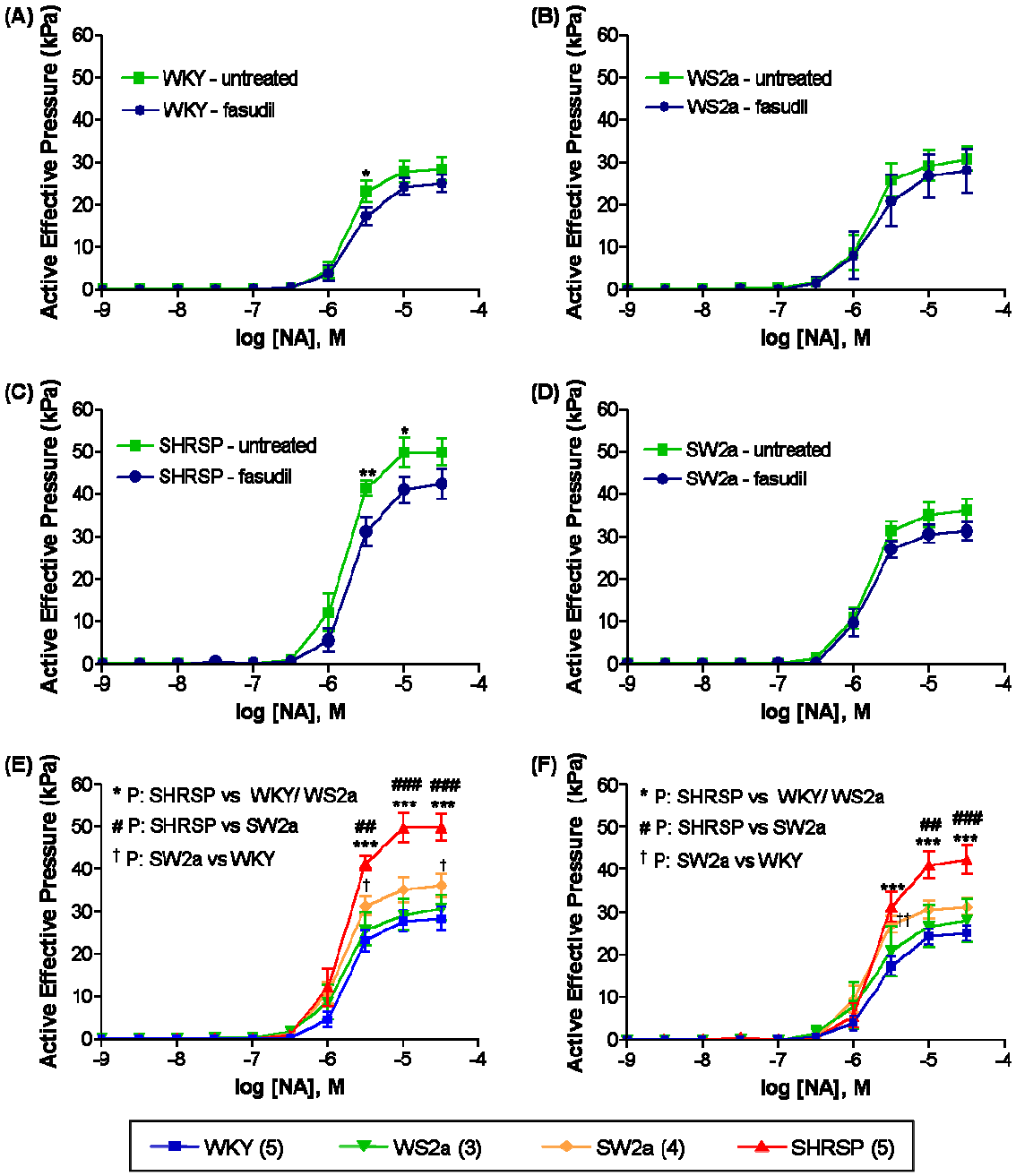


**Figure 4-4 - Contractile responses to noradrenaline (NA) in MRAs from 16 week old parental WKY and SHRSP and congenic WKY.SP$_{Gla}$2a and SP.WKY$_{Gla}$2a strains. Concentration-response curves of (A) WKY, (B) WKY.SP$_{Gla}$2a, (C) SHRSP and (D) SP.WKY$_{Gla}$2a to NA ($10^{-9}$ to $3x10^{-5}$M) before and after acute treatment with fasudil 3µM, using wire myography. (E) Comparison of contraction curves of untreated MRAs. (F) Comparison of contraction curves of fasudil-treated MRAs. Data are expressed as mean ±SEM; n=number of animals is indicated in parenthesis; *,**,*** P< 0.05, 0.01, 0.001 indicate significant statistical difference calculated by two-way ANOVA (treatment - [NA] or rat strain - [NA]), followed by Bonferroni test.**

Endothelium-mediated relaxation to cumulative doses of carbachol ($3x10^{-8}$ to $10^{-5}$ M) was measured in NA-pre-contracted MRAs, at baseline and after eNOS inhibition with L-NAME (100μM, 30min before stimulation with agonists), to evaluate function of endothelium and contribution of endothelial NO on relaxation, in each strain.

In the first series of experiments, fully (100%) pre-contracted arteries ($3x10^{-5}$M NA) from SHRSP and SP.WKY$_{Gla}$2a relaxed in a similar manner to carbachol ($3x10^{-7}$ to $10^{-5}$M) and significantly less compared to WKY and WKY.SP$_{Gla}$2a, under basal conditions (Figure 4-5). Data are summarised in Table 4-4.

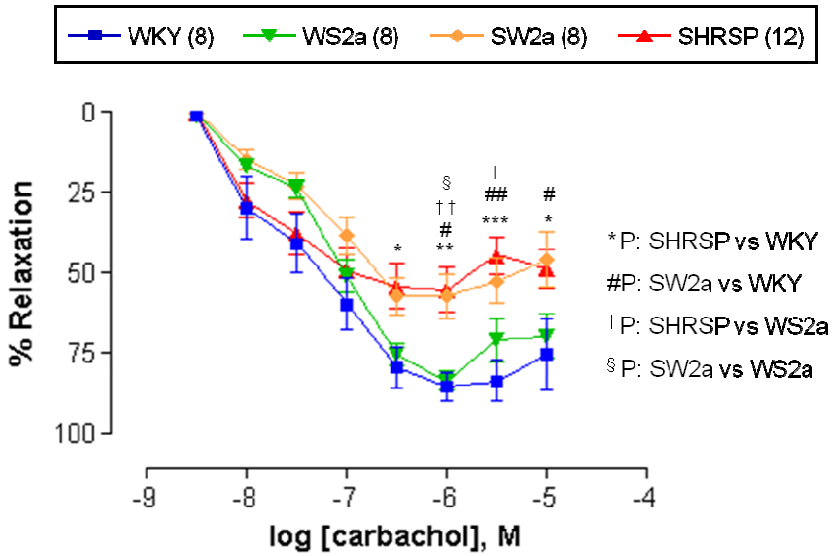


**Figure 4-5 - Endothelium-dependent relaxation to carbachol, in fully (100%) pre-contracted MRAs with noradrenaline, from 16 week old parental WKY and SHRSP and congenic WKY.SP$_{Gla}$2a and SP.WKY$_{Gla}$2a strains. MRAs were pre-contracted with $3x10^{-5}$M NA and concentration-response curves to carbachol ($3x10^{-8}$ to $10^{-5}$M) were generated using wire myography. Data are expressed as mean ±SEM; n=number of animals is indicated in parenthesis; *,**,*** P< 0.05, 0.01, 0.001 indicate statistical difference calculated by two-way ANOVA (rat strain - [carbachol]), followed by Bonferroni test.**

In a following set of experiments MRAs were pre-contracted to approximately 80% ($2x10^{-6}$M NA) before treatment with L-NAME. Untreated arteries relaxed completely in all four strains (Figure 4-6A). Inhibition of eNOS significantly decreased carbachol-induced relaxation of MRAs from SHRSP compared to WKY and the two congenic strains ($3x10^{-7}$ to $10^{-5}$ M). Responses of SP.$WKY_{Gla}$2a were affected to a lesser extent, without reaching significance against WKY and WKY.$SP_{Gla}$2a (Figure 4-6B). Looking specifically into each strain, L-NAME treatment partially reduced relaxation to carbachol in MRAs from WKY ($10^{-7}$ to $3x10^{-7}$ M), but had no significant effect on WKY.$SP_{Gla}$2a (Figure 4-6C and D). On the contrary, inhibition of eNOS highly impaired vasodilatation in MRAs from SHRSP and SP.$WKY_{Gla}$2a ($10^{-7}$ to $10^{-5}$ M) (Figure 4-6E and F). Moreover, upon treatment sensitivity to carbachol was reduced in all four strains, however to a different extent, as indicated by the rightward shift of the curve. Data are summarised in Table 4-4.

**Table 4-4. Relaxation responses of MRAs**

| Group | Carbachol % Relaxation ($3x10^{-6}$ M) (100% pre-contracted) | Carbachol % Relaxation ($3 x 10^{-6}$ M) (80% pre-contracted) | Carbachol + L-NAME % Relaxation ($3 x 10^{-6}$ M) (80% pre-contracted) | SNP % Relaxation ($3 x 10^{-6}$ M) (80% pre-contracted) |
|---|---|---|---|---|
| **WKY** | 83.50 ± 6.43***, ## | 98.36 ± 0.77 | 84.21 ± 10.53 * | 100 ± 0.26 |
| **WS2a** | 70.76 ± 6.57 * | 95.05 ± 2.83 | 93.41 ± 2.56 ** | 98.3 ± 1.67 |
| **SW2a** | 52.34 ± 7.10 | 95.12 ± 3.63 | 63.11 ± 12.25 §§ | 94.6 ± 2.77 |
| **SHRSP** | 44.53 ± 5.88 | 88.33 ± 3.05 | 47.21 ± 10.85 §§§ | 97.6 ± 0.66 |

**Values are means ± SEM**

*****,**,* P < 0.001, 0.01, 0.05 vs SHRSP ## P < 0.01 vs SW2a**

**§§§,§§ P < 0.001, 0.01 vs untreated**

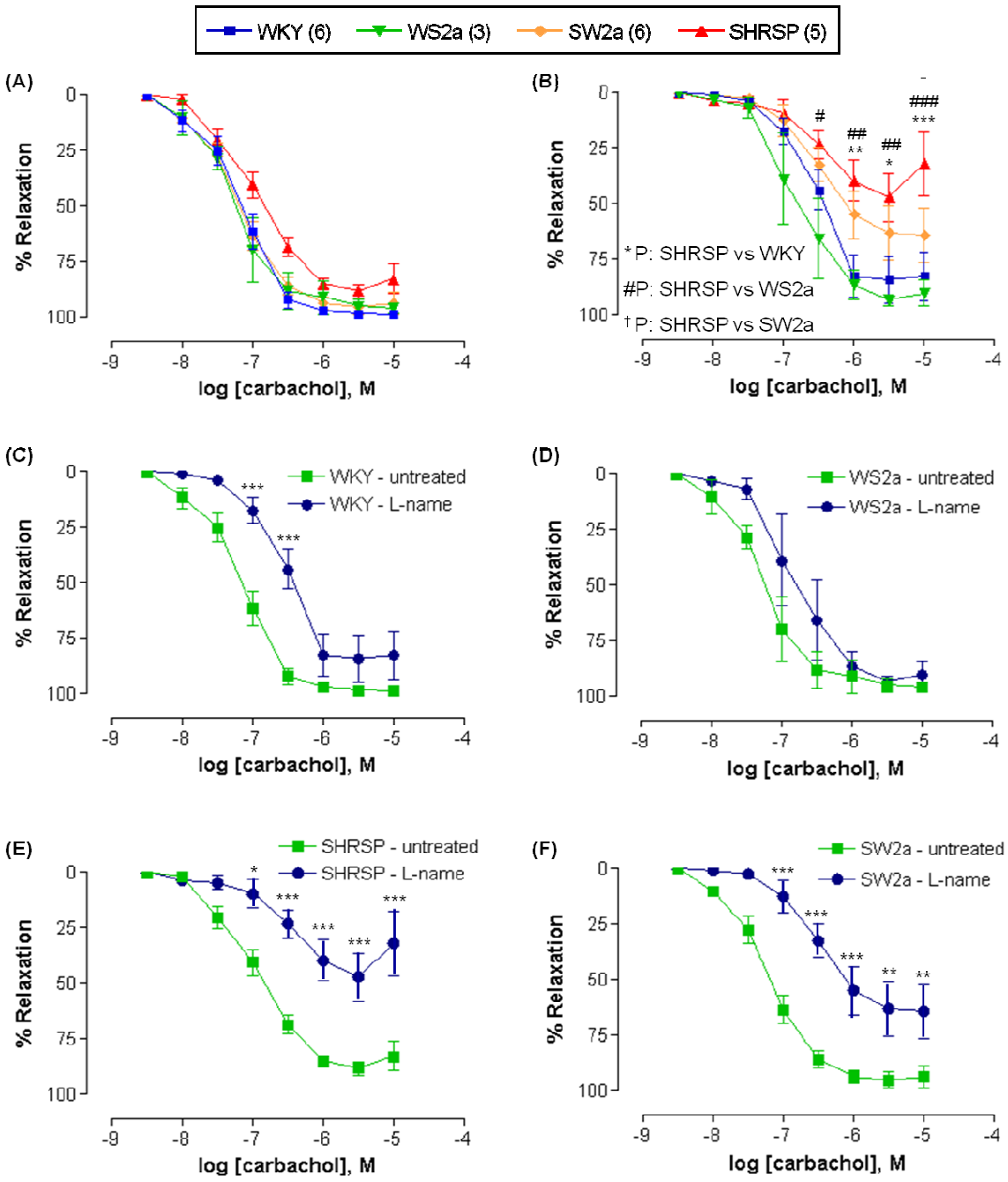


**Figure 4-6 - Endothelium-dependent vasodilatation responses to carbachol, in 80% NA pre-contracted MRAs from 16 weeks old parental WKY and SHRSP and congenic WKY.SP$_{Gla}$2a and SP.WKY$_{Gla}$2a strains. (A) Comparison of relaxation curves of untreated MRA. (B) Comparison of relaxation curves of L-name-treated MRA. Concentration-response curves of (C) WKY, (D) WKY.SP$_{Gla}$2a, (E) SHRSP and (F) SP.WKY$_{Gla}$2a to carbachol ($3x10^{-8}$ to $10^{-5}$M) before and after treatment with L-name (100μM), using wire myography. Data are expressed as mean ±SEM; n=number of animals is indicated in parenthesis; *,**,*** P< 0.05, 0.01, 0.001 indicate statistical difference calculated by two-way ANOVA (treatment - [carbachol] or rat strain - [carbachol]), followed by Bonferroni test.**

Endothelium-independent relaxation of NA-pre-contracted vessels ($2x10^{-6}$M) was assessed in response to cumulative doses of the external nitric oxide (NO) donor, sodium nitroprusside (SNP; 3x10-8 to 10-5 M). Relaxation curves did not differ between the four strains (Figure 4-7). Data are also summarised in Table 4.

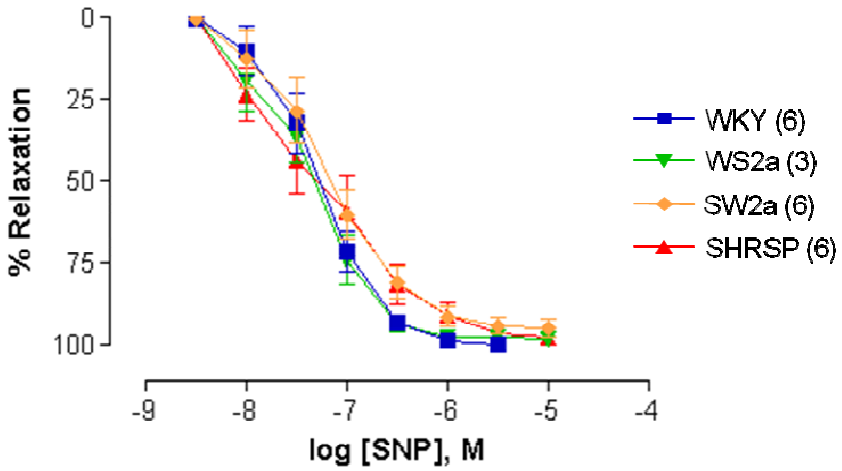


**Figure 4-7 - Endothelium-independent vasodilatation responses to the external nitric oxide donor, sodium nitroprusside (SNP) in noradrenaline pre-contracted (80%) MRAs. Concentration-response curves of WKY, WKY.SP$_{Gla}$2a, SHRSP, and SP.WKY$_{Gla}$2a, to SNP ($3x10^{-8}$ to $10^{-5}$M), using wire myography. Data are expressed as mean ±SEM; n=number of animals is indicated in parenthesis. Statistical difference between treatment groups was calculated by two-way ANOVA (rat strain - [SNP]).**

### 4.2.3 Isolation of primary VSMCs from MRAs and culture establishment

To investigate whether differences in physiology of MRAs are represented at the cellular and molecular level, primary VSMCs from MRAs of 16 week old WKY, SHRSP and 2a congenic strains were isolated and cell cultures were established (sections 2.2.1 and 2.2.2). Purity of primary VSMC cultures was assessed by positive immunofluerescent staining (ICC) for the smooth muscle cell type-specific marker SMC-α-actin (ACTA2), at passage 3, as described in section 2.2.4. Green fluorescent staining of actin microfilaments demonstrated clear domination of VSMCs (>90%) (Figure 4-8, middle). Negative species-specific IgG (rabbit) control showed no detectable staining (Figure 4-8, right).

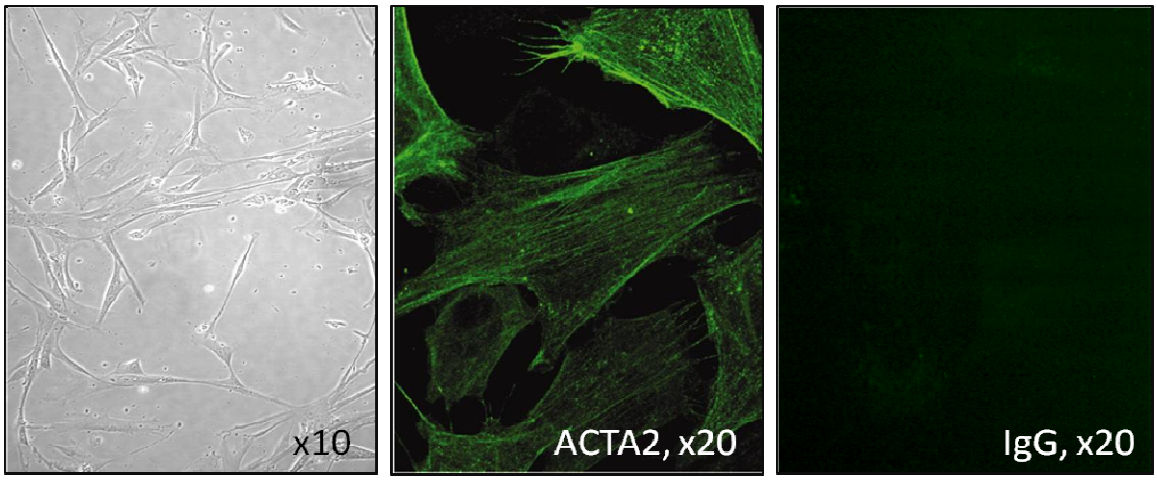


**Figure 4-8 - Characterisation of mesenteric VSMC cultures from 16 week old rats, by immunocytochemistry. VSMC cell culture at passage 3, x10 magnification (left). Immunofluorescent staining for ACTA2 (polyclonal rabbit-anti human, 1/100, ab5694), x20 magnification (middle). Isotype (rabbit IgG) negative control (right).**

### 4.2.4 S1P-Receptors expression in primary VSMCs from MRAs

Previous microarray and protein expression data from renal tissue and primary VSMCs, indicated S1PR1 as a positional candidate of salt-sensitivity and BP regulation in SHRSP (Graham et al., 2007). Following these observations, S1PR1 expression was investigated in primary mesenteric VSMCs relative to primary aortic VSMCs. Moreover, levels of S1PR2 and S1PR3 were tested in mesenteric primary VSMCs. WB analysis (section 2.3) was performed on whole cell lysates (section 2.2.7) from 16 weeks old WKY, SHRSP and the 2a congenics, probed with specific receptor antibodies. No bands corresponding to the size of S1PR1 (47kDa) were detected in any of the strains, for mesenteric or aortic VSMCs. Positive control of transfected CCL39 cells expressing human S1PR1 gave an intense band at the expected size. No signal was detected in negative control of untransfected CCL39 cells. (Figure 4-9; top panel). Similarly, expression levels of S1PR2 and S1PR3 were beyond detection in mesenteric VSMCs from WKY and SHRSP (Figure 4-9 B and C; top panels). β-actin was used as loading control.

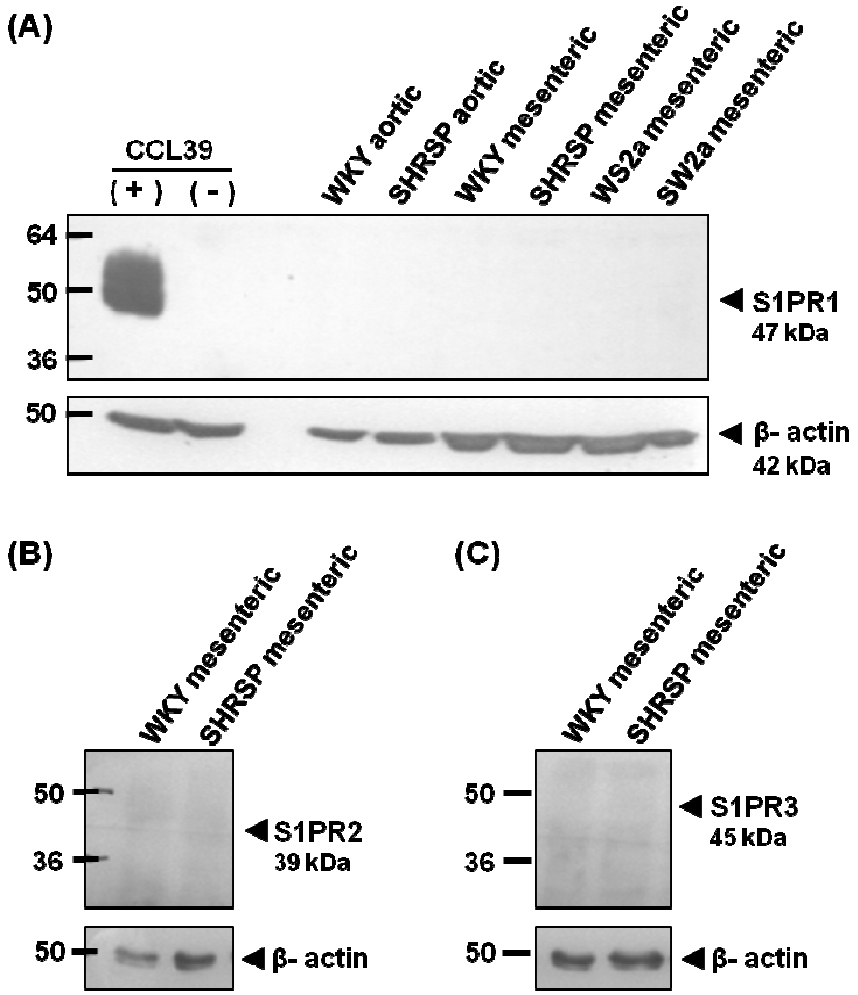


**Figure 4-9 - S1P-Receptors expression in whole cell lysates of primary VSMCs from 16 week old WKY, SHRSP and 2a congenic strains. Top panels: (A) immunoblot for S1PR1 (PA1-1040 antibody provided by Dr. Tim Palmer) in: transfected CCL39 hamster lung fibroblast cells stably expressing human S1PR1 protein ((+) positive control), CCL39 untransfected cells ((-) negative control), primary aortic VSMCs from WKY and SHRSP (lanes 3,4), primary VSMCs from MRAs of WKY, SHRSP, WKY.SP$_{Gla}$2a and SP.WKY$_{Gla}$2a (lanes 5 to 8). (B) immunoblot for S1PR2 and (C) S1PR3 in primary VSMCs from MRAs of WKY and SHRSP. Bottom panels: immunoblots for β-actin used as loading control. Protein loaded: 80 μg.**

### 4.2.5 S1PR1 signalling in primary VSMCs from MRAs

Despite expression levels of S1PR1 below the detection threshold of western analysis in mesenteric primary VSMCs from the four strains (section 4.2.4), investigation of receptor's downstream signalling was performed based on and in order to confirm data from previous studies, which demonstrated altered S1PR1 MAP kinase signalling between WKY and SHRSP in mesenteric VSMCs (Yogi et al., 2011). A drug agonist/antagonist intervention was applied to compare phosphorylation levels of signalling effectors and verify the receptor subtype through which S1P induces its effects, in primary VSMCs from the parental and congenic strains. As described in section 2.2.5, cells were either stimulated with the S1P agonist ($10^{-6}$M) for 30mins or pre-exposed to VPC23091 ($10^{-5}$M), a potent S1PR1 antagonist, for 30min before S1P stimulation. Levels of phosphorylation of the MAP kinases SAPK/JNK, ERK1/2 and p38MAPK were compared by WB analysis (section 2.3) on whole cell lysates (section 2.2.7). Membranes were probed with specific antibodies for total and phosphorylated forms of SAPK/JNK, ERK1/2 and p38MAPK. β-actin was used as loading control. Responses were expressed as percentages of the initial phosphorylation levels during control treatment with vehicle.

S1P-stimulation significantly increased SAPK/JNK phosphorylation in cells from all four strains. Responses were augmented in SP.WKY$_{Gla}$2a compared to the other three strains. VPC pre-treatment did not appear to have any inhibitory effects on the S1P-induced phosphorylation in any of the strains, but WKY.SP$_{Gla}$2a. However no statistics could be performed on the latter strain as there was only one experimental replicate. (Figure 4-10)

Moreover, stimulation with S1P induced significant p38MAPK phopshorylation of similar magnitude in cells from WKY and SP.WKY$_{Gla}$2a, but not in SHRSP and WKY.SP$_{Gla}$2a. Treatment with VPC did not abrogate this change in phosphorylation levels. (Figure 4-11)

Finally, S1P significantly stimulated ERK1/2 phosphorylation in parental strains as opposed to congenics. Effects were enhanced in cells for WKY relative to SHRSP, without reaching significance. VPC did not significantly block S1P-mediated ERK1/2 phosphorylation in any strain. (Figure 4-12)

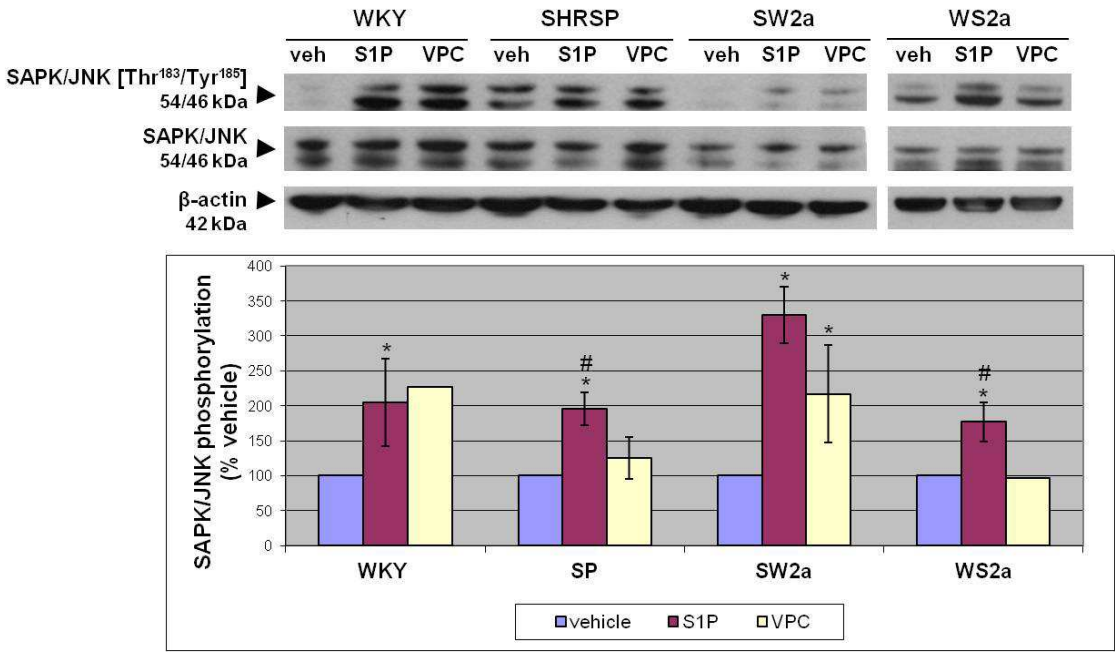


**Figure 4-10 - Effect of S1PR1 receptor stimulation and antagonism on S1P-induced SAPK/JNK phosphorylation in VSMCs from WKY, SHRSP and the 2a congenics. Mesenteric primary VSMCs from 16 week old WKY, SHRSP, SP.WKY$_{Gla}$2a and WKY.SP$_{Gla}$2a were stimulated with $10^{-6}$M S1P for 30mins or pre-treated with $10^{-5}$M VPC23091 for 30min prior to S1P stimulation. Top panels, representative immunoblots on whole cell lysates for SAPK/JNK [Thr$^{183}$/Tyr$^{185}$] (top), SAPK/JNK (middle) and β-actin (bottom). Protein loaded: 30 μg. Bottom, corresponding densitometry bar graph demonstrating the effect of S1P stimulation on SAPK/JNK phosphorylation and of VPC23091 on S1P-induced SAPK/JNK phosphorylation in VSMCs of the four strains. Results come either from one or are the mean ±SEM of 2 or 3 experiments and were compared by Student's t-test (unpaired, two-tailed). *P<0.05 vs vehicle; #P<0.05 vs S1P-stimulation in SP.WKY$_{Gla}$2a.**

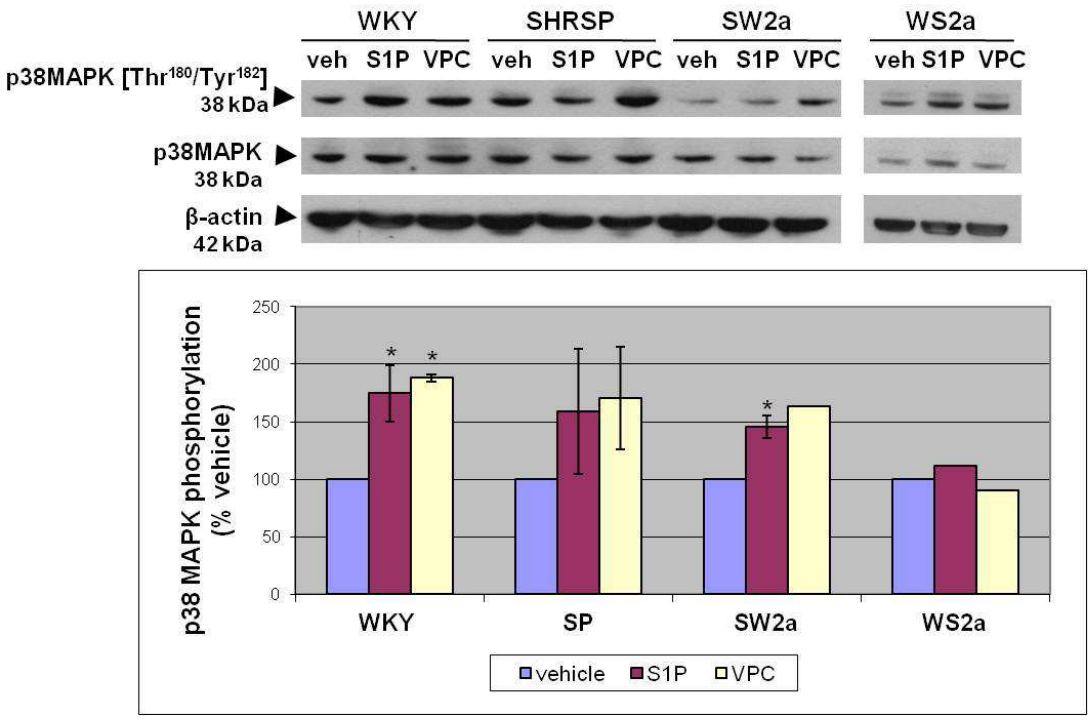


**Figure 4-11 - Effect of S1PR1 receptor stimulation and antagonism on S1P-induced p38MAPK phosphorylation in VSMCs from WKY, SHRSP and the 2a congenics. Top panels, representative immunoblots for p38MAPK [Thr$^{180}$/Tyr$^{182}$] (top), p38MAPK (middle) and β-actin (bottom). Protein loaded: 30 µg. Bottom, corresponding bar graph demonstrating the effect of S1P ($10^{-6}$M) stimulation on p38MAPK phosphorylation and of VPC23091 ($10^{-5}$M) on S1P-induced p38MAPK phosphorylation in VSMCs of the four strains. Results come either from one or are the mean ±SEM of 2 or 3 experiments and were compared by Student's t-test (unpaired, two-tailed). *P<0.05 vs vehicle.**

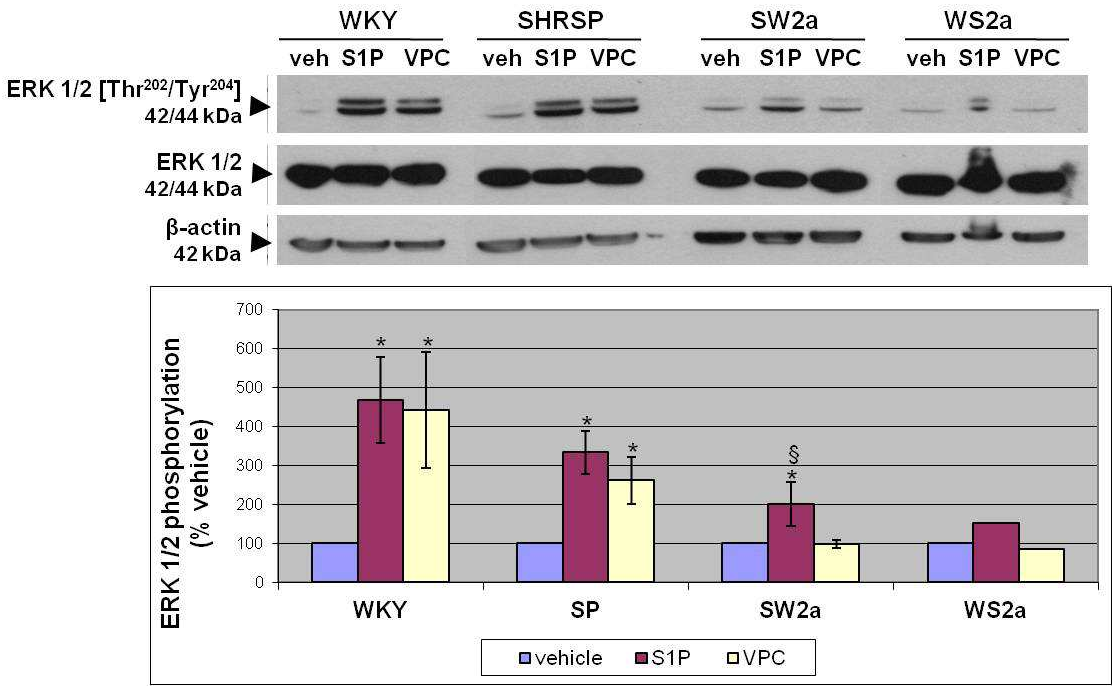


**Figure 4-12 - Effect of S1PR1 receptor stimulation and antagonism on S1P-induced ERK 1/2 phosphorylation in VSMCs from WKY, SHRSP and the 2a congenics. Top panels, representative immunoblots for ERK 1/2 [$Thr^{202}/Tyr^{204}$] (top), ERK 1/2 (middle) and β-actin (bottom). Protein loaded: 30 μg. Bottom, corresponding bar graph demonstrating the effect of S1P ($10^{-6}$M) stimulation on ERK 1/2 phosphorylation and of VPC23091 ($10^{-5}$M) on S1P-induced ERK 1/2 phosphorylation in VSMCs of the four strains. Results come either from one or are the mean ±SEM of 2 or 3 experiments and were compared by Student's t-test (unpaired, two-tailed). *P<0.05 vs vehicle; §P<0.05 vs S1P-stimulation in WKY.**

## 4.3 Discussion

Previous introgression of normotensive-WKY or hypertensive-SHRSP chromosome 2 interval into the reciprocal genetic background generated the SP.$WKY_{Gla}$2a and WKY.$SP_{Gla}$2a congenic strains of increased SBP phenotypes. This study aims to further investigate the significance of the interval on vascular/endothelial function and remodelling in mesenteric resistance arteries (MRA) from 16 week old parental and 2a congenic strains. *Ex vivo* studies compared structure, mechanics and function of arteries. *In vitro* experiments in primary VSMCs from MRAs focused on investigation of S1P/S1PR1-mediated mitogenic signalling.

Remodelling of MRAs was assessed by comparison of structural and mechanical vascular properties. Basic structure measurements of internal (Di) and external (Do) diameter, wall thickness, wall:lumen ratio and CSA were similar between WKY and SHRSP. Nonetheless, the decreased trends in Do, wall thickness and CSA in SHRSP, especially at high intravascular pressures (>60mmHg), indicate smaller vessel size and thinner walls, and imply a tendency of the hypertensive vessels to be stiffer. However, previous microscopic investigation of structure in MRAs from 8-10 month old SHRSP (Glasgow) has shown hypertrophic inward remodelling resulting from a reduced vessel lumen and an increased wall thickness and wall:lumen ratio compared to WKY (Arribas et al., 1997). This may suggest that structural alterations develop later in life as an adaptive response to increased BP, which is in agreement with studies on time course development of remodelling in MRAs from SHR demonstrating no structural alterations up to 1 month but present at 5 and 6 months old animals (Gonzalez et al., 2006, Intengan et al., 1999). Further, from the two congenic strains, SP.$WKY_{Gla}$2a exhibited characteristics very similar to WKY, implying a potential beneficial effect of the WKY congenic interval. Such an effect has already been evident through the reduced SBP of SP.$WKY_{Gla}$2a compared to SHRSP. On the other hand, WKY.$SP_{Gla}$2a demonstrated increased Di, associated with decreased wall thickness and consequently lower wall:lumen ratio and CSA compared to WKY. Such alterations indicate a vessel of similar size but thinner walls, which could be interpreted as adaptive responses (reduce peripheral vascular resistance) to the detrimental effect (increased hemodynamic load/SBP) introduced by the SHRSP congenic interval.

In line with the structural data, comparison of MRA mechanical properties, in SHRSP versus WKY, demonstrated significant decrease in wall strain, thus reduced ability to stretch (elasticity). This was also evident in the decreased trend of incremental distensibility (at

physiological intravascular pressures of 20 to 60 mmHg), which implies requirement of greater pressure in SHRSP to achieve similar percentage of Di change with WKY. However, wall stress (wall tension), which depends on the Di and wall thickness, did not differ between the parental stains, as expected. Nevertheless, the stress-strain relationship indicated a tendency of vessels from 16 week old SHRSP to be stiffer. Such observations are supported by previous studies on MRAs from 20-24 week old SHR that reported increased intrinsic wall stiffness and reduced stress and incremental distensibility compared to WKY (Intengan et al., 1999, Briones et al., 2003). This implies that the mechanical alterations probably develop later in life, following vascular remodelling. With respect to SP.WKY$_{Gla}$2a, MRA mechanical properties did not differ significantly to those of the parental animals. Nonetheless, elasticity of arteries (strain) at high pressures, as well as their stiffness tended to improve by introgression of the WKY congenic interval. In WKY.SP$_{Gla}$2a, the ability of arteries to stretch (strain and incremental distensibility) was similar to the one of WKY. However, introgression of the SHRSP congenic interval appeared to significantly elevate wall tension, which is not surprising, considering the significantly reduced wall thickness observed in this strain. Moreover, stiffness of the vessels tended to increase. In both congenic strains, the observed tendencies in stiffness are in agreement with the respective changes introduced in SBP by the congenic interval. However, the cause and effect relationship is still not clear, despite the fact that the above data collectively would support that changes in SBP occur as primary events leading to changes in stiffness at a later stage.

Taken together the above findings demonstrate no evident remodelling in SHRSP MRAs at the age of 16 weeks, despite the established hypertension. A possible explanation could be that structural and mechanical alterations develop later in life as adaptive responses to increased BP. From experiments on rat models of hypertension, it is known that primary structural abnormalities in distal resistance arteries (arterioles) seem to be responsible for increase in BP which finally leads to adaptive structural changes in proximal resistance arteries (small arteries) . It is also known that resistance artery structure is not entirely dependent on the development of hypertension, but it is also affected by neurohormonal (Folkow et al., 1988) and genetic factors. Data supporting this hypothesis showed that improvement in SHRSP vessel structure, such as reduction in wall:lumen ratio, did not reduce BP and *vice versa* (Morton et al., 1992, Hashimoto et al., 2010, Rigsby et al., 2011). Furthermore, introgression of the SHRSP-'diseased' congenic interval into WKY.SP$_{Gla}$2a seems to introduce great alterations in MRA structural and mechanical

properties as an attempt of the WKY-'healthy' background to correct the increased BP. On the other hand, introduction of the WKY congenic interval in SP.WKY$_{Gla}$2a does not manage to significantly improve the 'diseased' phenotype. Further evaluation of differences in MRA structure and mechanical properties by histological staining for markers of morphological changes, such as elastin and collagens content, would have been more supportive of our data, but there was a limitation of time.

Subsequently, assessment of contractile function in MRAs demonstrated hypercontractility of SHRSP arteries compared to the other strains, which could explain the increased BP in SHRSP at this age, in the lack of significant structural/mechanical alterations. In support of this observation, several studies have shown hypercontractility in hypertensive rat strains (Gradin et al., 2003). Moreover, the reduced contractile responses of SP.WKY$_{Gla}$2a in comparison to SHRSP imply that introgression of WKY congenic interval improves the hypercontratile phenotype. In contrast, insertion of the SHRSP congenic interval in WKY.SP$_{Gla}$2a did not seem to have any detrimental effect on the vascular tone of WKY. Therefore, it could be hypothesised that WKY control their contraction by components that lie both inside and outside chromosome 2 congenic interval and which could act synergistically or even compensate for each other's loss of functionality. Those components lying outside the interval seem to be predominant, as they maintain normal contractile function in WKY.SP$_{Gla}$2a, whereas in SP.WKY$_{Gla}$2a function is only partially improved. Further, acute inhibition of RhoK, to investigate the role of RhoA/RhoK signalling on contraction of the smooth muscle, demonstrated significant improvement of hypercontractility in SHRSP arteries, but had no effect on WKY and the congenic strains. Such observations are consistent with previous studies suggesting implication of RhoA/RhoK pathway in increased contractile responses of hypertensive rat models (Kitazono et al., 2002, Moriki et al., 2004). Moreover, reduction of hypercontractility in SHRSP could partially be attributed to decreased release of EDCFs, another effect of RhoK blockade. This is supported by studies on WKY aortas, in which inhibition of RhoK resulted in a significant decrease of endothelium-dependent contractions (Chan et al., 2009). On the other hand, contractions in MRAs from WKY, WKY.SP$_{Gla}$2a and SP.WKY$_{Gla}$2a seem to only partially be mediated by RhoA/RhoK pathway, considering the trend of reduced responses upon RhoK inhibition. It is therefore suggested that alternative contraction regulatory systems are predominant in these strains, such as potassium channels and PKC. This explanation further supports our earlier hypothesis suggesting existence of components, in this case other regulatory systems,

present within or outside the congenic interval of WKY having a beneficial effect on contractile responses in 2a congenics. Further experiments, including inhibition of the other contraction pathways, calcium sensitivity and cyclic GMP regulation studies, measurement of Rho kinase activity and expression levels of RhoA/RhoK activation markers, such as ezrin and MLC, would enable a better understanding and verification of the above data.

Moreover, assessment of vasodilatory responses of fully pre-contracted MRAs revealed significantly reduced ability of SHRSP and SP.WKY$_{Gla}$2a to relax in comparison to WKY and WKY.SP$_{Gla}$2a, at 16 weeks of age. Such observations indicate a predominant role of the genetic background over the congenic interval on regulation of relaxation**.** Further, based on the increased SBP phenotype of WKY.SP$_{Gla}$2a, it is implied that impaired relaxation is a secondary event to elevated BP in this strain. Whether this impairment is the result of smooth muscle or endothelial dysfunction was further examined. Endothelium-independent responses to an external vasodilator (SNP: NO donor) were similar in all four strains, indicating fully functional smooth muscle at this age. Endothelium-dependent relaxation was assessed by evaluating the contribution of endothelial NO bioavailability as relaxation mechanism in MRAs upon eNOS inhibition. A trend in WKY and WKY.SP$_{Gla}$2a arteries to dilate less than before eNOS blockade, imply that either NO is not the major vasodilator in MRAs of strains sharing WKY genetic background, but rather acts synergistically to alternative vasodilatory systems such as EDHF and prostacyclins, or that the alternative regulatory systems can effectively compensate for the reduced NO biovailability. Studies have previously demonstrated EDHF-signalling as the predominant vasodilatation mechanism in small resistance arteries, compensating for decreased NO availability (Ruiz-Marcos et al., 2001, Hussain et al., 2001, Madhani et al., 2003). On the contrary, in SHRSP and SP.WKY$_{Gla}$2a, eNOS inhibition was followed by significantly reduced dilatory responses, although introgression of the WKY congenic interval slightly, but not significantly, improved relaxation. This suggests that either NO bioavailability is the predominant mechanism in strains sharing SHRSP genetic background, as shown previously (Kerr et al., 1999, Ma et al., 2001, McIntyre et al., 1997), or that the predominant EDHF or prostacyclin pathway is impaired (Sunano et al., 1999, Goto et al., 2004, Giachini et al., 2009) and NO, as a secondary system, can only partially compensate for the impairment. The ability of different vasodilatation systems to act synergistically or substitute each other in situations of endothelial dysfunction has been previously shown in MRAs from hypertensive models (Chataigneau et al., 1999, Sofola et al., 2002). Taken together the results from eNOS

blockade unmasked an endothelial dysfunction in SHRSP and SP.WKY$_{Gla}$2a, as a combination of impaired and non-efficient relaxation mechanisms, which are primarily regulated by the genetic background rather the congenic interval. Moreover, based on the opposite relaxation responses of the 2a congenic strains, despite their increased-SBP phenotypes, it is implied that endothelial impairment is a secondary event to elevated BP. In agreement with this, studies on aorta from SHRSP demonstrated that only at a later stage, after hypertension is established, endothelial dysfunction develops (Kerr et al., 1999, Onda et al., 1994). Further experiments, including inhibition of alternative relaxation systems and measuring of NO levels in MRAs from the four strains, would elucidate the predominant vasodilatory mechanisms and impairments in each strain.

In order to investigate whether the above physiological differences in MRAs from our strains are represented at the cellular/molecular level, cell cultures of primary mesenteric VSMCs were established. S1PR1 expression and mitogenic signalling were chosen to be assessed in these cells, based on existing data identifying S1PR1 receptor as a positional candidate for hypertension and implicating S1P/S1PR1 signalling in vascular inflammatory responses and cell growth in VSMCs (Graham et al., 2007, Yogi et al., 2011), processes that impact on vascular remodelling and endothelial dysfunction in hypertension. In contrast to previous studies from Touyz's group demonstrating similar expression of S1PR1 and S1PR2 subtypes between WKY and SHRSP, but absence of S1PR3 in these cells (Yogi et al., 2011), our studies showed expression levels below detection for all three receptor subtypes in WKY and SHRSP. Similarly, S1PR1 levels were below detection in primary cells from 2a congenic strains MRAs, as well as from WKY and SHRSP aortas. These opposing results could be attributed to interstrain variability. Furthermore, it is known that GPCR receptors are generally expressed in low levels. Future studies could explore expression levels in enriched membrane fractions.

Considering growing evidence on the importance of S1P/S1PR signalling in development and regulation of vascular system and in pathogenesis of vascular diseases (Bolz et al., 2003, Allende and Proia, 2002, Deutschman et al., 2003), particularly from the work of Yogi *et* al. (Yogi et al., 2011) and in order to verify them, altered S1PR1 signalling through MAP kinase activation was investigated in cells from our strains. Phosphorylation levels of SAPK/JNK, ERK1/2 and p38MAPK as downstream signalling partners were assessed in response to the S1P stimulus and VPC blockade of S1PR1/3 receptors. Also, the 30min stimulation was chosen as the optimal time for maximal responses, according to previous

data (Yogi et al., 2011). Differential activation of MAPKs observed upon S1P stimulation is an indirect indication that our cells express at least one out of the three subtypes of S1PR receptors, despite their low levels as assessed by WB. However, the observation that VPC treatment was unable to significantly abrogate phosphorylation of MAPKs in mesenteric VSMCs from any strain indicates that these changes are potentially not mediated by S1PR1 or S1PR3. Such results contradict Yogi's data, and could suggest that S1PR2 may play a role in induction of MAPK pathways in these cells. However, no firm conclusions to support Yogi's data can be drawn regarding the extent of responses in each strain, due to the low number of repetitions of each experiment.

However, S1P signalling is still relevant, as involvement of other signalling pathways, apart from MAPKs, are known to influence vascular function (vascular remodelling and endothelial dysfunction), such as generation of ROS, activation of transcription factors and stimulation of cation channels (Mochizuki, 2009). To further investigate such pathways and to overcome difficulties on assessing contribution of the congenic interval to phenotypic differences by *ex vivo* and *in vitro* studies, a broader, high-throughput approach was followed, involving whole proteome profiling in our parental and 2a congenic strains in response to S1P stimulation, described in the following chapter. The ultimate aim would be to compare the outputs of signalling pathways in health and disease and to identify/predict the best points at which to intervene to redress the balance.

# 5 Proteome Profiling in S1P-Stimulated Mesenteric Primary VSMCs

# 5.1 Introduction

## 5.1.1 MS-based quantitative proteomics: SILAC

In the highly complex cellular environment, comprehensive characterisation of protein dynamic interactions and signalling networks is vital in revealing the mechanisms underlying biological processes. Development of high-throughput, MS-based quantitative proteomic approaches has enabled for large-scale mapping of interconnected protein networks (Aebersold and Mann, 2003).

Considering that MS is not essentially a quantitative method, molecules are stably labelled to assist quantification. Direct comparison of intensity signals between differentially labelled isotopes correspond to peptide and protein ratios.

Stable isotope labelling with amino acids of cells in culture (SILAC) is the most widespread metabolic labelling technique (Mann, 2006, Ong et al., 2002) applicable on both cell lines and primary cells. Combined with high-resolution LC-MS/MS and specialised data processing software, it provides a powerful strategy for rapid, unbiased screening of global proteomes and of post-translational modifications (PTM) occurring in response to particular stimuli (Olsen et al., 2006). Moreover, SILAC has been successfully used to study the temporal dynamics of signalling pathways by exploiting phosphorylation based enrichment methods coupled to MS (EGFR pathway; (Schulze and Mann, 2004)), as well as in the identification of prognostic disease biomarkers (Geiger et al., 2012). SILAC achieves highly reliable quantification of hundreds to thousands of proteins, within four orders of magnitude in protein abundance, including low level regulatory molecules and membrane proteins (de Godoy et al., 2008).

SILAC labelling is performed using media in which the normal isotopes $^{12}C$ and $^{14}N$ of arginine and lysine have been replaced by stable (non-radioactive) heavy isotopes $^{13}C$ or $^{13}C/^{15}N$, to be incorporated into proteins. Arginine and lysine are selected as sites of trypsin cleavage, thus generating chemically identical tryptic peptides (Olsen et al., 2004). Nevertheless, tryptic peptides derived from differentially labelled populations are isotopically distinct and thus distinguished by a defined mass shift of the peak in the mass spectra. Specific software quantifies intensity ratios of heavy labelled peptides over light isotopic pairs as relative abundance (Figure 5-1). Usually, protein ratios of 1.3 to 2.0-fold have been used as cut-offs for both statistical and biological significance (Mann, 2006). SILAC allows further for multiplex comparisons either in a single experiment using triple labelling,

or by linking several SILAC experiments through a common experimental state or through a 'spiked-in' labelled internal standard, without affecting quantitative accuracy (Andersen et al., 2005, Blagoev et al., 2004, Geiger et al., 2011, Kratchmarova et al., 2005).

### 5.1.2 Quantitative proteomics sample preparation and instrumentation

Recent advances in sample preparation strategies, instrument performance (Domon and Aebersold, 2006, Makarov et al., 2006) and bioinformatics tools (Mueller et al., 2008) have led to a spectacular progress and routine application of MS-based proteomics.

It is common practice for highly-complex protein mixtures to be enzymatically digested (e.g. trypsin) into mixtures of chemically identical peptides prior to MS analysis (Olsen et al., 2004). Further processing of digested peptides through liquid chromatography coupled to electrospray ionisation and high-resolution mass spectrometers (LC-ESI/MS) (Ho et al., 2003) has become the technique of choice for rapid analysis in shotgun quantitative proteomics (Aebersold and Mann, 2003, Cravatt et al., 2007). Amongst the existing mass analysers, linear iontrap quadrupole (LTQ) /orbitrap hybrids (Makarov et al., 2006) exhibit the highest resolving power and mass precision (5ppm m/z) and employ Fourier-transformation of peptide signals to generate MS spectra containing information on peptide mass and intensities. MS/MS fragmentation spectra are matched against sequence databases for peptide identification (Steen and Mann, 2004).

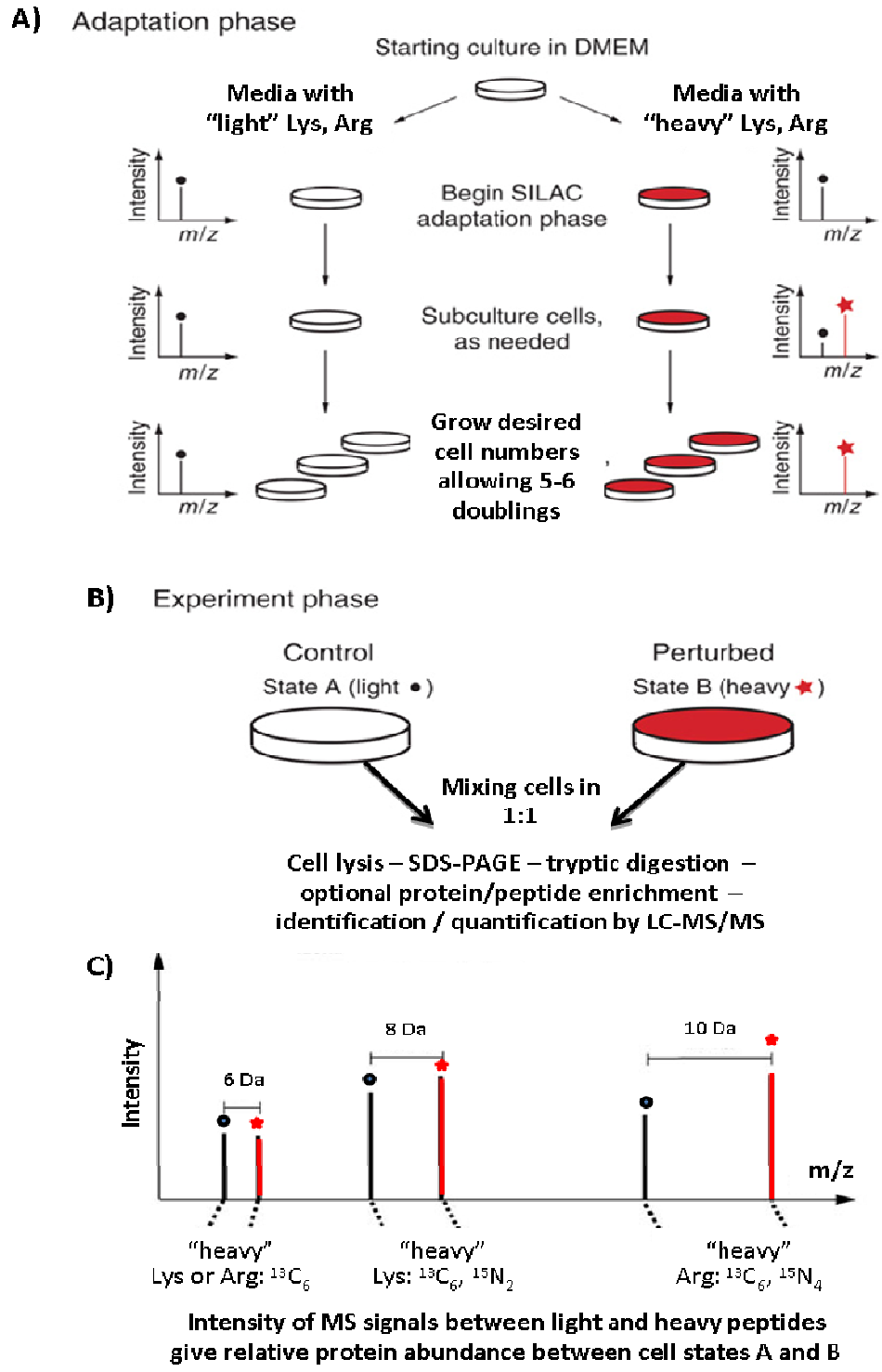


**Figure 5-1 - Stable isotope labelling by amino acids in cell culture (SILAC). (A) Adaptation phase. Cells are initially adapted to complete growth media supplemented with dialysed serum, for 24h. Subsequently, they are transferred into differentially isotope-labelled SILAC media for metabolic labelling. Control "light" media contain $^{12}C_6{}^{14}N_2$ L-lysine (Lys0) and/or $^{12}C_6{}^{14}N_4$ L-arginine (Arg0). "Heavy" media contain heavy isotopes of these amino-acids ($^{13}C_6$ L-lysine (Lys6) or $^{13}C_6{}^{15}N_2$ L-lysine (Lys8) and/or $^{13}C_6$ L-arginine (Arg6) or $^{13}C_6{}^{15}N_4$ L-arginine (Arg10)). Cells are propagated into SILAC media for 5-6 divisions, to ensure complete incorporation of labelled amino-acids. (B) Experimental phase. To quantify changes upon treatment of either cell population, labelled cells from both**

**populations (light and heavy) are harvested and combined in 1:1 ratio. Mixed cell lysate is then resolved by SDS-PAGE and visualized by Coomassie staining. Gel-lane slices or individual bands are extracted and subjected to trypsin digestion. Optional enrichment for a specific peptide fraction (e.g. phosphopeptides), is followed by separation of tryptic peptides by LC and identification/quantification by MS/MS analysis. (C) Exemplary mass spectra of isotopic peptide pairs. Differences in intensity ratios of peptide peaks reflect differences in relative protein abundance between the two states. (Adapted from Ong and Mann, 2006).**

### 5.1.3 Proteomic data processing and analysis: MaxQuant - Perseus

Large-scale proteomics analyses generate gigabytes of high-resolution MS data, requiring specialised software for efficient manipulation. MaxQuant is a widely applied computational proteomics platform (Cox et al., 2009), which uses a standardised workflow to process large numbers of LC-MS runs, including complex data from SILAC double or triple-labelling experiments (Andersen et al., 2005, Blagoev et al., 2004). Its high quantification accuracy lies upon algorithms that perform measurements at the level of individual peptides. In combination with robust peptide and protein scoring results, it enables high peptide identification rates, that are even higher on SILAC peptide pairs (Cox and Mann, 2008). In the case of SILAC experiments, raw data files generated by the mass analyser software are loaded into MaxQuant. Three-dimensional peak and isotope patterns are detected and assembled into SILAC pairs/triplets for quantification. SILAC-peptide ratios are normalised (log-ratio median = 0) to correct for unequal loading. Output files containing combined MS/MS fragmentation spectra from all LC-MS runs are submitted to either Mascot (commercial; (Perkins et al., 1999)) or Andromeda (MaxQuant-integrated; (Cox et al., 2011)) search engine, for peptide identification using a specified protein sequence database (e.g. IPI, Swissprot). Further processing in MaxQuant includes statistical validation of identifications, protein assembly and quantification and generation of summary tables containing all the information. Bioinformatics analysis and visualisation is performed on platforms such as Perseus, a separate module developed to complement MaxQuant workflow into a powerful, unified computational analysis pipeline for quantitative proteomics (http://www.perseus-framework.org), Scaffold (Searle, 2010) and IPA (http://www.ingenuity.com).

### 5.1.4 Aims

Previous microarray profiling of salt-loaded SHRSP, WKY and SP.WKY$_{Gla}$2a congenic strain indicated differential renal expression of *S1pr1*, in addition to a number of SNPs in the promoter region (Graham et al., 2007). Moreover, signalling through S1PR1 receptor was found to be altered in S1P-stimulated mesenteric VSMC from SHRSP compared to WKY (Yogi et al., 2011). In order to overcome the difficulties on assessing outputs in situations of health and disease by low-sensitivity, small-scale experiments and to further investigate the impact of the congenic interval on phenotype, high-throughput MS-based quantitative proteomics were employed. Comparison of global-proteome profiles of mesenteric primary VSMCs from 16-week-old WKY, SHRSP and 2a congenic strains (WKY.SP$_{Gla}$2a and SP.WKY$_{Gla}$2a) and characterisation of biological effects of a 30min S1P-stimulation on BP regulation were achieved using:

- high-throughput SILAC proteomic approach (triple-labelling) in the exploratory mode, to stably label global proteome for identification/monitoring of relative quantitative differences by LC-MS/MS analysis.

- bioinformatics analysis, to focus on significantly differentially expressed proteins and elucidate modulated biological processes, networks and pathways associated with S1P signalling and BP regulation.

- immunoblotting analysis, to validate SILAC results for significantly differentially expressed proteins as candidate molecules driving phenotypic changes in hypertension.

# 5.2 Results

## 5.2.1 Proteomics and bioinformatics analysis

Global proteomes of S1P-stimulated VSMCs from parental and 2a congenic strains were compared in two individual experiments using triple SILAC labelling (Light - Medium heavy - Heavy), as described in section 2.2.6: (A) $WKY_L$ - $WKY.SP_{Gla}2a_M$ - $SHRSP_H$ and (B) $WKY_L$ - $SP.WKY_{Gla}2a_M$ - $SHRSP_H$. Cell growth rates did not seem to be affected upon replacement of normal with isotopically labelled media supplemented with dFBS, during the adaptation phase. MS data were filtered down a stringent pipeline, combining high accuracy quantitative software, search engines and protein sequences databases, visualisation platforms and web-based functional analysis tools (Figure 5-2). Filtering removed noise and contaminants, leaving a substantially reduced number of proteins to be further analysed. Assessment of incorporation of labelled-amino acids into peptides seemed to be efficient, when MS/MS spectra were previewed in Mascot. Combined MS/MS data were then processed through multiple versions of MaxQuant (v1.1.1.25, 1.2.0.18 and 1.2.2.6) to overcome re-occurring issues with the triple-labelling quantification (inconsistencies between the raw data - intensities of individual peptides mapping to a protein - and relative protein abundance). Eventually, data analysed with the latest version, v1.2.2.6, were searched against the rat IPI database v3.68, using Mascot Server to accurately identify proteins (high probability scores). Proteins sharing a set of identified peptides were joined in a protein group, and protein quantification was performed based on unique and razor peptides (shared peptides associated with the group with the highest number of identified peptides). A total of 1998 proteins were identified across the two experiments, A and B. This number includes all isomers of each protein group which share at least half of the peptides with the leading protein of the group (majority isomers). Of these 1998 proteins, a small percentage represented highly abundant phosphorylated proteins, as visualised in Scaffold3 (v3.2.0). As shown in Figure 5-3, only six phosphoproteins were identified with a probability higher than 95%, when filtered for a minimum of 99% protein probability, 90% peptide probability and peptide number of 2. Raw data for all proteins identified using MaxQuant v1.2.2.6 are summarised in supplementary table 'PerseusDataTable_Expanded_MajorityIDs_1998', included in the hard copy (CD) accompanying the thesis.

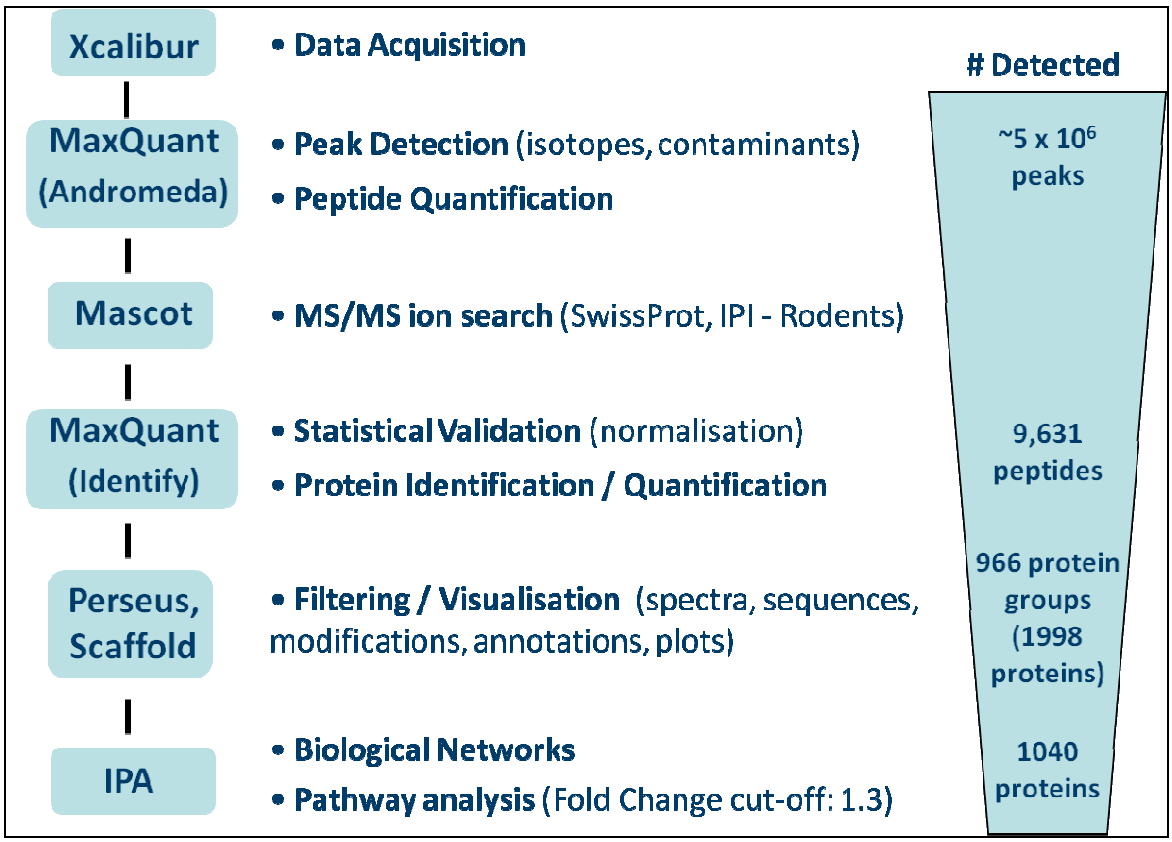


**Figure 5-2 – Proteomics analysis pipeline. MS/MS data from LTQ-Orbitrap Velos are extracted using Xcalibur, filtered and quantified through the MaxQuant workflow, associated with amino acid sequences on Mascot Server and uploaded to platforms such as Perseus and Scaffold for further manipulation and visualisation. Finally, Ingenuity Pathway Analysis (Ingenuity® Systems, www.ingenuity.com) is used for functional analysis and biological interpretation. Along the pipeline the number of detected features is remarkably reduced, allowing focus into a more manageable number of proteins.**

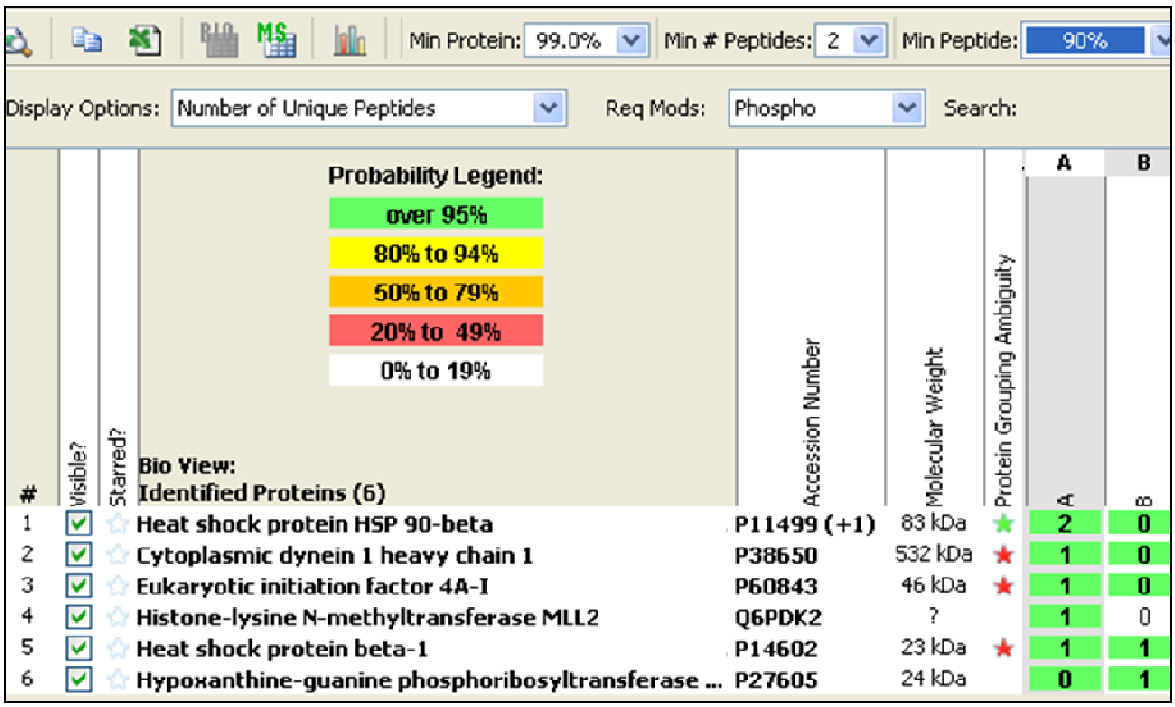


**Figure 5-3 - List of phosphorylated proteins identified at 95% probability, or higher, in Scaffold3 proteome software. Protein list generated by MaxQuant v1.2.2.6 was filtered for minimum protein probability: 99%, minimum peptide number: 2 and minimum peptide probability: 90%. Columns A and B include the number of unique peptides on which the identification was based for experiments A: WKY - WKY.SP$_{Gla}$2a - SHRSP and B: WKY - SP.WKY$_{Gla}$2a - SHRSP, respectively.**

Further processing and visualisation of the identified peptides/proteins was performed using Perseus v1.2.7.4. Data from pair-wise comparisons between strains were represented in histograms. Normalised relative log-ratios (subtract median from each distribution) of all proteins identified were plotted against summed peptide counts (light, medium and heavy), in each experiment (Figure 5-4). Comparisons of SHRSP vs WKY demonstrated normal distribution. However, skewed distributions were identified in comparisons including any of the medium-labelled congenic strains, in both experiments A and B. Specifically, a leftward shift was observed for congenic vs WKY (M/L) comparisons, indicating down-regulation of an unexpectedly large number of proteins in the congenics, whereas the rightward shift for SHRSP vs congenics (H/M) comparisons suggested up-regulation of the majority of proteins in SHRSP. Groups of proteins represented by bins (columns) adjacent to $\log_{10}$Ratio=0 (1:1 ratio) on the x-axis are not differentially expressed between the strains compared. In contrast, the longer the distance from 0, the greater the difference in expression levels.

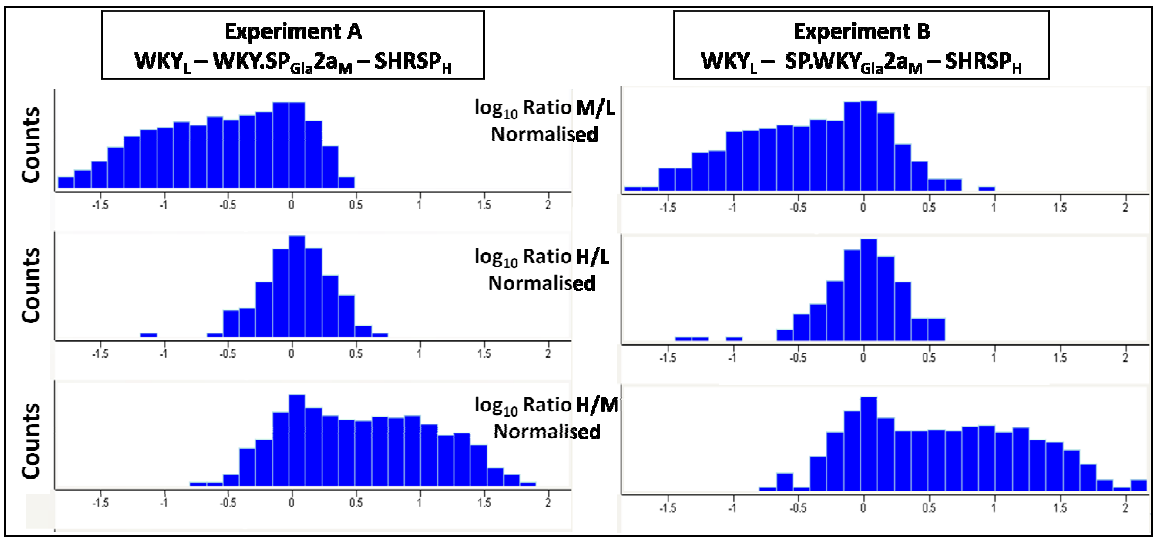


**Figure 5-4 - Distribution histograms of all proteins quantified per comparison in experiments A and B. Normalised protein ratios of each comparison (M/L: congenic vs WKY, H/L: SHRSP vs WKY, H/M: SHRSP vs congenic) are plotted on the x-axis using a log10 scale, against the summed peptide counts detected in each experiment, on the y-axis. Each bin (column) corresponds to a group of proteins sharing similar ratios. Proteins annotated to bins adjacent to $log_{10}$Ratio=0 (on the x-axis) show no or very small expression changes. Proteins groups of positive ratios include up-regulated proteins whereas groups of negative ratios contain down-regulated molecules. Data is acquired on MaxQuant v1.2.2.6 and histograms are generated on Perseus v1.2.7.4.**

Similar distribution-patterns were observed in scatterplot representation of relative log-ratios of all proteins identified, against summed peptide intensities (light, medium and heavy) detected for each protein, in each experiment (Figure 5-5). In this case proteins were represented by data points (coloured by density) exhibiting a colour gradient, ranging from light-blue to deep-red corresponding from unaltered up to high fold changes. In both experiments, distributions appeared shifted for comparisons including any of the medium-labelled (M) congenic populations, as opposed to normal distributions exhibited in the SHRSP vs WKY (H/L) comparisons, with the majority of proteins clustering around 0 (ratio 1:1). However, peptide distributions seemed to be slightly corrected when compared against analyses performed on previous versions of MaxQuant (v1.1.1.25, 1.2.0.18), but were still shifted compared to analysis on Mascot Distiller (Figure 5-6).

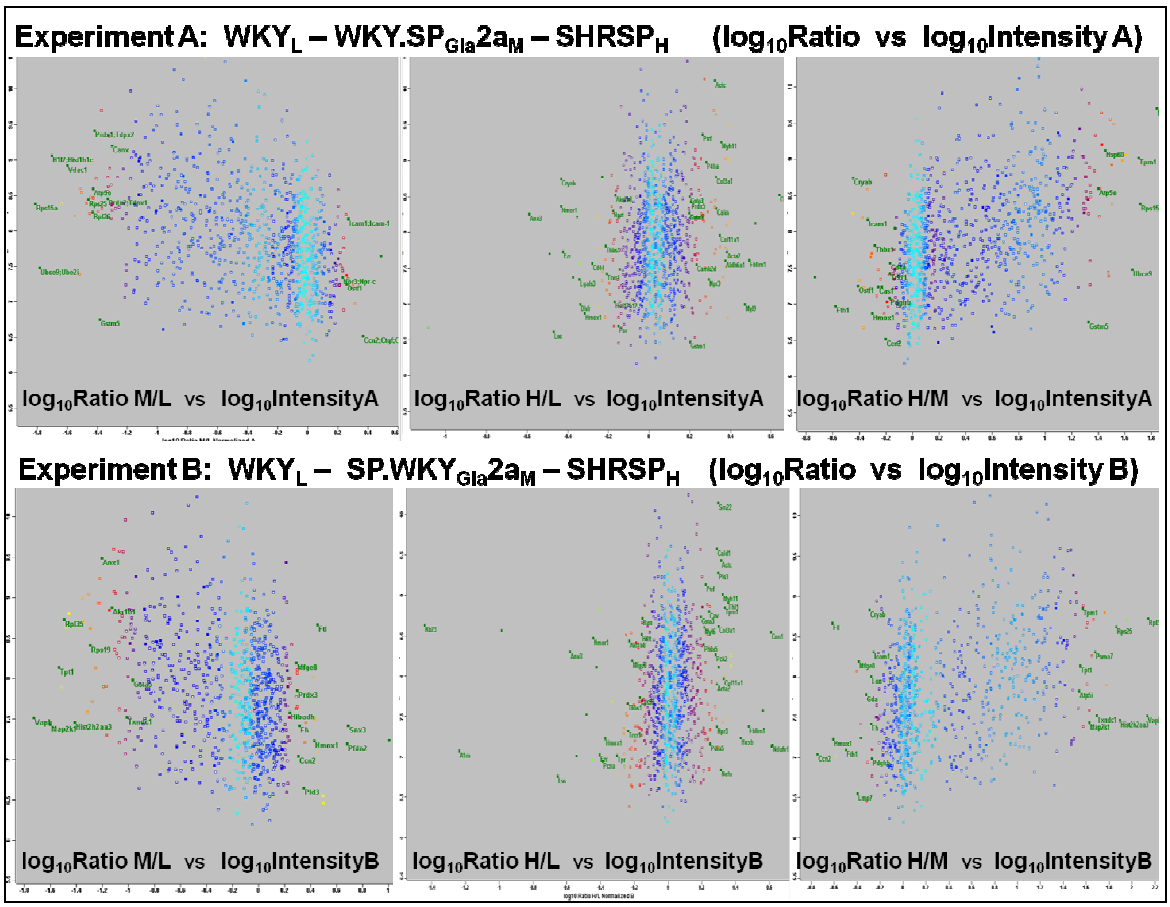


**Figure 5-5 – Quantitative scatterplots of all proteins quantified per comparison in experiments A and B. Relative protein ratios of each comparison (M/L: congenic vs WKY, H/L: SHRSP vs WKY, H/M: SHRSP vs congenic) are plotted on the x-axis using a $\log_{10}$ scale. The abundance of each protein is indicated on the y-axis as the sum of the individual peptide intensities detected for each protein, in each experiment. Proteins clustering around $\log_{10}$Ratio=0 (light blue dots) show no or very small expression changes. Data points are coloured for expression change, with dots in yellow/red corresponding to highly regulated proteins. Few of the most regulated molecules are annotated in green. Data is acquired on MaxQuant v1.2.2.6 and histograms are produced on Perseus v1.2.7.4.**

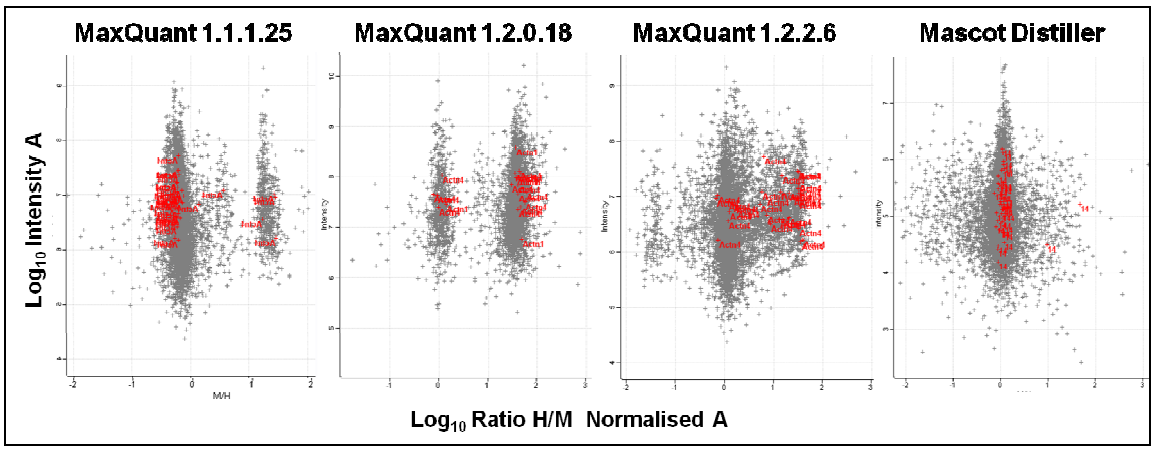


**Figure 5-6 - Software and version comparison. Quantitative scatterplots of all peptides quantified for the comparison H/M: SHRSP vs WKY.SP$_{Gla}$2a in experiment A, as acquired on MaxQuant v1.1.1.25, v1.2.0.18, v1.2.2.6 and on Mascot Distiller. Scatterplots are produced on Perseus. Relative peptide ratios (normalised) are plotted on the x-axis using a log$_{10}$ scale. The abundance of each peptide is indicated on the y-axis. The majority of peptides exhibit 1:1 ratio and cluster around log$_{10}$Ratio=0. In red: peptides mapping to protein alpha actinin 4 (IPI0023463 - MaxQuant; Swissprot q9qxq0 - Distiller). Distiller ratio is inverted to match MaxQuant.**

The unusual quantification pattern was also obvious when data were uploaded for biological interpretation onto IPA as protein lists containing SwissProt/IPI identifiers, expression values and FC. Specifically, from 1998 proteins (majority isomers) identified in total across experiments A and B by MaxQuant v1.2.2.6, 1736 had mapping IDs on IPA. Therefore, the primary focus during the discovery phase was on the SHRSP vs WKY (H/L) comparison, which was replicated in both A and B experiments. The reproducibility of the results in the two replicates was satisfactory (linear distribution along the diagonal axis) as indicated by correlation scatterplot of log-transformed normalised ratios, with no presence of distinct populations and the majority of hits clustering around 0 (1:1 ratio) (Figure 5-7A). Analysis on IPA identified 1148 proteins in union and 1056 in common (~92%) between $H/L_A$ and $H/L_B$. 338 and 288, respectively, were significantly differentially expressed (FC ≥ ±1.3), 'analysis-ready' proteins, exhibiting FC ranging from -12.18/-17.30 to 4.35/4.12 (in experiments A and B respectively) (Supplementary tables 'HLA_analysis ready_338' and 'HLB_analysis ready_288' included in the hard copy). Not surprisingly, the number of significantly differentially expressed proteins appeared to be much larger in comparisons that included any of the medium-labelled strains: experiment A: WKY.$SP_{Gla}$2a vs WKY ($M/L_A$): 778, SHRSP vs WKY.$SP_{Gla}$2a ($H/M_A$): 759; experiment B: SP.$WKY_{Gla}$2a vs WKY ($M/L_B$): 675, SHRSP vs SP.$WKY_{Gla}$2a ($H/M_B$): 638. Figure 5-7 illustrates Venn diagrams of these 'analysis-ready' proteins for several comparisons of interest (Figure 5-7 B,C and D). Overlap in the cases of $H/L_A$ - $H/L_B$ and $M/L_A$ - $H/M_B$ was substantial, whereas any of the comparisons including a medium-labelled strain (M/L, H/M) exhibited low overlap with the parental H/L comparisons.

Based on these outcomes, which support the unusual quantification pattern derived from MaxQuant, our further study focused mainly on the SHRSP vs WKY (H/L) comparison. From the 203 proteins that were changing significantly in both experiments A and B (Figure 5-7B), 141 were consistently up-regulated, 61 were consistently down-regulated (Supplementary table 'common_HLA_HLB_Fold change significant_203' included in the CD) and 18 (~10%) were encoded by genes mapping to chromosome 2 (Table 5-1). Ranking was performed on the 203 common IDs, individually in each experiment, and the mean ranks were calculated to prioritise proteins for further validation. Numerical data are summarised in Figure 5-8A.

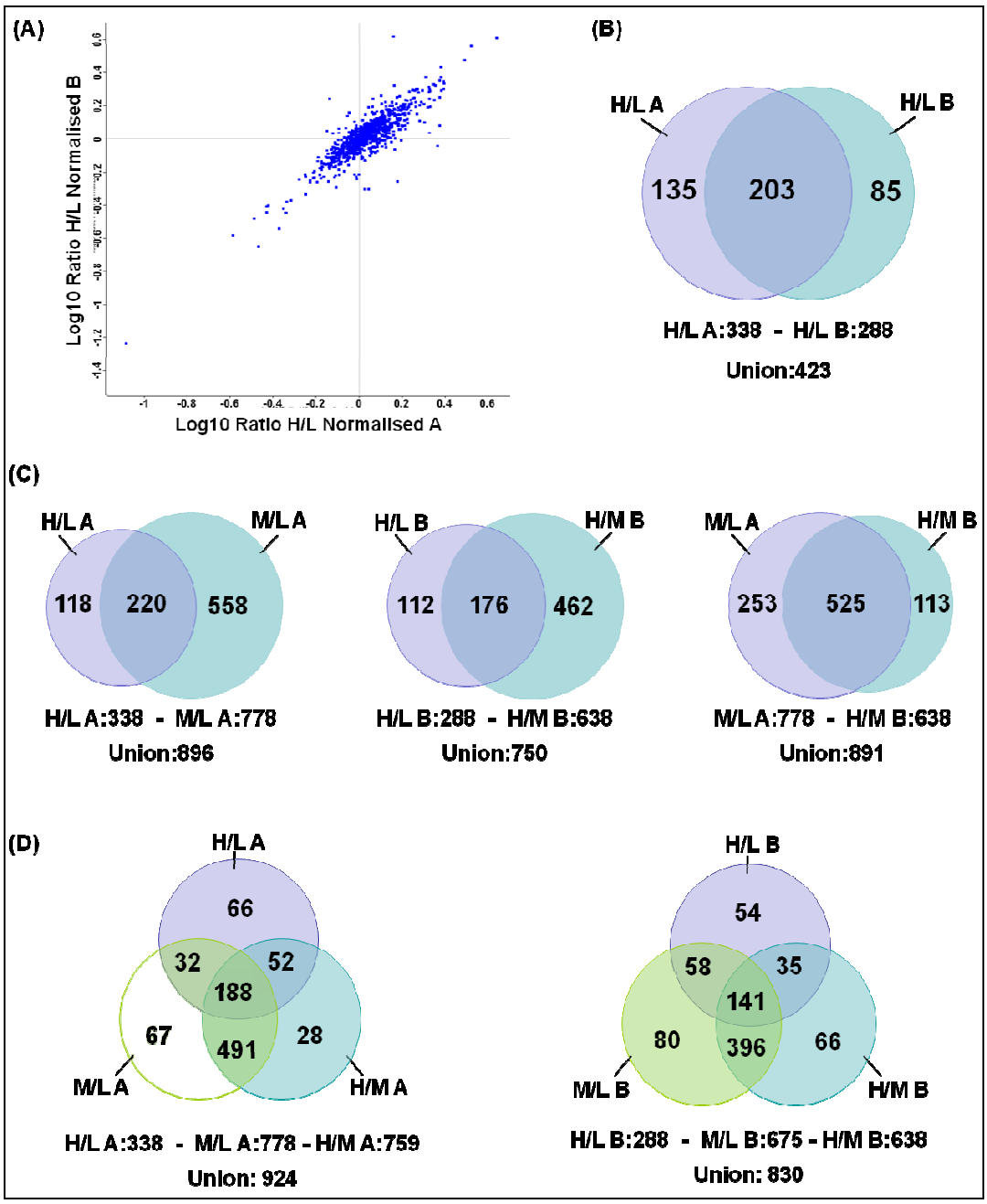


**Figure 5-7 - Bioinformatics analysis of data produced on MaxQuant v1.2.2.6. (A) Correlation scatterplot of log-transformed, normalised SILAC ratios determined in H/L A and H/L B independent replicates. Plot generated on Perseus v1.2.7.4. (B) Venn-diagram representing the overlap of differentially expressed majority proteins (FC≥ ±1.3) quantified in SHRSP vs WKY (H/L) A and B comparisons and identified as 'analysis ready' on IPA. (C) Venn-diagrams of comparisons of interest (M/L: congenic vs WKY, H/L: SHRSP vs WKY, H/M: SHRSP vs congenic).**

**Table 5-1. Differentially expressed proteins in SHRSP vs WKY (H/L) comparison, 'common' across experiments A and B, encoded by genes mapping to rat chromosome 2. Molecules exhibited consistent significant change (FC≥±1.3) and were identified on IPA as 'analysis ready'. Ranking was performed on the 203 'common' IDs. Green: down-regulation, red: up-regulation.**

| Symbol | Protein Names | IPI | Fold Change HLA | Fold Change HLB | Mean Ranks FC |
|---|---|---|---|---|---|
| DHFR | Dihydrofolate reductase | IPI00200419 | -2.184 | -2.428 | 11 |
| HMGCS1 | Hydroxymethylglutaryl-CoA synthase | IPI00188158 | -1.698 | -1.834 | 16 |
| LMNA | Lamin-A | IPI00188879 | -1.506 | -1.414 | 37.5 |
| HIST1H4A | Histone H4 | IPI00764726 | -1.432 | -1.439 | 38.5 |
| ARHGEF2 | Rho guanine nucleotide exchange factor 2 | IPI00368617 | -1.311 | -1.708 | 42 |
| LXN | Latexin | IPI00211758 | 1.327 | 1.506 | 101.5 |
| RAI14 | Ankycorbin; Retinoic acid-induced protein 14 | IPI00372146 | 1.414 | 1.655 | 124.5 |
| PDLIM5 | PDZ and LIM domain protein 5 | IPI00210187 | 1.457 | 1.360 | 95 |
| GSTM1 (*Gstm2;Gstm3*) | Glutathione S-transferase Mu 2; GST class-mu 3; GSTM2-2 | IPI00411230 | 1.569 | 1.492 | 124.5 |
| GSTM2 (*Gstm2;Gstm3*) | Glutathione S-transferase Mu 2; GST class-mu 3; GSTM2-2 | IPI00230942 | 1.569 | 1.492 | 123.5 |
| GSTM5 (*Gstm1*) | Glutathione S-transferase Mu 1; GSTM1-1; Rat glutathione S-transferase | IPI00231639 | 1.584 | 1.400 | 115.5 |
| Hist2h2aa1/ Hist2h2aa2 | H2A histone family, member X | IPI00368293 | 1.670 | 1.311 | 107 |
| HIST2H2AB | H2A histone family, member X | IPI00569279 | 1.670 | 1.311 | 111 |
| HIST2H2AC | H2A histone family, member X | IPI00566481 | 1.670 | 1.311 | 109 |
| ITGA1 | Integrin alpha-1 | IPI00324585 | 1.739 | 1.470 | 136.5 |
| SELENBP1 | Selenium-binding protein 1 | IPI00208026 | 1.768 | 1.958 | 173 |
| NPR3 | Atrial natriuretic peptide clearance receptor type C | IPI00195882 | 1.961 | 1.938 | 178.5 |
| HEXB | Beta-hexosaminidase subunit beta | IPI00464518 | 2.386 | 2.687 | 196 |

Subsequently, biological functions and diseases, pathways and toxicological lists relevant to the common (203) differentially regulated proteins (FC ≥ ±1.3) were explored on IPA (Figure 5-8B). The analysis revealed ~20% of the changing proteins to be associated with "cardiovascular disease" and the "cardiovascular system development and function", including regulation of BP. "Inflammation" was also highly affected by ~10% of the identified proteins. Oxidative stress, hypertrophy and fibrosis were amongst the top regulated tox functions/pathways and were upregulated in SHRSP. Canonical pathway analysis highlighted signalling involved in oxidative stress, myogenic tone and vascular remodelling as highly regulated. The degree of regulation was expressed as correlation between H/L A (338) or H/L B (288) datasets (FC ≥ ±1.3) with each pathway, indicated by -log(p-value). The most regulated pathways were "Integrin signalling" (5.72e-15 / 2.35e-10), "NRF-mediated oxidative stress response" (1.55e-09 / 3.19e-09), "ILK signalling" (2.46e-09 / 4.01e-08) and "RhoA signalling" (5.92e-09 / 3.81 e-0.8); numbers in brackets correspond to -log(p-value) in experiment A / B.

(A)

| Comparison | Union IDs | Common IDs | Chrom2 IDs | IPA 'analysis ready' molecules FC ≥ ± 1.3 |
|---|---|---|---|---|
| SHRSP v WKY ($H/L_A$ - $H/L_B$) | 423 | 203<br>141-UP<br>61-DOWN | 18<br>13-UP<br>5-DOWN | |

(B)

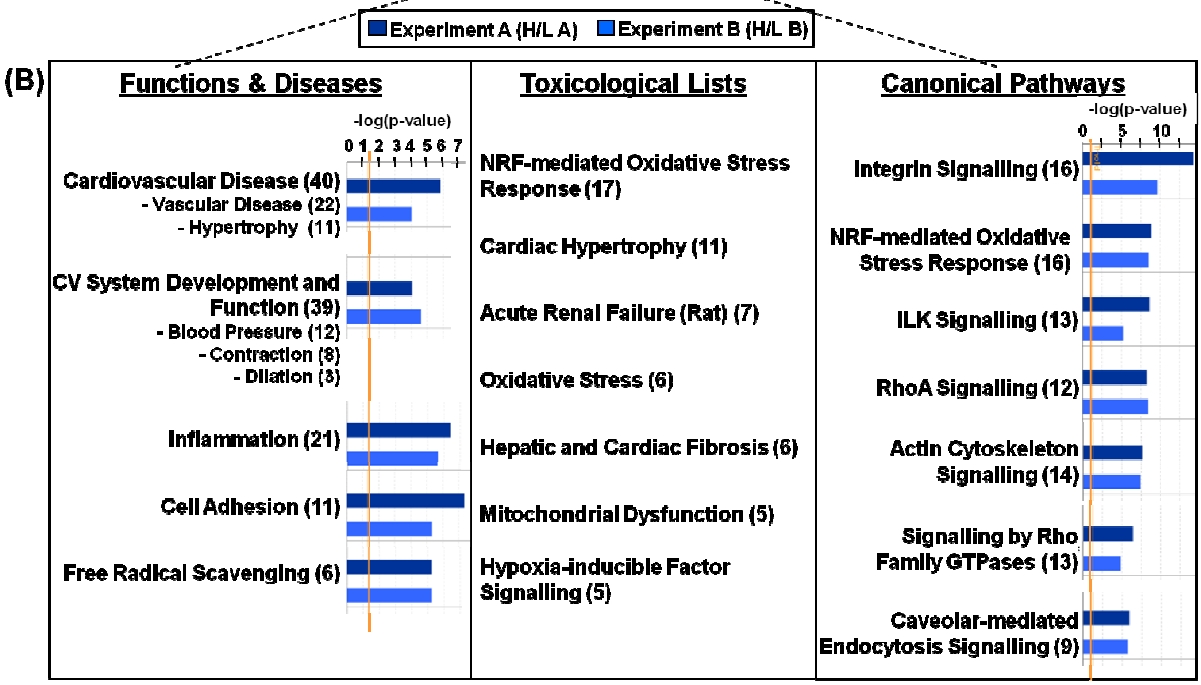


**Figure 5-8 - Correlation analysis in IPA. (A) Table summarising numbers of significantly differentially expressed proteins (FC≥±1.3) in the SHRSP vs WKY (H/L) comparison, identified to be in union, in common and encoded by chromosome 2 genes across the two experimental replicates, H/L A and H/L B. Majority was up-regulated in SHRSP. (B) Lists of top Functions & Diseases, Toxicological processes and Canonical Pathways, related to the 203 'common' proteins. Numbers in brackets correspond to mapped proteins found to be associated with the respective function/pathway. Bar-graphs demonstrate the degree of correlation (-log(p-value)) of the entire H/L A (dark blue) and H/L B (light blue) datasets (FC≥±1.3). Orange line on the bar-graphs represents the threshold of correlation significance. Green: down-regulation, red: up-regulation.**

Following the basic function/pathway correlation analysis, top related proteins and pathways were investigated further on IPA. Out of the 18 significantly regulated (FC≥±1.3) proteins encoded by the chromosome 2 congenic interval (Table 5-1), glutathione S-transferases (GSTM1, GSTM2: 1.569 / 1.492; GSTM5: 1.584 / 1.400), were up-regulated in SHRSP and linked to oxidative stress and free radical scavenging. On the contrary, dihydrofolate reductase (DHFR: -2.184 / -2.428) and Rho-guanine nucleotide exchange factor 2 (ARHGEF2: -1.311 / -1.708) were down-regulated and related to regulation of myogenic tone. Lastly, levels of natriuretic peptide receptor C (NPR3: 1.961 / 1.938) and integrin alpha-1 (ITGA1: 1.739 / 1.470) were enhanced in the hypertensive strain and associated with vasodilatation and hypertrophy, and vascular remodelling and fibrosis, respectively. (Numbers in brackets correspond to fold change in experiments A / B and data are summarised in Table 5-2).

Further, altered proteins encoded by genes lying outside the congenic interval were mapped to pathways involved in BP regulation. In RhoA signalling, one of the regulatory SM-contraction systems, actin (ACTA1/ACTC1: 2.097 / 2.058, ACTA2/ACTG2: 2.405 / 1.935), myosin light-chain (MYL12A/MYL12B: 1.641 / 1.710; MYL6B: 1.750 / 1.636) and MLC-kinase (MYLK: 3.316 / 3.617) levels were significantly increased in SHRSP as opposed to down-regulated ezrin (EZR: -2.656 / -2.547) (Figure 5-9). Caveolin-1 (CAV1: 1.784 / 1.741), also increased in SHRSP, was implicated in a number of pathways related to hypertension, such as "Caveolar-mediated endocytosis signalling" (Figure 5-10A), "NO signalling in the cardiovascular system" (Figure 5-10B). Investigation of the "sphingosine-1 phosphate signalling" of interest did not demonstrate any significant regulation across WKY and SHRSP, with expression levels of most proteins remaining unaltered. (Figure 5-11A). However, assessment of the interconnection between S1P/S1PR1 and the list of differentially expressed proteins generated an interesting network (Figure 5-11B). Members of this network were implicated in hypertension phenotypes, including vascular remodelling, regulation of myogenic tone and oxidative stress. In specific, collagen alpha-1 type III (COL3A1: 2.121 / 1.988), cathepsin D (CTSD: 1.301 / 1.362) and superoxide dismutase 2 (SOD2: 1.374 / 1.378) were up-regulated in SHRSP, as opposed to decreased levels of ezrin (EZR: -2.656 / -2.547) and milk fat globule-EGF factor 8 (MFGE8: -1.794 / -1.639). (Numbers in brackets correspond to fold change in experiments A / B and data are summarised in Table 5-2).

**Table 5-2. List of highly regulated proteins identified on IPA to be related to processes and pathways implicated in hypertension. Proteins exhibited consistent differential expression (FC≥±1.3) in the SHRSP vs WKY (H/L) comparisons. Regulation is shown across all SILAC comparisons: SHRSP vs WKY (H/L), WKY.SP$_{Gla}$2a vs WKY (M/L A), SHRSP vs WKY.SP$_{Gla}$2a (H/M A), SP.WKY$_{Gla}$2a vs WKY (M/L B), SHRSP vs SP.WKY$_{Gla}$2a (H/M B). Red: up-regulation, green: down-regulation.**

| Protein name | IPI identifier | Fold change (H/L) A B | Fold change (M/L A) | Fold change (H/M A) | Fold change (M/L B) | Fold change (H/M B) |
|---|---|---|---|---|---|---|
| GSTM1/GSTM2 | IPI00778234/ 00230942 | 1.569 / 1.492 | -10.254 | 10.024 | 1.649 | 1.055 |
| GSTM5 | IPI00231639 | 1.584 / 1.400 | -1.463 | 1.557 | 1.288 | -1.005 |
| DHFR | IPI00200419 | -2.184 / -2.428 | -3.169 | -1.034 | -2.196 | -1.767 |
| ARHGEF2 | IPI00949206 | -1.311 / -1.708 | -1.598 | -1.104 | -1.842 | -1.131 |
| NPR3 | IPI00195882 | 1.961 / 1.938 | 1.695 | 1.143 | -2.006 | 3.278 |
| ITGA1 | IPI00324585 | 1.739 / 1.470 | -2.363 | 3.746 | 1.790 | -1.126 |
| ACTA1/ACTC1 | IPI00189813/ 00194087 | 2.097 / 2.058 | -3.231 | 5.008 | 1.183 | 1.330 |
| ACTA2/ACTG2 | IPI00197129/ 00560160 | 2.405 / 1.935 | -1.737 | 1.412 | -6.556 | 5.025 |
| MYL12A/MYL12B | IPI00564409/ 00914162 | 1.641 / 1.710 | 1.270 | 1.324 | 1.356 | 1.247 |
| MYL6B | IPI00870820 | 1.750 / 1.636 | -6.094 | 8.196 | -2.918 | 9.690 |
| MYLK | IPI00779078 | 3.316 / 3.617 | 1.278 | 5.559 | -1.015 | 3.265 |
| EZR | IPI00948980 | -2.656 / -2.547 | -1.410 | 1.102 | -1.663 | -1.496 |
| CAV1 | IPI00475476 | 1.784 / 1.741 | -2.421 | 3.746 | -1.812 | 3.731 |
| PDGFRB | IPI00199968 | 1.065 / -1.216 | 1.401 | -1.487 | 1.649 | -1.863 |
| ERK1 | IPI00231081 | 1.136 / 1.010 | -1.015 | 1.059 | 1.083 | 1.010 |
| ERK2 | IPI00199688 | -1.074 / -1.163 | -1.000 | 1.062 | -1.039 | -1.163 |
| COL3A1 | IPI00366944 | 2.121 / 1.988 | -2.086 | 5.012 | 1.485 | 2.990 |
| CTSD | IPI00421525 | 1.301 / 1.362 | -2.751 | 4.136 | -1.788 | 5.412 |
| SOD2 | IPI00211593 | 1.374 / 1.378 | -12.107 | 11.540 | -2.305 | 13.659 |
| MFGE8 | IPI00188896 | -1.794 / -1.639 | -1.579 | 2.372 | 1.941 | -2.427 |
| NQO1 | IPI00231595 | -2.711 / -2.784 | -20.144 | 4.768 | -5.684 | 6.748 |
| HMOX1 | IPI00206626 | -2.080 / -2.364 | -1.179 | -2.008 | 2.666 | -4.067 |

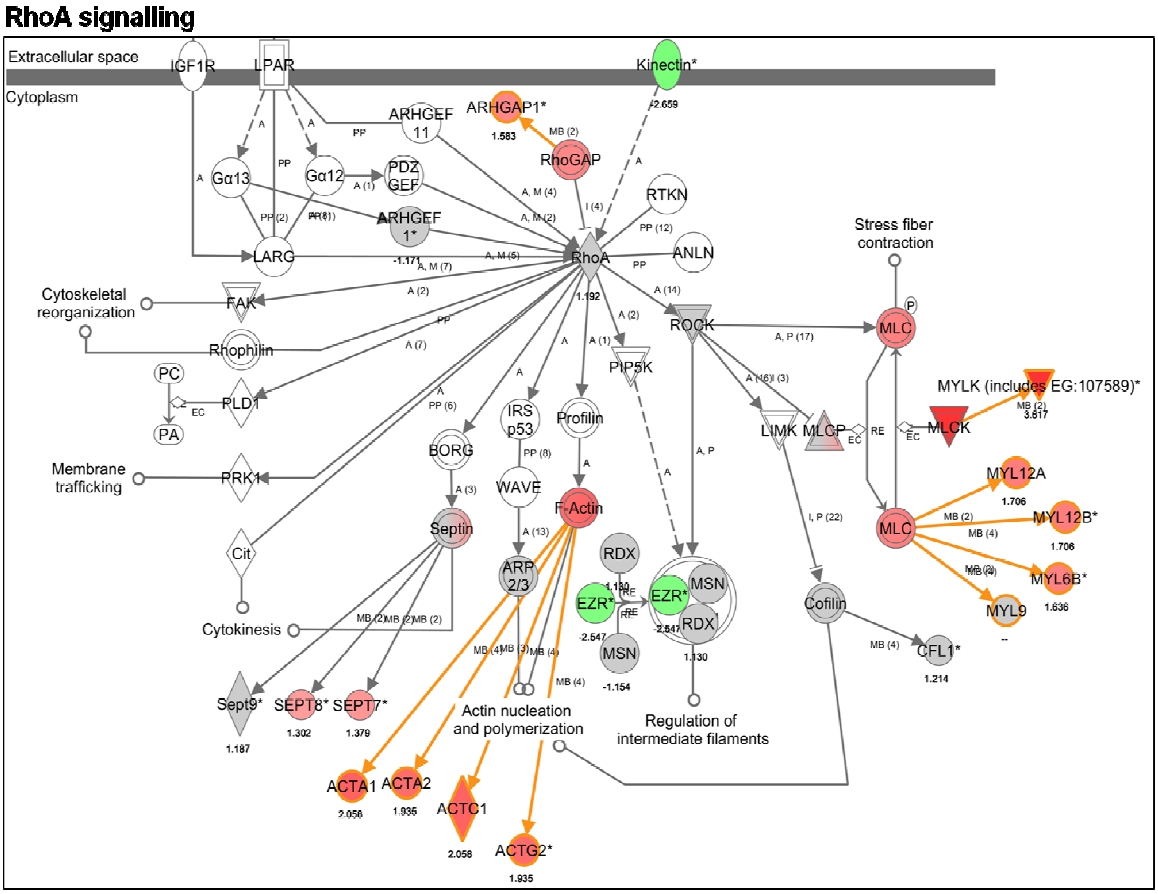


**Figure 5-9 - Schematic representation of RhoA signalling and mapping of differentially expressed proteins identified in SHRSP vs WKY (H/L) comparison. Actins (ACTA1/ACTC1, ACTA2/ACTG2) myosin light-chain (MLC: MYL12A/MYL12B, MYL6B) and MLC kinase (MLCK) were consistently up-regulated in SHRSP, in both A and B experiments. Ezrin (EZR) was consistently down-regulated. The pathway was generated on IPA and overlaid with the H/L A dataset of the 203 'common' with H/L B proteins. Proteins involved in the pathway are indicated with their IPA names and FC. Colour key: red: up-regulated, green: down-regulated, grey: not changing, white: not identified. For molecule shapes and relationship labels and types see Figure 2.4 in M&M.**

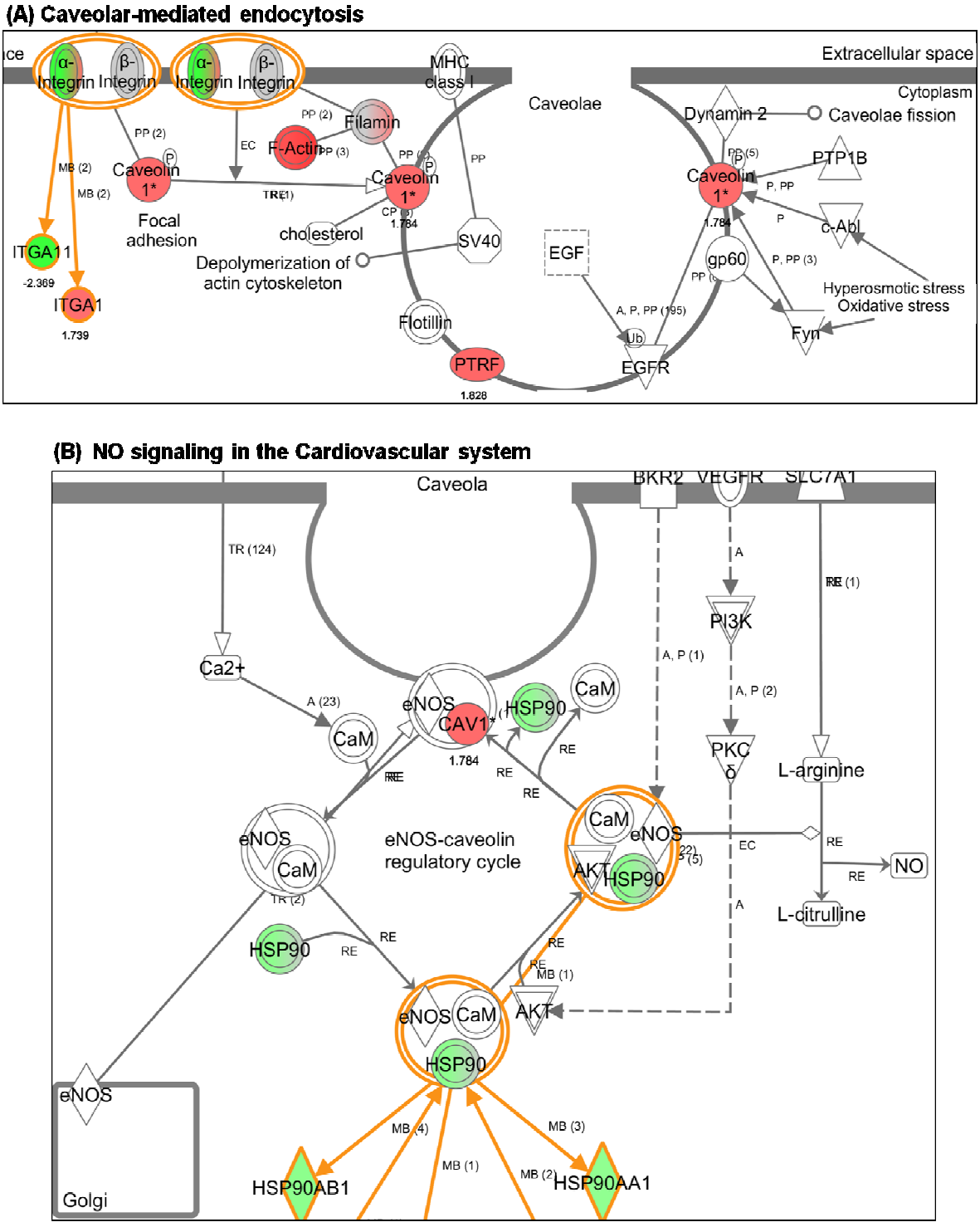


**Figure 5-10 - Schematic representation of top canonical pathways of caveolin-1 (CAV1). CAV1 was consistently up-regulated in SHRSP vs WKY, in both A and B experiments (FC= 1.784 / 1.741) and was associated with pathways related to BP regulation, such as caveolar-mediated endocytosis (A) and nitric oxide signalling in the cardiovascular system (B). Pathways were generated on IPA and overlaid with the H/L A dataset of the 203 'common' with H/L B proteins. Proteins involved in the pathways are indicated with their IPA names and FC. Colour key: red: up-regulated, green: down-regulated, grey: not changing, white: not identified. For molecule shapes and relationship labels and types see Figure 2.4 in M&M.**

**(A) Sphingosine 1-phosphate (S1P) signalling**

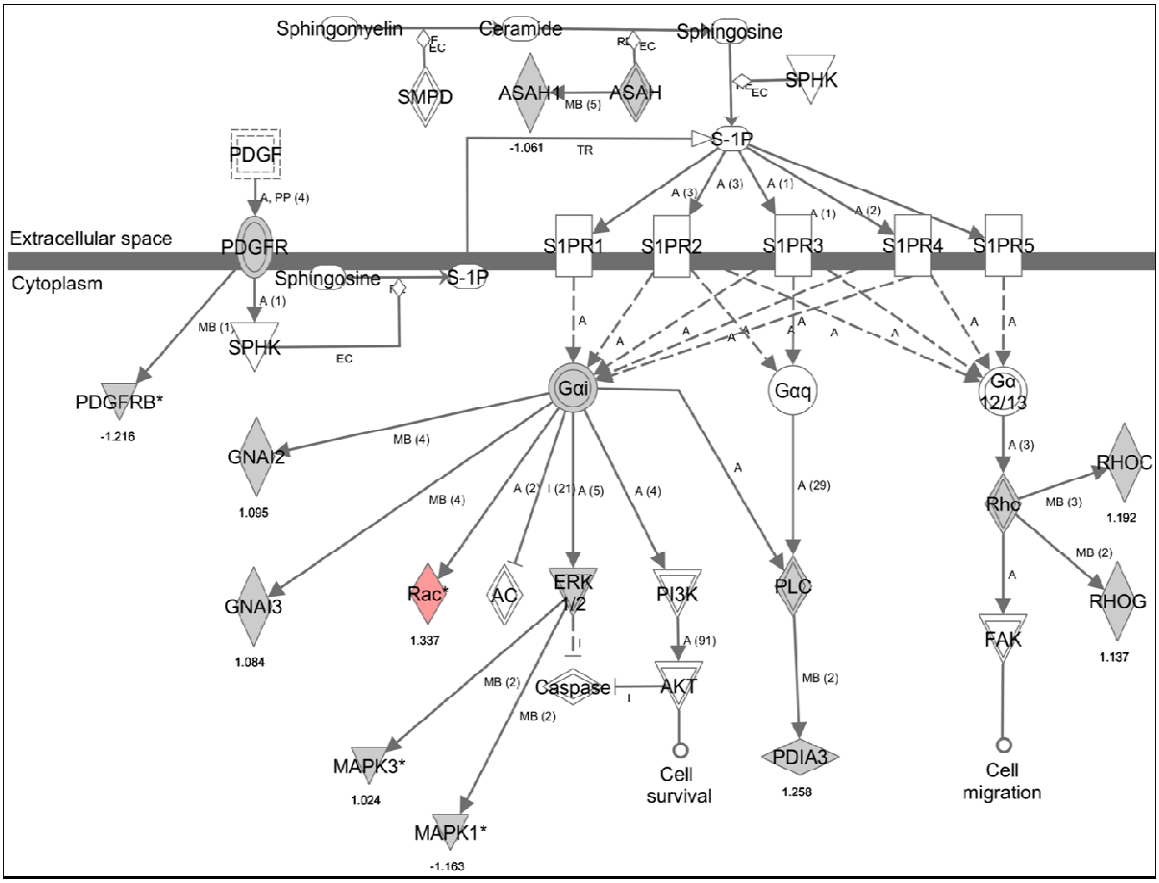


**(B) S1P / S1PR network**

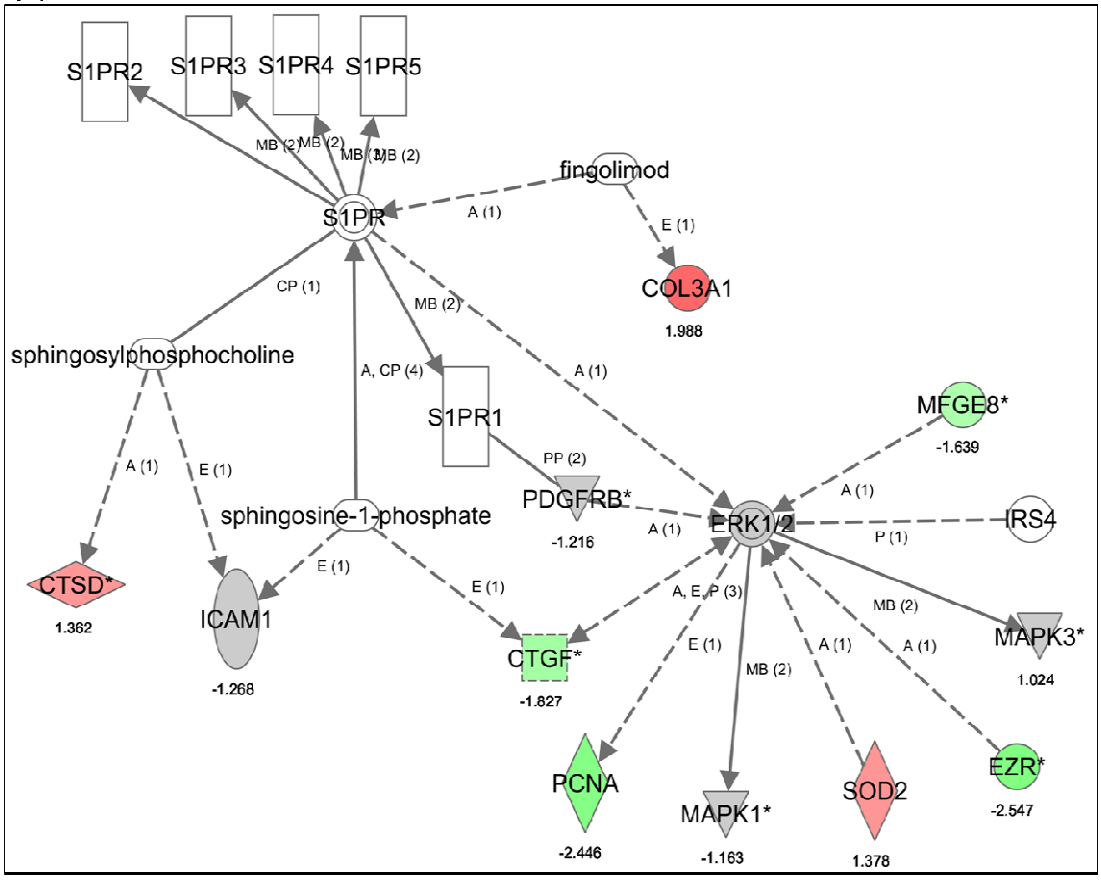

**Figure 5-11 - Schematic representation of sphingosine-1 phosphate (S1P) signalling and mapping of differentially expressed proteins identified in SHRSP vs WKY (H/L) comparison. (A) The S1P signalling pathway was not significantly regulated. (B) The network generated by S1P/S1PR and the list of differentially expressed proteins (203) was highly-regulated. Collagen alpha-1 type III (COL3A1), cathepsin D (CTSD) and superoxide dismutase 2 (SOD2) were up-regulated in SHRSP. Ezrin (EZR) and milk fat globule-EGF factor 8 (MFGE8) were decreased, whereas platelet-derived growth factor receptor (PDGFRB) and extracellular signal-regulated kinase (ERK1: 1.136 / 1.010; ERK2) remained unaltered. The pathway and network were generated on IPA and overlaid with the H/L B dataset of the 203 'common' with H/L A proteins. Proteins involved are indicated with their IPA names and FC. Colour key: red: up-regulation, green: down-regulation, grey: not changing, white: not identified. For molecule shapes and relationship labels and types see Figure 2.4 in M&M.**

Lastly, DHFR and NPR3 were two proteins that demonstrated significant regulation of a particular pattern of interest across comparisons with the 2a congenic strains (medium-labelled). Specifically, when WKY.SP$_{Gla}$2a was compared to WKY (M/L A: -3.169_DHFR, 1.695_NPR3), the differential expression followed same direction of change as in the SHRSP vs WKY (H/L A: -2.184_DHFR, 1.691_NPR3) comparison. Moreover, protein levels remained unaltered between SHRSP and WKY.SP$_{Gla}$2a (H/M A: -1.034_DHFR, 1.143_NPR3). In contrast, comparisons of the SP.WKY$_{Gla}$2a with the parental strains did not reveal a consistent pattern between the two protein levels. DHFR levels were decreased in SP.WKY$_{Gla}$2a compared to WKY (M/L B: -2.196) and increased compared to SHRSP (H/M B: -1.767). NPR3 regulation was down in the SP.WKY$_{Gla}$2a when compared to either of the parental strains (i.e. M/L B: -2.006 and H/M B: 3.278).

### 5.2.2 Immunoblotting validation

To validate proteomic changes revealed by SILAC, eight of the significantly regulated proteins in the SHRSP vs WKY (H/L) comparisons were chosen to be analysed by WB, in the same VSMCs used for the proteomic analysis (section 2.3). The candidate proteins were: NAD(P)H quinone oxireductase-1 (NQO1) and heme oxygenase-1 (HMOX) - down-regulated in SHRSP in the proteomics analysis; glutathione S-transferase mu-1 (GSTM5), caveolin-1 (CAV1), natriuretic peptide receptor C (NPR3) and alpha-SM-actin2 (ACTA2) - up-regulated in SHRSP in the proteomics analysis (Table 5-3). The 2a congenic strains were also included in the WB analysis. The experimental design of the 30min S1P-stimulation of mesenteric, primary VSMCs, was identical to the one used for the SILAC-proteomic analysis, excluding the use of isotopically labelled-media.

The 30min S1P-stimulation did not cause any changes in the levels of the proteins examined, as expected (Figure 5-12). HMOX1 exhibited a trend to decrease in SHRSP vs WKY, unlike NQO1 which seemed unaltered. CAV1, GSTM1 and ACTA2 also showed a trend to increase in the hypertensive strain. Finally, NPR3 demonstrated a trend for up-regulation in SHRSP vs WKY. More specifically, NPR3 levels tended to be higher in the WKY-congenic ($SP.WKY_{Gla}2a$) compared to WKY and at the same levels as SHRSP. Further, the SHRSP-congenic ($WKY.SP_{Gla}2a$) showed a decreased trend compared to SHRSP and similar levels to WKY.

**Table 5-3. List of proteins selected for immunoblotting validation. Proteins were identified in the SILAC-proteomics analysis as differentially regulated (FC ≥ ±1.3) in SHRSP vs WKY (H/L), 'common' across experiments A and B. Ranking was performed on these 203 'common' IDs.**

| Protein name | Rank (FC_H/L) | FC H/L A | FC H/L B | FC M/L A | FC H/M A | FC M/L B | FC H/M B |
|---|---|---|---|---|---|---|---|
| **NQO1 NAD(P)H dehydrogenase quinone 1** | 5.5 | **-2.711** | **-2.784** | -20.144 | 4.768 | -5.684 | 6.748 |
| **HMOX1 Heme oxygenase 1** | 12 | **-2.080** | **-2.364** | -1.179 | -2.008 | 2.666 | -4.067 |
| **GSTM1 Glutathion S-transferase mu 1** | 115.5 | **1.584** | **1.400** | -1.463 | 1.557 | 1.288 | -1.005 |
| **CAV1 Caveolin 1** | 167 | **1.784** | **1.741** | -2.421 | 3.746 | -1.812 | 3.731 |
| **NPR3 Natriuretic peptide receptor C** | 178.5 | **1.961** | **1.938** | 1.695 | 1.143 | -2.006 | 3.278 |
| **ACTA2 Alpha-actin-2, smooth muscle** | 184.5 | **2.405** | **1.935** | -1.737 | 1.412 | -6.556 | 5.025 |

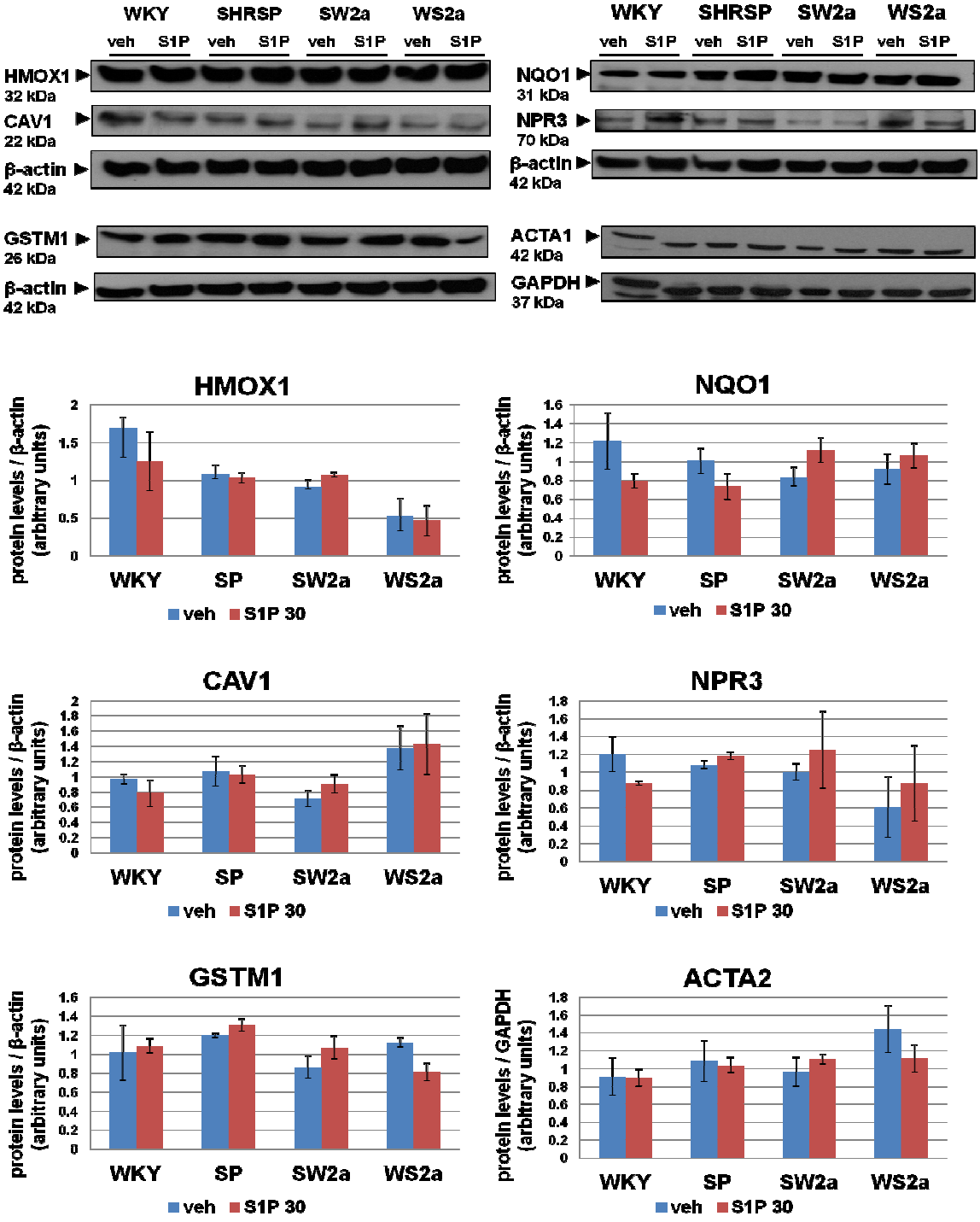


**Figure 5-12 - Western blot analysis of selected proteins identified in the SILAC study. Primary VSMCs from WKY, SHRSP and the 2a congenics were treated with vehicle (control) or stimulated with S1P ($10^{-6}$M), for 30mins in the same way as in the SILAC experiments. Protein loaded: 40-50μg. Membranes were probed with the indicated antibodies. Top panels, representative immunoblots for HMOX1, CAV1, GSTM1 (left); NQO1, NPR3, ACTA2 (right) and respective β-actin and GAPDH loading controls. Bottom, corresponding bar graphs demonstrating the change (arbitrary units) in protein levels before and after stimulation, across the four strains. Quantification data were normalised to either GAPDH or β-actin. Results are the mean ±SEM of 2 or 3 individual experiments, compared by Student's t-test (unpaired, two-tailed).**

## 5.3 Discussion

Previous microarray analysis and sphingosine signalling studies identified altered *S1pr1* expression and signalling profiles between WKY and SHRSP. To overcome difficulties faced during low-throughput characterisation of S1PR1 expression and signalling (chapter4) and to further investigate effects of altered sphingosine signalling on BP regulation, comprehensive MS-based proteomic screening was employed. By combining the power of SILAC labelling and reciprocal congenic strains, SP.WKY$_{Gla}$2a and WKY.SP$_{Gla}$2a, along with the WKY and SHRSP parental strains, we aimed to more accurately and reliably characterise traits underlying phenotypic differences in hypertensive rat models. Proteomic alterations occurring upon 30min S1P-stimulation, as well as genetically driven proteomic differences across the four strains were quantified in whole cell proteome of primary VSMCs from 16 week old animals.

Using triple-SILAC labelling, optimal comparison of four strains proteome was achieved in just two experiments. Moreover, the WKY vs SHRSP comparison was replicated twice allowing for testing of the technique reproducibility. Cell growth rate and morphology was not affected when cells were transferred in SILAC/dFBS media, minimising the chances that the observed proteome differences are the result of this treatment. Mixing equal numbers of differentially SILAC-labelled intact-cell populations at an early stage in the process minimised relative quantification errors, as an identical workflow was followed thereafter. The increased quantitative accuracy of this method was evident by similar abundance (score) of L(light), M(medium) and H(heavy) SILAC-peptides of housekeeping proteins, according to MS/MS spectra preview on Mascot. Extensive separation of intact proteins, with SDS-PAGE and subsequent LC, significantly reduced complexity of samples, permitting deeper proteome coverage. Trypsin digestion of protein mixtures generated chemically identical peptides, yet isotopically distinct, allowing for accurate identification and relative quantification of SILAC-peptides by MS. Finally, extensive processing of MS/MS data in MaxQuant removed noise, contaminants and low confidence hits, and normalised SILAC-peptide ratios to further correct for any cell-mixing errors, while assuming that the majority of proteins were not deferentially expressed.

Despite the initial objective of the experiment to detect effects of the 30min S1P-stimulation, expressed mainly as changes in the phosphoproteome, only a small number of highly abundant phospho-peptides were detected. Generally, detection of phosphoproteins is considered challenging as they comprise only ~10% of the entire proteome in a cell. It is

lately becoming common practice to perform enrichment for particular fractions of interest previous to digestion, in order to achieve deeper coverage of fraction specific or low abundance proteins (Olsen et al., 2006, Zhang and Peck, 2011). Consequently, in our experiment, it is expected that the majority of detected protein differences would most likely be driven by genetic differences across strains rather than the S1P stimulation.

During the discovery phase of this work, we identified proteins of potential interest by setting the fold change (FC) threshold to ±1.3, based on literature reports (Blagoev et al., 2003, Mann, 2006). This cut-off is stringent enough to filter out the majority of proteins with ratios close to 1, without however excluding potentially interesting hits with a small magnitude of change. Lists of differentially regulated proteins were subjected to pathway analysis on IPA, allowing for biological interpretation of SILAC results in the context of published experimental data.

Our primary focus was on the comparison between the two extreme phenotypes of hypertension, SHRSP(H) vs WKY(L), which was replicated twice. Satisfactory reproducibility of normalised H/L ratios between A and B experiments, as well as 1:1 H/L ratios for the majority of proteins in each experiment indicated good performance and SILAC quantification accuracy. Using IPA, significantly regulated proteins, in common between H/L A and H/L B, were highly correlated with CVD and a number of biologically relevant phenotypes and processes including BP, vascular reactivity, hypertrophy, oxidative stress and inflammation. Moreover, canonical pathway analysis further highlighted signalling associated with these processes, such as NRF2-mediated oxidative stress response (antioxidant pathway), Rho family GTPases / RhoA signalling (vascular contractility) and integrin / actin cytoskeleton signalling (cytoskeletal reorganisation). Interestingly, several of the regulated proteins involved in these pathways and almost 10% of all significantly regulated proteins in the H/L comparisons, mapped to chrom.2 congenic interval, including: GSTM1/GSTM2, GSTM5, DHFR, ARHGEF2, NPR3 and ITGA1. However, examination of their direction of change across parental and congenic strains sharing the chrom.2 interval did not reveal any consistent patterns of interest. Such results highlight the fact that protein expression levels do not solely depend upon the origin of the gene, but also on the epigenetics and cellular state.

- Glutathione S-transferases (GSTM1/GSTM2 and GSTM5), implicated in ROS detoxification, were up-regulated in SHRSP, indicating a protective role against increased superoxide levels observed in their vasculature (Kerr et al., 1999). However, reduced mRNA

and protein levels of GSTM1 detected in their kidneys, compared to WKY (McBride et al., 2005), most likely imply differences in renal and vascular antioxidant mechanisms.

- Dihydrofolate reductase (DHFR), associated with oxidative stress and regulation of SM tone, was decreased in SHRSP. However, its role is mainly studied in endothelial cells, where DHFR regulates tetrahydrobiopterin ($BH_4$) bioavailability, essential in eNOS coupling (Crabtree et al., 2009). Reduced DHFR levels in SHRSP are in line with increased superoxide in their vasculature (Kerr et al., 1999), as well as the impaired relaxation observed in our functional studies (chapter 4). As protein levels are consistent with the WKY.$SP_{Gla}$2a congenic data, this suggests that regulation of DHFR expression is dependent on the congenic interval and may directly contribute to the pathogenesis of hypertension in this model. In addition, increased expression in SP.$WKY_{Gla}$2a vs SHRSP, could support the partial correction of endothelial dysfunction demonstrated in chapter 4.
- Rho-guanine nucleotide exchange factor 2 (ARHGEF2), which activates Rho proteins to increase formation of actin stress fibres and regulate SM tone, was decreased in SHRSP. According to Yu et al. (Yu et al., 2011), ARHGEF2 down-regulation imply reduced SMC proliferation, and it may therefore represent a protective adaptation against the hypertrophic phenotype of SHRSP.
- Natriuretic peptide receptor C (NPR3), primarily expressed in the mesenterium of SHRSP (Nagase et al., 1997), was up-regulated compared to WKY. NPR3 mediates C natriuretic peptide (CNP) signalling known to be associated with lowering of BP, and exerts anti-hypertrophic and anti-inflammatory properties (Scotland et al., 2005a). Further, CNP was recently identified as an EDHF factor, therefore implicating NPR3 in regulation of vascular reactivity (Chauhan et al., 2003). Increased NPR3 levels in SHRSP are consistent with previous data demonstrating higher density in VSMCs from SHRSP vs WKY (Liao et al., 1991). This could be interpreted as an attempt to correct high BP, hypertrophy and inflammation phenotypes, as well as the hypercontractility and endothelial dysfunction observed in chapter 4, or even to compensate for reduced affinity and responsiveness of the receptor, as previously shown (Liao et al., 1991). Moreover, the direction of change in the congenic strains, imply that NPR3 expression is principally controlled by the interval and is a secondary response to the already established hypertensive phenotypes.
- Integrin alpha-1 (ITGA1), associated with negative regulation of ROS production and collagen synthesis, hallmarks of fibrosis (Chen et al., 2004), was increased in SHRSP. Integrins are also known to participate in detection of pressure and contraction changes (Martinez-

Lemus et al., 2005). Therefore, ITGA1 increase could be a protective response against pronounced oxidative stress and hypercontractility in SHRSP (chapter 4). Considering the direction of change in the congenic strains, it can be assumed that ITGA1 expression is primarily regulated by the genetic background rather the congenic interval.

Apart from the proteins mapping to the congenic interval, differentially regulated proteins lying outside the interval were also associated with pathways related to hypertension phenotypes, BP regulation and S1P signalling.

- RhoA/Rock pathway, a regulator of cytoskeletal re-organisation and thus vascular tone, was most regulated in SHRSP. Consistent with this finding, previous studies have shown up-regulation in mesenteric and aortic VSMC from SHRSP (Moriki et al., 2004, Savoia et al., 2005). Moreover, our vascular reactivity data (chapter 4) demonstrated RhoA/Rock as the major contraction mechanism in SHRSP MRAs which was impaired, promoting hypercontractility. Therefore, the up-regulation of MLC-kinase (MYLK), myosin light-chain (MYL12A/MYL12B, MYL6B) and actin (ACTA1, ACTA2) could imply increased contractile activity in SHRSP vs WKY, despite no differences in RhoA and Rock levels, which is consistent with previous findings in aortic VSMCs (Moriki et al., 2004). On the contrary, a downstream target of Rock, ezrin (EZR), an actin-binding protein, was down-regulated, perhaps as a defence mechanism attempting to lower the activity of the pathway.
- Caveolin-1 (CAV1), the main component of caveolae, highly expressed in rat vascular SM (Voldstedlund et al., 2001), was up-regulated in SHRSP compared to WKY and SP.WKY$_{Gla}$2a. It is known to induce RhoA activation in rat MRAs (Dubroca et al, 2007), consistent with the hypercontractility we observed in SHRSP (chapter 4). Furthermore, CAV1 overexpression in vascular myocytes has been shown to attenuate growth by inhibiting PDGF proliferative responses (Peterson et al., 2003), which is critical since PDGFR signalling is up-regulated in hypertension (Tabet et al., 2005, Yogi et al., 2011). In addition, CAV1 has been implicated in S1P/S1PR1 signalling in endothelial cells, through direct interaction with S1PR1 in caveolae, which is crucial for endothelial barrier integrity and eNOS activation (Igarashi and Michel, 2000, Singleton et al., 2009). Such findings encourage further studies on the role of CAV1 in VSMC of hypertensive animals.
- The S1P/S1PR1 signalling canonical pathway was not significantly altered between WKY and SHRSP and the receptor levels were below detection. Moreover, PTMs mediating enhanced signalling in SHRSP upon 30min S1P-stimulation (Yogi et al., 2011) could not be observed in global proteome screening. Nevertheless, in a broader S1P/S1PR1 interaction

network a number of interesting proteins were highly changing. More specifically, enzymes positively related to oxidative stress responses, including superoxide dismutase 2 (SOD2) and cathepsin D (CTSD) (Roberg, 1998, Tiwari et al., 2008), were increased in SHRSP, exerting a potentially protective role. These enzymes have also been implicated in attenuation of VSMC proliferation and migration (Wang et al., 2012a) and hypertrophy of aortic VSMC from SHR (Fukuda et al., 1999), respectively. Other regulated proteins of the network were also associated with vascular structure and mechanics. Increased mRNA levels of collagen alpha-1 type III (COL3A1) have been related to fibrotic stiffness of MRA in aged rats (Briones et al., 2007, Campbell et al., 1991) and the increased protein levels observed here could therefore explain the increased stiffness of MRAs from SHRSP observed in our functional studies (chapter 4). Further, up-regulated levels of ezrin (EZR) and milk fat globule-EGF factor 8 protein (MFGE8) have been detected in proteomic screenings of pulmonary hypertensive mice (Veith et al., 2013) and of aortas from rats with chronic kidney disease exhibiting arterial stiffness (Lin et al., 2010), respectively. EZR has also been associated with SMC hypertrophy and increased vascular resistance in pulmonary artery of rats with induced inflammation (Dai et al., 2006), while MFGE8 has been shown to induce aortic VSMC proliferation in aged rats (Wang et al., 2012b). Hence, the decreased levels observed in our SHRSP may reflect protective adaptations. Interestingly, the above proteins exhibited consistent direction of change across the comparisons between SHRSP vs WKY and SP.WKY$_{Gla}$2a, reflecting regulation of their expression by the WKY congenic interval.

- Finally, two proteins important in the protection against oxidative stress were highly down-regulated in SHRSP, which may contribute further to the hypertensive phenotypes. Heme oxygenase-1 (HMOX1) is an enzyme shown to regulate myogenic tone, reduce BP in SHR and counteract oxidative stress (Datla et al., 2007, Escalante et al., 1991, Sammut et al., 1998), as well as to restore high-blood-flow-dependent remodelling and impaired endothelial function in MRAs from old Wistar rats (Freidja et al., 2011). The second protein, the detoxification enzyme NAD(P)H quinone oxireductase-1 (NQO1) (Zhu et al., 2007), is highly expressed in cardiovascular cells and has anti-proliferative effects on VSMCs (Kim et al., 2009).

Despite the fact that several protein expression data from the congenic strains could be interpreted in a meaningful way, we have to be careful due to the unusual quantification patterns observed in the congenics' comparisons. It is highly likely that such patterns reflect issues of the MaxQuant version used in performing triple-SILAC quantification. This

assumption is supported by the fact that when MS/MS spectra of housekeeping proteins were previewed on Mascot, similar abundance (score) of L, M and H SILAC-peptides was observed. Moreover, when data were quantified using Mascot Distiller normal distributions were acquired for every (pair) comparison. To confirm our assumption a control, 'cross-over' experiment with inverted SILAC labels between the strains could be performed, had there not been time limitations.

Validation of changes observed with MS was performed for some proteins of interest, which were identified as single isoforms and exhibited FC>1.5, to enable more accurate and easier detection by WB. As expected, levels of these proteins were not changing upon the 30min S1P-stimulation, consistent with the hypothesis that the observed differences were genetically driven. However, WB results did not provide any solid confirmation of the proteomic data. Possible explanations could be the small number of WB replicates, the small magnitude of protein FC or the sensitivity and specificity of the antibodies. Generally, due to inherent variability in a WB, which makes the technique less accurate and reliable, only 'dramatic' changes can be confirmed.

In conclusion, identification of proteins previously known to be related with the disease, as well as expression changes consistent with the literature validate our workflow design, giving more confidence to our data. On the other hand, changing proteins not previously reported to associate with the disease, could provide novel knowledge and the motive for generation of new testable hypothesis. To further investigate the effect of S1P-signalling on hypertension and assess contribution of the congenic interval, metabolomic screening was conducted on the S1P-treated VSMC used in our proteomics analysis, described in chapter 5.

# 6 Metabolome Profiling in S1P-stimulated Mesenteric Primary VSMCs

# 6.1 Introduction

One of the major strategies in systems biology is integration of data from high-throughput 'omics' analyses, which promises valuable insights into cellular biology and a more holistic and accurate characterisation of the living systems. In the past, such approaches were prevented due to the high-complexity of such datasets and the lack of powerful analytical software. However, the recent advances in high-resolution and accuracy instrumentation, in combination with developed quantitative and statistical platforms and databases have opened the way to large-scale integrating studies. To date, the majority of such studies come from the areas of plant biology and microbiology (Kromer et al., 2004, Maier et al., 2013), primarily due to the lower complexity of such systems. So far, there are many less studies integrating data from different platforms for highly complex biological systems (Ly-Verdu et al., 2013, Geiger et al., 2010, Zhang et al., 2013). Yet, the number of 'omics' analyses on complex organisms, including animal models of human diseases as well as on biofluids and tissues from human subjects, grows exponentially. This provides the potential for a rapid rise of 'omics'-integrating studies in the near future, towards a better understanding of the pathophysiology and treatment of chronic diseases, such as EH.

Upon perturbations of a biological system, response of its homeostatic mechanisms results in alterations on its proteome and metabolome. Therefore, comprehensive analysis of dynamic changes in the molecular characterisation of living systems should include both proteomic and metabolomic profiling. Variations in the metabolic profile, represented by changes in metabolites levels, comprise a useful complementary analysis to proteomic studies, which identify changes in protein levels, protein-protein interactions and PTMs.

## 6.1.1 Aims

Following the global proteomic profiling of mesenteric primary VSMCs, conducted in chapter 5, and studies demonstrating altered sphingosine signalling in VSMCs from SHRSP (Yogi et al., 2011), an untargeted metabolomic profiling of these cells was performed in this chapter. Metabolome from mesenteric primary VSMCs from 16-week-old WKY, SHRSP and the SP.WKY$_{Gla}$2a (SW2a) congenic strains was subjected to HILIC/MS and IDEOM bioinformatics analysis aiming to:

- investigate metabolic differences under basal conditions (vehicle), across the hypertensive SHRSP, the normotensive WKY and the SW2a congenic strain of improved BP phenotype (Figure 3-1A),
- elucidate the metabolic effects of sphingosine signalling (30min S1P-stimulation) within each strain and compare the effects across the three strains (Figure 3-1C).

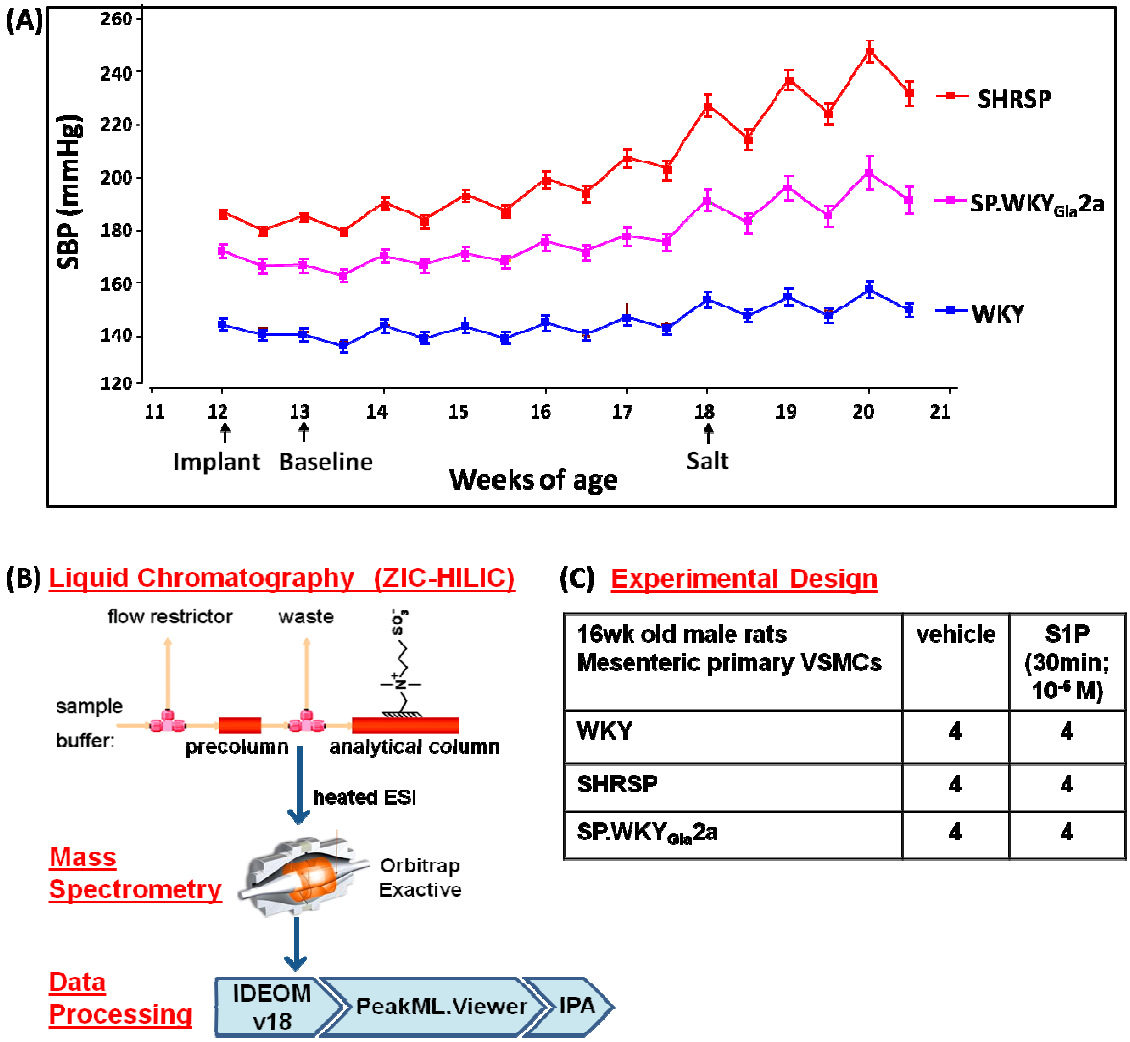


| 16wk old male rats Mesenteric primary VSMCs | vehicle | S1P (30min; $10^{-6}$ M) |
|---|---|---|
| WKY | 4 | 4 |
| SHRSP | 4 | 4 |
| SP.WKY$_{Gla}$2a | 4 | 4 |

**Figure 6-1 - Metabolomics analysis in S1P-stimulated mesenteric primary VSMCs isolated from 16-week-old WKY, SHRSP and SP.WKY$_{Gla}$2a-congenic strains. (A) Averaged weekly radiotelemetry recordings of night-time and day-time SBP in male animals, under baseline and salt-loaded periods (high-salt diet at 18 weeks of age) (Edited from Graham et al., 2007). (B) Experimental process. Metabolites were separated by ZIC-HILIC, ionised by ESI and directed to Orbitrap Exactive mass analyser. Raw peaks were filtered, identified, quantified and statistically analysed through IDEOM v18, visualised on PeakML.Viewer and finally uploaded to databases for biological interpretation. (C) Experimental design. Four biological replicates of each strain were analysed at basal conditions (vehicle) and upon 30min stimulation with spingosine-1-phosphate (S1P).**

## 6.2 Results

Metabolites were extracted from mesenteric primary VSMCs, which had been treated with vehicle or S1P for 30min (section 2.2.5), and processed on a ZIC-HILIC/MS platform, as detailed in section 2.7. Stringent processing of raw MS data containing thousands of peaks (~50.000) using IDEOM v18, led to identification of a relatively small number of positively (691_Pos) and negatively (374_Neg) ionised putative metabolites (Figure 6-2A). Correction for total MS intensity (TIC; metabolite intensity / sum of all metabolite intensities) was then performed to minimise the uncontrollable effect of exogenous factors (quantification errors). Identification lists of positive and negative modes were then combined (PosNeg) to give the list of putative metabolites to be further analysed: 920_PosNeg (Figure 6-2A).

The quality of filtered data was assessed by generation of principal component analysis (PCA) plots (Figure 6-2B), which represent the profile of a linear combination of the metabolites identified for each sample. In the PCA for the PosNeg dataset, in which all samples (vehicle and S1P-stimulated) were plotted together, the percentage of PC1 was 13.9% and of PC2 was 12.7%. Clustering of samples according to strain or to differential treatments was not clear.

(A)

| Mesenteric primary VSMCs (IDEOM v18) | Positive | Negative | PosNeg (TIC) |
|---|---|---|---|
| Peaks Detected (mzMatch filtered) | 4773 | 2697 | |
| Metabolites Identified (central database) | 691 | 374 | 920 |

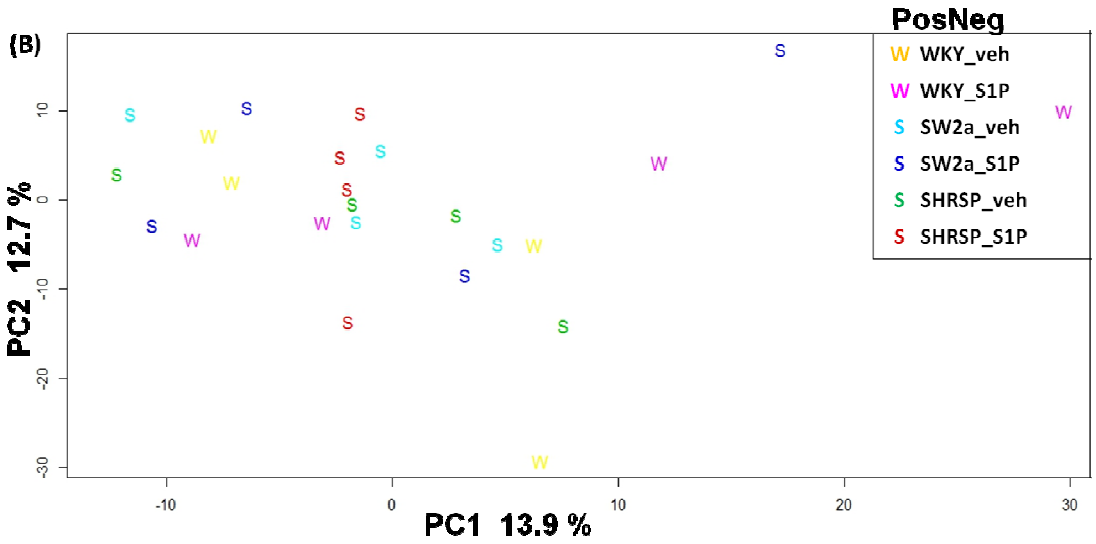


**Figure 6-2 - Orbitrap Exactive MS-data filtering and visualisation on IDEOM v18. (A) Peaks were picked using XCMS, filtered using mzMatch and matched to a set of databases for metabolite identification. The table summarises numbers of putative metabolites identified in the positive and negative modes and collectively (posneg), after correcting for total intensity (TIC), across all samples and stains. (B) PCA score plots for PosNeg list of putative metabolites, was generated in R using data from all strains and both vehicle and S1P-stimulated samples. PC1 and PC2 represent the percentages of metabolites that drive the separation of samples along the axes.**

Subsequently, pair-wise comparisons were performed across strains under vehicle or S1P treatment, as well as within each strain before and after the S1P-stimulation. Unpaired t-test was utilised to determine significance (p-val <0.05). Approximately 1/10 to 1/30 of the identified metabolites were found to be significantly changed in each of the comparisons. Around one half of these had KEGG IDs and were qualified as 'analysis ready' molecules on IPA (Figure 6-3A). During further exploration on IPA, the majority of 'analysis ready' metabolites were related to 'lipid metabolism' and 'small molecule biochemistry' processes. When associated to canonical pathways, diseases and toxicological functions, the relatively few metabolites were, mostly, individually mapped to different processes rather than highlighting a few common ones. Therefore, an individual investigation of potentially interesting molecules was followed, including the significant metabolites that were not mapped on IPA (no KEGG ID) (Figure 6-3B).

(A)

| Mesenteric primary VSMCs (IDEOM v18) | PosNeg | | |
|---|---|---|---|
| | Total | p-val <0.05 | IPA (analysis ready) |
| SHRSP v WKY (vehicle) | 778 | 20 | 10 |
| SHRSP v SW2a (vehicle) | 782 | 25 | 17 |
| SW2a v WKY (vehicle) | 776 | 12 | 6 |
| SHRSP v WKY (S1P) | 784 | 45 | 28 |
| SHRSP v SW2a (S1P) | 784 | 11 | 5 |
| SW2a v WKY (S1P) | 786 | 22 | 10 |
| $SHRSP_{S1P}$ v $SHRSP_{veh}$ | 780 | 20 | 14 |
| $WKY_{S1P}$ v $WKY_{veh}$ | 783 | 32 | 18 |
| $SW2a_{S1P}$ v $SW2a_{veh}$ | 784 | 26 | 19 |

(B)

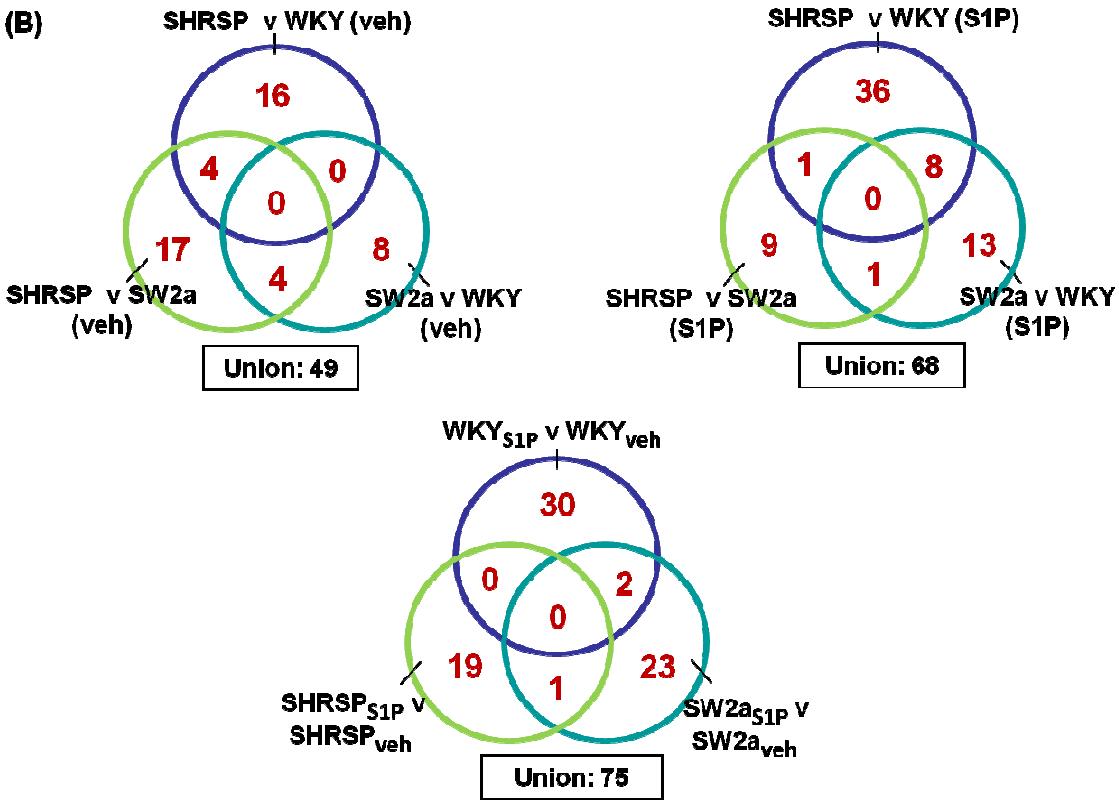


**Figure 6-3 - Comparisons of interest across WKY, SHRSP and SW2a-congenic strains, under control and S1P-treated conditions. (A) Comparisons were performed either across the stains or within each stain, before and after S1P-stimulation. Table summarises numbers of putative metabolites identified in positive and negative modes collectively (total), of metabolites changing significantly (p-val <0.05), and of significant metabolites mapped on IPA ('analysis ready'), in each comparison. (B) Venn-diagrams of significantly changing metabolites for comparisons of interest. Data acquired on IDEOM v18.**

### 6.2.1 Metabolic differences across strains at basal conditions

To investigate the metabolic components that are potentially implicated in BP regulation the metabolome of VSMCs was compared across the three strains, under basal conditions (vehicle). The ratio of significantly changing metabolites to total metabolites identified for each of the comparisons was: SHRSP_v_WKY (20/778); SHRSP_v_SW2a (25/782); SW2a_v_WKY (12/776) (Figure 6-3A). Most changes were observed between SHRSP_v_WKY (16 unique) and SHRSP_v_SW2a (17 unique) (Figure 6-3B; top left venn-diagram). The main focus was on intersects between comparisons, as they are likely to include metabolites regulated by the congenic interval and be beneficial on the VSMC phenotype. When SHRSP or SW2a were compared to WKY, no 'in common' metabolites were identified. In the comparisons between SHRSP versus WKY or SW2a, four metabolites were found to be changing 'in common', consistently decreased in SHRSP. In addition, potentially protective metabolites could be included in the 17 unique metabolites identified in SHRSP versus SW2a comparison, from which 10 were decreased and 7 increased in SHRSP. The decreased metabolites were implicated in nucleotide, amino acid and carbohydrate metabolism. Of similar interest were the 16 unique metabolites identified to be changing in SHRSP compared to WKY, from which 15 were reduced and one raised in SHRSP. From the decreased metabolites, 8 were related to lipid metabolism. Table 6-1 summarises data for some of the above significant metabolites. Full data are included in ‘vehicle comparisons; venns’ supplementary table.

Additional checking of peak quality for the above metabolites on peakML.Viewer, in order to exclude false-positives (e.g. present only in 'standards' or 'quality control' samples, peak reproducibility), directed the focus on the four metabolites, whose peaks are illustrated in Figure 6-4. [SP (16:0)] N-(hexadecanoyl)-sphing-4-enine-1-phosphocholine was found to be consistently decreased in SHRSP compared to WKY and SW2a: FC= -1.314 and -1.242, respectively. Homoarginine was reduced in SHRSP versus WKY: FC= -2.040. L-ornithine and inosine were also decreased in SHRSP in comparison to SW2a: FC= -14.974 and -1.581, respectively.

Network analysis on IPA mapped few of the metabolites changing significantly in SHRSP versus WKY and SW2a to a network implicating molecules related to vascular tone modulation and BP regulation. The network included nitric oxide synthase (NOS), tumor necrosis factor (TNF), xanthine dehydrogenase (XDH), calcium, cAMP and hydrogen peroxide (Figure 6-5).

**Table 6-1. Subset of metabolites exhibiting significant change in the comparisons across WKY, SHRSP and SW2a, under basal conditions. Data were generated on IDEOM v18. Green: decreased and red: increased metabolite levels.**

| KEGG id | Isomers | Putative metabolite | Map | Pathway | Fold Change | Pvalue (<0.05) |
|---|---|---|---|---|---|---|
| SHRSP_v_WKY ∩ SHRSP_v_SW2a (vehicle) | | | | | | |
| C13876 | 14 | 1-Hexadecanoyl-2-(9Z-octadecenoyl)-sn-glycero-3-phosphonocholine | Lipids: Glycerophospholipids | Glycerophosphonocholines | -1.797 / -1.692 | 0.0209 / 0.0343 |
| C01234 | 5 | 1-Aminocyclopropane-1-carboxylate | Amino Acid Metabolism | Methionine metabolism__ Propanoate metabolism | -1.410 / -1.376 | 0.0165 / 0.0274 |
| 0 | 1 | [SP (16:0)] N-(hexadecanoyl)-sphing-4-enine-1-phosphocholine | Lipids: Sphingolipids | Ceramide phosphocholines (sphingomyelins) | -1.314 / -1.242 | 0.0246 / 0.0496 |
| 0 | 3 | Ile-Phe-Thr-Pro | Peptide (tetra-) | Hydrophobic peptide | -1.258 / -1.349 | 0.0449 / 0.0194 |
| SHRSP _v_ SW2a (vehicle) - unique | | | | | | |
| C00294 | 3 | Inosine | Nucleotide Metabolism | Purine metabolism | -14.979 | 0.0012 |
| C00262 | 3 | Hypoxanthine | Nucleotide Metabolism | Purine metabolism | -4.189 | 0.0278 |
| C00497 | 4 | (R)-Malate | Carbohydrate Metabolism | Butanoate metabolism | -1.731 | 0.0493 |
| C00077 | 6 | L-Ornithine | Amino Acid Metabolism | D-Arginine and D-ornithine metabolism | -1.581 | 0.0043 |
| C01796 | 9 | D-Erythrose | Carbohydrate Metabolism | 0 | -1.426 | 0.0117 |
| C01043 | 6 | N-Carbamoylsarcosine | Amino Acid Metabolism | Arginine and proline metabolism | -1.422 | 0.0066 |
| C00299 | 3 | Uridine | Nucleotide Metabolism | Pyrimidine metabolism | -1.364 | 0.0234 |
| C06144 | 2 | 3-Butynoate | Carbohydrate Metabolism | Butanoate metabolism | 1.607 | 0.0250 |
| C10165 | 1 | Pinidine | 0 | Glycerophosphoinositols | 5.329 | 0.0186 |
| SHRSP _v_ WKY (vehicle) - unique | | | | | | |
| C01190 | 3 | Glucosylceramide (d18:1/16:0) | Lipids: Sphingolipids | Sphingolipid metabolism | -2.198 | 0.0274 |
| C01924 | 5 | Homoarginine | Amino Acid Metabolism | 0 | -2.040 | 0.0354 |
| C13914 | 1 | N,N-Dimethylsphing-4-enine | Lipids: Sphingolipids | Sphingoid bases | -1.551 | 0.0232 |
| C00157 | 15 | PC(18:1(11Z)/P-18:1(11Z)) | Lipids: Glycerophospholipids | Glycerophosphocholines | -1.523 | 0.0212 |
| C16512 | 6 | [FA (16:2)] N-hexadecyl-ethanolamine | Lipids: Fatty Acyls | Fatty amides | -1.342 | 0.0003 |
| C05465 | 3 | [ST hydrox] N-(3alpha, 7alpha-dihydroxy-5beta-cholan-24-oyl)-taurine | Lipids: Sterol lipids | Bile acid biosynthesis | 4.581 | 0.0127 |

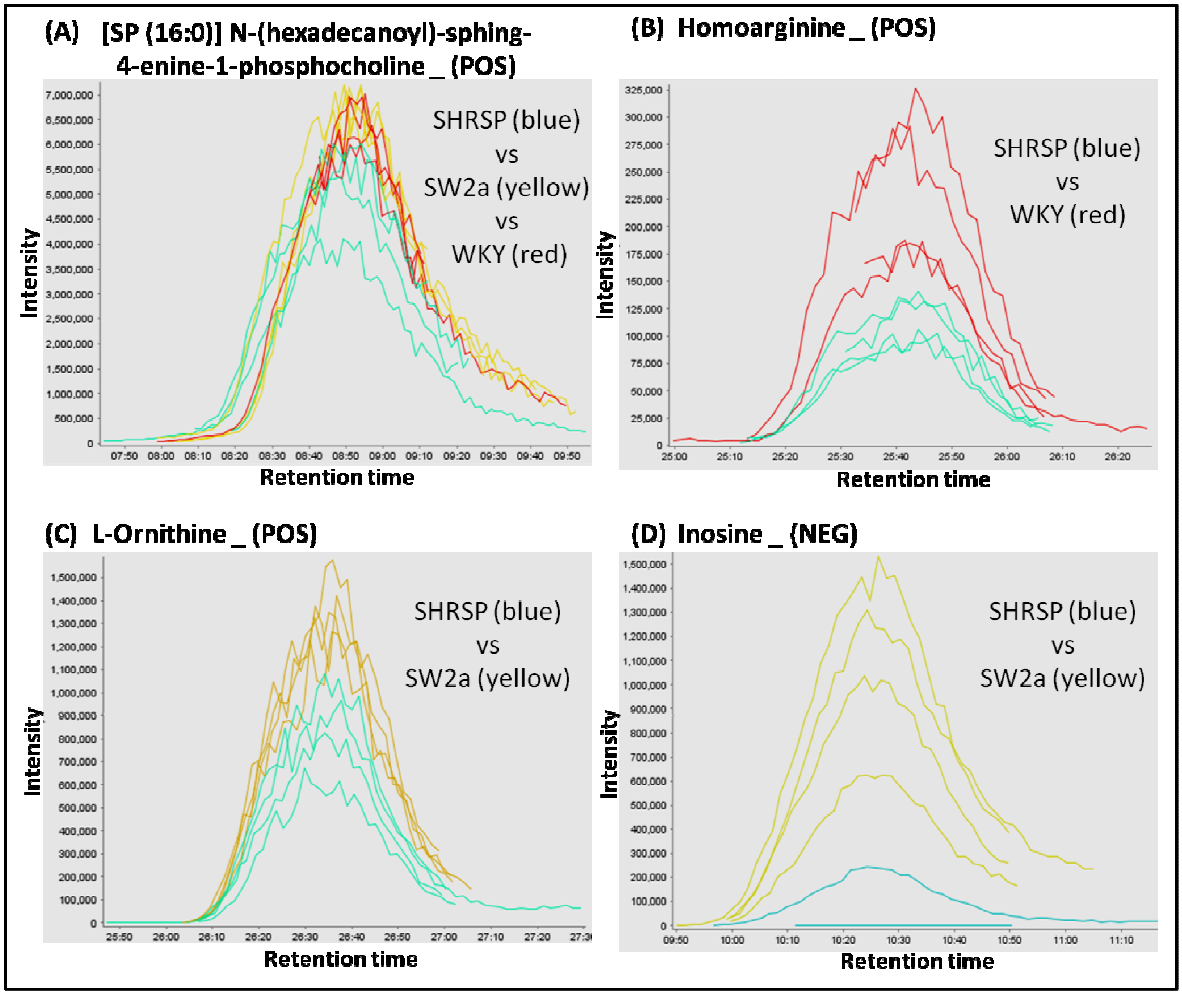


**Figure 6-4 - Levels of significantly changing metabolites in the comparisons across WKY, SHRSP and SW2a, at basal conditions (vehicle). PeakML chromatograms illustrate significant ($p<0.05$) decrease of: (A) [SP (16:0)] N-(hexadecanoyl)-sphing-4-enine-1-phosphocholine, in SHRSP versus WKY and SW2a; (B) homoarginine, in SHRSP versus WKY; (C) L-ornithine and (D) inosine, in SHRSP versus SW2a. The x-axis indicates the retention time and the y-axis the intensity.**

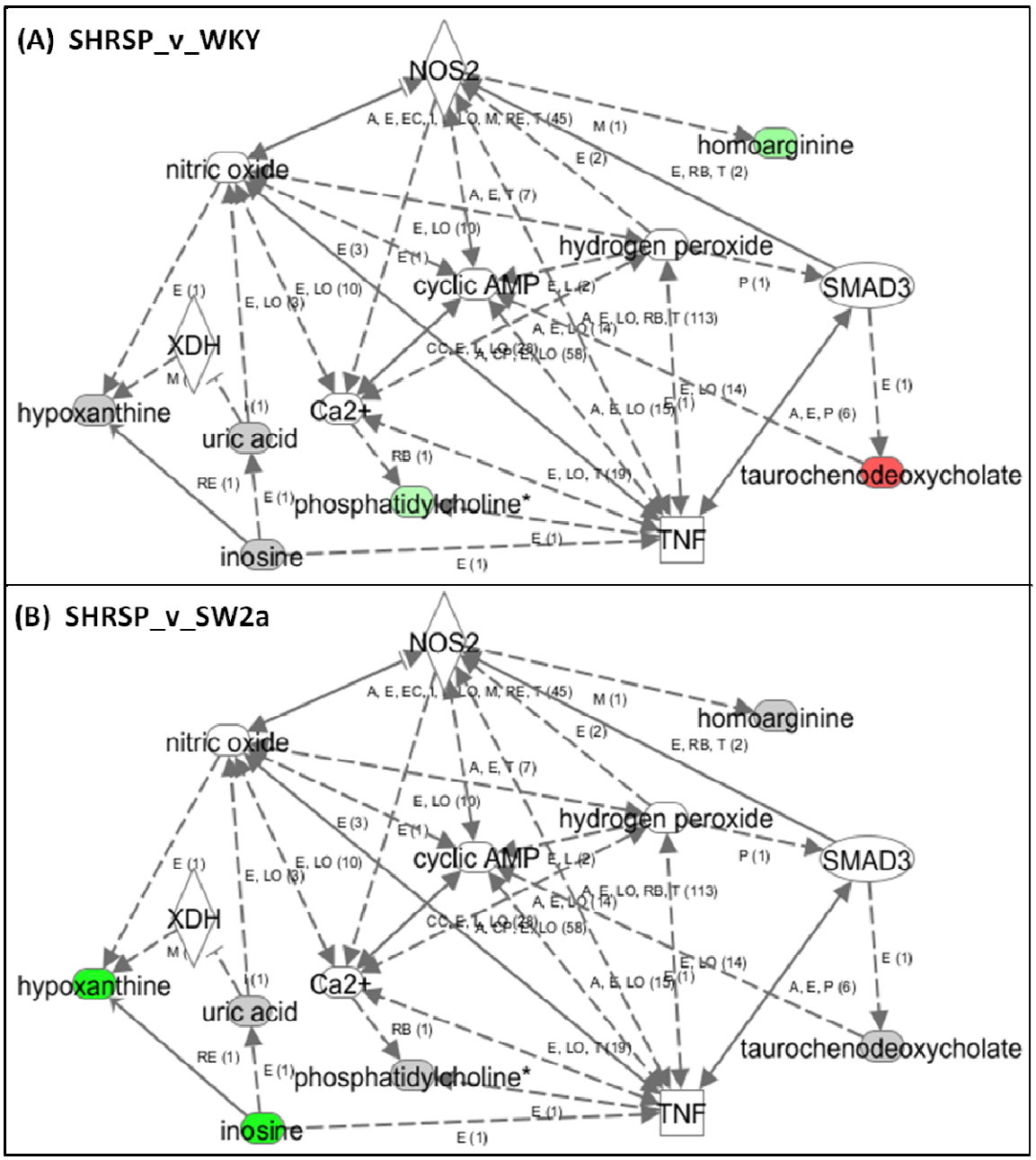


**Figure 6-5 - Ingenuity Pathway Analysis (IPA) network of metabolic changes in SHRSP versus WKY and SW2a, in VSMCs under basal conditions. Significantly changing molecules from the two comparisons are related to TNF (tumor necrosis factor), NOS (nitric oxide synthase), SMAD3 signalling protein, calcium ($Ca^{2+}$), xanthine dehydrogenase (XDH), hydrogen peroxide and cyclic AMP. (A) Metabolites changing in the SHRSP_v_WKY comparison. (B) Metabolites changing in the SHRSP_v_SW2a comparison. Colour indications: green - decrease, red - increase, gray - no change, white - not detected. Asterisk indicated more than one potential isomers.**

### 6.2.2 Metabolic differences across strains upon S1P-stimulation

To investigate the metabolic effect of sphingosine stimulation across the strains and its association with processes and pathways related to BP regulation, the metabolome of S1P-stimulated VSMCs was compared across the three strains. The ratio of significantly changing metabolites to total metabolites identified in the three comparisons was: SHRSP_v_WKY (45/784); SHRSP_v_SW2a (11/784); SW2a_v_WKY (22/786) (Figure 6-3A). The majority of changes were observed between SHRSP_v_WKY (36 unique), with SHRSP_v_SW2a exhibiting the fewest (9 unique). The main focus was on intersects between comparisons, as they are likely to include metabolites affected by the congenic interval and having protective or detrimental effect on BP regulation (Figure 6-3B; top right venn-diagram). In the comparisons between SHRSP versus WKY or SW2a, one metabolite was found to be consistently decreased in SHRSP and it was involved in lipid metabolism. When SHRSP and SW2a were compared to WKY, 8 'in common' metabolites were identified. All 8 displayed reduced levels in SHRSP and SW2a and they were mapping to different metabolic pathways. Moreover, the 36 unique metabolites changing in SHRSP versus WKY were further investigated. 20 of them were related to lipid or amino acid metabolism, 22 were decreased and 14 increased in SHRSP. Table 6-2 summarises the data for some of the above significant metabolites. Full data are included in 'S1Pcomparisons; venns' supplementary table.

Further inspection of peak quality for the above metabolites on peakML.Viewer, brought up the three metabolites illustrated in Figure 6-6 as potentially interesting. (S)-3-methyl-2-oxopentanoic acid was found to be consistently decreased in SHRSP and SW2a compared to WKY: FC= -1.649 and -1.362, respectively. Inosine and tyramine displayed increased concentrations in SHRSP versus WKY: FC= 2.777 and 5.487, respectively.

Generation of S1P-network on IPA involved significantly changing metabolites from the SHRSP versus WKY comparison, including inosine and tyramine. The metabolites were associated with S1P through calcium, cAMP and hydrogen peroxide (Figure 6-7).

**Table 6-2. Subset of metabolites exhibiting significant change in comparisons across S1P-stimulated VSMCs from WKY, SHRSP and SW2a. Data were generated on IDEOM v18. Green: decreased and red: increased metabolite levels.**

| KEGG id | Isomers | Putative metabolite | Map | Pathway | Fold Change | Pvalue (<0.05) |
|---|---|---|---|---|---|---|
| SHRSP_v_WKY ∩ SHRSP_v_SW2a (S1P) | | | | | | |
| C02804 | 12 | 5-Hydroxypentanoate | Lipids: Fatty Acyls | Fatty Acids and Conjugates | -1.516 / -1.645 | 0.0493 / 0.0414 |
| SHRSP_v_WKY ∩ SW2a_v_WKY (S1P) | | | | | | |
| 0 | 5 | [FA (13:0/2:0)] Tridecanedioic acid | Lipids: Fatty Acyls | Fatty Acids and Conjugates | -1.842 / -1.799 | 0.0018 / 0.0019 |
| C00671 | 17 | (S)-3-Methyl-2-oxopentanoic acid | Amino Acid Metabolism | Valine, leucine and isoleucine degradation / biosynthesis | -1.649 / -1.362 | 0.0280 / 0.0171 |
| C06463 | 9 | D-Threose | Carbohydrate Metabolism | 0 | -1.529 / -1.392 | 0.0110 / 0.0382 |
| C05817 | 1 | (1R,6R)-6-Hydroxy-2-succinylcyclohexa-2,4-diene-1-carboxylate | Metabolism of Cofactors and Vitamins | Ubiquinone biosynthesis | -1.575 / -1.378 | 0.0248 / 0.0381 |
| SHRSP_v_WKY (S1P) - unique | | | | | | |
| C00989 | 13 | 4-Hydroxybutanoic acid | Carbohydrate Metabolism | Butanoate metabolism | -1.882 | 0.0253 |
| C14827 | 39 | [FA (18:2)] 9S-hydroperoxy-10E,12Z-octadecadienoic acid | Lipids: Fatty Acyls | Linoleic acid metabolism | -1.815 | 0.0481 |
| 0 | 6 | Leu-Asn | Peptide(di-) | Hydrophobic peptide | -1.809 | 0.0253 |
| C00137 | 57 | myo-Inositol | Carbohydrate Metabolism | Inositol /Galactose metabolism | -1.510 | 0.0140 |
| C00626 | 9 | PI(16:0/18:2(9Z,12Z)) | Lipids: Glycerophospholipids | Glycerophosphoinositols | 1.611 | 0.0369 |
| C05332 | 6 | Phenethylamine | Amino Acid Metabolism | Phenylalanine metabolism | 2.519 | 0.0051 |
| C00483 | 7 | Tyramine | Amino Acid Metabolism | Tyrosine metabolism | 2.777 | 0.0059 |
| C00020 | 7 | AMP | Nucleotide Metabolism | Purine metabolism | 3.731 | 0.0316 |
| C00294 | 3 | Inosine | Nucleotide Metabolism | Purine metabolism | 5.487 | 0.0457 |

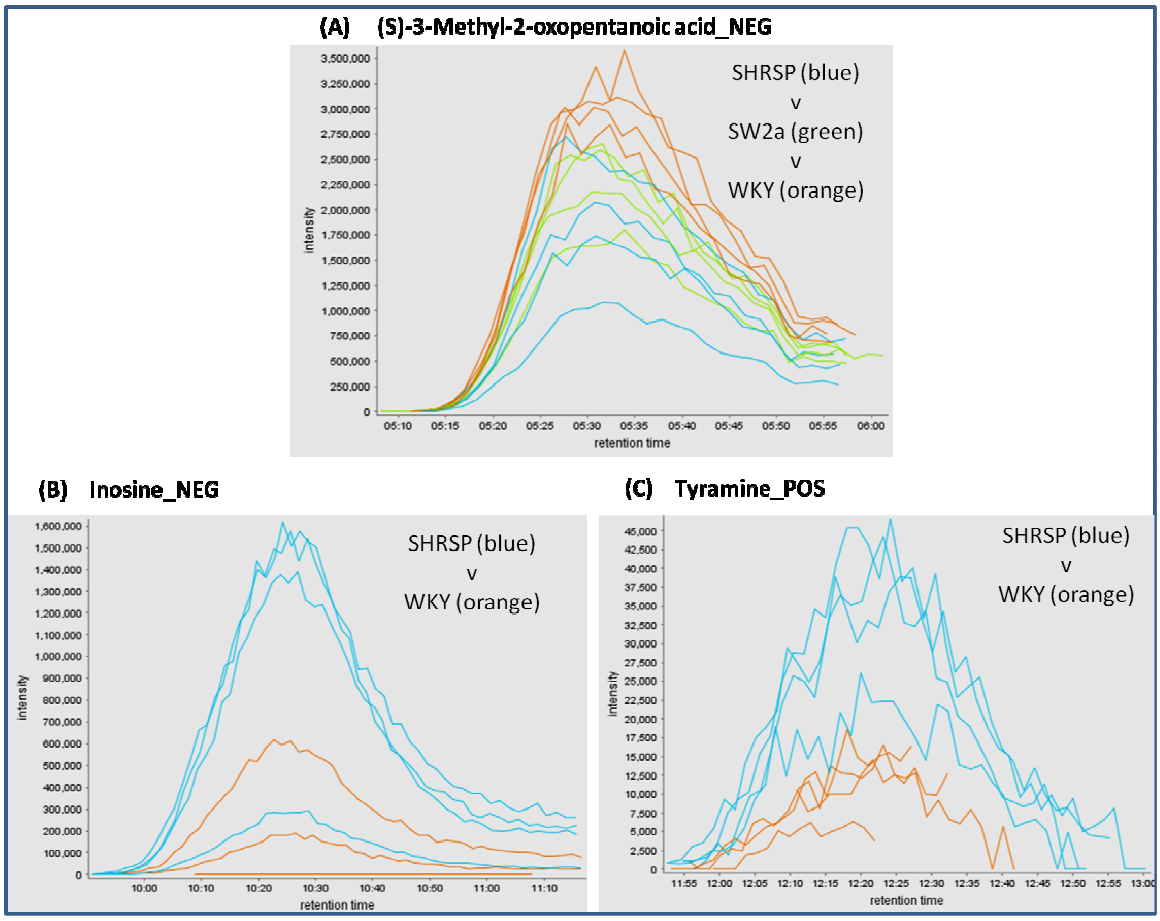


**Figure 6-6 - Levels of significantly changing metabolites in the comparisons across S1P-stimulated VSMCs from WKY, SHRSP and SW2a. PeakML chromatograms demonstrate significant ($p<0.05$) decrease of (S)-3-methyl-2-oxopentanoic acid in SHRSP and SW2a compared to WKY (A) and increase in the levels of inosine (B) and tyramine (C) in SHRSP versus WKY. The x-axis indicates the retention time and the y-axis the intensity.**

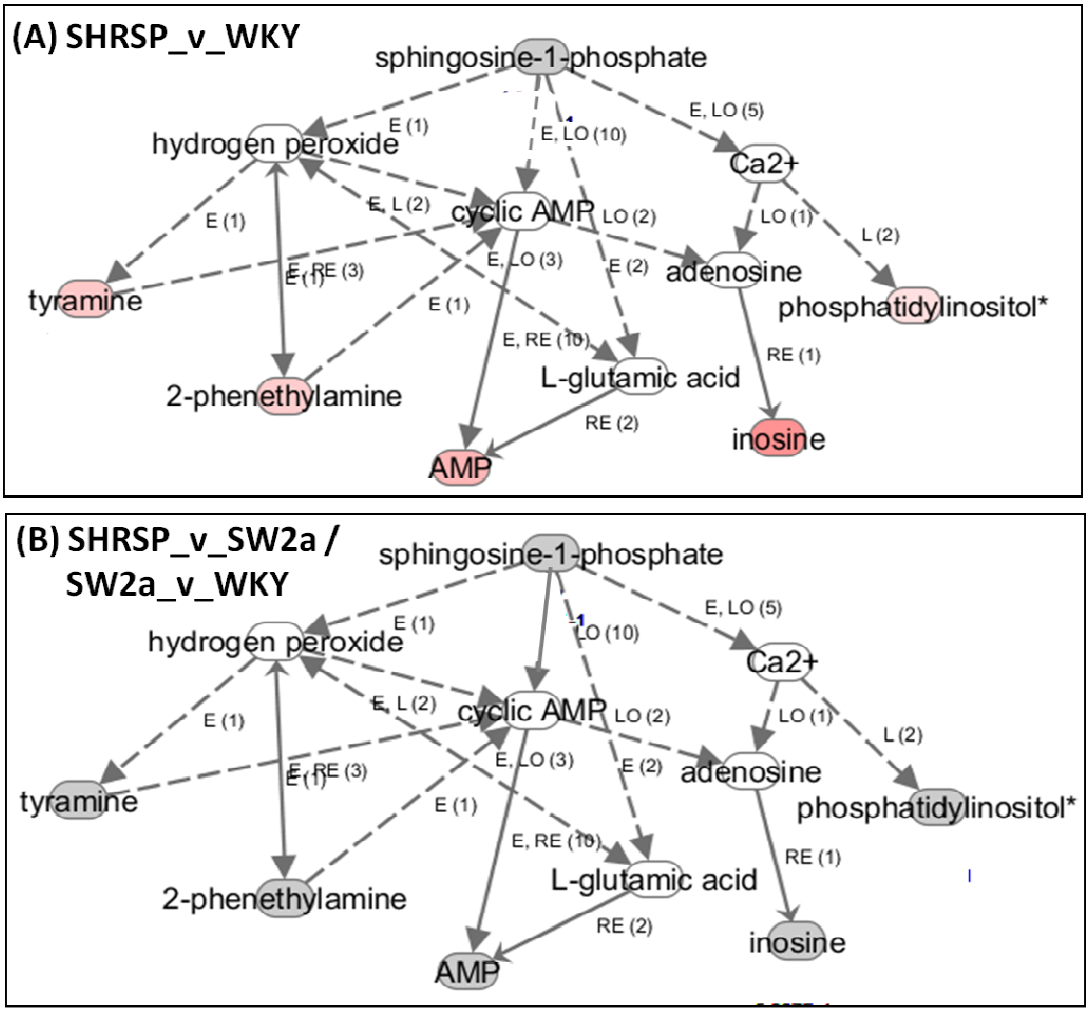


**Figure 6-7 - IPA comparison of S1P-network across S1P-stimulated VSMCs from SHRSP, WKY and SW2a. (A) Significantly changing metabolites in the SHRSP_v_WKY comparison are associated to sphingosine signalling, involving hydrogen peroxide, cAMP and calcium. These metabolites are unique to the comparison and are not changing in (B) SHRSP_v_SW2a and SW2a_v_WKY comparisons. Colour indications: red - increase, gray - no change, white - not detected. Asterisk indicates more than one isomers.**

### 6.2.3 Metabolic effects of S1P-stimulation within strains

The metabolic effect of sphingosine stimulation was assessed in each strain individually, by comparing metabolic profiles under basal conditions and upon S1P-stimulation. The number of significantly changing metabolites compared to the total number of metabolites identified in each strain was: $WKY_{S1P}$_v_$WKY_{veh}$ (32/783); $SHRSP_{S1P}$_v_$SHRSP_{veh}$ (20/780); $SW2a_{S1P}$_v_$SW2a_{veh}$ (26/784) (Figure 3-7A). The majority of changed metabolites were unique to each strain: union (75); $WKY_{S1P}$_v_$WKY_{veh}$ (31); $SHRSP_{S1P}$_v_$SHRSP_{veh}$ (19); $SW2a_{S1P}$_v_$SW2a_{veh}$ (22), with no molecules identified 'in common' (e.g. Figure 6-3B; bottom venn-diagram). In WKY the number of metabolites exhibiting reduced levels (12) upon stimulation was similar to those with elevated levels (19). Many of the decreased metabolites (5) mapped to lipid metabolism, whilst most of the increased (8) were related to amino acid and carbohydrate metabolism. In stimulated SHRSP the larger number of metabolites was increased (14 out of 19) and related to lipid metabolism. Lastly, in stimulated SW2a most metabolites were decreased (17 out of 22) and also mapped to lipid metabolic pathways. The 30 unique metabolites in WKY comparison, along with the two common between SW2a and WKY comparisons, were further investigated as potentially protective in the sphingosine-related BP regulation. Likewise, the 19 SHRSP unique metabolites and the one common metabolite between SW2a and SHRSP comparisons were examined as potentially deleterious upon S1P-stimulation (Table 6-3). Full data are included in ‘S1P_v_veh_comparisons; venns’ supplementary table.

**Table 6-3. Subsets of metabolites exhibiting significant change upon S1P-stimulation in VSMCs from WKY, SHRSP and SW2a. Data were generated on IDEOM v18. Green: decreased and red: increased metabolite levels.**

| KEGG id | Isomers | Putative metabolite | Map | Pathway | Fold Change | Pvalue (<0.05) |
|---|---|---|---|---|---|---|
| | | | $WKY_{S1P}\_v\_WKY_{veh}$ | | | |
| C04840 | 7 | 3beta-Hydroxy-4beta-methyl-5alpha-cholest-7-ene-4alpha-carboxylate | 0 | 0 | -2.46 | 0.0092 |
| C13877 | 17 | [PE (16:0/18:1)] 1-Hexadecanoyl-2-(9Z-octadecenoyl)-sn-glycero-3-phosphoethanolamine | Lipids: Glycerophospholipids | Glycerophospho-ethanolamines | -2.009 | 0.0126 |
| C00350 | 12 | PE(18:1(11Z)/P-18:1(11Z)) | Lipids: Glycerophospholipids | Glycerophospho-ethanolamines | -1.969 | 0.0076 |
| C01924 | 5 | Homoarginine | Amino Acid Metabolism | 0 | -1.908 | 0.0425 |
| 0 | 1 | Cholesterolsulfate | Lipids: Sterol lipids | 0 | -1.686 | 0.0172 |
| C00626 | 15 | PI(16:0/20:4(5Z,8Z,11Z,14Z)) | Lipids: Glycerophospholipids | Glycerophospho-inositols | -1.624 | 0.0099 |
| 0 | 4 | DL-2-Aminooctanoicacid | 0 | 0 | -1.590 | 0.0143 |
| C00624 | 4 | N-Acetyl-L-glutamate | Amino Acid Metabolism | Arginine and proline metabolism | -1.561 | 0.0265 |
| C00166 | 13 | Phenylpyruvate | Amino Acid Metabolism | Phenylalanine, tyrosine, tryptophan biosynthesis | 1.360 | 0.0439 |
| C06002 | 8 | (S)-Methylmalonate semialdehyde | Amino Acid Metabolism | Valine, leucine and isoleucine degradation__ Propanoate metabolism | 1.434 | 0.0105 |
| C00137 | 57 | myo-Inositol | Carbohydrate Metabolism | Inositol / Galactose / Ascorbate and aldarate metabolism | 1.477 | 0.0023 |
| C15117 | 1 | 3-Methyl-19-nor-17alpha-pregna-1,3,5(10)-trien-17-ol | 0 | 0 | 2.923 | 0.0353 |
| C05465 | 3 | [ST hydrox] N-(3alpha,7alpha-dihydroxy-5beta-cholan-24-oyl)-taurine | Lipids: Sterol lipids | Bile acid biosynthesis | 3.889 | 0.0439 |
| | | | $SHRSP_{S1P}\_v\_SHRSP_{veh}$ | | | |
| C15025 | 2 | (S)-Carnitine | 0 | carnitine degradation II | -1.850 | 0.0401 |
| C06144 | 2 | 3-Butynoate | Carbohydrate Metabolism | Butanoate metabolism | -1.587 | 0.0317 |
| C00906 | 3 | 5,6-Dihydrothymine | Nucleotide Metabolism | Pyrimidine metabolism | -1.443 | 0.0487 |
| C01234 | 5 | 1-Aminocyclopropane-1-carboxylate | Amino Acid Metabolism | Methionine metabolism_ Propanoate metabolism | 1.416 | 0.0108 |
| C00350 | 14 | PE(20:4(5Z,8Z,11Z,14Z)/P-18:1(11Z)) | Lipids: Glycerophospholipids | Glycerophospho-ethanolamines | 1.838 | 0.0213 |
| C13914 | 1 | N,N-Dimethylsphing-4-enine | Lipids: Sphingolipids | Sphingoid bases | 1.894 | 0.0389 |
| C00350 | 6 | [PE (16:1/22:6)] 1-O-(1Z-hexadecenyl)-2-(4Z,7Z,10Z,13Z,16Z,19Z-docosahexaenoyl)-sn-glycero-3-phosphoethanolamine | Lipids: Glycerophospholipids | Glycerophospho-ethanolamines | 2.132 | 0.0187 |
| 0 | 1 | Asp-Cys-Cys-Pro | Peptide (tetra-) | Acidic peptide | 7.415 | 0.0366 |
| | | | $WKY_{S1P}\_v\_WKY_{veh} \cap SW2a_{S1P}\_v\_SW2a_{veh}$ | | | |
| 0 | 3 | Ile-Phe-Thr-Pro | Peptide(tetra-) | Hydrophobic peptide | -1.340 / -1.370 | 0.0395 / 0.0298 |
| | | | $SHRSP_{S1P}\_v\_SHRSP_{veh} \cap SW2a_{S1P}\_v\_SW2a_{veh}$ | | | |
| C00294 | 3 | Inosine | Nucleotide Metabolism | Purine metabolism | 17.152 / -2.775 | 0.0349 / 0.0499 |

Subsequent assessment of peak quality for the above metabolites was performed on peakML.Viewer. Figure 6-8 illustrates selected peaks of potential interest. Myo-inositol (FC=1.477) was increased in S1P-stimulated WKY as opposed to reduced levels of homoarginine (FC=-1.908) (Figure 6-8A). In SHRSP, S1P-stimulation caused significant increase in inosine (FC=17.152) and N,N-dimethylsphing-4-enine (FC=1.894) concentrations (Figure 6-8B). The significance in inosine reduction in S1P-stimulated SW2a (FC=-2.775) appeared to be a 'false positive' indication, driven by outliers (Figure 6-8C).

Generation of S1P-network on IPA involved significantly changing metabolites from stimulated WKY, SHRSP and SW2a strains, including homoarginine, N,N-dimethylsphing-4-enine and inosine (Figure 6-9). In WKY the metabolites were connected to S1P through calcium, L-glutamic acid, NOS (nitric oxide synthase) and SMAD3 protein. In SHRSP the connections were either direct or involved cAMP-adenosine. Finally, in SW2a the network implicated the inflammatory molecules, TNF (tumour necrosis factor), IFNG (interferon gamma) and IL6 (interleukin 6).

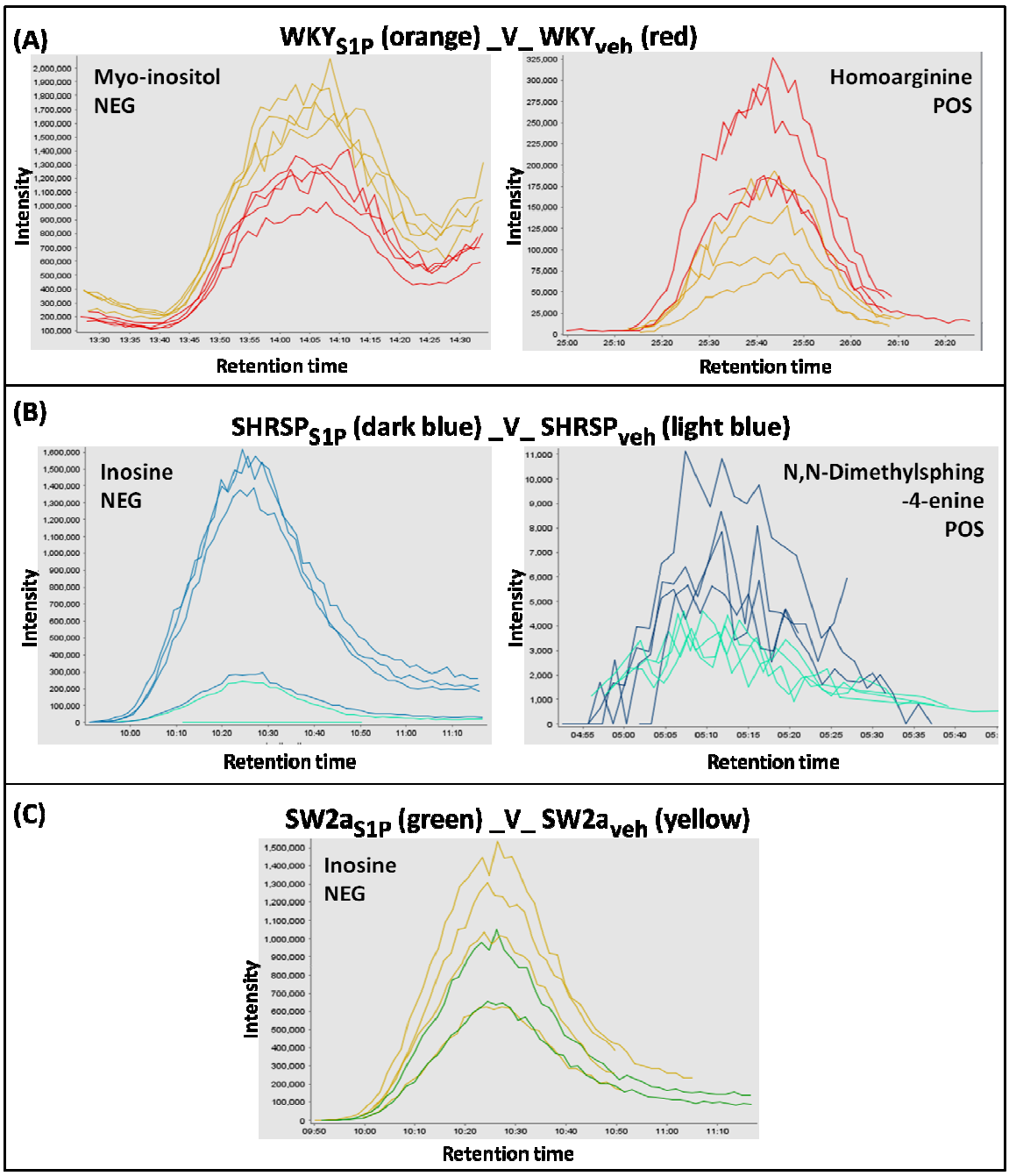


**Figure 6-8 - Levels of significantly changing metabolites upon S1P-stimulation of the three strains, illustrated as peakML chromatograms. (A) S1P-stimulated WKY demonstrate significant ($p<0.05$) increase of myo-inositol (FC=1.477)) and decrease of homoarginine (FC=-1.908). (B) In S1P-stimulated SHRSP, inosine (FC=17.152) and N,N-dimethylsphing-4-enine (FC=1.894) exhibit increased concentrations. (C) S1P-stimulation in SW2a did not affect inosine levels, despite the achieved significance ($p=0.0499$) due to poor reproducibility of peaks. The x-axis indicates the retention time and the y-axis the intensity.**

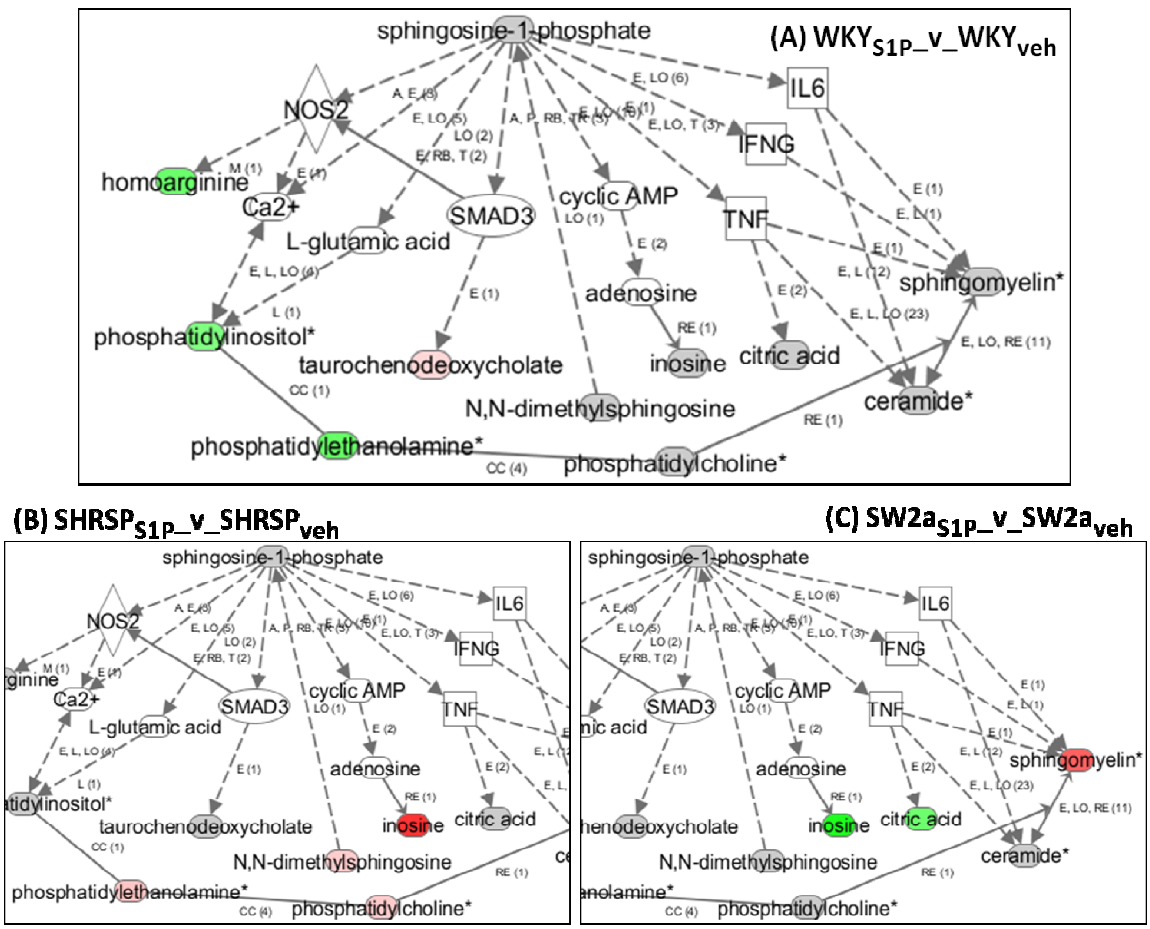


**Figure 6-9 - Metabolic changes induced by S1P-stimulation of VSMCs in SHRSP, WKY and SW2a and mapping to S1P-network. (A) Significantly changing metabolites in stimulated WKY are related to NOS (nitric oxide synthase), calcium ($Ca^{2+}$), L-glutamic acid and SMAD3 protein. (B) Changing metabolites in stimulated SHRSP are either directly associated with S1P or through cyclic AMP-adenosine, NOS, ($Ca^{2+}$) and L-glutamic acid. (C) In SW2a the changes are mediated through cyclic AMP-adenosine or mainly through inflammatory components (TNF: tumour necrosis factor; IL6: interleukin 6; IFNG: interferon gamma). The network was generated on IPA. Colour indications: red - increase, gray - no change, white - not detected. Asterisk indicates more than one isomers.**

## 6.3 Discussion

To complement previous proteomic profiling of primary mesenteric VSMCs across WKY, SHRSP and reciprocal 2a-congenic strains, and in order to further investigate the altered sphingosine signalling in HTN (Yogi et al., 2011), untargeted metabolomic profiling was conducted in primary VSMCs from WKY, SHRSP and SW2a, under basal and S1P-stimulated conditions.

Initially, data quality was assessed by PCA plots, where all samples (vehicle and S1P-stimulated) were plotted together for increased reliability. Relatively low percentages of PC1 and PC2 as well as not clear clustering of samples imply small differences across and within strains, before and after S1P-stimulation. This is further supported by the relatively small ratio of significantly changing metabolites to total metabolites identified, across all comparisons. However, such a result could be attributed to the small number of replicates (N=4) and the dynamic nature of metabolome, which can compromise reproducibility. Alternatively, the fact that metabolome is a highly diverse entity which may not be entirely characterised by a single analytical platform, may suggest that more significant differences exist in a different component of the metabolome that were not identified in this analysis. Further investigation of this assumption would be worthwhile by conducting analysis on a different platform, or a more specified lipidomic analysis.

Considering time limitations, from a large number of comparisons across strains and conditions, we focused on particular intersects according to the most interesting questions to be tested in each case.

At basal conditions, the SHRSP had more different profile to SW2a and WKY, than the SW2a to WKY. This suggests that the congenic interval is having a profound effect on the SW2a metabolic profile, which is likely to contribute to their improved BP phenotype. Specifically, the majority of changes in SHRSP compared to SW2a indicated decreased nucleotide, amino acid and carbohydrate metabolism, whereas comparison with WKY showed altered lipid metabolism. This demonstrates that metabolic processes are genetically regulated in a different manner across the strains, which are likely to also regulate BP. Therefore, the main focus was to identify 'unique' metabolites changing in SHRSP versus SW2a and in SHRSP versus WKY, and more importantly to identify 'in common' metabolites between these two comparisons, changing in the same direction. These molecules were investigated as potentially deleterius against high BP. On an IPA-generated

network, several of the altered metabolites were connected, directly or indirectly, to NO, $Ca^{2+}$, cAMP and $H_2O_2$, indicating potential association with pathways implicated in vascular tone regulation and oxidative stress.

Inosine and hypoxanthine, two sequential products of the adenine-adenosine (purine) metabolic pathway, mapped to the above network through association with NO, uric acid and xanthine dehydrogenase (XDH), and were significantly reduced in SHRSP versus SW2a. The purine degradation pathway has been implicated in oxidative stress and enzymes such as XDH, which uses hypoxanthine as substrate, are known drug targets for CVD (Rekhraj et al., 2013, Feig et al., 2008). Moreover, both hypoxanthine and inosine have been identified as plasma metabolic biomarkers for myocardial injury (Lewis et al., 2008). The observed decreased levels in SHRSP imply increased XDH activity and elevated oxidative stress, which is corrected in SW2a by introduction of the congenic interval. Another interesting metabolite, which exhibited small but significant reduction in SHRSP compared to SW2a, was L-ornithine. In VSMCs arginase hydrolyses L-arginine to produce L-ornithine, which is further metabolised into polyamines to promote SMC proliferation and collagen synthesis (Morrison and Seidel, 1995, Durante et al., 1998, Durante et al., 2001). Decreased levels in SHRSP may imply increased polyamine synthesis and vascular remodelling of MRAs, which is attempted to be prevented by the congenic interval in SW2a. In addition, homoarginine, an aminoacid derived from lysine and known to inhibit arginase (Hrabak et al., 1994), was decreased in SHRSP compared to WKY. Low levels could suggest increased arginase activity influencing vascular remodelling in SHRSP. Moreover, low homoarginine concentrations, in plasma, have been associated with myocardial dysfunction and increased risk of fatal cardiovascular events in human studies (Pilz et al., 2011). Finally, [SP (16:0)] N-(hexadecanoyl)-sphing-4-enine-1-phosphocholine, also known as palmitoyl sphingomyelin, was an interesting metabolite displaying slight, yet significant decrease in SHRSP compared both to WKY and SW2a. Not much is known about the specific role of palmyitoyl sphingomyelin in cell function and disease. However, the family of sphingomyelins are known to be metabolised in ceramide and bioactive lipids, which mediate VSMC proliferation, apoptosis and constriction in a number of cardiovascular diseases (Pavoine and Pecker, 2009). Therefore, the observed low concentrations in SHRSP could reflect potentially increased levels of ceramides in SHRSP, which have not been detected on this analytical platform.

Upon S1P-stimulation, metabolic profiles of the parental strains exhibited the larger number of differences, supporting Yogi's data (Yogi et al., 2011) on significantly altered

signalling induced by S1P between the two strains. Further, SHRSP and SW2a displayed the most comparable profiles, which imply similar responses to stimulation. Such result is in contrast to the findings under basal conditions, which demonstrated greater similarities between SW2a and WKY. Therefore, it becomes obvious that S1P signalling is most likely regulated by components lying outside the congenic interval. For this reason, the most interesting metabolites to be further examined were those changing 'in common' between SHRSP versus WKY and SW2a versus WKY. (S)-3-methyl-2-oxopentanoic acid was one of the above metabolites having a consistently decreased trend across SHRSP and SW2a. It is known to participate in isoleucine degradation, and has not been related to any other processes or diseases. Therefore further investigation on its potential association to BP regulation processes is needed. The rest of the 'in common' metabolites presented low confidence due to either noisy peakML chromatograms or significance driven by one outlier, and they were not pursued further. Subsequently, focus was on the 'unique metabolites changing between SHRSP and WKY. Tyramine, a trace amine derived from tyrosine and involved in the release of catecholamines, displayed increased concentrations in SHRSP versus WKY. Tyramine has been reported to induce vasodilatation in raised-perfusion-pressure MRAs from Sprague-Dawley rats (Anwar et al., 2012), in contrast to its vasoconstrictive effects on mesentery from Wistar (Elliott et al., 1989) and on rat aortic rings (Fehler et al., 2010). Consequently, addressing the effects of tyramine on SHRSP mesenterium would aid the interpretation of its increased levels in SHRSP. Lastly, inosine concentration was elevated in SHRSP compared to WKY but not SW2a. S1P is known to regulate accumulation of cAMP in VSMCs (Damirin et al., 2005), which in turn is involved in the purine metabolism and can be associated with observed increases in levels of AMP and inosine. Considering the significantly decreased levels of inosine in SHRSP versus SW2a at baseline, it is obvious that S1P stimulation causes an increase in SHRSP to reach SW2a levels. This effect seems to be dependent on the congenic interval and is a priority finding for further investigation.

The last set of comparisons examined changes in the metabolic profiles of each strain before and after S1P-stimulation. The majority of changed metabolites were unique to each strain, with very few 'in common' metabolites identified. This finding demonstrates differential responses of each animal to the stimulation and suggests a combined effect of the genetic background and the congenic interval in S1P-signalling. Indeed, on a network generated on IPA, with S1P at the apex, metabolites identified in the three comparisons

were connected to S1P through intermediate molecules associated with different processes. Nonetheless, all three strains appeared to respond to S1P-stimulation mainly through alterations in their lipid profile. However, the lack of a larger number of common consistent changes between SHRSP and SW2a limits identification of potentially interesting metabolites implicated in the altered sphingosine signalling in HTN. This finding may suggest further that filtering through SW2a and WKY for identification of candidates for S1P-mediated BP regulation is not the most appropriate strategy, at least for the metabolite profile, or that another analytical platform is needed to capture these metabolic changes.

In WKY, S1P-stimulation induced increase in myo-inositol levels. This carbohydrate, apart from being the structural component in the synthesis of inositol phosphates, it has been reported to prevent and reverse endothelial dysfunction in rat mesenteric vessels, through scavenging of superoxide (Nascimento et al., 2006). Therefore, further characterisation of its relation to S1P signalling in VSMCs would be of interest. Moreover, stimulated WKY exhibited diminished levels of homoarginine, which may impact on arginase activity towards VSMC proliferation and collagen synthesis (Hrabak et al., 1994). In SHRSP, S1P-stimulation elevated concentration of N,N-Dimethylsphing-4-enine, which is a sphingosine kinase inhibitor (Edsall et al., 1998). This metabolite has been implicated in reduction of MAPK and NADPH oxidase activities, VCAM1 expression, intracellular calcium and formation of actin stress fibres (Wu et al., 2004, Ibrahim et al., 2004, Xia et al., 1998, Meyer zu Heringdorf et al., 1998, Hanna et al., 2001). Thus, increased levels upon S1P stimulation could be potentially beneficial on VSMC function and structure and consequently on BP regulation. Furthermore, inosine was considerably elevated in stimulated SHRSP, which suggests that in this strain sphingosine signalling significantly affects purine metabolism. This could be mediated by cAMP, which participates in purine metabolism and its intracellular levels are known to be regulated by S1P (Damirin et al., 2005, Van Brocklyn et al., 1998).

In conclusion, the effect of the congenic interval on the metabolic profile appears to be more profound under basal conditions, whereas S1P signalling may be predominantly regulated by components lying outside the interval. However, metabolic responses to stimulation seem to be, not surprisingly, a combined effect of the genetic background and the congenic interval. Further investigation by use of complementary analytical platforms would allow more comprehensive capturing of metabolic changes. Moreover, the putative metabolites identified in this analysis, will have to be validated to authentic standards by

MS/MS fractionation and verified by WB and enzymatic activity assays, on control and S1P-stimulated cells, before generation of new testable hypothesis.

# 7 General Discussion

The growing problem of elevated blood pressure (BP) over the last decades has become one of the major contributors to the present pandemic of cardiovascular disease (CVD) (Levenson et al., 2002b, Carretero and Oparil, 2000). Hypertension (HTN) is a trait of large phenotypic variance with a clear genetic predisposition (Franceschini et al., 2011). By 2025, approximately 1.56 billion adults are predicted to suffer from essential hypertension (EH), which makes the need for better understanding of its pathophysiology and genetics highly pressing. Over the past few years, an increasing number of large scale-genetic studies in human, including several GWAS (Levy et al., 2009, Ehret, 2011, Johnson et al., 2011), has accelerated the current understanding of the polygenic nature of BP regulation. However, only in few cases the reported SNPs implicate a specific gene of high effect (Padmanabhan et al., 2010) and, collectively, they represent, only a small fraction of BP heritability and have small size effects that do not explain BP phenotypic variance. This could be attributed to multifactorial upstream regulation of the candidate gene expression, as well as downstream regulation of the protein levels and activity, which would be reflected on the metabolic profiles of cells, tissues, organs and ultimately on the phenotype.

To further dissect the genetic components of EH, the present study employed high-throughput, untargeted proteomic and metabolomic profiling, on a well characterised animal model of human EH, the SHRSP. These high-resolution powerful approaches were combined with chr.2 congenic stains, which had been previously generated in our laboratory using the SHRSP and WKY parental strains and had confirmed that the congenic interval is involved in BP regulation. Our results demonstrate that the chr.2 congenic interval affects BP phenotype through regulation of vascular reactivity and mechanics of resistance arteries, and that these events are primary to vascular remodelling. Alterations in vascular reactivity are confirmed at the molecular level in the proteomic and metabolomic screenings, along with highly de-regulated antioxidant responses. Finally, proteomics analysis identifies up-regulation of NPR3 in SHRSP, a protein which is correlated to a GWAS discovery in humans.

Below are discussed in more detail the aims of this work, the results in association to existing knowledge as well as the potential and limitations of our studies.

The SHRSP is an experimental rat model resembles the human pathophysiology of HTN and has been used extensively in high-throughput genomic studies, offering the advantage of increased genetic homogeneity. Previous genetic linkage studies have identified QTLs associated with BP regulation and salt-sensitivity on chr. 2, 3 and 14 (Luft et al., 1988, McBride et al., 2005, McBride et al., 2003). Construction of chr.2 reciprocal congenic stains

in our laboratory, using SHRSP and WKY as the parental stains, combined with microarray gene expression profiling in kidney from salt-loaded rats, identified positional candidate genes for salt-sensitive hypertension. Sphingosine-1-phosphate receptor 1 (*S1pr1*) and vascular adhesion molecule (*Vcam1*) lie on the chr.2 congenic interval implicated in salt-sensitivity and were differentially expressed across the strains (Graham et al., 2007). Additionally, glutathione S-transferase mu 1 (*Gstm1*) was identified as another chr.2 positional and functional candidate for BP regulation, lying outside the region implicated in salt-sensitivity (McBride et al., 2003). Construction of congenic strains has been widely used for the dissection of QTLs and identification of candidate genes underlying complex, multifactorial diseases (Wallace et al., 2004, Kumarasamy et al., 2011, Ariyarajah et al., 2004).

However, as differential expression profiling of candidate genes at the mRNA level, does not always correlate with phenotypic variance, alterations at the protein and metabolite levels need to be investigated in order to obtain a clearer picture of multifactorial traits such as HTN. Use of large-scale proteomic and metabolomic screenings are becoming essential for comprehensive characterisation and comparison of phenotypic alterations induced by genomic changes, at health and disease (Geiger et al., 2010, Mittler et al., 2009). Such high-resolution, system-wide, (semi)-quantitative approaches offer new potential in post genomics and systems biology. However, analysis and interpretation of such gigabyte-large datasets remain challenging.

The present study combined shotgun proteomics and metabolomics, with chr.2 congenic and *Gstm1*-transgenic strains, aiming to identify potential biomarkers for EH and salt-sensitivity, as well as altered processes in HTN related to S1P/S1PR1 signalling and regulated by the congenic interval. Comparison of the parental WKY and SHRSP strains, exhibiting two extreme BP and salt-sensitivity phenotypes, with the SW2k-congenic, the SW2a and WS2a reciprocal-congenic and the *Gstm1*-transgenic strains of intermediate BP and salt-sensitivity phenotypes, offered the potential of more restrictive identification of components underlying these differences. Moreover, during these studies, 3 major disciplines were combined: biology for sample preparation, analytical chemistry for sample processing and bioinformatics for data analysis.

Initially, untargeted metabolomic profiling was performed in urine and plasma from normal-salt and salt-loaded parental, SW2k-congenic and *Gstm1*-transgenic rats. Given the different BP phenotypes, the aim was to assess the role of the congenic interval and *Gstm1*

on salt-sensitivity and BP-regulation and identify putative biomarkers. The rich metabolic content of urine and plasma, consisting of building blocks and by-products of processes occurring throughout the organism, classifies them as biological samples of high prognostic and diagnostic value in the biomarker research (Giovane et al., 2008, Barderas et al., 2011). Moreover, recent untargeted metabolomic studies were able to associate distinct urine metabolite signatures to specific QTLs, suggesting a global impact of genetic loci on metabolic pathways (Cazier et al., 2012). In our study, quantitative changes of L-proline and linoleic acid in plasma, under normal-salt, were unique to SHRSP, indicating regulation of their metabolic pathway by the congenic interval and potential association with *Gstm1.* Upon salt-loading, oleic acid in urine and glutathione disulfide and S1P in plasma, exhibited different pattern of change in salt-sensitive versus salt-resistant strains. This demonstrates a regulatory role of the congenic interval in salt-loaded conditions, but not of *Gstm1*, which was expected, as this gene is not a candidate for salt-sensitivity. The majority of altered metabolites were associated with lipid metabolism, inflammatory response and free radical scavenging processes previously shown to be altered in salt-sensitive rats and associated with cardiovascular disorders (Spijkers et al., 2011, Liu et al., 2012).

Subsequently, due to the importance of the resistance vasculature in BP regulation, the effect of the congenic interval on structure, mechanical properties and vascular reactivity of MRAs was investigated, in parental and 2a-reciprocal congenic strains. Remodelling of vessels at 16 weeks of age was not observed across the strains, suggesting that structural alterations develop later in life as an adaptive response to increased BP. However, MRAs from SHRSP exhibited a tendency to be stiffer, whereas the congenic strains displayed an intermediate phenotype, implicating the congenic interval. The above data are supported by studies in 24-week-old animals, which demonstrated no significant alterations in vessel structure but increased intrinsic wall stiffness in SHRSP/SHR versus WKY (Arribas et al., 1997, Gonzalez et al., 2006). However, the effect of the congenic interval was more obvious in the vascular reactivity studies, where it corrected for hypercontractility but not for the endothelial dysfunction observed in SHRSP, when introgressed into SW2a congenic rats. Hypercontractility in SHRSP implicated RhoA/RhoK pathway which is supported by studies on hypertensive rat models (Moriki et al., 2004, Kitazono et al., 2002) and is potentially affected by the congenic interval. Endothelial dysfunction in the SHRSP and SW2a was mediated by NO bioavailability, as shown previously (McIntyre et al., 1997, Kerr et al., 1999, Ma et al., 2001) and appeared to be independent of the congenic interval. In the

reciprocal WS2a congenic strains detrimental effects were not identified, suggesting that elements outside the interval regulate these processes or compensate for the loss of the 'healthy' genes.

Further investigation of these differences in the vasculature between the stains was performed at the molecular level, through MS-based quantitative proteomic analysis of primary mesenteric VSMC from the parental and 2a-reciprocal congenic strains. Use of triple-SILAC labelling allowed for three-way comparisons across the strains. However, challenges in the bioinformatics analysis directed the focus on the comparison between WKY and SHRSP. Not surprisingly, differentially regulated proteins were associated to processes implicated in BP regulation and HTN, including oxidative stress, vascular tone regulation and remodelling. Increased GSTM1 levels in the primary VSMCs from SHRSP, as opposed to previously described reduced mRNA and protein levels in the kidney (McBride et al., 2005), suggest differences in vascular and renal antioxidant mechanisms. This is further supported by the observed reduction in SHRSP, of HMOX and NQO1 detoxification enzymes of the Nrf2 (nuclear factor (erythroid-derived 2)-like 2) pathway, which has been found to be up-regulated in the kidney antioxidant response (Wilmes et al., 2011, Zoja et al., 2013). Moreover, NPR3, which maps to the chr.2 congenic interval, was up-regulated in SHRSP. As a receptor of C natriuretic peptide (CNP), an identified EDHF factor (Laurant et al., 1997), NPR3 increased levels could be interpreted as an attempt of SHRSP to correct for hypercontractility and endothelial dysfunction, which was observed in MRAs. Furthermore, in support of the data implicating RhoA/Rock signalling in MRA hypercontractility, this pathway was found to be significantly altered in SHRSP during the proteomics analysis and CAV1 which induces RhoA activation (Dubroca et al., 2007) was also up-regulated in SHRSP. Lastly, proteins related to sphingosine signalling were also differentially expressed in SHRSP, including down-regulated EZR, a member of the RhoA/Rock pathway, and up-regulated SOD2 and CTSD antioxidant enzymes, as well as COL3A1, which has been implicated in stiffness of MRAs and therefore supports the findings of the myography functional studies (Briones et al., 2007, Campbell et al., 1991).

To further investigate the effect of S1P-signalling on HTN and assess contribution of the congenic interval, metabolomic screening was conducted on VSMC used in the proteomics analysis, at basal conditions and upon S1P-stimulation. Under basal conditions, the effect of the congenic interval was more profound on the metabolic profile of SW2a, which may be linked to their improved BP phenotype. S1P-stimulation induced more

differences in the metabolic profiles of SHRSP v WKY, which is supported by altered S1P signalling in VSMCs (Yogi et al., 2011). Differences between SHRSP and SW2a were fewer, suggesting that S1P signalling is predominantly regulated by components outside the congenic interval. However, responses to stimulation were different across all strains which suggests a combined effect of the genetic background and the congenic interval on S1P signalling regulation and implies that filtering through the SW2a congenic strain for identification of candidates for S1P-mediated BP regulation, may not by the most appropriate strategy, at least in the VSMC metabolite profiling. Two interesting metabolites were elevated in stimulated SHRSP compared to the other strains. Effects of S1P-signalling on inosine levels appeared to be mediated by the congenic interval, which suggests that in SHRSP, sphingosine signalling significantly affects purine metabolism potentially through cAMP (Damirin et al., 2005, Van Brocklyn et al., 1998). Additionally, S1P-signalling in SHRSP may be related to BP-regulation through tyramine, which has vasodilatory properties in rat MRAs (Anwar et al., 2012) and could have a protective role against the hypercontractility described in the myography studies.

Collectively, this study followed a holistic approach aiming to capture a clearer picture of the genetic determinants underlying BP regulation in the SHRSP. Combination of high-throughput proteome and metabolome profiling with chr.2 congenic and transgenic strains allowed identification of candidate metabolites and proteins whose altered quantitative profiles may underlie salt-sensitivity, sphingosine signalling and BP regulation in SHRSP. Validation and functional characterisation of these candidates and the implicated pathways is the essential step before any further translational studies are curried out in humans. One major finding of our study, which could be correlated to a GWAS discovery in humans, is the differential protein expression levels of NPR3 in SHRSP. The largest GWAS meta-analysis of >200.000 human subjects identified *NPR3 - C5orf23* as one of the 29 loci harbouring validated SNPs associated with systolic BP (Ehret, 2011). Therefore, further work needs to be prioritised towards the elucidation of the pathways linking NPR3 and HTN. Particular focus should be placed on pathways implicated in regulation of vascular reactivity in resistance arteries, based on the results from our vessel-myography functional studies and the knowledge that CNP has been identified as a potential EDHF in vasodilation (Chauhan et al., 2003). However, it should be kept in mind that translating results from animal models into human HTN has proven challenging. The best maybe example coming from GWAS studies, to this day, is uromodulin (*UMOD*), whose discovery in humans was extended to a *umod* KO

mouse model, identifying a novel pathway linking UMOD, sodium homeostasis, and HTN (Graham et al., 2014). Moreover, the challenge of multiple causative genes mapping to a single GWAS locus, making genetic dissection of the polygenic trait of HTN more complex, needs to be circumvented. Recent studies, have shown phenotypic contributions of the five out of six genes within the *AGTRAP-PLOD1* GWAS locus (Johnson et al., 2011) on CVD phenotypes in a rat model of HTN, many of which were previously unattainable in the human population. The approach used was introduction of mutations to each of the genes within the locus. (Flister et al., 2013).

The fact that GWAS studies have been unable to identify genetic variants of relatively large influence on physiologic responses in HTN, can be attributed to multifactorial determination of expression of such traits, as discussed above, and compensatory mechanisms. Transcriptional regulation, protein post-translational modifications (PTM) and protein-protein interactions could either alter or abolish the function of proteins encoded by GWAS candidate genes. Altered protein function could in turn lead to dramatic changes in the metabolite profile of cells, tissues, organs and to an ultimately changed phenotype. The potential regulatory interactions across the different layers of information in a biological system are illustrated in Figure 7-1A. Integration of large 'omics' datasets appears to be the next step in studying causal relationships between genes and phenotypic endpoints. A growing number of studies support the importance of this integrative approach by demonstrating direct functional links between GWAS variants, quantitative metabolic traits and an end-point of cardiovascular diseases and identifying new underlying biological processes and pathways (Illig et al., 2010, Suhre et al., 2011, Kettunen et al., 2012). In this light, the recent generation of SHRSP and WKY genome sequence (Glasgow strains) permits integration of transcriptomic with our proteomic and metabolomic studies, towards the investigation of the pathophysiology of EH in the SHRSP (Atanur et al., 2013). Rapid and continuous development of platforms such as Ingenuity Pathway Analysis (IPA) allow for quantitative data integration in cells, tissues or biofluids. Curated knowledge databases are used for generation of networks and pathway mapping, which improve the understanding of causal network connections across diseases, genes, upstream regulators and intermediate metabolic traits. Implementing an integrative approach of high-throughput analyses (Geiger et al., 2010, Maier et al., 2013) could lead to identification of genetic variants, signalling pathways and metabolic processes that are altered in human disease. (Figure 7-1B)

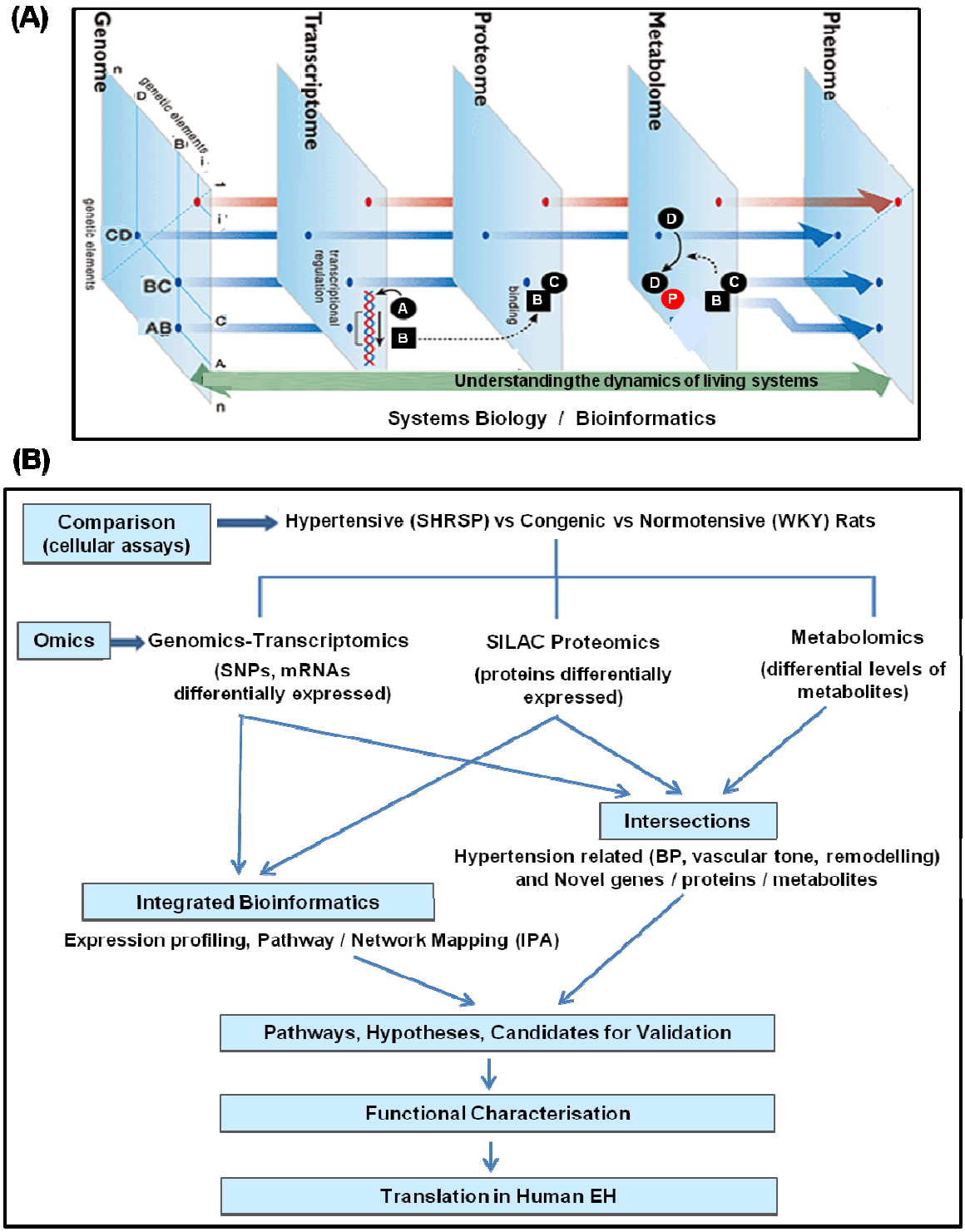


**Figure 7-1 - Data integration across the various layers of information. (A) High-level view of biological information flow from expression of genes to expression of phenotypes, via the multiple 'omics' levels of regulation. Adapted from Genomics Sciences Research Complex. (B) Simplified schematic of how information from our proteomic and metabolomic studies could be integrated, on IPA, with existing genomic and tanscriptomic data, towards identification of candidate gene/proteins/metabolites/pathways for further functional validation and generation of new hypotheses. Assessment of if and how such findings translate in human EH could lead to a better understanding of the disease pathophysiology and lead to generation of new therapeutic targets.**

Using systems biology tools, data integration could feed into reconstruction of dynamic networks with increasing reliability. Moving from working on individual molecules to work on networks, which constitute functional processes that link genetic and biochemical incidents with biological phenotypes, provide holistic information on living systems. Mathematical modelling of network maps provides the means to predict the emergent properties of complex systems, such as biological systems, by using sets of mathematical rules describing interactions of molecular components (Calder et al., 2010). Combination of dynamic network maps with models simulating their mean behaviour allows rigorous predictions of the output to specific stimuli, as well as validation of experimental data. Applying the predicted models in patho-biological systems at the molecular, cellular, tissue/organ and whole animal levels facilitate discovery of novel mechanistic pathways and predict the best points at which to intervene to redress the balance.

Irrespective of how informative robust 'omics' characterisations can be, they still pose big challenges during data analysis and interpretation, due to the high technical and biological variability as well as complexity of the samples. A simple, basic strategy to ensure reproducibility and increase confidence is the use of large numbers (>10) of replicates (biological, technical, analytical) in every experimental design (Jankevics et al., 2011). A weak point of our work was the small numbers of replicates (N=4) included in our metabolomic studies, which may explain the substantial variability observed within groups. Another challenge in the application of highly sensitive and automated technologies in 'omics' studies has been the identification of false-positives. To circumvent such issues, data normalisation, multiple testing analyses and the use of appropriate statistical tests are crucial for detection of statistically significant signals. However, in-house packages used in this study were under constant development, which made the data analysis process long and exigent. A limitation of IDEOM, in the case of the metabolomics analysis, was the use of t-test statistical filtering for such a large number of comparisons, which may have led to identification of false-positive, as it does not account for multiple testing. Therefore, the statistically significant results were always confirmed through reviewing of the original raw data. A more appropriate statistical test for such large datasets would be the Rank Products (RP) non-parametric statistical test (Breitling et al., 2004). RP is based on ranks of fold changes and multiple testing, using false discovery rate (FDR) significance cut-off, and is about to be implemented in the next versions of IDEOM. Furthermore, the limited ability of a single analytical platform to screen for the global, highly diverse metabolome makes the use of

multi-platform approaches demanding, towards the characterisation of complex diseases like EH (Mandal et al., 2012, Suhre et al., 2010, Naz et al., 2013). Moreover, due to the fact that several chronic diseases are characterised by altered lipid metabolic profile, including CVD, there is a growing interest in the area of shotgun lipidomics (Min et al., 2011, Han et al., 2011). In the case of proteomics analysis, the imperfect overlap of identifications from different search engines, which is reflected on partial overlap of results from different quantification algorithms (Searle et al., 2008, Yu et al., 2010), limits an even more robust protein identification. In addition, we still need to understand the issues MaxQuant presented during the processing of the triple-labelling SILAC datasets. As several new versions of MaxQuant have been released since our analysis, it would be worthwhile re-processing our proteomic data. Another challenge in proteomics analysis is the validation of findings through western blot (WB). The fact that our SILAC-proteomics results were not reproducible by WB could be attributed to the small number of WB replicates, the small magnitude of protein FC or the sensitivity and specificity of the antibodies. However, it is important to stress that, despite generally increased sensitivity of antibodies, the inherent variability in a WB makes the technique less accurate and reliable, and only substantial MS changes can be confirmed. Moreover, in WB only a single signal-band is quantified, whereas MS methods measure several individual peptides per quantified protein and generate independent measurements, thus increasing the accuracy of the mean (relative) quantification. Therefore WB is seriously questioned as a validation method for MS results and maybe reproducibility and consistency of the results across multiple replicates is the answer to validity.

In conclusion, this study combined MS-based (semi-)quantitative proteomics and metabolomics approaches with congenic strains, to improve our understanding on fundamental pathophysiological processes underlying HTN in SHRSP. Despite big challenges in the data analysis process, this work identified altered quantitative profiles of molecules and processes in health and disease, which once integrated with data from 'omics' studies at the gene level will set the basis for generation of new testable hypothesis, aiming to elucidate the underpinning molecular mechanisms of these processes. Furthermore, findings from our proteomic and metabolomic analyses that are associated with GWAS genetic loci could potentially identify novel pathways which would be translated into new drug therapies for human EH.

# 8 References


AALKJAER, C., HEAGERTY, A. M., PETERSEN, K. K., SWALES, J. D. & MULVANY, M. J. 1987. Evidence for increased media thickness, increased neuronal amine uptake, and depressed excitation--contraction coupling in isolated resistance vessels from essential hypertensives. *Circ Res,* 61**,** 181-6.

ABDEL-SAYED, S., NUSSBERGER, J., AUBERT, J. F., GOHLKE, P., BRUNNER, H. R. & BRAKCH, N. 2003. Measurement of plasma endothelin-1 in experimental hypertension and in healthy subjects. *Am J Hypertens,* 16**,** 515-21.

AEBERSOLD, R. & MANN, M. 2003. Mass spectrometry-based proteomics. *Nature,* 422**,** 198-207.

AGABITI-ROSEI, E., HEAGERTY, A. M. & RIZZONI, D. 2009. Effects of antihypertensive treatment on small artery remodelling. *J Hypertens,* 27**,** 1107-14.

ALENCAR, J. L., LOBYSHEVA, I., GEFFARD, M., SARR, M., SCHOTT, C., SCHINI-KERTH, V. B., NEPVEU, F., STOCLET, J. C. & MULLER, B. 2003. Role of S-nitrosation of cysteine residues in long-lasting inhibitory effect of nitric oxide on arterial tone. *Mol Pharmacol,* 63**,** 1148-58.

ALLENDE, M. L. & PROIA, R. L. 2002. Sphingosine-1-phosphate receptors and the development of the vascular system. *Biochim Biophys Acta,* 1582**,** 222-7.

ANDERSEN, J. S., LAM, Y. W., LEUNG, A. K. L., ONG, S.-E., LYON, C. E., LAMOND, A. I. & MANN, M. 2005. Nucleolar proteome dynamics. *Nature,* 433**,** 77-83.

ANWAR, M. A., FORD, W. R., BROADLEY, K. J. & HERBERT, A. A. 2012. Vasoconstrictor and vasodilator responses to tryptamine of rat-isolated perfused mesentery: comparison with tyramine and beta-phenylethylamine. *Br J Pharmacol,* 165**,** 2191-202.

ARITA, M. 2009. What can metabolomics learn from genomics and proteomics? *Current Opinion in Biotechnology,* 20**,** 610-615.

ARIYARAJAH, A., PALIJAN, A., DUTIL, J., PRITHIVIRAJ, K., DENG, Y. & DENG, A. Y. 2004. Dissecting quantitative trait loci into opposite blood pressure effects on Dahl rat chromosome 8 by congenic strains. *J Hypertens,* 22**,** 1495-502.

ARRIBAS, S. M., HILLIER, C., GONZÁLEZ, C., MCGRORY, S., DOMINICZAK, A. F. & MCGRATH, J. C. 1997. Cellular Aspects of Vascular Remodeling in Hypertension Revealed by Confocal Microscopy. *Hypertension,* 30**,** 1455-1464.

ARTWOHL, M., RODEN, M., WALDHAUSL, W., FREUDENTHALER, A. & BAUMGARTNER-PARZER, S. M. 2004. Free fatty acids trigger apoptosis and inhibit cell cycle progression in human vascular endothelial cells. *FASEB J,* 18**,** 146-8.

ASANO, T., IKEGAKI, I., SATOH, S., SUZUKI, Y., SHIBUYA, M., TAKAYASU, M. & HIDAKA, H. 1987. Mechanism of action of a novel antivasospasm drug, HA1077. *J Pharmacol Exp Ther,* 241, 1033-1040.

ATANUR, S. S., DIAZ, A. G., MARATOU, K., SARKIS, A., ROTIVAL, M., GAME, L., TSCHANNEN, M. R., KAISAKI, P. J., OTTO, G. W., MA, M. C., KEANE, T. M., HUMMEL, O., SAAR, K., CHEN, W., GURYEV, V., GOPALAKRISHNAN, K., GARRETT, M. R., JOE, B., CITTERIO, L., BIANCHI, G., MCBRIDE, M., DOMINICZAK, A., ADAMS, D. J., SERIKAWA, T., FLICEK, P., CUPPEN, E., HUBNER, N., PETRETTO, E., GAUGUIER, D., KWITEK, A., JACOB, H. & AITMAN, T. J. 2013. Genome sequencing reveals loci under artificial selection that underlie disease phenotypes in the laboratory rat. *Cell,* 154**,** 691-703.

AWAD, A. S., YE, H., HUANG, L., LI, L., FOSS, F. W., MACDONALD, T. L., LYNCH, K. R. & OKUSA, M. D. 2006. Selective sphingosine 1-phosphate 1 receptor activation reduces ischemia-reperfusion injury in mouse kidney. *American Journal of Physiology - Renal Physiology,* 290**,** F1516-F1524.

BARDERAS, M. G., LABORDE, C. M., POSADA, M., DE LA CUESTA, F., ZUBIRI, I., VIVANCO, F. & ALVAREZ-LLAMAS, G. 2011. Metabolomic profiling for identification of novel potential biomarkers in cardiovascular diseases. *J Biomed Biotechnol,* 2011**,** 790132.

BARTON, M., BENY, J. L., D'USCIO, L. V., WYSS, T., NOLL, G. & LUSCHER, T. F. 1998. Endothelium-independent relaxation and hyperpolarization to C-type natriuretic peptide in porcine coronary arteries. *J Cardiovasc Pharmacol,* 31**,** 377-83.

BAUMBACH, G. L. & Heistad, D. D. 1989. Remodeling of cerebral arterioles in chronic hypertension. *Hypertension,* 13, 968-972.

BEDIR, A., ARIK, N., ADAM, B., KILINC, K., GUMUS, T. & GUNER, E. 1999. Angiotensin converting enzyme gene polymorphism and activity in Turkish patients with essential hypertension. *Am J Hypertens,* 12**,** 1038-43.

BEEKS, E., KESSELS, A. G., KROON, A. A., VAN DER KLAUW, M. M. & DE LEEUW, P. W. 2004. Genetic predisposition to salt-sensitivity: a systematic review. *J Hypertens,* 22**,** 1243-9.

BENJAFIELD, A. V. & MORRIS, B. J. 2000. Association analyses of endothelial nitric oxide synthase gene polymorphisms in essential hypertension. *Am J Hypertens,* 13**,** 994-8.

BLAGOEV, B., KRATCHMAROVA, I., ONG, S.-E., NIELSEN, M., FOSTER, L. J. & MANN, M. 2003. A proteomics strategy to elucidate functional protein-protein interactions applied to EGF signaling. *Nat Biotech,* 21**,** 315-318.

BLAGOEV, B., ONG, S.-E., KRATCHMAROVA, I. & MANN, M. 2004. Temporal analysis of phosphotyrosine-dependent signaling networks by quantitative proteomics. *Nat Biotech,* 22**,** 1139-1145.

BLAUSTEIN, M. P., LEENEN, F. H., CHEN, L., GOLOVINA, V. A., HAMLYN, J. M., PALLONE, T. L., VAN HUYSSE, J. W., ZHANG, J. & WIER, W. G. 2012. How NaCl raises blood pressure: a new paradigm for the pathogenesis of salt-dependent hypertension. *Am J Physiol Heart Circ Physiol,* 302**,** H1031-49.

BLEKHERMAN, G., LAUBENBACHER, R., CORTES, D. F., MENDES, P., TORTI, F. M., AKMAN, S., TORTI, S. V. & SHULAEV, V. 2011. Bioinformatics tools for cancer metabolomics. *Metabolomics,* 7**,** 329-343.

BOHLEN, H. G. 1986. Localization of vascular resistance changes during hypertension. *Hypertension,* 8**,** 181-183.

BOLICK, D. T., SRINIVASAN, S., KIM, K. W., HATLEY, M. E., CLEMENS, J. J., WHETZEL, A., FERGER, N., MACDONALD, T. L., DAVIS, M. D., TSAO, P. S., LYNCH, K. R. & HEDRICK, C. C. 2005. Sphingosine-1-phosphate prevents tumor necrosis factor-{alpha}-mediated monocyte adhesion to aortic endothelium in mice. *Arterioscler Thromb Vasc Biol,* 25**,** 976-81.

BOLZ, S. S., VOGEL, L., SOLLINGER, D., DERWAND, R., BOER, C., PITSON, S. M., SPIEGEL, S. & POHL, U. 2003. Sphingosine kinase modulates microvascular tone and myogenic responses through activation of RhoA/Rho kinase. *Circulation,* 108**,** 342-7.

BORDERS, J. L. & GRANGER, H. J. 1986. Power dissipation as a measure of peripheral resistance in vascular networks. *Hypertension,* 8**,** 184-191.

BREITLING, R., ARMENGAUD, P., AMTMANN, A. & HERZYK, P. 2004. Rank products: a simple, yet powerful, new method to detect differentially regulated genes in replicated microarray experiments. *FEBS Letters,* 573**,** 83-92.

BREITLING, R., PITT, A. R. & BARRETT, M. P. 2006. Precision mapping of the metabolome. *Trends in Biotechnology,* 24**,** 543-548.

BREITLING, R., VITKUP, D. & BARRETT, M. P. 2008. New surveyor tools for charting microbial metabolic maps. *Nat Rev Micro,* 6**,** 156-161.

BRINDLE, J. T., ANTTI, H., HOLMES, E., TRANTER, G., NICHOLSON, J. K., BETHELL, H. W., CLARKE, S., SCHOFIELD, P. M., McKILLIGIN, E., MOSEDALE, D. E. & GRAINGER, D. J. 2002. Rapid and noninvasive diagnosis of the presence and severity of coronary heart disease using 1H-NMR-based metabonomics. *Nat Med,* 8, 1439-44.

BRIONES, A. M., GONZALEZ, J. M., SOMOZA, B., GIRALDO, J., DALY, C. J., VILA, E., GONZALEZ, M. C., MCGRATH, J. C. & ARRIBAS, S. M. 2003. Role of elastin in spontaneously hypertensive rat small mesenteric artery remodelling. *J Physiol,* 552**,** 185-95.

BRIONES, A. M., RODRIGUEZ-CRIADO, N., HERNANZ, R., GARCIA-REDONDO, A. B., RODRIGUES-DIEZ, R. R., ALONSO, M. J., EGIDO, J., RUIZ-ORTEGA, M. & SALAICES, M. 2009. Atorvastatin prevents angiotensin II-induced vascular remodeling and oxidative stress. *Hypertension,* 54**,** 142-9.

BRIONES, A. M., SALAICES, M. & VILA, E. 2007. Mechanisms Underlying Hypertrophic Remodeling and Increased Stiffness of Mesenteric Resistance Arteries From Aged Rats. *The Journals of Gerontology Series A: Biological Sciences and Medical Sciences,* 62**,** 696-706.

BROWN, M., DUNN, W. B., DOBSON, P., PATEL, Y., WINDER, C. L., FRANCIS-MCINTYRE, S., BEGLEY, P., CARROLL, K., BROADHURST, D., TSENG, A., SWAINSTON, N., SPASIC, I., GOODACRE, R. & KELL, D. B. 2009. Mass spectrometry tools and metabolite-specific databases for molecular identification in metabolomics. *Analyst,* 134**,** 1322-32.

BUUS, N. H., BOTTCHER, M., JORGENSEN, C. G., CHRISTENSEN, K. L., THYGESEN, K., NIELSEN, T. T. & MULVANY, M. J. 2004. Myocardial perfusion during long-term angiotensin-converting enzyme inhibition or beta-blockade in patients with essential hypertension. *Hypertension,* 44**,** 465-70.

CALDER, M., GILMORE, S., HILLSTON, J. & VYSHEMIRSKY, V. 2010. *Formal Methods for Biochemical Signalling Pathways,* Godalming, Springer-Verlag London Ltd.

CAMPBELL, J. H., TACHAS, G., BLACK, M. J., COCKERILL, G. & CAMPBELL, G. R. 1991. Molecular biology of vascular hypertrophy. *Basic Res Cardiol,* 86 Suppl 1**,** 3-11.

CARRETERO, O. A. & OPARIL, S. 2000. Essential Hypertension: Part I: Definition and Etiology. *Circulation,* 101**,** 329-335.

CAULFIELD, M., MUNROE, P., PEMBROKE, J., SAMANI, N., DOMINICZAK, A., BROWN, M., BENJAMIN, N., WEBSTER, J., RATCLIFFE, P., O'SHEA, S., PAPP, J., TAYLOR, E., DOBSON, R., KNIGHT, J., NEWHOUSE, S., HOOPER, J., LEE, W., BRAIN, N., CLAYTON, D., LATHROP, G. M., FARRALL, M. & CONNELL, J. 2003. Genome-wide mapping of human loci for essential hypertension. *Lancet,* 361**,** 2118-23.

CAZIER, J. B., KAISAKI, P. J., ARGOUD, K., BLAISE, B. J., VESELKOV, K., EBBELS, T. M., TSANG, T., WANG, Y., BIHOREAU, M. T., MITCHELL, S. C., HOLMES, E. C., LINDON, J. C., SCOTT, J., NICHOLSON, J. K., DUMAS, M. E. & GAUGUIER, D. 2012. Untargeted metabolome quantitative trait locus mapping associates variation in urine glycerate to mutant glycerate kinase. *J Proteome Res,* 11**,** 631-42.

CHAN, C. K., MAK, J. C., MAN, R. Y. & VANHOUTTE, P. M. 2009. Rho kinase inhibitors prevent endothelium-dependent contractions in the rat aorta. *J Pharmacol Exp Ther,* 329**,** 820-6.

CHAN, S. Y., MANCINI, G. B., KURAMOTO, L., SCHULZER, M., FROHLICH, J. & IGNASZEWSKI, A. 2003. The prognostic importance of endothelial dysfunction and carotid atheroma burden in patients with coronary artery disease. *J Am Coll Cardiol,* 42**,** 1037-43.

CHATAIGNEAU, T., FELETOU, M., HUANG, P. L., FISHMAN, M. C., DUHAULT, J. & VANHOUTTE, P. M. 1999. Acetylcholine-induced relaxation in blood vessels from endothelial nitric oxide synthase knockout mice. *Br J Pharmacol,* 126**,** 219-26.

CHAUHAN, S. D., NILSSON, H., AHLUWALIA, A. & HOBBS, A. J. 2003. Release of C-type natriuretic peptide accounts for the biological activity of endothelium-derived hyperpolarizing factor. *Proceedings of the National Academy of Sciences,* 100**,** 1426-1431.

CHEN, X., MOECKEL, G., MORROW, J. D., COSGROVE, D., HARRIS, R. C., FOGO, A. B., ZENT, R. & POZZI, A. 2004. Lack of Integrin α1β1 Leads to Severe Glomerulosclerosis after Glomerular Injury. *The American Journal of Pathology,* 165**,** 617-630.

CHEN, X., TOUYZ, R. M., PARK, J. B. & SCHIFFRIN, E. L. 2001. Antioxidant effects of vitamins C and E are associated with altered activation of vascular NADPH oxidase and superoxide dismutase in stroke-prone SHR. *Hypertension,* 38**,** 606-11.

CHOBANIAN, A. V., BAKRIS, G. L., BLACK, H. R., CUSHMAN, W. C., GREEN, L. A., IZZO, J. L., JR., JONES, D. W., MATERSON, B. J., OPARIL, S., WRIGHT, J. T., JR., ROCCELLA, E. J., JOINT NATIONAL COMMITTEE ON PREVENTION, D. E., TREATMENT OF HIGH BLOOD PRESSURE. NATIONAL HEART, L., BLOOD, I. & NATIONAL HIGH BLOOD PRESSURE EDUCATION PROGRAM COORDINATING, C. 2003. Seventh report of the Joint National Committee on Prevention, Detection, Evaluation, and Treatment of High Blood Pressure. *Hypertension,* 42**,** 1206-52.

CLARK, J. S., JEFFS, B., DAVIDSON, A. O., LEE, W. K., ANDERSON, N. H., BIHOREAU, M. T., BROSNAN, M. J., DEVLIN, A. M., KELMAN, A. W., LINDPAINTNER, K. & DOMINICZAK, A. F. 1996. Quantitative trait loci in genetically hypertensive rats. Possible sex specificity. *Hypertension,* 28**,** 898-906.

CLEMITSON, J. R., DIXON, R. J., HAINES, S., BINGHAM, A. J., PATEL, B. R., HALL, L., LO, M., SASSARD, J., CHARCHAR, F. J. & SAMANI, N. J. 2007. Genetic dissection of a blood pressure quantitative trait locus on rat chromosome 1 and gene expression analysis identifies SPON1 as a novel candidate hypertension gene. *Circ Res,* 100**,** 992-9.

COUSSIN, F., SCOTT, R. H., WISE, A. & NIXON, G. F. 2002. Comparison of Sphingosine 1-Phosphate–Induced Intracellular Signaling Pathways in Vascular Smooth Muscles: Differential Role in Vasoconstriction. *Circulation Research,* 91**,** 151-157.

COWLEY, A. W., JR. 2006. The genetic dissection of essential hypertension. *Nat Rev Genet,* 7**,** 829-40.

COX, J. & MANN, M. 2008. MaxQuant enables high peptide identification rates, individualized p.p.b.-range mass accuracies and proteome-wide protein quantification. *Nat Biotech,* 26**,** 1367-1372.

COX, J., MATIC, I., HILGER, M., NAGARAJ, N., SELBACH, M., OLSEN, J. V. & MANN, M. 2009. A practical guide to the MaxQuant computational platform for SILAC-based quantitative proteomics. *Nat Protoc,* 4**,** 698-705.

COX, J., NEUHAUSER, N., MICHALSKI, A., SCHELTEMA, R. A., OLSEN, J. V. & MANN, M. 2011. Andromeda: a peptide search engine integrated into the MaxQuant environment. *J Proteome Res,* 10**,** 1794-805.

CRABTREE, M. J., TATHAM, A. L., HALE, A. B., ALP, N. J. & CHANNON, K. M. 2009. Critical Role for Tetrahydrobiopterin Recycling by Dihydrofolate Reductase in Regulation of Endothelial Nitric-oxide Synthase Coupling: RELATIVE IMPORTANCE OF THE DE NOVO BIOPTERIN SYNTHESIS VERSUS SALVAGE PATHWAYS. *Journal of Biological Chemistry,* 284**,** 28128-28136.

CRAVATT, B. F., SIMON, G. M. & YATES III, J. R. 2007. The biological impact of mass-spectrometry-based proteomics. *Nature,* 450**,** 991-1000.

CREEK, D. J., JANKEVICS, A., BURGESS, K. E., BREITLING, R. & BARRETT, M. P. 2012. IDEOM: an Excel interface for analysis of LC-MS-based metabolomics data. *Bioinformatics,* 28**,** 1048-9.

CUBBON, S., ANTONIO, C., WILSON, J. & THOMAS-OATES, J. 2010. Metabolomic applications of HILIC–LC–MS. *Mass Spectrometry Reviews,* 29**,** 671-684.

DAI, Y.-P., BONGALON, S., TIAN, H., PARKS, S. D., MUTAFOVA-YAMBOLIEVA, V. N. & YAMBOLIEV, I. A. 2006. Upregulation of profilin, cofilin-2 and LIMK2 in cultured pulmonary artery smooth muscle cells and in pulmonary arteries of monocrotaline-treated rats. *Vascular Pharmacology,* 44**,** 275-282.

DAMIRIN, A., TOMURA, H., KOMACHI, M., TOBO, M., SATO, K., MOGI, C., NOCHI, H., TAMOTO, K. & OKAJIMA, F. 2005. Sphingosine 1-phosphate receptors mediate the lipid-induced cAMP accumulation through cyclooxygenase-2/prostaglandin I2 pathway in human coronary artery smooth muscle cells. *Mol Pharmacol,* 67**,** 1177-85.

DASKALOPOULOU, S. S., KHAN, N. A., QUINN, R. R., RUZICKA, M., MCKAY, D. W., HACKAM, D. G., RABKIN, S. W., RABI, D. M., GILBERT, R. E., PADWAL, R. S., DAWES, M., TOUYZ, R. M., CAMPBELL, T. S., CLOUTIER, L., GROVER, S., HONOS, G., HERMAN, R. J., SCHIFFRIN, E. L., BOLLI, P., WILSON, T., FELDMAN, R. D., LINDSAY, M. P., HEMMELGARN, B. R., HILL, M. D., GELFER, M., BURNS, K. D., VALLEE, M., PRASAD, G. V., LEBEL, M., MCLEAN, D., ARNOLD, J. M., MOE, G. W., HOWLETT, J. G., BOULANGER, J. M., LAROCHELLE, P., LEITER, L. A., JONES, C., OGILVIE, R. I., WOO, V., KACZOROWSKI, J., TRUDEAU, L., BACON, S. L., PETRELLA, R. J., MILOT, A., STONE, J. A., DROUIN, D., LAMARRE-CLICHE, M., GODWIN, M., TREMBLAY, G., HAMET, P., FODOR, G., CARRUTHERS, S. G., PYLYPCHUK, G., BURGESS, E., LEWANCZUK, R., DRESSER, G. K., PENNER, B., HEGELE, R. A., MCFARLANE, P. A., SHARMA, M., CAMPBELL, N. R., REID, D., POIRIER, L. & TOBE, S. W. 2012. The 2012 Canadian hypertension education program recommendations for the management of hypertension: blood pressure measurement, diagnosis, assessment of risk, and therapy. *Can J Cardiol,* 28**,** 270-87.

DATLA, S. R., DUSTING, G. J., MORI, T. A., TAYLOR, C. J., CROFT, K. D. & JIANG, F. 2007. Induction of heme oxygenase-1 in vivo suppresses NADPH oxidase derived oxidative stress. *Hypertension,* 50**,** 636-42.

DAVIGNON, J. & GANZ, P. 2004. Role of endothelial dysfunction in atherosclerosis. *Circulation,* 109**,** III27-32.

DE ARAUJO, M., ANDRADE, L., COIMBRA, T. M., RODRIGUES, A. C., JR. & SEGURO, A. C. 2005. Magnesium supplementation combined with N-acetylcysteine protects against postischemic acute renal failure. *J Am Soc Nephrol,* 16**,** 3339-49.

DE GODOY, L. M., OLSEN, J. V., COX, J., NIELSEN, M. L., HUBNER, N. C., FROHLICH, F., WALTHER, T. C. & MANN, M. 2008. Comprehensive mass-spectrometry-based proteome quantification of haploid versus diploid yeast. *Nature,* 455**,** 1251-4.

DE HOOG, C. L., FOSTER, L. J. & MANN, M. 2004. RNA and RNA Binding Proteins Participate in Early Stages of Cell Spreading through Spreading Initiation Centers. *Cell,* 117**,** 649-662.

DE VOS, R. C. H., MOCO, S., LOMMEN, A., KEURENTJES, J. J. B., BINO, R. J. & HALL, R. D. 2007. Untargeted large-scale plant metabolomics using liquid chromatography coupled to mass spectrometry. *Nat. Protocols,* 2**,** 778-791.

DENG, L. Y. & SCHIFFRIN, E. L. 1991. Morphological and functional alterations of mesenteric small resistance arteries in early renal hypertension in rats. *American Journal of Physiology - Heart and Circulatory Physiology,* 261**,** H1171-H1177.

DEUTSCHMAN, D. H., CARSTENS, J. S., KLEPPER, R. L., SMITH, W. S., PAGE, M. T., YOUNG, T. R., GLEASON, L. A., NAKAJIMA, N. & SABBADINI, R. A. 2003. Predicting obstructive coronary artery disease with serum sphingosine-1-phosphate. *Am Heart J,* 146**,** 62-8.

DOGGRELL, S. A. & BROWN, L. 1998. Rat models of hypertension, cardiac hypertrophy and failure. *Cardiovasc Res,* 39**,** 89-105.

DOMON, B. & AEBERSOLD, R. 2006. Mass spectrometry and protein analysis. *Science,* 312**,** 212-7.

DONALD, S. P., SUN, X. Y., HU, C. A., YU, J., MEI, J. M., VALLE, D. & PHANG, J. M. 2001. Proline oxidase, encoded by p53-induced gene-6, catalyzes the generation of proline-dependent reactive oxygen species. *Cancer Res,* 61**,** 1810-5.

DORNAS, W. C. & SILVA, M. E. 2011. Animal models for the study of arterial hypertension. *J Biosci,* 36**,** 731-7.

DUBROCA, C., LOYER, X., RETAILLEAU, K., LOIRAND, G., PACAUD, P., FERON, O., BALLIGAND, J.-L., LÉVY, B. I., HEYMES, C. & HENRION, D. 2007. RhoA activation and interaction with Caveolin-1 are critical for pressure-induced myogenic tone in rat mesenteric resistance arteries. *Cardiovascular Research,* 73**,** 190-197.

DUFFY, S. J., KEANEY, J. F., JR., HOLBROOK, M., GOKCE, N., SWERDLOFF, P. L., FREI, B. & VITA, J. A. 2001. Short- and long-term black tea consumption reverses endothelial dysfunction in patients with coronary artery disease. *Circulation,* 104**,** 151-6.

DUNN, W. B., BROADHURST, D. I., ATHERTON, H. J., GOODACRE, R. & GRIFFIN, J. L. 2011. Systems level studies of mammalian metabolomes: the roles of mass spectrometry and nuclear magnetic resonance spectroscopy. *Chem Soc Rev,* 40**,** 387-426.

DURANTE, W., LIAO, L., PEYTON, K. J. & SCHAFER, A. I. 1998. Thrombin stimulates vascular smooth muscle cell polyamine synthesis by inducing cationic amino acid transporter and ornithine decarboxylase gene expression. *Circ Res,* 83**,** 217-23.

DURANTE, W., LIAO, L., REYNA, S. V., PEYTON, K. J. & SCHAFER, A. I. 2001. Transforming growth factor-beta(1) stimulates L-arginine transport and metabolism in vascular smooth muscle cells: role in polyamine and collagen synthesis. *Circulation,* 103**,** 1121-7.

EDSALL, L. C., VAN BROCKLYN, J. R., CUVILLIER, O., KLEUSER, B. & SPIEGEL, S. 1998. N,N-Dimethylsphingosine is a potent competitive inhibitor of sphingosine kinase but not of protein kinase C: modulation of cellular levels of sphingosine 1-phosphate and ceramide. *Biochemistry,* 37**,** 12892-8.

EGUCHI, S., DEMPSEY, P. J., FRANK, G. D., MOTLEY, E. D. & INAGAMI, T. 2001. Activation of MAPKs by angiotensin II in vascular smooth muscle cells. Metalloprotease-dependent EGF receptor activation is required for activation of ERK and p38 MAPK but not for JNK. *J Biol Chem,* 276**,** 7957-62.

EHRET, G. B. M. P., RICE KM, BOCHUD M, JOHNSON AD, CHASMAN DI, SMITH AV, TOBIN MD, VERWOERT GC, HWANG SJ, PIHUR V, VOLLENWEIDER P, O'REILLY PF, AMIN N, BRAGG-GRESHAM JL, TEUMER A, GLAZER NL, LAUNER L, ZHAO JH, AULCHENKO Y, HEATH S, SÕBER S, PARSA A, LUAN J, ARORA P, DEHGHAN A, ZHANG F, LUCAS G, HICKS AA, JACKSON AU, PEDEN JF, TANAKA T, WILD SH, RUDAN I, IGL W, MILANESCHI Y, PARKER AN, FAVA C, CHAMBERS JC, FOX ER, KUMARI M, GO MJ, VAN DER HARST P, KAO WH, SJÖGREN M, VINAY DG, ALEXANDER M, TABARA Y, SHAW-HAWKINS S, WHINCUP PH, LIU Y, SHI G, KUUSISTO J, TAYO B, SEIELSTAD M, SIM X, NGUYEN KD, LEHTIMÄKI T, MATULLO G, WU Y, GAUNT TR, ONLAND-MORET NC, COOPER MN, PLATOU CG, ORG E, HARDY R, DAHGAM S, PALMEN J, VITART V, BRAUND PS, KUZNETSOVA T, UITERWAAL CS, ADEYEMO A, PALMAS W, CAMPBELL H, LUDWIG B, TOMASZEWSKI M, TZOULAKI I, PALMER ND; CARDIOGRAM CONSORTIUM; CKDGEN CONSORTIUM; KIDNEYGEN CONSORTIUM; ECHOGEN CONSORTIUM; CHARGE-HF CONSORTIUM, ASPELUND T, GARCIA M, CHANG YP, O'CONNELL JR, STEINLE NI, GROBBEE DE, ARKING DE, KARDIA SL, MORRISON AC, HERNANDEZ D, NAJJAR S,

MCARDLE WL, HADLEY D, BROWN MJ, CONNELL JM, HINGORANI AD, DAY IN, LAWLOR DA, BEILBY JP, LAWRENCE RW, CLARKE R, HOPEWELL JC, ONGEN H, DREISBACH AW, LI Y, YOUNG JH, BIS JC, KÄHÖNEN M, VIIKARI J, ADAIR LS, LEE NR, CHEN MH, OLDEN M, PATTARO C, BOLTON JA, KÖTTGEN A, BERGMANN S, MOOSER V, CHATURVEDI N, FRAYLING TM, ISLAM M, JAFAR TH, ERDMANN J, KULKARNI SR, BORNSTEIN SR, GRÄSSLER J, GROOP L, VOIGHT BF, KETTUNEN J, HOWARD P, TAYLOR A, GUARRERA S, RICCERI F, EMILSSON V, PLUMP A, BARROSO I, KHAW KT, WEDER AB, HUNT SC, SUN YV, BERGMAN RN, COLLINS FS, BONNYCASTLE LL, SCOTT LJ, STRINGHAM HM, PELTONEN L, PEROLA M, VARTIAINEN E, BRAND SM, STAESSEN JA, WANG TJ, BURTON PR, SOLER ARTIGAS M, DONG Y, SNIEDER H, WANG X, ZHU H, LOHMAN KK, RUDOCK ME, HECKBERT SR, SMITH NL, WIGGINS KL, DOUMATEY A, SHRINER D, VELDRE G, VIIGIMAA M, KINRA S, PRABHAKARAN D, TRIPATHY V, LANGEFELD CD, ROSENGREN A, THELLE DS, CORSI AM, SINGLETON A, FORRESTER T, HILTON G, MCKENZIE CA, SALAKO T, IWAI N, KITA Y, OGIHARA T, OHKUBO T, OKAMURA T, UESHIMA H, UMEMURA S, EYHERAMENDY S, MEITINGER T, WICHMANN HE, CHO YS, KIM HL, LEE JY, SCOTT J, SEHMI JS, ZHANG W, HEDBLAD B, NILSSON P, SMITH GD, WONG A, NARISU N, STANČÁKOVÁ A, RAFFEL LJ, YAO J, KATHIRESAN S, O'DONNELL CJ, SCHWARTZ SM, IKRAM MA, LONGSTRETH WT JR, MOSLEY TH, SESHADRI S, SHRINE NR, WAIN LV, MORKEN MA, SWIFT AJ, LAITINEN J, PROKOPENKO I, ZITTING P, COOPER JA, HUMPHRIES SE, DANESH J, RASHEED A, GOEL A, HAMSTEN A, WATKINS H, BAKKER SJ, VAN GILST WH, JANIPALLI CS, MANI KR, YAJNIK CS, HOFMAN A, MATTACE-RASO FU, OOSTRA BA, DEMIRKAN A, ISAACS A, RIVADENEIRA F, LAKATTA EG, ORRU M, SCUTERI A, ALA-KORPELA M, KANGAS AJ, LYYTIKÄINEN LP, SOININEN P, TUKIAINEN T, WÜRTZ P, ONG RT, DÖRR M, KROEMER HK, VÖLKER U, VÖLZKE H, GALAN P, HERCBERG S, LATHROP M, ZELENIKA D, DELOUKAS P, MANGINO M, SPECTOR TD, ZHAI G, MESCHIA JF, NALLS MA, SHARMA P, TERZIC J, KUMAR MV, DENNIFF M, ZUKOWSKA-SZCZECHOWSKA E, WAGENKNECHT LE, FOWKES FG, CHARCHAR FJ, SCHWARZ PE, HAYWARD C, GUO X, ROTIMI C, BOTS ML, BRAND E, SAMANI NJ, POLASEK O, TALMUD PJ, NYBERG F, KUH D, LAAN M, HVEEM K, PALMER LJ, VAN DER SCHOUW YT, CASAS JP, MOHLKE KL, VINEIS P, RAITAKARI O, GANESH SK, WONG TY, TAI ES, COOPER RS, LAAKSO M, RAO DC, HARRIS TB, MORRIS RW, DOMINICZAK AF, KIVIMAKI M, MARMOT MG, MIKI T, SALEHEEN D, CHANDAK GR, CORESH J, NAVIS G, SALOMAA V, HAN BG, ZHU X, KOONER JS, MELANDER O, RIDKER PM, BANDINELLI S, GYLLENSTEN UB, WRIGHT AF, WILSON JF, FERRUCCI L, FARRALL M, TUOMILEHTO J, PRAMSTALLER PP, ELOSUA R, SORANZO N, SIJBRANDS EJ, ALTSHULER D, LOOS RJ, SHULDINER AR, GIEGER C, MENETON P, UITTERLINDEN AG, WAREHAM NJ, GUDNASON V, ROTTER JI, RETTIG R, UDA M, STRACHAN DP, WITTEMAN JC, HARTIKAINEN AL, BECKMANN JS, BOERWINKLE E, VASAN RS, BOEHNKE M, LARSON MG, JÄRVELIN MR, PSATY BM, ABECASIS GR, CHAKRAVARTI A, ELLIOTT P, VAN DUIJN CM, NEWTON-CHEH C, LEVY D, CAULFIELD MJ, JOHNSON T. 2011. Genetic variants in novel pathways influence blood pressure and cardiovascular disease risk. *Nature,* 478**,** 103-109.

ELLIOTT, J., CALLINGHAM, B. A. & SHARMAN, D. F. 1989. The influence of amine metabolizing enzymes on the pharmacology of tyramine in the isolated perfused mesenteric arterial bed of the rat. *Br J Pharmacol,* 98**,** 515-22.

ESCALANTE, B., SACERDOTI, D., DAVIDIAN, M. M., LANIADO-SCHWARTZMAN, M. & MCGIFF, J. C. 1991. Chronic treatment with tin normalizes blood pressure in spontaneously hypertensive rats. *Hypertension,* 17**,** 776-9.

FALLON, B. J., STEPHENS, N., TULIP, J. R. & HEAGERTY, A. M. 1995. Comparison of small artery sensitivity and morphology in pressurized and wire-mounted preparations. *Am J Physiol*, 268, H670-678.

FEHLER, M., BROADLEY, K. J., FORD, W. R. & KIDD, E. J. 2010. Identification of trace-amine-associated receptors (TAAR) in the rat aorta and their role in vasoconstriction by beta-phenylethylamine. *Naunyn Schmiedebergs Arch Pharmacol,* 382**,** 385-98.

FEIG, D. I., SOLETSKY, B. & JOHNSON, R. J. 2008. Effect of allopurinol on blood pressure of adolescents with newly diagnosed essential hypertension: a randomized trial. *JAMA,* 300**,** 924-32.

FELETOU, M., KOHLER, R. & VANHOUTTE, P. M. 2012. Nitric oxide: orchestrator of endothelium-dependent responses. *Ann Med,* 44**,** 694-716.

FELETOU, M., TANG, E. H. & VANHOUTTE, P. M. 2008. Nitric oxide the gatekeeper of endothelial vasomotor control. *Front Biosci,* 13**,** 4198-217.

FELETOU, M. & VANHOUTTE, P. M. 2009. EDHF: an update. *Clin Sci (Lond),* 117**,** 139-55.

FÉLÉTOU, M. & VANHOUTTE, P. M. 2006. Endothelial dysfunction: a multifaceted disorder (The Wiggers Award Lecture). *American Journal of Physiology - Heart and Circulatory Physiology,* 291**,** H985-H1002.

FENNELL, J. P., BROSNAN, M. J., FRATER, A. J., HAMILTON, C. A., ALEXANDER, M. Y., NICKLIN, S. A., HEISTAD, D. D., BAKER, A. H. & DOMINICZAK, A. F. 2002. Adenovirus-mediated overexpression of extracellular superoxide dismutase improves endothelial dysfunction in a rat model of hypertension. *Gene Ther,* 9**,** 110-7.

FERNANDEZ, M. L., WILSON, T. A., CONDE, K., VERGARA-JIMENEZ, M. & NICOLOSI, R. J. 1999. Hamsters and guinea pigs differ in their plasma lipoprotein cholesterol distribution when fed diets varying in animal protein, soluble fiber, or cholesterol content. *J Nutr,* 129**,** 1323-32.

FLISTER, M. J., TSAIH, S. W., O'MEARA, C. C., ENDRES, B., HOFFMAN, M. J., GEURTS, A. M., DWINELL, M. R., LAZAR, J., JACOB, H. J. & MORENO, C. 2013. Identifying multiple causative genes at a single GWAS locus. *Genome Res,* 23, 1996-2002.

FOLCH, J., LEES, M. & STANLEY, G. H. S. 1957. A SIMPLE METHOD FOR THE ISOLATION AND PURIFICATION OF TOTAL LIPIDES FROM ANIMAL TISSUES. *J Biol Chem, 226*, 497-509.

FOLKOW, B., GRIMBY, G, THULESIUS, O 1958. Adaptive structural changes of the vascular walls in hypertension and their relation to the control of peripheral resistance. . *Acta Physiologica Scandinavica,* 44**,** 255-272.

FOLKOW, B., ISAKSSON, O. P., KARLSTROM, G., LEVER, A. F. & NORDLANDER, M. 1988. The importance of hypophyseal hormones for structural cardiovascular adaptation in hypertension. *J Hypertens Suppl,* 6**,** S166-9.

FRANCESCHINI, N. & LE, T. 2013. Invited Review- Genetics of Hypertension: discoveries from the bench to human populations. *Am J Physiol Renal Physiol*.

FRANCESCHINI, N., REINER, A. P. & HEISS, G. 2011. Recent findings in the genetics of blood pressure and hypertension traits. *Am J Hypertens,* 24**,** 392-400.

FRANK, J. 2008. Managing hypertension using combination therapy. *Am Fam Physician,* 77**,** 1279-86.

FREIDJA, M. L., VESSIERES, E., CLERE, N., DESQUIRET, V., GUIHOT, A. L., TOUTAIN, B., LOUFRANI, L., JARDEL, A., PROCACCIO, V., FAURE, S. & HENRION, D. 2011. Heme oxygenase-1 induction restores high-blood-flow-dependent remodeling and endothelial function in mesenteric arteries of old rats. *J Hypertens,* 29**,** 102-12.

FUJII, Y., UEDA, Y., OHTAKE, H., ONO, N., TAKAYAMA, T., NAKAZAWA, K., IGARASHI, Y. & GOITSUKA, R. 2012. Blocking S1P interaction with S1P(1) receptor by a novel

competitive S1P(1)-selective antagonist inhibits angiogenesis. *Biochem Biophys Res Commun,* 419**,** 754-60.

FUKUDA, N., SATOH, C., HU, W.-Y., SOMA, M., KUBO, A., KISHIOKA, H., WATANABE, Y., IZUMI, Y. & KANMATSUSE, K. 1999. Production of Angiotensin II by Homogeneous Cultures of Vascular Smooth Muscle Cells From Spontaneously Hypertensive Rats. *Arteriosclerosis, Thrombosis, and Vascular Biology,* 19**,** 1210-1217.

GARCIA, D. E., BAIDOO, E. E., BENKE, P. I., PINGITORE, F., TANG, Y. J., VILLA, S. & KEASLING, J. D. 2008. Separation and mass spectrometry in microbial metabolomics. *Curr Opin Microbiol,* 11**,** 233-9.

GAVIN, A.-C., ALOY, P., GRANDI, P., KRAUSE, R., BOESCHE, M., MARZIOCH, M., RAU, C., JENSEN, L. J., BASTUCK, S., DUMPELFELD, B., EDELMANN, A., HEURTIER, M.-A., HOFFMAN, V., HOEFERT, C., KLEIN, K., HUDAK, M., MICHON, A.-M., SCHELDER, M., SCHIRLE, M., REMOR, M., RUDI, T., HOOPER, S., BAUER, A., BOUWMEESTER, T., CASARI, G., DREWES, G., NEUBAUER, G., RICK, J. M., KUSTER, B., BORK, P., RUSSELL, R. B. & SUPERTI-FURGA, G. 2006. Proteome survey reveals modularity of the yeast cell machinery. *Nature,* 440**,** 631-636.

GEIGER, T., COX, J. & MANN, M. 2010. Proteomic Changes Resulting from Gene Copy Number Variations in Cancer Cells. *PLoS Genet,* 6**,** e1001090.

GEIGER, T., MADDEN, S. F., GALLAGHER, W. M., COX, J. & MANN, M. 2012. Proteomic Portrait of Human Breast Cancer Progression Identifies Novel Prognostic Markers. *Cancer Research,* 72**,** 2428-2439.

GEIGER, T., WISNIEWSKI, J. R., COX, J., ZANIVAN, S., KRUGER, M., ISHIHAMA, Y. & MANN, M. 2011. Use of stable isotope labeling by amino acids in cell culture as a spike-in standard in quantitative proteomics. *Nat. Protocols,* 6**,** 147-157.

GHIADONI, L., TADDEI, S. & VIRDIS, A. 2012. Hypertension and endothelial dysfunction: therapeutic approach. *Curr Vasc Pharmacol,* 10**,** 42-60.

GIACHINI, F. R., CARNEIRO, F. S., LIMA, V. V., CARNEIRO, Z. N., DORRANCE, A., WEBB, R. C. & TOSTES, R. C. 2009. Upregulation of intermediate calcium-activated potassium channels counterbalance the impaired endothelium-dependent vasodilation in stroke-prone spontaneously hypertensive rats. *Transl Res,* 154**,** 183-93.

GINGRAS, A.-C., GSTAIGER, M., RAUGHT, B. & AEBERSOLD, R. 2007. Analysis of protein complexes using mass spectrometry. *Nat Rev Mol Cell Biol,* 8**,** 645-654.

GIOVANE, A., BALESTRIERI, A. & NAPOLI, C. 2008. New insights into cardiovascular and lipid metabolomics. *J Cell Biochem,* 105**,** 648-54.

GOLDBLATT, H., LYNCH, J., HANZAL, R. F. & SUMMERVILLE, W. W. 1934. STUDIES ON EXPERIMENTAL HYPERTENSION : I. THE PRODUCTION OF PERSISTENT ELEVATION OF SYSTOLIC BLOOD PRESSURE BY MEANS OF RENAL ISCHEMIA. *J Exp Med,* 59**,** 347-79.

GONZALEZ, J. M., BRIONES, A. M., SOMOZA, B., DALY, C. J., VILA, E., STARCHER, B., MCGRATH, J. C., GONZALEZ, M. C. & ARRIBAS, S. M. 2006. Postnatal alterations in elastic fiber organization precede resistance artery narrowing in SHR. *Am J Physiol Heart Circ Physiol,* 291**,** H804-12.

GOTO, K., FUJII, K., KANSUI, Y. & IIDA, M. 2004. Changes in endothelium-derived hyperpolarizing factor in hypertension and ageing: response to chronic treatment with renin-angiotensin system inhibitors. *Clin Exp Pharmacol Physiol,* 31**,** 650-5.

GRADIN, K. A., LI, J. Y., ANDERSSON, O. & SIMONSEN, U. 2003. Enhanced neuropeptide Y immunoreactivity and vasoconstriction in mesenteric small arteries from spontaneously hypertensive rats. *J Vasc Res,* 40**,** 252-65.

GRAHAM, D., HUYNH, N. N., HAMILTON, C. A., BEATTIE, E., SMITH, R. A., COCHEME, H. M., MURPHY, M. P. & DOMINICZAK, A. F. 2009. Mitochondria-targeted antioxidant

MitoQ10 improves endothelial function and attenuates cardiac hypertrophy. *Hypertension,* 54**,** 322-8.

GRAHAM, D., MCBRIDE, M. W., BRAIN, N. J. & DOMINICZAK, A. F. 2005. Congenic/consomic models of hypertension. *Methods Mol Med,* 108**,** 3-15.

GRAHAM, D., MCBRIDE, M. W., GAASENBEEK, M., GILDAY, K., BEATTIE, E., MILLER, W. H., MCCLURE, J. D., POLKE, J. M., MONTEZANO, A., TOUYZ, R. M. & DOMINICZAK, A. F. 2007. Candidate Genes That Determine Response to Salt in the Stroke-Prone Spontaneously Hypertensive Rat: Congenic Analysis. *Hypertension,* 50**,** 1134-1141.

GRAHAM, L. A., PADMANABHAN, S., FRAZER, N. J., KUMAR, S., BATES, J. M., RAFFI, H. S., WELSH, P., BEATTIE, W., HAO, S., LEH, S., HULTSTOM, M., FERRERI, N. R., DOMINICZAK, A. F., GRAHAM, D. & McBRIDE, M. W. 2014. Validation of uromodulin as a candidate gene for human essential hypertension. *Hypertension,* 63, 551-8.

GRAUMANN, J., HUBNER, N. C., KIM, J. B., KO, K., MOSER, M., KUMAR, C., COX, J., SCHOLER, H. & MANN, M. 2008. Stable isotope labeling by amino acids in cell culture (SILAC) and proteome quantitation of mouse embryonic stem cells to a depth of 5,111 proteins. *Mol Cell Proteomics,* 7**,** 672-83.

GRATZFELD-HUSGEN, A. & SCHUSTER, R. 1996. HPLC for Food Analysis. A Primer. Hewlett-Packard, Palo Alto, Calif, USA, 43–44.

GRIENDLING, K. K. & FITZGERALD, G. A. 2003a. Oxidative stress and cardiovascular injury: Part I: basic mechanisms and in vivo monitoring of ROS. *Circulation,* 108**,** 1912-6.

GRIENDLING, K. K. & FITZGERALD, G. A. 2003b. Oxidative stress and cardiovascular injury: Part II: animal and human studies. *Circulation,* 108**,** 2034-40.

GRUNFELD, S., HAMILTON, C. A., MESAROS, S., MCCLAIN, S. W., DOMINICZAK, A. F., BOHR, D. F. & MALINSKI, T. 1995. Role of superoxide in the depressed nitric oxide production by the endothelium of genetically hypertensive rats. *Hypertension,* 26**,** 854-7.

GUAN, S. J., MA, Z. H., WU, Y. L., ZHANG, J. P., LIANG, F., WEISS, J. W., GUO, Q. Y., WANG, J. Y., JI, E. S. & CHU, L. 2012. Long-term administration of fasudil improves cardiomyopathy in streptozotocin-induced diabetic rats. *Food Chem Toxicol,* 50**,** 1874-82.

GUYARD-DANGREMONT, V., DESRUMAUX, C., GAMBERT, P., LALLEMANT, C. & LAGROST, L. 1998. Phospholipid and cholesteryl ester transfer activities in plasma from 14 vertebrate species. Relation to atherogenesis susceptibility. *Comp Biochem Physiol B Biochem Mol Biol,* 120**,** 517-25.

GYGI, S. P., RIST, B., GERBER, S. A., TURECEK, F., GELB, M. H. & AEBERSOLD, R. 1999. Quantitative analysis of complex protein mixtures using isotope-coded affinity tags. *Nat Biotech,* 17**,** 994-999.

HALPERN, W. & OSOL, G. 1986. Resistance vessels in hypertension. *Prog Clin Biol Res,* 219**,** 211-23.

HAMILTON, C. A., BROSNAN, M. J., AL-BENNA, S., BERG, G. & DOMINICZAK, A. F. 2002. NAD(P)H oxidase inhibition improves endothelial function in rat and human blood vessels. *Hypertension,* 40**,** 755-62.

HAMILTON, C. A., BROSNAN, M. J., MCINTYRE, M., GRAHAM, D. & DOMINICZAK, A. F. 2001. Superoxide excess in hypertension and aging: a common cause of endothelial dysfunction. *Hypertension,* 37**,** 529-34.

HAMILTON, C. A., MILLER, W. H., AL-BENNA, S., BROSNAN, M. J., DRUMMOND, R. D., MCBRIDE, M. W. & DOMINICZAK, A. F. 2004. Strategies to reduce oxidative stress in cardiovascular disease. *Clin. Sci.,* 106**,** 219-234.

HAN, X., ROZEN, S., BOYLE, S. H., HELLEGERS, C., CHENG, H., BURKE, J. R., WELSH-BOHMER, K. A., DORAISWAMY, P. M. & KADDURAH-DAOUK, R. 2011. Metabolomics in early Alzheimer's disease: identification of altered plasma sphingolipidome using shotgun lipidomics. *PLoS One,* 6**,** e21643.

HANNA, A. N., BERTHIAUME, L. G., KIKUCHI, Y., BEGG, D., BOURGOIN, S. & BRINDLEY, D. N. 2001. Tumor necrosis factor-alpha induces stress fiber formation through ceramide production: role of sphingosine kinase. *Mol Biol Cell,* 12**,** 3618-30.

HARRISON, C. B., DRUMMOND, G. R., SOBEY, C. G. & SELEMIDIS, S. 2010. Evidence that nitric oxide inhibits vascular inflammation and superoxide production via a p47phox-dependent mechanism in mice. *Clin Exp Pharmacol Physiol,* 37**,** 429-34.

HASHIMOTO, R., UMEMOTO, S., GUO, F., UMEJI, K., ITOH, S., KISHI, H., KOBAYASHI, S. & MATSUZAKI, M. 2010. Nifedipine activates PPARgamma and exerts antioxidative action through Cu/ZnSOD independent of blood-pressure lowering in SHRSP. *J Atheroscler Thromb,* 17**,** 785-95.

HAYES, J. D. & PULFORD, D. J. 1995. The glutathione S-transferase supergene family: regulation of GST and the contribution of the isoenzymes to cancer chemoprotection and drug resistance. *Crit Rev Biochem Mol Biol,* 30**,** 445-600.

HEITZER, T., BALDUS, S., VON KODOLITSCH, Y., RUDOLPH, V. & MEINERTZ, T. 2005. Systemic endothelial dysfunction as an early predictor of adverse outcome in heart failure. *Arterioscler Thromb Vasc Biol,* 25**,** 1174-9.

HILBERT, P., LINDPAINTNER, K., BECKMANN, J. S., SERIKAWA, T., SOUBRIER, F., DUBAY, C., CARTWRIGHT, P., DE GOUYON, B., JULIER, C., TAKAHASI, S., VINCENT, M., GANTEN, D., GEORGES, M. & LATHROP, G. M. 1991. Chromosomal mapping of two genetic loci associated with blood-pressure regulation in hereditary hypertensive rats. *Nature,* 353, 521 - 529.

HO, C. S., LAM, C. W., CHAN, M. H., CHEUNG, R. C., LAW, L. K., LIT, L. C., NG, K. F., SUEN, M. W. & TAI, H. L. 2003. Electrospray ionisation mass spectrometry: principles and clinical applications. *Clin Biochem Rev,* 24**,** 3-12.

HOBBS, A. J. 1997. Soluble guanylate cyclase: the forgotten sibling. *Trends Pharmacol Sci,* 18**,** 484-91.

HOLZMANN, S., KUKOVETZ, W. R. & SCHMIDT, K. 1980. Mode of action of coronary arterial relaxation by prostacyclin. *J Cyclic Nucleotide Res,* 6**,** 451-60.

HORTON, J. D., CUTHBERT, J. A. & SPADY, D. K. 1995. Regulation of hepatic 7 alpha-hydroxylase expression and response to dietary cholesterol in the rat and hamster. *J Biol Chem,* 270**,** 5381-7.

HRABAK, A., BAJOR, T. & TEMESI, A. 1994. Comparison of substrate and inhibitor specificity of arginase and nitric oxide (NO) synthase for arginine analogues and related compounds in murine and rat macrophages. *Biochem Biophys Res Commun,* 198**,** 206-12.

HUSSAIN, M. B., MACALLISTER, R. J. & HOBBS, A. J. 2001. Reciprocal regulation of cGMP-mediated vasorelaxation by soluble and particulate guanylate cyclases. *American Journal of Physiology - Heart and Circulatory Physiology,* 280**,** H1151-H1159.

IBRAHIM, F. B., PANG, S. J. & MELENDEZ, A. J. 2004. Anaphylatoxin signaling in human neutrophils. A key role for sphingosine kinase. *J Biol Chem,* 279**,** 44802-11.

IGARASHI, J. & MICHEL, T. 2000. Agonist-modulated Targeting of the EDG-1 Receptor to Plasmalemmal Caveolae: eNOS ACTIVATION BY SPHINGOSINE 1-PHOSPHATE AND THE ROLE OF CAVEOLIN-1 IN SPHINGOLIPID SIGNAL TRANSDUCTION. *Journal of Biological Chemistry,* 275**,** 32363-32370.

ILLIG, T., GIEGER, C., ZHAI, G., ROMISCH-MARGL, W., WANG-SATTLER, R., PREHN, C., ALTMAIER, E., KASTENMULLER, G., KATO, B. S., MEWES, H.W., MEITINGER, T., HRABE DE ANGELIS, M., KRONENBERG, F., SORANZO, N., WICHMANN, H. E., D SPECTOR, T. D., ADAMSKI, J. & SUHRE, K. 2010. A genome-wide perspective of genetic variation in human metabolism. *Nat Genet,* 42, 137–141.

INTENGAN, H. D., THIBAULT, G., LI, J.-S. & SCHIFFRIN, E. L. 1999. Resistance Artery Mechanics, Structure, and Extracellular Components in Spontaneously Hypertensive Rats: Effects of Angiotensin Receptor Antagonism and Converting Enzyme Inhibition. *Circulation,* 100**,** 2267-2275.

ISHIHAMA, Y., SATO, T., TABATA, T., MIYAMOTO, N., SAGANE, K., NAGASU, T. & ODA, Y. 2005. Quantitative mouse brain proteomics using culture-derived isotope tags as internal standards. *Nat Biotech,* 23**,** 617-621.

ISHII, I., YE, X., FRIEDMAN, B., KAWAMURA, S., CONTOS, J. J., KINGSBURY, M. A., YANG, A. H., ZHANG, G., BROWN, J. H. & CHUN, J. 2002. Marked perinatal lethality and cellular signaling deficits in mice null for the two sphingosine 1-phosphate (S1P) receptors, S1P(2)/LP(B2)/EDG-5 and S1P(3)/LP(B3)/EDG-3. *J Biol Chem,* 277**,** 25152-9.

ITO, S. & CARRETERO, O. A. 1992. Impaired response to acetylcholine despite intact endothelium-derived relaxing factor/nitric oxide in isolated microperfused afferent arterioles of the spontaneously hypertensive rat. *J Cardiovasc Pharmacol,* 20 Suppl 12**,** S187-9.

JACOB, H. J., LINDPAINTNER, K., LINCOLN, S, E., KUSUMI, K., BUNKER, R. K., MAO, Y., GANTEN, D., DZAU, V. J., LANDER, E. S. 1991. Genetic mapping of a gene causing hypertension in the stroke-prone spontaneously hypertensive rat. *Cell,* 67, 213–224

JAGER, A., VAN HINSBERGH, V. W., KOSTENSE, P. J., EMEIS, J. J., NIJPELS, G., DEKKER, J. M., HEINE, R. J., BOUTER, L. M. & STEHOUWER, C. D. 2000. Increased levels of soluble vascular cell adhesion molecule 1 are associated with risk of cardiovascular mortality in type 2 diabetes: the Hoorn study. *Diabetes,* 49**,** 485-491.

JANG, Y., LINCOFF, A. M., PLOW, E. F. & TOPOL, E. J. 1994. Cell adhesion molecules in coronary artery disease. *J Am Coll Cardiol,* 24**,** 1591-601.

JANKEVICS, A., MERLO, M. E., DE VRIES, M., VONK, R. J., TAKANO, E. & BREITLING, R. 2011. Metabolomic analysis of a synthetic metabolic switch in Streptomyces coelicolor A3(2). *Proteomics,* 11**,** 4622-31.

JEFFS, B., NEGRIN, C. D., GRAHAM, D., CLARK, J. S., ANDERSON, N. H., GAUGUIER, D. & DOMINICZAK, A. F. 2000. Applicability of a "speed" congenic strategy to dissect blood pressure quantitative trait loci on rat chromosome 2. *Hypertension,* 35**,** 179-87.

JIN, N., PACKER, C. S. & RHOADES, R. A. 1991. Reactive oxygen-mediated contraction in pulmonary arterial smooth muscle: cellular mechanisms. *Can J Physiol Pharmacol,* 69**,** 383-8.

JOHNSON, M. D., HE, L., HERMAN, D., WAKIMOTO, H., WALLACE, C. A., ZIDEK, V., MLEJNEK, P., MUSILOVA, A., SIMAKOVA, M., VORLICEK, J., KREN, V., VIKLICKY, O., QI, N. R., WANG, J., SEIDMAN, C. E., SEIDMAN, J., KURTZ, T. W., AITMAN, T. J. & PRAVENEC, M. 2009. Dissection of chromosome 18 blood pressure and salt-sensitivity quantitative trait loci in the spontaneously hypertensive rat. *Hypertension,* 54**,** 639-45.

JOHNSON, T., GAUNT, T. R., NEWHOUSE, S. J., PADMANABHAN, S., TOMASZEWSKI, M., KUMARI, M., MORRIS, R. W., TZOULAKI, I., O'BRIEN, E. T., POULTER, N. R., SEVER, P., SHIELDS, D. C., THOM, S., WANNAMETHEE, S. G., WHINCUP, P. H., BROWN, M. J., CONNELL, J. M., DOBSON, R. J., HOWARD, P. J., MEIN, C. A., ONIPINLA, A., SHAW-HAWKINS, S., ZHANG, Y., SMITH, G. D., DAY, I. N. M., LAWLOR, D. A., GOODALL, A. H., FOWKES, F. G., ABECASIS, G. R., ELLIOTT, P., GATEVA, V., BRAUND, P. S., BURTON,

PAUL R., NELSON, CHRISTOPHER P., TOBIN, MARTIN D., VAN DER HARST, P., GLORIOSO, N., NEUVRITH, H., SALVI, E., STAESSEN, J. A., STUCCHI, A., DEVOS, N., JEUNEMAITRE, X., PLOUIN, P.-F., TICHET, J., JUHANSON, P., ORG, E., PUTKU, M., SÕBER, S., VELDRE, G., VIIGIMAA, M., LEVINSSON, A., ROSENGREN, A., THELLE, D. S., HASTIE, C. E., HEDNER, T., LEE, W. K., MELANDER, O., WAHLSTRAND, B., HARDY, R., WONG, A., COOPER, J. A., PALMEN, J., CHEN, L., STEWART, A. F. R., WELLS, G. A., WESTRA, H.-J., WOLFS, M. G. M., CLARKE, R., FRANZOSI, M. G., GOEL, A., HAMSTEN, A., LATHROP, M., PEDEN, J. F., SEEDORF, U., WATKINS, H., OUWEHAND, W. H., SAMBROOK, J., STEPHENS, J., CASAS, J.-P., DRENOS, F., HOLMES, MICHAEL V., KIVIMAKI, M., SHAH, S., SHAH, T., TALMUD, P. J., WHITTAKER, J., WALLACE, C., DELLES, C., LAAN, M., KUH, D., HUMPHRIES, S. E., NYBERG, F., CUSI, D., ROBERTS, R., NEWTON-CHEH, C., FRANKE, L., STANTON, A. V., DOMINICZAK, A. F., FARRALL, M., et al. 2011. Blood Pressure Loci Identified with a Gene-Centric Array. *The American Journal of Human Genetics,* 89**,** 688-700.

JULIUS, S. 1993. Corcoran Lecture. Sympathetic hyperactivity and coronary risk in hypertension. *Hypertension,* 21**,** 886-93.

KAMLEH, A., BARRETT, M. P., WILDRIDGE, D., BURCHMORE, R. J., SCHELTEMA, R. A. & WATSON, D. G. 2008. Metabolomic profiling using Orbitrap Fourier transform mass spectrometry with hydrophilic interaction chromatography: a method with wide applicability to analysis of biomolecules. *Rapid Commun Mass Spectrom,* 22**,** 1912-8.

KATHIRESAN, S. & SRIVASTAVA, D. 2012. Genetics of human cardiovascular disease. *Cell,* 148**,** 1242-57.

KAWASHIMA, S. & YOKOYAMA, M. 2004. Dysfunction of endothelial nitric oxide synthase and atherosclerosis. *Arterioscler Thromb Vasc Biol,* 24**,** 998-1005.

KEARNEY, P. M., WHELTON, M., REYNOLDS, K., MUNTNER, P., WHELTON, P. K. & HE, J. 2005. Global burden of hypertension: analysis of worldwide data. *The Lancet,* 365**,** 217-223.

KELL, D. B. 2006. Systems biology, metabolic modelling and metabolomics in drug discovery and development. *Drug Discovery Today,* 11**,** 1085-1092.

KERR, S., BROSNAN, M. J., MCINTYRE, M., REID, J. L., DOMINICZAK, A. F. & HAMILTON, C. A. 1999. Superoxide anion production is increased in a model of genetic hypertension: role of the endothelium. *Hypertension,* 33**,** 1353-8.

KETTUNEN, J., TUKIAINEN, T., SARIN, A. P , ORTENGA-ALONSO, A., TIKKANEN, E., LYYTIKAINEN, L. P., KANGAS, A. J., SOININEN, P., WURTZ, P., SILANDER, K., DICK, D. M., ROSE, R. J., SAVOLAINEN, M. J., VIIKARI, J., KAHONEN, M., LEHTIMAKI, T., PIETILAINEN, K. H., INOUYE, M., McCARTHY, M. I., JULA, A., ERIKSSON, J., RAITAKARI, O. T., SALOMAA, V., KAPRIO, J., JARVELIN, M. R., PELTONEN, L., PEROLA, M., FREIMER, N. B., ALA-KORPELA, M., PALOTIE, A. & RIPATTI, S. 2012. Genome-wide association study identifies multiple loci influencing human serum metabolite levels. *Nat Genet*, 44, 269-76.

KIM, M. G., LEE, S. Y., KO, Y. S., LEE, H. Y., JO, S. K., CHO, W. Y. & KIM, H. K. 2011. CD4+ CD25+ regulatory T cells partially mediate the beneficial effects of FTY720, a sphingosine-1-phosphate analogue, during ischaemia/reperfusion-induced acute kidney injury. *Nephrol Dial Transplant,* 26**,** 111-24.

KIM, S.-Y., JEOUNG, N. H., OH, C. J., CHOI, Y.-K., LEE, H.-J., KIM, H.-J., KIM, J.-Y., HWANG, J. H., TADI, S., YIM, Y.-H., LEE, K.-U., PARK, K.-G., HUH, S., MIN, K.-N., JEONG, K.-H., PARK, M. G., KWAK, T. H., KWEON, G. R., INUKAI, K., SHONG, M. & LEE, I.-K. 2009. Activation of NAD(P)H:Quinone Oxidoreductase 1 Prevents Arterial Restenosis by Suppressing Vascular Smooth Muscle Cell Proliferation. *Circulation Research,* 104**,** 842-850.

KIMURA, T., WATANABE, T., SATO, K., KON, J., TOMURA, H., TAMAMA, K., KUWABARA, A., KANDA, T., KOBAYASHI, I., OHTA, H., UI, M. & OKAJIMA, F. 2000. Sphingosine 1-phosphate stimulates proliferation and migration of human endothelial cells possibly through the lipid receptors, Edg-1 and Edg-3. *Biochem J,* 348 Pt 1**,** 71-6.

KITAZONO, T., AGO, T., KAMOUCHI, M., SANTA, N., OOBOSHI, H., FUJISHIMA, M. & IBAYASHI, S. 2002. Increased activity of calcium channels and Rho-associated kinase in the basilar artery during chronic hypertension in vivo. *J Hypertens,* 20**,** 879-84.

KOCHER, T. & SUPERTI-FURGA, G. 2007. Mass spectrometry-based functional proteomics: from molecular machines to protein networks. *Nat Meth,* 4**,** 807-815.

KOETH, R. A., WANG, Z., LEVISON, B. S., BUFFA, J. A., ORG, E., SHEEHY, B. T., BRITT, E. B., FU, X., WU, Y., LI, L., SMITH, J. D., DiDONATO, J. A., CHEN, J., LI, H., WU, G. D., LEWIS, J. D., WARRIER, M., BROWN, J.M., KRAUSS, R. M., TANG, W. H., BUSHMAN, F. D., LUSIS, A. J. & HAZEN, S.L. 2013. Intestinal microbiota metabolism of L-carnitine, a nutrient in red meat, promotes atherosclerosis. *Nat Med*, 19, 576-85.

KOH-TAN, H. H., GRAHAM, D., HAMILTON, C. A., NICOLL, G., FIELDS, L., MCBRIDE, M. W., YOUNG, B. & DOMINICZAK, A. F. 2009. Renal and vascular glutathione S-transferase mu is not affected by pharmacological intervention to reduce systolic blood pressure. *J Hypertens,* 27**,** 1575-84.

KRATCHMAROVA, I., BLAGOEV, B., HAACK-SORENSEN, M., KASSEM, M. & MANN, M. 2005. Mechanism of Divergent Growth Factor Effects in Mesenchymal Stem Cell Differentiation. *Science,* 308**,** 1472-1477.

KROGAN, N. J., CAGNEY, G., YU, H., ZHONG, G., GUO, X., IGNATCHENKO, A., LI, J., PU, S., DATTA, N., TIKUISIS, A. P., PUNNA, T., PEREGRÍN-ALVAREZ, J. M., SHALES, M., ZHANG, X., DAVEY, M., ROBINSON, M. D., PACCANARO, A., BRAY, J. E., SHEUNG, A., BEATTIE, B., RICHARDS, D. P., CANADIEN, V., LALEV, A., MENA, F., WONG, P., STAROSTINE, A., CANETE, M. M., VLASBLOM, J., WU, S., ORSI, C., COLLINS, S. R., CHANDRAN, S., HAW, R., RILSTONE, J. J., GANDI, K., THOMPSON, N. J., MUSSO, G., ST ONGE, P., GHANNY, S., LAM, M. H. Y., BUTLAND, G., ALTAF-UL, A. M., KANAYA, S., SHILATIFARD, A., O'SHEA, E., WEISSMAN, J. S., INGLES, C. J., HUGHES, T. R., PARKINSON, J., GERSTEIN, M., WODAK, S. J., EMILI, A. & GREENBLATT, J. F. 2006. Global landscape of protein complexes in the yeast Saccharomyces cerevisiae. *Nature,* 440**,** 637-643.

KROMER, J. O., SORGENFREI, O., KLOPPROGGE, K., HEINZLE, E. & WITTMANN, C. 2004. In-depth profiling of lysine-producing Corynebacterium glutamicum by combined analysis of the transcriptome, metabolome, and fluxome. *J Bacteriol,* 186**,** 1769-84.

KRÜGER, M., MOSER, M., USSAR, S., THIEVESSEN, I., LUBER, C. A., FORNER, F., SCHMIDT, S., ZANIVAN, S., FÄSSLER, R. & MANN, M. 2008. SILAC Mouse for Quantitative Proteomics Uncovers Kindlin-3 as an Essential Factor for Red Blood Cell Function. *Cell,* 134**,** 353-364.

KSHIRSAGAR, A. V., CARPENTER, M., BANG, H., WYATT, S. B. & COLINDRES, R. E. 2006. Blood pressure usually considered normal is associated with an elevated risk of cardiovascular disease. *Am J Med,* 119**,** 133-41.

KUBO-INOUE, M., EGASHIRA, K., USUI, M., TAKEMOTO, M., OHTANI, K., KATOH, M., SHIMOKAWA, H. & TAKESHITA, A. 2002. Long-term inhibition of nitric oxide synthesis increases arterial thrombogenecity in rat carotid artery. *Am J Physiol Heart Circ Physiol,* 282**,** H1478-84.

KUMAR, N., CALHOUN, D. A. & DUDENBOSTEL, T. 2013. Management of patients with resistant hypertension: current treatment options. *Integr Blood Press Control,* 6**,** 139-151.

KUMARASAMY, S., GOPALAKRISHNAN, K., TOLAND, E. J., YERGA-WOOLWINE, S., FARMS, P., MORGAN, E. E. & JOE, B. 2011. Refined mapping of blood pressure quantitative trait loci using congenic strains developed from two genetically hypertensive rat models. *Hypertens Res,* 34**,** 1263-70.

KUSAMA, N., KAJIKURI, J., YAMAMOTO, T., WATANABE, Y., SUZUKI, Y., KATSUYA, H. & ITOH, T. 2005. Reduced hyperpolarization in endothelial cells of rabbit aortic valve following chronic nitroglycerine administration. *Br J Pharmacol,* 146**,** 487-97.

LAFFER, C. L., BOLTERMAN, R. J., ROMERO, J. C. & ELIJOVICH, F. 2006. Effect of salt on isoprostanes in salt-sensitive essential hypertension. *Hypertension,* 47**,** 434-40.

LASSEGUE, B. & CLEMPUS, R. E. 2003. Vascular NAD(P)H oxidases: specific features, expression, and regulation. *Am J Physiol Regul Integr Comp Physiol,* 285**,** R277-97.

LAURANT, P., TOUYZ, R. M. & SCHIFFRIN, E. L. 1997. Effect of pressurization on mechanical properties of mesenteric small arteries from spontaneously hypertensive rats. *J Vasc Res,* 34**,** 117-25.

LE NOBLE, F. A., STASSEN, F. R., HACKING, W. J. & STRUIJKER BOUDIER, H. A. 1998. Angiogenesis and hypertension. *J Hypertens,* 16**,** 1563-72.

LEE, M.-J., VAN BROCKLYN, J. R., THANGADA, S., LIU, C. H., HAND, A. R., MENZELEEV, R., SPIEGEL, S. & HLA, T. 1998. Sphingosine-1-Phosphate as a Ligand for the G Protein-Coupled Receptor EDG-1. *Science,* 279**,** 1552-1555.

LEE, O. H., KIM, Y. M., LEE, Y. M., MOON, E. J., LEE, D. J., KIM, J. H., KIM, K. W. & KWON, Y. G. 1999. Sphingosine 1-phosphate induces angiogenesis: its angiogenic action and signaling mechanism in human umbilical vein endothelial cells. *Biochem Biophys Res Commun,* 264**,** 743-50.

LEE, R. M., OWENS, G. K., SCOTT-BURDEN, T., HEAD, R. J., MULVANY, M. J. & SCHIFFRIN, E. L. 1995. Pathophysiology of smooth muscle in hypertension. *Can J Physiol Pharmacol,* 73**,** 574-84.

LEVENSON, J. W., SKERRETT, P. J. & GAZIANO, J. M. 2002a. Reducing the Global Burden of Cardiovascular Disease: The Role of Risk Factors. *Preventive Cardiology,* 5**,** 188-199.

LEVENSON, J. W., SKERRETT, P. J. & GAZIANO, J. M. 2002b. Reducing the global burden of cardiovascular disease: the role of risk factors. *Prev Cardiol,* 5**,** 188-99.

LEVY, D., EHRET, G. B., RICE, K., VERWOERT, G. C., LAUNER, L. J., DEHGHAN, A., GLAZER, N. L., MORRISON, A. C., JOHNSON, A. D., ASPELUND, T., AULCHENKO, Y., LUMLEY, T., KOTTGEN, A., VASAN, R. S., RIVADENEIRA, F., EIRIKSDOTTIR, G., GUO, X., ARKING, D. E., MITCHELL, G. F., MATTACE-RASO, F. U. S., SMITH, A. V., TAYLOR, K., SCHARPF, R. B., HWANG, S.-J., SIJBRANDS, E. J. G., BIS, J., HARRIS, T. B., GANESH, S. K., O'DONNELL, C. J., HOFMAN, A., ROTTER, J. I., CORESH, J., BENJAMIN, E. J., UITTERLINDEN, A. G., HEISS, G., FOX, C. S., WITTEMAN, J. C. M., BOERWINKLE, E., WANG, T. J., GUDNASON, V., LARSON, M. G., CHAKRAVARTI, A., PSATY, B. M. & VAN DUIJN, C. M. 2009. Genome-wide association study of blood pressure and hypertension. *Nat Genet,* 41**,** 677-687.

LEWIS, G. D., WEI, R., LIU, E., YANG, E., SHI, X., MARTINOVIC, M., FARRELL, L., ASNANI, A., CYRILLE, M., RAMANATHAN, A., SHAHAM, O., BERRIZ, G., LOWRY, P. A., PALACIOS, I. F., TASAN, M., ROTH, F. P., MIN, J., BAUMGARTNER, C., KESHISHIAN, H., ADDONA, T., MOOTHA, V. K., ROSENZWEIG, A., CARR, S. A., FIFER, M. A., SABATINE, M. S. & GERSZTEN, R. E. 2008. Metabolite profiling of blood from individuals undergoing planned myocardial infarction reveals early markers of myocardial injury. *J Clin Invest,* 118**,** 3503-12.

LIAO, Y. B., ZHANG, Q. & DING, J. F. 1991. [Regulation of atrial natriuretic peptide receptor in cultured aortic vascular smooth muscle cells from stroke-prone spontaneously hypertensive and Wistar-Kyoto rats]. *Sheng Li Xue Bao,* 43**,** 368-75.

LIEN, Y. H., YONG, K. C., CHO, C., IGARASHI, S. & LAI, L. W. 2006. S1P1-selective agonist, SEW2871, ameliorates ischemic acute renal failure. *Kidney Int,* 69**,** 1601-1608.

LIFTON, R. P., GHARAVI, A. G. & GELLER, D. S. 2001. Molecular Mechanisms of Human Hypertension. *Cell,* 104**,** 545-556.

LIGHTHALL, G. K., HAMILTON, B. P. & HAMLYN, J. M. 2004. Identification of salt-sensitive genes in the kidneys of Dahl rats. *J Hypertens,* 22**,** 1487-94.

LIN, Y. P., HSU, M. E., CHIOU, Y. Y., HSU, H. Y., TSAI, H. C., PENG, Y. J., LU, C. Y., PAN, C. Y., YU, W. C., CHEN, C. H., CHI, C. W. & LIN, C. H. 2010. Comparative proteomic analysis of rat aorta in a subtotal nephrectomy model. *Proteomics,* 10**,** 2429-43.

LINSEMAN, D. A., BENJAMIN, C. W. & JONES, D. A. 1995. Convergence of angiotensin II and platelet-derived growth factor receptor signaling cascades in vascular smooth muscle cells. *J Biol Chem,* 270**,** 12563-8.

LIU, Y., BLEDSOE, G., HAGIWARA, M., SHEN, B., CHAO, L. & CHAO, J. 2012. Depletion of endogenous kallistatin exacerbates renal and cardiovascular oxidative stress, inflammation, and organ remodeling. *Am J Physiol Renal Physiol,* 303**,** F1230-8.

LIU, Y., BUBOLZ, A. H., SHI, Y., NEWMAN, P. J., NEWMAN, D. K. & GUTTERMAN, D. D. 2006. Peroxynitrite reduces the endothelium-derived hyperpolarizing factor component of coronary flow-mediated dilation in PECAM-1-knockout mice. *Am J Physiol Regul Integr Comp Physiol,* 290**,** R57-65.

LIU, Y., WADA, R., YAMASHITA, T., MI, Y., DENG, C.-X., HOBSON, J. P., ROSENFELDT, H. M., NAVA, V. E., CHAE, S.-S., LEE, M.-J., LIU, C. H., HLA, T., SPIEGEL, S. & PROIA, R. L. 2000. Edg-1, the G protein–coupled receptor for sphingosine-1-phosphate, is essential for vascular maturation. *The Journal of Clinical Investigation,* 106**,** 951-961.

LOSCALZO, J., KOHANE, I. & BARABASI, A. L. 2007. Human disease classification in the postgenomic era: a complex systems approach to human pathobiology. *Mol Syst Biol,* 3**,** 124.

LU, G., GREENE, E. L., NAGAI, T. & EGAN, B. M. 1998. Reactive oxygen species are critical in the oleic acid-mediated mitogenic signaling pathway in vascular smooth muscle cells. *Hypertension,* 32**,** 1003-10.

LUDMER, P. L., SELWYN, A. P., SHOOK, T. L., WAYNE, R. R., MUDGE, G. H., ALEXANDER, R. W. & GANZ, P. 1986. Paradoxical vasoconstriction induced by acetylcholine in atherosclerotic coronary arteries. *N Engl J Med,* 315**,** 1046-51.

LUFT, F. C., MILLER, J. Z., WEINBERGER, M. H., CHRISTIAN, J. C. & SKRABAL, F. 1988. Genetic influences on the response to dietary salt reduction, acute salt loading, or salt depletion in humans. *J Cardiovasc Pharmacol,* 12 Suppl 3**,** S49-55.

LUFT, F. C., WEINBERGER, M. H., GRIM, C. E. & FINEBERG, N. S. 1986. Natriuresis and the renin axis in sodium-sensitive man. *J Hypertens Suppl,* 4**,** S198-201.

LUSCHER, T. F. & VANHOUTTE, P. M. 1986. Endothelium-dependent contractions to acetylcholine in the aorta of the spontaneously hypertensive rat. *Hypertension,* 8**,** 344-8.

LY-VERDU, S., SCHAEFER, A., KAHLE, M., GROEGER, T., NESCHEN, S., ARTEAGA-SALAS, J. M., UEFFING, M., DE ANGELIS, M. H. & ZIMMERMANN, R. 2013. The impact of blood on liver metabolite profiling - a combined metabolomic and proteomic approach. *Biomed Chromatogr*.

MA, X. L., GAO, F., NELSON, A. H., LOPEZ, B. L., CHRISTOPHER, T. A., YUE, T. L. & BARONE, F. C. 2001. Oxidative inactivation of nitric oxide and endothelial dysfunction in stroke-prone spontaneous hypertensive rats. *J Pharmacol Exp Ther,* 298**,** 879-85.

MA, Z., ZHANG, J., JI, E., CAO, G., LI, G. & CHU, L. 2011. Rho kinase inhibition by fasudil exerts antioxidant effects in hypercholesterolemic rats. *Clin Exp Pharmacol Physiol,* 38**,** 688-94.

MADHANI, M., SCOTLAND, R. S., MACALLISTER, R. J. & HOBBS, A. J. 2003. Vascular natriuretic peptide receptor-linked particulate guanylate cyclases are modulated by nitric oxide–cyclic GMP signalling. *British Journal of Pharmacology,* 139**,** 1289-1296.

MADSEN, R., LUNDSTEDT, T. & TRYGG, J. 2010. Chemometrics in metabolomics—A review in human disease diagnosis. *Analytica Chimica Acta,* 659**,** 23-33.

MAIER, T., MARCOS, J., WODKE, J. A., PAETZOLD, B., LIEBEKE, M., GUTIERREZ-GALLEGO, R. & SERRANO, L. 2013. Large-scale metabolome analysis and quantitative integration with genomics and proteomics data in Mycoplasma pneumoniae. *Mol Biosyst,* 9**,** 1743-55.

MAKAROV, A., DENISOV, E., KHOLOMEEV, A., BALSCHUN, W., LANGE, O., STRUPAT, K. & HORNING, S. 2006. Performance Evaluation of a Hybrid Linear Ion Trap/Orbitrap Mass Spectrometer. *Analytical Chemistry,* 78**,** 2113-2120.

MANDAL, R., GUO, A. C., CHAUDHARY, K. K., LIU, P., YALLOU, F. S., DONG, E., AZIAT, F. & WISHART, D. S. 2012. Multi-platform characterization of the human cerebrospinal fluid metabolome: a comprehensive and quantitative update. *Genome Med,* 4**,** 38.

MANN, M. 2006. Functional and quantitative proteomics using SILAC. *Nat Rev Mol Cell Biol,* 7**,** 952-958.

MANNING, R. D., JR., TIAN, N. & MENG, S. 2005. Oxidative stress and antioxidant treatment in hypertension and the associated renal damage. *Am J Nephrol,* 25**,** 311-7.

MANSANO, A. M., VIANNA, P. T., FABRIS, V. E., SILVA, L. M., BRAZ, L. G. & CASTIGLIA, Y. M. 2012. Prevention of renal ischemia/reperfusion injury in rats using acetylcysteine after anesthesia with isoflurane. *Acta Cir Bras,* 27**,** 340-5.

MARTEAU, J. B., ZAIOU, M., SIEST, G. & VISVIKIS-SIEST, S. 2005. Genetic determinants of blood pressure regulation. *J Hypertens,* 23**,** 2127-43.

MARTINEZ-LEMUS, L. A., CROW, T., DAVIS, M. J. & MEININGER, G. A. 2005. alpha(v)beta(3)- and alpha(5)beta(1)-integrin blockade inhibits myogenic constriction of skeletal muscle resistance arterioles. *American Journal of Physiology-Heart and Circulatory Physiology,* 289**,** H322-H329.

MATHIASSEN, O. N., BUUS, N. H., SIHM, I., THYBO, N. K., MORN, B., SCHROEDER, A. P., THYGESEN, K., AALKJAER, C., LEDERBALLE, O., MULVANY, M. J. & CHRISTENSEN, K. L. 2007. Small artery structure is an independent predictor of cardiovascular events in essential hypertension. *J Hypertens,* 25**,** 1021-6.

MCBRIDE, M. W., BROSNAN, M. J., MATHERS, J., MCLELLAN, L. I., MILLER, W. H., GRAHAM, D., HANLON, N., HAMILTON, C. A., POLKE, J. M., LEE, W. K. & DOMINICZAK, A. F. 2005. Reduction of Gstm1 Expression in the Stroke-Prone Spontaneously Hypertension Rat Contributes to Increased Oxidative Stress. *Hypertension,* 45**,** 786-792.

MCBRIDE, M. W., CARR, F. J., GRAHAM, D., ANDERSON, N. H., CLARK, J. S., LEE, W. K., CHARCHAR, F. J., BROSNAN, M. J. & DOMINICZAK, A. F. 2003. Microarray Analysis of Rat Chromosome 2 Congenic Strains. *Hypertension,* 41**,** 847-853.

MCINTYRE, M., HAMILTON, C. A., REES, D. D., REID, J. L. & DOMINICZAK, A. F. 1997. Sex differences in the abundance of endothelial nitric oxide in a model of genetic hypertension. *Hypertension,* 30**,** 1517-24.

MEI, H., GU, D., HIXSON, J. E., RICE, T. K., CHEN, J., SHIMMIN, L. C., SCHWANDER, K., KELLY, T. N., LIU, D. P., CHEN, S., HUANG, J. F., JAQUISH, C. E., RAO, D. C. & HE, J. 2012. Genome-wide linkage and positional association study of blood pressure response to dietary sodium intervention: the GenSalt Study. *Am J Epidemiol,* 176 Suppl 7**,** S81-90.

MEYER ZU HERINGDORF, D., LASS, H., ALEMANY, R., LASER, K. T., NEUMANN, E., ZHANG, C., SCHMIDT, M., RAUEN, U., JAKOBS, K. H. & VAN KOPPEN, C. J. 1998. Sphingosine kinase-mediated Ca2+ signalling by G-protein-coupled receptors. *EMBO J,* 17**,** 2830-7.

MIN, H. K., LIM, S., CHUNG, B. C. & MOON, M. H. 2011. Shotgun lipidomics for candidate biomarkers of urinary phospholipids in prostate cancer. *Anal Bioanal Chem,* 399**,** 823-30.

MISTRY, H. D., WILSON, V., RAMSAY, M. M., SYMONDS, M. E. & BROUGHTON PIPKIN, F. 2008. Reduced selenium concentrations and glutathione peroxidase activity in preeclamptic pregnancies. *Hypertension,* 52**,** 881-8.

MITTLER, G., BUTTER, F. & MANN, M. 2009. A SILAC-based DNA protein interaction screen that identifies candidate binding proteins to functional DNA elements. *Genome Research,* 19**,** 284-293.

MOCCI, E., CONCAS, M. P., FANCIULLI, M., PIRASTU, N., ADAMO, M., CABRAS, V., FRAUMENE, C., PERSICO, I., SASSU, A., PICCIAU, A., PRODI, D. A., SERRA, D., BIINO, G., PIRASTU, M. & ANGIUS, A. 2009. Microsatellites and SNPs linkage analysis in a Sardinian genetic isolate confirms several essential hypertension loci previously identified in different populations. *BMC Med Genet,* 10**,** 81.

MOCHIZUKI, N. 2009. Vascular integrity mediated by vascular endothelial cadherin and regulated by sphingosine 1-phosphate and angiopoietin-1. *Circ J,* 73**,** 2183-91.

MOCO, S., VERVOORT, J., MOCO, S., BINO, R. J., DE VOS, R. C. H. & BINO, R. 2007. Metabolomics technologies and metabolite identification. *TrAC Trends in Analytical Chemistry,* 26**,** 855-866.

MORIKI, N., ITO, M., SEKO, T., KUREISHI, Y., OKAMOTO, R., NAKAKUKI, T., KONGO, M., ISAKA, N., KAIBUCHI, K. & NAKANO, T. 2004. RhoA activation in vascular smooth muscle cells from stroke-prone spontaneously hypertensive rats. *Hypertens Res,* 27**,** 263-70.

MORRISON, R. F. & SEIDEL, E. R. 1995. Vascular endothelial cell proliferation: regulation of cellular polyamines. *Cardiovasc Res,* 29**,** 841-7.

MORTON, J. J., BEATTIE, E. C. & MACPHERSON, F. 1992. Angiotensin II receptor antagonist losartan has persistent effects on blood pressure in the young spontaneously hypertensive rat: lack of relation to vascular structure. *J Vasc Res,* 29**,** 264-9.

MUELLER, L. N., BRUSNIAK, M.-Y., MANI, D. R. & AEBERSOLD, R. 2008. An Assessment of Software Solutions for the Analysis of Mass Spectrometry Based Quantitative Proteomics Data. *Journal of Proteome Research,* 7**,** 51-61.

MUIESAN, M. L., RIZZONI, D., SALVETTI, M., PORTERI, E., MONTEDURO, C., GUELFI, D., CASTELLANO, M., GARAVELLI, G. & AGABITI-ROSEI, E. 2002. Structural changes in small resistance arteries and left ventricular geometry in patients with primary and secondary hypertension. *J Hypertens,* 20**,** 1439-44.

MUKAI, Y., SHIMOKAWA, H., MATOBA, T., KANDABASHI, T., SATOH, S., HIROKI, J., KAIBUCHI, K. & TAKESHITA, A. 2001. Involvement of Rho-kinase in hypertensive vascular disease -a novel therapeutic target in hypertension. *The FASEB Journal*.

MULVANY, M. J. 1988. Biophysical aspects of resistance vessels studied in spontaneous and renal hypertensive rats. *Acta Physiol Scand Suppl,* 571**,** 129-37.

MULVANY, M. J. 2005. Abnormalities of the resistance vasculature in hypertension: correction by vasodilator therapy. *Pharmacol Rep,* 57 Suppl**,** 144-50.

MULVANY, M. J. 2012. Small artery remodelling in hypertension. *Basic Clin Pharmacol Toxicol,* 110**,** 49-55.

MULVANY, M. J. & AALKJAER, C. 1990. Structure and function of small arteries. *Physiol Rev,* 70**,** 921-61.

MULVANY, M. J., BAUMBACH, G. L., AALKJAER, C., HEAGERTY, A. M., KORSGAARD, N., SCHIFFRIN, E. L., HEISTAD, D. D. 1996. Vascular remodeling. *Hypertension*, 28(3), 505-6.

MUNROE, P. B., BARNES, M. R. & CAULFIELD, M. J. 2013. Advances in blood pressure genomics. *Circ Res,* 112**,** 1365-79.

MÜNZEL, T., DAIBER, A., ULLRICH, V. & MÜLSCH, A. 2005. Vascular Consequences of Endothelial Nitric Oxide Synthase Uncoupling for the Activity and Expression of the Soluble Guanylyl Cyclase and the cGMP-Dependent Protein Kinase. *Arteriosclerosis, Thrombosis, and Vascular Biology,* 25**,** 1551-1557.

MURAKAMI, A., TAKASUGI, H., OHNUMA, S., KOIDE, Y., SAKURAI, A., TAKEDA, S., HASEGAWA, T., SASAMORI, J., KONNO, T., HAYASHI, K., WATANABE, Y., MORI, K., SATO, Y., TAKAHASHI, A., MOCHIZUKI, N. & TAKAKURA, N. 2010. Sphingosine 1-phosphate (S1P) regulates vascular contraction via S1P3 receptor: investigation based on a new S1P3 receptor antagonist. *Mol Pharmacol,* 77**,** 704-13.

NABHA, L., GARBERN, J. C., BULLER, C. L. & CHARPIE, J. R. 2005. Vascular oxidative stress precedes high blood pressure in spontaneously hypertensive rats. *Clin Exp Hypertens,* 27**,** 71-82.

NAGASE, M., KATAFUCHI, T., HIROSE, S. & FUJITA, T. 1997. Tissue distribution and localization of natriuretic peptide receptor subtypes in stroke-prone spontaneously hypertensive rats. *J Hypertens,* 15**,** 1235-43.

NASCIMENTO, N. R., LESSA, L. M., KERNTOPF, M. R., SOUSA, C. M., ALVES, R. S., QUEIROZ, M. G., PRICE, J., HEIMARK, D. B., LARNER, J., DU, X., BROWNLEE, M., GOW, A., DAVIS, C. & FONTELES, M. C. 2006. Inositols prevent and reverse endothelial dysfunction in diabetic rat and rabbit vasculature metabolically and by scavenging superoxide. *Proc Natl Acad Sci U S A,* 103**,** 218-23.

NAZ, S., GARCIA, A. & BARBAS, C. 2013. Multiplatform analytical methodology for metabolic fingerprinting of lung tissue. *Anal Chem,* 85**,** 10941-8.

NEUMANN, S. & BOCKER, S. 2010. Computational mass spectrometry for metabolomics: identification of metabolites and small molecules. *Anal Bioanal Chem,* 398**,** 2779-88.

OHANIAN, J., FORMAN, S. P., KATZENBERG, G. & OHANIAN, V. 2012. Endothelin-1 stimulates small artery VCAM-1 expression through p38MAPK-dependent neutral sphingomyelinase. *J Vasc Res,* 49**,** 353-62.

OHTAKA, M. 1980. Vectorcardiographical and pathological approach to the relationship between cardiac hypertrophy and coronary arteriosclerosis in spontaneously hypertensive rats (SHR). *Jpn Circ J,* 44**,** 283-93.

OKAMOTO, K. & AOKI, K. 1963. Development of a strain of spontaneously hypertensive rats. *Jpn Circ J,* 27**,** 282-93.

OLSEN, J. V., BLAGOEV, B., GNAD, F., MACEK, B., KUMAR, C., MORTENSEN, P. & MANN, M. 2006. Global, In Vivo, and Site-Specific Phosphorylation Dynamics in Signaling Networks. *Cell,* 127**,** 635-648.

OLSEN, J. V., DE GODOY, L. M. F., LI, G., MACEK, B., MORTENSEN, P., PESCH, R., MAKAROV, A., LANGE, O., HORNING, S. & MANN, M. 2005. Parts per Million Mass Accuracy on an Orbitrap Mass Spectrometer via Lock Mass Injection into a C-trap. *Molecular & Cellular Proteomics,* 4**,** 2010-2021.

OLSEN, J. V., ONG, S.-E. & MANN, M. 2004. Trypsin Cleaves Exclusively C-terminal to Arginine and Lysine Residues. *Molecular & Cellular Proteomics,* 3**,** 608-614.

OLSZEWSKI, K. L., MATHER, M. W., MORRISEY, J. M., GARCIA, B. A., VAIDYA, A. B., RABINOWITZ, J. D. & LLINAS, M. 2010. Branched tricarboxylic acid metabolism in Plasmodium falciparum. *Nature,* 466**,** 774-8.

ONAKA, U., FUJII, K., ABE, I. & FUJISHIMA, M. 1998. Antihypertensive treatment improves endothelium-dependent hyperpolarization in the mesenteric artery of spontaneously hypertensive rats. *Circulation,* 98**,** 175-82.

ONDA, T., MASHIKO, S., HAMANO, M., TOMITA, I. & TOMITA, T. 1994. Enhancement of endothelium-dependent relaxation in the aorta from stroke-prone spontaneously hypertensive rats at developmental stages of hypertension. *Clin Exp Pharmacol Physiol,* 21**,** 857-63.

ONG, S.-E., BLAGOEV, B., KRATCHMAROVA, I., KRISTENSEN, D. B., STEEN, H., PANDEY, A. & MANN, M. 2002. Stable Isotope Labeling by Amino Acids in Cell Culture, SILAC, as a Simple and Accurate Approach to Expression Proteomics. *Molecular & Cellular Proteomics,* 1**,** 376-386.

ONG, S.-E., MITTLER, G. & MANN, M. 2004. Identifying and quantifying in vivo methylation sites by heavy methyl SILAC. *Nat Meth,* 1**,** 119-126.

ONG, S. E. & MANN, M. 2006. A practical recipe for stable isotope labeling by amino acids in cell culture (SILAC). *Nat Protoc,* 1**,** 2650-60.

OPITZ, C. A., WICK, W., STEINMAN, L. & PLATTEN, M. 2007. Tryptophan degradation in autoimmune diseases. *Cell Mol Life Sci,* 64**,** 2542-63.

PADMANABHAN, S., MELANDER, O., JOHNSON, T., DI BLASIO, A. M., LEE, W. K., GENTILINI, D., HASTIE, C. E., MENNI, C., MONTI, M. C., DELLES, C., LAING, S., CORSO, B., NAVIS, G., KWAKERNAAK, A. J., VAN DER HARST, P., BOCHUD, M., MAILLARD, M., BURNIER, M., HEDNER, T., KJELDSEN, S., WAHLSTRAND, B., SJÖGREN, M., FAVA, C., MONTAGNANA, M., DANESE, E., TORFFVIT, O., HEDBLAD, B., SNIEDER, H., CONNELL, J. M. C., BROWN, M., SAMANI, N. J., FARRALL, M., CESANA, G., MANCIA, G., SIGNORINI, S., GRASSI, G., EYHERAMENDY, S., WICHMANN, H. E., LAAN, M., STRACHAN, D. P., SEVER, P., SHIELDS, D. C., STANTON, A., VOLLENWEIDER, P., TEUMER, A., VÖLZKE, H., RETTIG, R., NEWTON-CHEH, C., ARORA, P., ZHANG, F., SORANZO, N., SPECTOR, T. D., LUCAS, G., KATHIRESAN, S., SISCOVICK, D. S., LUAN, J. A., LOOS, R. J. F., WAREHAM, N. J., PENNINX, B. W., NOLTE, I. M., MCBRIDE, M., MILLER, W. H., NICKLIN, S. A., BAKER, A. H., GRAHAM, D., MCDONALD, R. A., PELL, J. P., SATTAR, N., WELSH, P., MUNROE, P., CAULFIELD, M. J., ZANCHETTI, A., DOMINICZAK, A. F. 2010. Genome-Wide Association Study of Blood Pressure Extremes Identifies Variant near *UMOD* Associated with Hypertension. *PLoS Genet,* 6(10)**,** e1001177.

PADMANABHAN, S., NEWTON-CHEH, C. & DOMINICZAK, A. F. 2012. Genetic basis of blood pressure and hypertension. *Trends in Genetics,* 28**,** 397-408.

PANZA, J. A., CASINO, P. R., KILCOYNE, C. M. & QUYYUMI, A. A. 1993. Role of endothelium-derived nitric oxide in the abnormal endothelium-dependent vascular relaxation of patients with essential hypertension. *Circulation,* 87**,** 1468-74.

PANZA, J. A., QUYYUMI, A. A., BRUSH, J. E., JR. & EPSTEIN, S. E. 1990. Abnormal endothelium-dependent vascular relaxation in patients with essential hypertension. *N Engl J Med,* 323**,** 22-7.

PARK, J. B. & SCHIFFRIN, E. L. 2001. Small artery remodeling is the most prevalent (earliest?) form of target organ damage in mild essential hypertension. *J Hypertens,* 19**,** 921-30.

PARK, J. B., TOUYZ, R. M., CHEN, X. & SCHIFFRIN, E. L. 2002. Chronic treatment with a superoxide dismutase mimetic prevents vascular remodeling and progression of hypertension in salt-loaded stroke-prone spontaneously hypertensive rats. *Am J Hypertens,* 15**,** 78-84.

PAVOINE, C. & PECKER, F. 2009. Sphingomyelinases: their regulation and roles in cardiovascular pathophysiology. *Cardiovasc Res,* 82**,** 175-83.

PERKINS, D. N., PAPPIN, D. J. C., CREASY, D. M. & COTTRELL, J. S. 1999. Probability-based protein identification by searching sequence databases using mass spectrometry data. *ELECTROPHORESIS,* 20**,** 3551-3567.

PETERS, S. L. & ALEWIJNSE, A. E. 2007. Sphingosine-1-phosphate signaling in the cardiovascular system. *Curr Opin Pharmacol,* 7**,** 186-92.

PETERSON, T. E., GUICCIARDI, M. E., GULATI, R., KLEPPE, L. S., MUESKE, C. S., MOOKADAM, M., SOWA, G., GORES, G. J., SESSA, W. C. & SIMARI, R. D. 2003. Caveolin-1 Can Regulate Vascular Smooth Muscle Cell Fate by Switching Platelet-Derived Growth Factor Signaling From a Proliferative to an Apoptotic Pathway. *Arteriosclerosis, Thrombosis, and Vascular Biology,* 23**,** 1521-1527.

PICKERING, G. W. 1955. THE GENETIC FACTOR IN ESSENTIAL HYPERTENSION*. *Annals of Internal Medicine,* 43**,** 457-464.

PILZ, S., MEINITZER, A., TOMASCHITZ, A., DRECHSLER, C., RITZ, E., KRANE, V., WANNER, C., BOEHM, B. O. & MARZ, W. 2011. Low homoarginine concentration is a novel risk factor for heart disease. *Heart,* 97**,** 1222-7.

POMPELLA, A., VISVIKIS, A., PAOLICCHI, A., TATA, V. D. & CASINI, A. F. 2003. The changing faces of glutathione, a cellular protagonist. *Biochemical Pharmacology,* 66**,** 1499-1503.

POTENZA, M. A., MARASCIULO, F. L., CHIEPPA, D. M., BRIGIANI, G. S., FORMOSO, G., QUON, M. J. & MONTAGNANI, M. 2005. Insulin resistance in spontaneously hypertensive rats is associated with endothelial dysfunction characterized by imbalance between NO and ET-1 production. *Am J Physiol Heart Circ Physiol,* 289**,** H813-22.

POULTER, N. 2003. Global risk of cardiovascular disease. *Heart,* 89 Suppl 2**,** ii2-5; discussion ii35-7.

PURVES, W. K., ORIANS, G. H., SADAVA, D. E., HELLER, H. C. 1995. Life: The Science of Biology, 4th Edition. Sinauer Associates, Sunderland.

PYNE, S. & PYNE, N. 2000a. Sphingosine 1-phosphate signalling via the endothelial differentiation gene family of G-protein-coupled receptors. *Pharmacol Ther,* 88**,** 115-31.

PYNE, S. & PYNE, N. J. 2000b. Sphingosine 1-phosphate signalling in mammalian cells. *Biochem J,* 349**,** 385-402.

RAO, D. C., PROVINCE, M. A., LEPPERT, M. F., OBERMAN, A., HEISS, G., ELLISON, R. C., ARNETT, D. K., ECKFELDT, J. H., SCHWANDER, K., MOCKRIN, S. C. & HUNT, S. C. 2003. A genome-wide affected sibpair linkage analysis of hypertension: the HyperGEN network. *Am J Hypertens,* 16**,** 148-50.

RAPP, J. P. 2000. Genetic analysis of inherited hypertension in the rat. *Physiol Rev,* 80**,** 135-72.

REKHRAJ, S., GANDY, S. J., SZWEJKOWSKI, B. R., NADIR, M. A., NOMAN, A., HOUSTON, J. G., LANG, C. C., GEORGE, J. & STRUTHERS, A. D. 2013. High-dose allopurinol reduces left ventricular mass in patients with ischemic heart disease. *J Am Coll Cardiol,* 61**,** 926-32.

RIGSBY, C. S., ERGUL, A., PORTIK DOBOS, V., POLLOCK, D. M. & DORRANCE, A. M. 2011. Effects of spironolactone on cerebral vessel structure in rats with sustained hypertension. *Am J Hypertens,* 24**,** 708-15.

RIZZONI, D., CASTELLANO, M., PORTERI, E., BETTONI, G., MUIESAN, M. L. & AGABITI-ROSEI, E. 1994. Vascular structural and functional alterations before and after the development of hypertension in SHR. *Am J Hypertens,* 7**,** 193-200.

RIZZONI, D., PORTERI, E., BOARI, G. E., DE CIUCEIS, C., SLEIMAN, I., MUIESAN, M. L., CASTELLANO, M., MICLINI, M. & AGABITI-ROSEI, E. 2003. Prognostic significance of small-artery structure in hypertension. *Circulation,* 108**,** 2230-5.

RIZZONI, D., PORTERI, E., PICCOLI, A., CASTELLANO, M., BETTONI, G., MUIESAN, M. L., PASINI, G., GUELFI, D., MULVANY, M. J. & AGABITI ROSEI, E. 1998. Effects of losartan and enalapril on small artery structure in hypertensive rats. *Hypertension,* 32**,** 305-10.

ROBERG, K. O., K 1998. OXIDATIVE STRESS CAUSES RELOCATION OF THE LYSOSOMAL-ENZYME CATHEPSIN-D WITH ENSUING APOPTOSIS IN NEONATAL RAT CARDIOMYOCYTES. *The American journal of pathology,* 152**,** 1151-1156.

ROBERT, P., TSUI, P., LAVILLE, M. P., LIVI, G. P., SARAU, H. M., BRIL, A. & BERREBI-BERTRAND, I. 2001. EDG1 Receptor Stimulation Leads to Cardiac Hypertrophy in Rat Neonatal Myocytes. *Journal of Molecular and Cellular Cardiology,* 33**,** 1589-1606.

ROBERTSON, D. G. 2005. Metabonomics in toxicology: a review. *Toxicol Sci,* 85**,** 809-22.

RODRIGUEZ-ITURBE, B., QUIROZ, Y., NAVA, M., BONET, L., CHAVEZ, M., HERRERA-ACOSTA, J., JOHNSON, R. J. & PONS, H. A. 2002. Reduction of renal immune cell infiltration results in blood pressure control in genetically hypertensive rats. *Am J Physiol Renal Physiol,* 282**,** F191-201.

RODRIGUEZ-ITURBE, B. & VAZIRI, N. D. 2007. Salt-sensitive hypertension--update on novel findings. *Nephrol Dial Transplant,* 22**,** 992-5.

ROECKER, R., JUNGES, G. M., DE LIMA, D. D., DA CRUZ, J. G., WYSE, A. T. & DAL MAGRO, D. D. 2012. Proline alters antioxidant enzyme defenses and lipoperoxidation in the erythrocytes and plasma of rats: in vitro and in vivo studies. *Biol Trace Elem Res,* 147**,** 172-9.

ROSNER, M. H. 2009. Urinary biomarkers for the detection of renal injury. *Adv Clin Chem,* 49**,** 73-97.

ROSS, P. L., HUANG, Y. N., MARCHESE, J. N., WILLIAMSON, B., PARKER, K., HATTAN, S., KHAINOVSKI, N., PILLAI, S., DEY, S., DANIELS, S., PURKAYASTHA, S., JUHASZ, P., MARTIN, S., BARTLET-JONES, M., HE, F., JACOBSON, A. & PAPPIN, D. J. 2004. Multiplexed Protein Quantitation in Saccharomyces cerevisiae Using Amine-reactive Isobaric Tagging Reagents. *Molecular & Cellular Proteomics,* 3**,** 1154-1169.

ROSSI, M., TADDEI, S., FABBRI, A., TINTORI, G., CREDIDIO, L., VIRDIS, A., GHIADONI, L., SALVETTI, A. & GIUSTI, C. 1997. Cutaneous vasodilation to acetylcholine in patients with essential hypertension. *J Cardiovasc Pharmacol,* 29**,** 406-11.

RUIZ-MARCOS, F. M., ORTIZ, M. C., FORTEPIANI, L. A., NADAL, F. J., ATUCHA, N. M. & GARCIA-ESTAN, J. 2001. Mechanisms of the increased pressor response to vasopressors in the mesenteric bed of nitric oxide-deficient hypertensive rats. *Eur J Pharmacol,* 412**,** 273-9.

SALVI, E., KUTALIK, Z., GLORIOSO, N., BENAGLIO, P., FRAU, F., KUZNETSOVA, T., ARIMA, H., HOGGART, C., TICHET, J., NIKITIN, Y. P., CONTI, C., SEIDLEROVA, J., TIKHONOFF, V., STOLARZ-SKRZYPEK, K., JOHNSON, T., DEVOS, N., ZAGATO, L., GUARRERA, S., ZANINELLO, R., CALABRIA, A., STANCANELLI, B., TROFFA, C., THIJS, L., RIZZI, F., SIMONOVA, G., LUPOLI, S., ARGIOLAS, G., BRAGA, D., D'ALESSIO, M. C., ORTU, M. F., RICCERI, F., MERCURIO, M., DESCOMBES, P., MARCONI, M., CHALMERS, J., HARRAP,

S., FILIPOVSKY, J., BOCHUD, M., IACOVIELLO, L., ELLIS, J., STANTON, A. V., LAAN, M., PADMANABHAN, S., DOMINICZAK, A. F., SAMANI, N. J., MELANDER, O., JEUNEMAITRE, X., MANUNTA, P., SHABO, A., VINEIS, P., CAPPUCCIO, F. P., CAULFIELD, M. J., MATULLO, G., RIVOLTA, C., MUNROE, P. B., BARLASSINA, C., STAESSEN, J. A., BECKMANN, J. S. & CUSI, D. 2012. Genomewide Association Study Using a High-Density Single Nucleotide Polymorphism Array and Case-Control Design Identifies a Novel Essential Hypertension Susceptibility Locus in the Promoter Region of Endothelial NO Synthase. *Hypertension,* 59**,** 248-255.

SAMMUT, I. A., FORESTI, R., CLARK, J. E., EXON, D. J., VESELY, M. J. J., SARATHCHANDRA, P., GREEN, C. J. & MOTTERLINI, R. 1998. Carbon monoxide is a major contributor to the regulation of vascular tone in aortas expressing high levels of haeme oxygenase-1. *British Journal of Pharmacology,* 125**,** 1437-1444.

SANO, T., BAKER, D., VIRAG, T., WADA, A., YATOMI, Y., KOBAYASHI, T., IGARASHI, Y. & TIGYI, G. 2002. Multiple mechanisms linked to platelet activation result in lysophosphatidic acid and sphingosine 1-phosphate generation in blood. *J Biol Chem,* 277**,** 21197-206.

SAUZEAU, V., LE JEUNE, H., CARIO-TOUMANIANTZ, C., SMOLENSKI, A., LOHMANN, S. M., BERTOGLIO, J., CHARDIN, P., PACAUD, P. & LOIRAND, G. 2000. Cyclic GMP-dependent Protein Kinase Signaling Pathway Inhibits RhoA-induced Ca2+ Sensitization of Contraction in Vascular Smooth Muscle. *Journal of Biological Chemistry,* 275**,** 21722-21729.

SAVOIA, C., EBRAHIMIAN, T., HE, Y., GRATTON, J. P., SCHIFFRIN, E. L. & TOUYZ, R. M. 2006. Angiotensin II/AT2 receptor-induced vasodilation in stroke-prone spontaneously hypertensive rats involves nitric oxide and cGMP-dependent protein kinase. *J Hypertens,* 24**,** 2417-22.

SAVOIA, C., TABET, F., YAO, G., SCHIFFRIN, E. L. & TOUYZ, R. M. 2005. Negative regulation of RhoA/Rho kinase by angiotensin II type 2 receptor in vascular smooth muscle cells: role in angiotensin II-induced vasodilation in stroke-prone spontaneously hypertensive rats. *J Hypertens,* 23**,** 1037-45.

SCALBERT, A., BRENNAN, L., FIEHN, O., HANKEMEIER, T., KRISTAL, B. S., VAN OMMEN, B., PUJOS-GUILLOT, E., VERHEIJ, E., WISHART, D. & WOPEREIS, S. 2009. Mass-spectrometry-based metabolomics: limitations and recommendations for future progress with particular focus on nutrition research. *Metabolomics,* 5**,** 435-458.

SCHELTEMA, R., DECUYPERE, S., DUJARDIN, J., WATSON, D., JANSEN, R. & BREITLING, R. 2009. Simple data-reduction method for high-resolution LC-MS data in metabolomics. *Bioanalysis,* 1**,** 1551-7.

SCHELTEMA, R. A., JANKEVICS, A., JANSEN, R. C., SWERTZ, M. A. & BREITLING, R. 2011. PeakML/mzMatch: a file format, Java library, R library, and tool-chain for mass spectrometry data analysis. *Anal Chem,* 83**,** 2786-93.

SCHIFFRIN, E., DENG, LY 1999. Relationship between small-artery structure and systolic, diastolic and pulse pressure in essential hypertension. *Journal of Hypertension,* 17.

SCHIFFRIN, E. L. 1998. Vascular remodeling and endothelial function in hypertensive patients: effects of antihypertensive therapy. *Scand Cardiovasc J Suppl,* 47**,** 15-21.

SCHIFFRIN, E. L. 2010. Circulatory therapeutics: use of antihypertensive agents and their effects on the vasculature. *J Cell Mol Med,* 14**,** 1018-29.

SCHULZE, W. X. & MANN, M. 2004. A Novel Proteomic Screen for Peptide-Protein Interactions. *Journal of Biological Chemistry,* 279**,** 10756-10764.

SCOTLAND, R. S., AHLUWALIA, A. & HOBBS, A. J. 2005a. C-type natriuretic peptide in vascular physiology and disease. *Pharmacol Ther,* 105**,** 85-93.

SCOTLAND, R. S., MADHANI, M., CHAUHAN, S., MONCADA, S., ANDRESEN, J., NILSSON, H., HOBBS, A. J. & AHLUWALIA, A. 2005b. Investigation of vascular responses in endothelial nitric oxide synthase/cyclooxygenase-1 double-knockout mice: key role for endothelium-derived hyperpolarizing factor in the regulation of blood pressure in vivo. *Circulation,* 111**,** 796-803.

SEARLE, B. C. 2010. Scaffold: A bioinformatic tool for validating MS/MS-based proteomic studies. *PROTEOMICS,* 10**,** 1265-1269.

SEARLE, B. C., TURNER, M. & NESVIZHSKII, A. I. 2008. Improving Sensitivity by Probabilistically Combining Results from Multiple MS/MS Search Methodologies. *Journal of Proteome Research,* 7**,** 245-253.

SEKO, T., ITO, M., KUREISHI, Y., OKAMOTO, R., MORIKI, N., ONISHI, K., ISAKA, N., HARTSHORNE, D. J. & NAKANO, T. 2003. Activation of RhoA and inhibition of myosin phosphatase as important components in hypertension in vascular smooth muscle. *Circ Res,* 92**,** 411-8.

SHAH, S. H., HAUSER, E. R., BAIN, J. R., MUEHLBAUER, M. J., HAYNES, C., STEVENS, R. D., WENNER, B. R., DOWDY, Z. E., GRANGER, C. B., GINSBURG, G. S., NEWGARD, C. B. & KRAUS, W. E. 2009. High heritability of metabolomic profiles in families burdened with premature cardiovascular disease. *Mol Syst Biol,* 5**,** 258.

SHEVCHENKO, A., WILM, M., VORM, O. & MANN, M. 1996. Mass Spectrometric Sequencing of Proteins from Silver-Stained Polyacrylamide Gels. *Analytical Chemistry,* 68**,** 850-858.

SHIMOKAWA, H., YASUTAKE, H., FUJII, K., OWADA, M. K., NAKAIKE, R., FUKUMOTO, Y., TAKAYANAGI, T., NAGAO, T., EGASHIRA, K., FUJISHIMA, M. & TAKESHITA, A. 1996. The importance of the hyperpolarizing mechanism increases as the vessel size decreases in endothelium-dependent relaxations in rat mesenteric circulation. *J Cardiovasc Pharmacol,* 28**,** 703-11.

SINGLETON, P. A., CHATCHAVALVANICH, S., FU, P., XING, J., BIRUKOVA, A. A., FORTUNE, J. A., KLIBANOV, A. M., GARCIA, J. G. & BIRUKOV, K. G. 2009. Akt-mediated transactivation of the S1P1 receptor in caveolin-enriched microdomains regulates endothelial barrier enhancement by oxidized phospholipids. *Circ Res,* 104**,** 978-86.

SMITH, C. A., WANT, E. J., O'MAILLE, G., ABAGYAN, R. & SIUZDAK, G. 2006a. XCMS: processing mass spectrometry data for metabolite profiling using nonlinear peak alignment, matching, and identification. *Anal Chem,* 78**,** 779-87.

SMITH, C. A., WANT, E. J., O'MAILLE, G., ABAGYAN, R. & SIUZDAK, G. 2006b. XCMS: Processing Mass Spectrometry Data for Metabolite Profiling Using Nonlinear Peak Alignment, Matching, and Identification. *Analytical Chemistry,* 78**,** 779-787.

SOFOLA, O. A., KNILL, A., HAINSWORTH, R. & DRINKHILL, M. 2002. Change in endothelial function in mesenteric arteries of Sprague-Dawley rats fed a high salt diet. *J Physiol,* 543**,** 255-60.

SPIEGEL, S. & MILSTIEN, S. 2003a. Exogenous and intracellularly generated sphingosine 1-phosphate can regulate cellular processes by divergent pathways. *Biochem Soc Trans,* 31**,** 1216-9.

SPIEGEL, S. & MILSTIEN, S. 2003b. Sphingosine-1-phosphate: an enigmatic signalling lipid. *Nat Rev Mol Cell Biol,* 4**,** 397-407.

SPIJKERS, L. J., VAN DEN AKKER, R. F., JANSSEN, B. J., DEBETS, J. J., DE MEY, J. G., STROES, E. S., VAN DEN BORN, B. J., WIJESINGHE, D. S., CHALFANT, C. E., MACALEESE, L., EIJKEL,

G. B., HEEREN, R. M., ALEWIJNSE, A. E. & PETERS, S. L. 2011. Hypertension is associated with marked alterations in sphingolipid biology: a potential role for ceramide. *PLoS One,* 6**,** e21817.

SREEKUMAR, A., POISSON, L. M., RAJENDIRAN, T. M., KHAN, A. P., CAO, Q., YU, J., LAXMAN, B., MEHRA, R., LONIGRO, R. J., LI, Y., NYATI, M. K., AHSAN, A., KALYANA-SUNDARAM, S., HAN, B., CAO, X., BYUN, J., OMENN, G. S., GHOSH, D., PENNATHUR, S., ALEXANDER, D. C., BERGER, A., SHUSTER, J. R., WEI, J. T., VARAMBALLY, S., BEECHER, C. & CHINNAIYAN, A. M. 2009. Metabolomic profiles delineate potential role for sarcosine in prostate cancer progression. *Nature,* 457**,** 910-914.

STEEN, H. & MANN, M. 2004. The abc's (and xyz's) of peptide sequencing. *Nat Rev Mol Cell Biol,* 5**,** 699-711.

STEINMETZ, M., POTTHAST, R., SABRANE, K. & KUHN, M. 2004. Diverging vasorelaxing effects of C-type natriuretic peptide in renal resistance arteries and aortas of GC-A-deficient mice. *Regulatory Peptides,* 119**,** 31-37.

SUHRE, K., MEISINGER, C., DORING, A., ALTMAIER, E., BELCREDI, P., GIEGER, C., CHANG, D., MILBURN, M. V., GALL, W. E., WEINBERGER, K. M., MEWES, H. W., HRABE DE ANGELIS, M., WICHMANN, H. E., KRONENBERG, F., ADAMSKI, J. & ILLIG, T. 2010. Metabolic footprint of diabetes: a multiplatform metabolomics study in an epidemiological setting. *PLoS One,* 5**,** e13953.

SUHRE, K., SHIN, S. Y., PETERSEN, A. K., MOHNEY R. P., MEREDITH, D., WAGELE, B., ALTMAIER, E., CARDIoGRAM, DELOUKAS, P., ERDMANN, J., GRUNDBERG, E., HAMMOND, C. J., HRABE DE ANGELIS, M., KASTENMULLER, G., KOTTGEN, A., KRONENBERG, F., MANGINO, M., MEISINGER, C., MEITINGER, T., MEWES, H. W., MILBURN, M. C., PREHN, C., RAFFLER, J., RIED, J. S., ROMISCH-MARGL, W., SAMANI, N. J., SMALL, K., S., WICHMANN, H. E., ZHAI, G., ILLIG, T., SPECTOR, T. D., ADAMSKI, J., SORANZO, N. & GIEGER, C. 2011. Human metabolic individuality in biomedical and pharmaceutical research. *Nature* 477, 54–60.

SUHRE, K., WALLASCHOFSKI, H., RAFFLER, J., FRIEDRICH, N., HARING, R., MICHAEL, K., WASNER, C., KREBS, A., KRONENBERG, F., CHANG, D., MEISINGER, C., WICHMANN, H. E., HOFFMANN, W., VOLZKE, H., VOLKER, U., TEUMER, A., BIFFAR, R., KOCHER, T., FELIX, S. B , ILLIG, T., KROEMER, H. K , GIEGER, C., ROMISCH-MARGL, W. & NAUCK, M. 2011. A genome-wide association study of metabolic traits in human urine. *Nat Genet,* 43, 565-9.

SUNANO, S., WATANABE, H., TANAKA, S., SEKIGUCHI, F. & SHIMAMURA, K. 1999. Endothelium-derived relaxing, contracting and hyperpolarizing factors of mesenteric arteries of hypertensive and normotensive rats. *Br J Pharmacol,* 126**,** 709-16.

SURY, M. D., CHEN, J.-X. X. & SELBACH, M. 2010. The SILAC fly allows for accurate protein quantification in vivo. *Molecular & Cellular Proteomics*.

SUZUKI, H., DELANO, F. A., PARKS, D. A., JAMSHIDI, N., GRANGER, D. N., ISHII, H., SUEMATSU, M., ZWEIFACH, B. W. & SCHMID-SCHONBEIN, G. W. 1998. Xanthine oxidase activity associated with arterial blood pressure in spontaneously hypertensive rats. *Proc Natl Acad Sci U S A,* 95**,** 4754-9.

SVETKEY, L. P., MCKEOWN, S. P. & WILSON, A. F. 1996. Heritability of salt sensitivity in black Americans. *Hypertension,* 28**,** 854-8.

TABET, F., SCHIFFRIN, E. L. & TOUYZ, R. M. 2005. Mitogen-activated protein kinase activation by hydrogen peroxide is mediated through tyrosine kinase-dependent, protein kinase C-independent pathways in vascular smooth muscle cells: upregulation in spontaneously hypertensive rats. *J Hypertens,* 23**,** 2005-12.

TADDEI, S., GHIADONI, L., VIRDIS, A., BURALLI, S. & SALVETTI, A. 1999. Vasodilation to bradykinin is mediated by an ouabain-sensitive pathway as a compensatory mechanism for impaired nitric oxide availability in essential hypertensive patients. *Circulation,* 100**,** 1400-5.

TADDEI, S., VIRDIS, A., GHIADONI, L., MAGAGNA, A., PASINI, A. F., GARBIN, U., COMINACINI, L. & SALVETTI, A. 2001. Effect of calcium antagonist or beta blockade treatment on nitric oxide-dependent vasodilation and oxidative stress in essential hypertensive patients. *J Hypertens,* 19**,** 1379-86.

TADDEI, S., VIRDIS, A., GHIADONI, L., MATTEI, P. & SALVETTI, A. 1998. Effects of angiotensin converting enzyme inhibition on endothelium-dependent vasodilatation in essential hypertensive patients. *J Hypertens,* 16**,** 447-56.

TADDEI, S., VIRDIS, A., MATTEI, P., ARZILLI, F. & SALVETTI, A. 1992. Endothelium-dependent forearm vasodilation is reduced in normotensive subjects with familial history of hypertension. *J Cardiovasc Pharmacol,* 20 Suppl 12**,** S193-5.

TADDEI, S., VIRDIS, A., MATTEI, P., GHIADONI, L., SUDANO, I. & SALVETTI, A. 1996. Defective L-arginine-nitric oxide pathway in offspring of essential hypertensive patients. *Circulation,* 94**,** 1298-303.

TANG, X. D., GARCIA, M. L., HEINEMANN, S. H. & HOSHI, T. 2004. Reactive oxygen species impair Slo1 BK channel function by altering cysteine-mediated calcium sensing. *Nat Struct Mol Biol,* 11**,** 171-8.

TANIMOTO, T., LUNGU, A. O. & BERK, B. C. 2004. Sphingosine 1-phosphate transactivates the platelet-derived growth factor beta receptor and epidermal growth factor receptor in vascular smooth muscle cells. *Circ Res,* 94**,** 1050-8.

TESFAMARIAM, B. & HALPERN, W. 1988. Endothelium-dependent and endothelium-independent vasodilation in resistance arteries from hypertensive rats. *Hypertension,* 11**,** 440-4.

TIWARI, M., HEMALATHA, T., GANESAN, K., NAYEEM, M., MURALI MANOHAR, B., BALACHANDRAN, C., VAIRAMUTHU, S., SUBRAMANIAM, S. & PUVANAKRISHNAN, R. 2008. Myocardial ischemia and reperfusion injury in rats: lysosomal hydrolases and matrix metalloproteinases mediated cellular damage. *Molecular and Cellular Biochemistry,* 312**,** 81-91.

TODOROV, V. T., DESCH, M., SCHMITT-NILSON, N., TODOROVA, A. & KURTZ, A. 2007. Peroxisome proliferator-activated receptor-gamma is involved in the control of renin gene expression. *Hypertension,* 50**,** 939-44.

TOUYZ, R. M. & SCHIFFRIN, E. L. 2004. Reactive oxygen species in vascular biology: implications in hypertension. *Histochem Cell Biol,* 122**,** 339-52.

TOUYZ, R. M., TABET, F. & SCHIFFRIN, E. L. 2003. Redox-dependent signalling by angiotensin II and vascular remodelling in hypertension. *Clin Exp Pharmacol Physiol,* 30**,** 860-6.

TREASURE, C. B., KLEIN, J. L., VITA, J. A., MANOUKIAN, S. V., RENWICK, G. H., SELWYN, A. P., GANZ, P. & ALEXANDER, R. W. 1993. Hypertension and left ventricular hypertrophy are associated with impaired endothelium-mediated relaxation in human coronary resistance vessels. *Circulation,* 87**,** 86-93.

TRUDU, M., JANAS, S., LANZANI, C., DEBAIX, H., SCHAEFFER, C., IKEHATA, M., CITTERIO, L., DEMARETZ, S., TREVISANI, F., RISTAGNO, G., GLAUDEMANS, B., LAGHMANI, K., DELL'ANTONIO, G., BOCHUD, M., BURNIER, M., DEVUYST, O., MARTIN, P. Y., MOHAUPT, M., PACCAUD, F., PECHERE-BERTSCHI, A., VOGT, B., ACKERMANN, D., EHRET, G., GUESSOUS, I., PONTE, B., PRUIJM, M., LOFFING, J., RASTALDI, M. P., MANUNTA, P., DEVUYST, O. & RAMPOLDI, L. 2013. Common noncoding UMOD gene

variants induce salt-sensitive hypertension and kidney damage by increasing uromodulin expression. *Nat Med*.

TSOUNAPI, P., SAITO, M., KITATANI, K., DIMITRIADIS, F., OHMASA, F., SHIMIZU, S., KINOSHITA, Y., TAKENAKA, A. & SATOH, K. 2012. Fasudil improves the endothelial dysfunction in the aorta of spontaneously hypertensive rats. *Eur J Pharmacol,* 691**,** 182-9.

TUNCER, M. & VANHOUTTE, P. M. 1993. Response to the endothelium-dependent vasodilator acetylcholine in perfused kidneys of normotensive and spontaneously hypertensive rats. *Blood Press,* 2**,** 217-20.

UDALI, S., GUARINI, P., MORUZZI, S., CHOI, S.-W. & FRISO, S. 2013. Cardiovascular epigenetics: From DNA methylation to microRNAs. *Molecular Aspects of Medicine,* 34**,** 883-901.

UEHATA, M., ISHIZAKI, T., SATOH, H., ONO, T., KAWAHARA, T., MORISHITA, T., TAMAKAWA, H., YAMAGAMI, K., INUI, J., MAEKAWA, M. & NARUMIYA, S. 1997. Calcium sensitization of smooth muscle mediated by a Rho-associated protein kinase in hypertension. *Nature,* 389**,** 990-994.

VAN BROCKLYN, J. R., LEE, M. J., MENZELEEV, R., OLIVERA, A., EDSALL, L., CUVILLIER, O., THOMAS, D. M., COOPMAN, P. J., THANGADA, S., LIU, C. H., HLA, T. & SPIEGEL, S. 1998. Dual actions of sphingosine-1-phosphate: extracellular through the Gi-coupled receptor Edg-1 and intracellular to regulate proliferation and survival. *J Cell Biol,* 142**,** 229-40.

VANDER, A., SHERMAN, J., LUCIANO, D. 2001a. Circulation. *Human Physiology: The mechanisms of body function.* Eighth Edition ed.

VANDER, A., SHERMAN, J., LUCIANO, D. 2001b. The kidneys and regulation of water and inorganic ions. *Human Physiology: The Mechanisms of Body Function.* Eighth Edition ed.

VANHOUTTE, P. M., FELETOU, M. & TADDEI, S. 2005. Endothelium-dependent contractions in hypertension. *British Journal of Pharmacology,* 144**,** 449-458.

VANHOUTTE, P. M. & TANG, E. H. C. 2008. Endothelium-dependent contractions: when a good guy turns bad! *The Journal of Physiology,* 586**,** 5295-5304.

VEITH, C., SCHMITT, S., VEIT, F., DAHAL, B. K., WILHELM, J., KLEPETKO, W., MARTA, G., SEEGER, W., SCHERMULY, R. T., GRIMMINGER, F., GHOFRANI, H. A., FINK, L., WEISSMANN, N. & KWAPISZEWSKA, G. 2013. Cofilin, a hypoxia-regulated protein in murine lungs identified by 2DE: Role of the cytoskeletal protein cofilin in pulmonary hypertension. *PROTEOMICS,* 13**,** 75-88.

VIDT, D. G. & BORAZANIAN, R. A. 2003. Treat high blood pressure sooner: tougher, simpler JNC 7 guidelines. *Cleveland Clinic Journal of Medicine,* 70**,** 721-728.

VILLAR, I. C., PANAYIOTOU, C. M., SHERAZ, A., MADHANI, M., SCOTLAND, R. S., NOBLES, M., KEMP-HARPER, B., AHLUWALIA, A. & HOBBS, A. J. 2007. Definitive role for natriuretic peptide receptor-C in mediating the vasorelaxant activity of C-type natriuretic peptide and endothelium-derived hyperpolarising factor. *Cardiovasc Res,* 74**,** 515-25.

VOLDSTEDLUND, M., VINTEN, J. & TRANUM-JENSEN, J. 2001. cav-p60 expression in rat muscle tissues. *Cell and Tissue Research,* 306**,** 265-276.

VON ZUR MUHLEN, C., SCHIFFER, E., ZUERBIG, P., KELLMANN, M., BRASSE, M., MEERT, N., VANHOLDER, R. C., DOMINICZAK, A. F., CHEN, Y. C., MISCHAK, H., BODE, C. & PETER, K. 2009. Evaluation of urine proteome pattern analysis for its potential to reflect coronary artery atherosclerosis in symptomatic patients. *J Proteome Res,* 8**,** 335-45.

WALLACE, K. J., WALLIS, R. H., COLLINS, S. C., ARGOUD, K., KAISAKI, P. J., KTORZA, A., WOON, P. Y., BIHOREAU, M. T. & GAUGUIER, D. 2004. Quantitative trait locus dissection in

congenic strains of the Goto-Kakizaki rat identifies a region conserved with diabetes loci in human chromosome 1q. *Physiol Genomics,* 19**,** 1-10.

WANG, J.-N., SHI, N. & CHEN, S.-Y. 2012a. Manganese superoxide dismutase inhibits neointima formation through attenuation of migration and proliferation of vascular smooth muscle cells. *Free Radical Biology and Medicine,* 52**,** 173-181.

WANG, M., FU, Z., WU, J., ZHANG, J., JIANG, L., KHAZAN, B., TELLJOHANN, R., ZHAO, M., KRUG, A. W., PIKILIDOU, M., MONTICONE, R. E., WERSTO, R., VAN EYK, J. & LAKATTA, E. G. 2012b. MFG-E8 activates proliferation of vascular smooth muscle cells via integrin signaling. *Aging Cell,* 11**,** 500-508.

WATERMAN, C. L., KIAN-KAI, C. & GRIFFIN, J. L. 2010. Metabolomic strategies to study lipotoxicity in cardiovascular disease. *Biochim Biophys Acta,* 1801**,** 230-4.

WEBB, R. C. 2003. SMOOTH MUSCLE CONTRACTION AND RELAXATION. *Advances in Physiology Education,* 27**,** 201-206.

WEINBERGER, M. H., MILLER, J. Z., LUFT, F. C., GRIM, C. E., FINEBERG, N. S. 1986. Definitions and characteristics of sodium sensitivity and blood pressure resistance. *Hypertension*, 8(suppl II):II-127-II-134.

WHO 2012. World Health Report. Geneva, Switzerland.

WIDLANSKY, M. E., GOKCE, N., KEANEY, J. F., JR. & VITA, J. A. 2003. The clinical implications of endothelial dysfunction. *J Am Coll Cardiol,* 42**,** 1149-60.

WILMES, A., CREAN, D., AYDIN, S., PFALLER, W., JENNINGS, P. & LEONARD, M. O. 2011. Identification and dissection of the Nrf2 mediated oxidative stress pathway in human renal proximal tubule toxicity. *Toxicol In Vitro,* 25**,** 613-22.

WINDH, R. T., LEE, M. J., HLA, T., AN, S., BARR, A. J. & MANNING, D. R. 1999. Differential coupling of the sphingosine 1-phosphate receptors Edg-1, Edg-3, and H218/Edg-5 to the G(i), G(q), and G(12) families of heterotrimeric G proteins. *J Biol Chem,* 274**,** 27351-8.

WU, W., MOSTELLER, R. D. & BROEK, D. 2004. Sphingosine kinase protects lipopolysaccharide-activated macrophages from apoptosis. *Mol Cell Biol,* 24**,** 7359-69.

WU, X., SOMLYO, A. V. & SOMLYO, A. P. 1996. Cyclic GMP-Dependent Stimulation Reverses G-Protein-Coupled Inhibition of Smooth Muscle Myosin Light Chain Phosphatase. *Biochemical and Biophysical Research Communications,* 220**,** 658-663.

WYNNE, B. M., CHIAO, C. W. & WEBB, R. C. 2009. Vascular Smooth Muscle Cell Signaling Mechanisms for Contraction to Angiotensin II and Endothelin-1. *J Am Soc Hypertens,* 3**,** 84-95.

XIA, P., GAMBLE, J. R., RYE, K. A., WANG, L., HII, C. S., COCKERILL, P., KHEW-GOODALL, Y., BERT, A. G., BARTER, P. J. & VADAS, M. A. 1998. Tumor necrosis factor-alpha induces adhesion molecule expression through the sphingosine kinase pathway. *Proc Natl Acad Sci U S A,* 95**,** 14196-201.

YAGIL, C., HUBNER, N., KREUTZ, R., GANTEN, D. & YAGIL, Y. 2003. Congenic strains confirm the presence of salt-sensitivity QTLs on chromosome 1 in the Sabra rat model of hypertension. *Physiol Genomics,* 12**,** 85-95.

YAMORI, Y. & OKAMOTO, K. 1974. Spontaneous hypertension in the rat. A model for human "essential" hypertension. *Verh Dtsch Ges Inn Med,* 80**,** 168-70.

YANG, Q., XUE, H. M., WONG, W. T., TIAN, X. Y., HUANG, Y., TSUI, S. K., NG, P. K., WOHLFART, P., LI, H., XIA, N., TOBIAS, S., UNDERWOOD, M. J. & HE, G. W. 2011. AVE3085, an enhancer of endothelial nitric oxide synthase, restores endothelial function and reduces blood pressure in spontaneously hypertensive rats. *Br J Pharmacol,* 163**,** 1078-85.

YOGI, A., CALLERA, G. E., ARANHA, A. B., ANTUNES, T. T., GRAHAM, D., MCBRIDE, M., DOMINICZAK, A. & TOUYZ, R. M. 2011. Sphingosine-1-Phosphate-Induced Inflammation Involves Receptor Tyrosine Kinase Transactivation in Vascular Cells: Upregulation in Hypertension. *Hypertension,* 57**,** 809-818.

YU, L., QUINN, D. A., GARG, H. G. & HALES, C. A. 2011. Heparin Inhibits Pulmonary Artery Smooth Muscle Cell Proliferation through Guanine Nucleotide Exchange Factor–H1/RhoA/Rho Kinase/p27. *American Journal of Respiratory Cell and Molecular Biology,* 44**,** 524-530.

YU, W., TAYLOR, J. A., DAVIS, M. T., BONILLA, L. E., LEE, K. A., AUGER, P. L., FARNSWORTH, C. C., WELCHER, A. A. & PATTERSON, S. D. 2010. Maximizing the sensitivity and reliability of peptide identification in large-scale proteomic experiments by harnessing multiple search engines. *PROTEOMICS,* 10**,** 1172-1189.

YUSUF, S., REDDY, S., OUNPUU, S. & ANAND, S. 2001. Global burden of cardiovascular diseases: part I: general considerations, the epidemiologic transition, risk factors, and impact of urbanization. *Circulation,* 104**,** 2746-53.

ZALBA, G., BEAUMONT, F. J., SAN JOSE, G., FORTUNO, A., FORTUNO, M. A., ETAYO, J. C. & DIEZ, J. 2000. Vascular NADH/NADPH oxidase is involved in enhanced superoxide production in spontaneously hypertensive rats. *Hypertension,* 35**,** 1055-61.

ZHANG, G., HE, P., TAN, H., BUDHU, A., GAEDCKE, J., GHADIMI, B. M., RIED, T., YFANTIS, H. G., LEE, D. H., MAITRA, A., HANNA, N., ALEXANDER, H. R. & HUSSAIN, S. P. 2013. Integration of metabolomics and transcriptomics revealed a fatty acid network exerting growth inhibitory effects in human pancreatic cancer. *Clin Cancer Res,* 19**,** 4983-93.

ZHANG, Q. Y., DENE, H., DENG, A. Y., GARRETT, M. R., JACOB, H. J. & RAPP, J. P. 1997. Interval mapping and congenic strains for a blood pressure QTL on rat chromosome 13. *Mamm Genome,* 8**,** 636-41.

ZHANG, Z. J. & PECK, S. C. 2011. Simplified enrichment of plasma membrane proteins for proteomic analyses in Arabidopsis thaliana. *PROTEOMICS,* 11**,** 1780-1788.

ZHU, H., JIA, Z., MAHANEY, J., ROSS, D., MISRA, H., TRUSH, M. & LI, Y. 2007. The Highly Expressed and Inducible Endogenous NAD(P)H:quinone Oxidoreductase 1 in Cardiovascular Cells Acts as a Potential Superoxide Scavenger. *Cardiovascular Toxicology,* 7**,** 202-211.

ZOJA, C., BENIGNI, A. & REMUZZI, G. 2013. The Nrf2 pathway in the progression of renal disease. *Nephrol Dial Transplant*.

ZOU, M. H., COHEN, R. & ULLRICH, V. 2004. Peroxynitrite and vascular endothelial dysfunction in diabetes mellitus. *Endothelium,* 11**,** 89-97.